

INVESTIGATING THE ROLE OF ION CHANNELS ACROSS THE FETOMATERNAL INTERFACE OF THE HUMAN PLACENTA

Tayyba Yasmin Ali

Thesis submitted to the University of Nottingham for the degree of Doctor
of Philosophy
March 2012

LIST OF CONTENTS

DECLARATION	V
ACKNOWLEDGEMENTS	VI
PUBLICATIONS	VIII
ABSTRACT	IX
ABBREVIATIONS	X
1. INTRODUCTION	1
1.1. Maternal adaptations to pregnancy	1
1.2. Maternal vascular remodelling	3
1.3. Early placental development	6
1.4. The term placenta	10
1.5. Transport across the placenta	13
1.6. Control of vascular tone in the placenta	17
1.6.1. Vasoconstrictors	22
1.6.2. Vasodilators	24
1.6.3. Biophysical factors	26
1.6.3.1. Tissue oxygenation	26
1.6.3.2. Acid base homeostasis	30
1.7. The role of Ion channels	34
1.7.1. L Type calcium channel ($Ca_v1.2$)	36
1.7.2. Potassium channels (K^+)	37
1.7.2.1. Large conductance potassium channel (BK_{Ca})	38
1.7.2.2. ATP sensitive potassium channel (K_{ATP})	40
1.7.3. The two pore domain family of potassium channels ($K2P$)	42
1.8. Vascular dysfunctions linked with the placenta	50
1.8.1. PE	51
1.8.2. IUGR	53
1.9. Methods used to study the placenta	54
1.9.1. Whole placentae	55
1.9.2. Resistance vessels	56
1.10. BACKGROUND TO THE STUDY	59
2. HYPOTHESIS	61
2.1. OBJECTIVES	61
3. MATERIALS AND METHODS	62
3.1. PATIENT RECRUITMENT	62
3.2. Tissue collection	62
3.2.1. Isolation of placental arteries	64
3.3. IHC	66
3.3.1. Cryostat tissue sectioning	67
3.3.2. Haematoxylin and eosin (H&E) staining	68
3.3.3. IHC staining for vascular SMC	69
3.4. WESTERN BLOTTING	72
3.4.1. Tissue collection	72
3.4.2. Control tissue	72
3.4.3. Tissue homogenisation	73
3.4.4. Protein determination	74
3.4.5. SDS PAGE Electrophoresis	76
3.4.6. Electroblothing	78
3.4.7. Blocking & antibody application	80
3.4.8. Control peptide blocking	81
3.4.9. β actin measurement	81
3.4.10. Secondary antibody & data analysis	82
3.5. CULTURING SMC	84
3.5.1. Culturing SMC from CPA and SVA explants	84

3.5.2.	<i>Culturing SMC from MYO</i>	87
3.5.3.	<i>SH SY57 cells</i>	87
3.6.	IMMUNOFLUORESCENCE (IF) OF SMC	88
3.6.1.	<i>Fixation of cells</i>	89
3.6.2.	<i>Blocking of non-specific binding sites</i>	90
3.6.3.	<i>Secondary antibody application & evaluation</i>	90
3.6.4.	<i>Slide preparation</i>	91
3.6.5.	<i>Confocal IF</i>	92
3.6.6.	<i>3D images</i>	95
3.6.7.	<i>Confocal image analysis</i>	95
3.6.8.	<i>Method optimisation</i>	96
3.7.	WIRE MYOGRAPHY	98
3.7.1.	<i>Artery preparation</i>	99
3.7.2.	<i>Wire mounted arteries</i>	100
3.7.3.	<i>Calibration of force transducers</i>	102
3.7.4.	<i>Normalisation procedure</i>	103
3.7.5.	<i>Initial experiment settings</i>	106
3.7.5.1.	<i>Determining the ideal resting tension</i>	106
3.7.5.2.	<i>Optimal working diameter (L_{100})</i>	108
3.7.6.	<i>Assessment of vessel viability</i>	111
3.7.7.	<i>Effect of pO_2</i>	112
3.7.8.	<i>Drugs and solutions</i>	113
3.7.9.	<i>Measurement of vasoconstriction and vasodilatation</i>	115
3.7.10.	<i>Drug assessment</i>	116
3.7.11.	<i>Data analysis</i>	116
4.	COMPARING THE STRUCTURE OF CPA AND SVA	119
4.1.	INTRODUCTION	119
4.2.	OBJECTIVES	119
4.3.	MATERIALS AND METHODS	119
4.4.	RESULTS	120
4.4.1.	<i>H&E of CPA and SVA</i>	120
4.4.2.	<i>IHC to identify SMC</i>	123
4.5.	DISCUSSION	125
4.5.1.	<i>Conclusion</i>	131
5.	ASSESSING THE FUNCTIONAL CHARACTERISTICS OF CPA AND SVA	132
5.1.	INTRODUCTION	132
5.2.	OBJECTIVES	132
5.3.	MATERIALS AND METHODS	133
5.4.	RESULTS	133
5.4.1.	<i>Sample number</i>	133
5.4.2.	<i>Vessel size</i>	133
5.5.	PHARMACOLOGICAL INVESTIGATIONS WITH CPA	135
5.5.1.	<i>Response to contractile agonists</i>	135
5.5.1.1.	<i>AVP</i>	135
5.5.1.2.	<i>Thromboxane mimetic U46619</i>	135
5.5.2.	RESPONSE TO ENDOTHELIUM-DEPENDENT VASODILATORS	137
5.5.2.1.	<i>ACh</i>	137
5.5.2.2.	<i>BK</i>	138
5.5.3.	RESPONSE TO ENDOTHELIUM-INDEPENDENT VASODILATORS	138
5.5.3.1.	<i>SNP</i>	138
5.6.	COMPARING CPA TO SVA	141
5.6.1.	<i>Effect of changing pO_2</i>	141
5.6.2.	<i>Contractile responses</i>	142
5.6.3.	<i>Vasodilatation responses</i>	145
5.6.4.	<i>Response to RIL</i>	148
5.6.5.	<i>Response to H_2O_2</i>	151
5.6.6.	<i>Effect of alkaline pH at 20% pO_2</i>	156

5.6.7.	<i>Effect of acidic pH</i>	158
5.7.	<i>Response of PE-CPA at 20% pO₂</i>	165
5.7.1.	<i>Response of PE CPA to SNP</i>	167
5.7.2.	<i>Response of PE CPA to RIL</i>	168
5.7.3.	<i>Response of PE CPA to stress</i>	170
5.7.3.1.	<i>Response of PE CPA to H₂O₂</i>	170
5.7.3.2.	<i>Response of PE CPA to acidic pH</i>	172
5.8.	DISCUSSION	175
5.8.1.	<i>Comparing CPA to SVA</i>	175
5.8.2.	<i>Contractile responses</i>	177
5.8.3.	<i>Vasodilatation in the placenta</i>	178
5.8.4.	<i>Response to RIL</i>	180
5.8.5.	<i>Response to stress stimuli</i>	183
5.8.5.1.	<i>Importance of pO₂</i>	183
5.8.5.2.	<i>H₂O₂</i>	185
5.8.5.3.	<i>pH</i>	186
5.8.6.	<i>CPA from PE samples</i>	190
5.8.7.	<i>Future research</i>	191
5.8.8.	<i>Conclusion</i>	193
6.	EXPRESSION OF ION CHANNELS IN CPA AND SVA	194
6.1.	INTRODUCTION	194
6.2.	OBJECTIVES.....	194
6.3.	MATERIALS AND METHODS	195
6.4.	RESULTS	195
6.4.1.	<i>Patient population</i>	195
6.4.2.	<i>Expression of BK_{Ca}</i>	197
6.4.3.	<i>Expression of K_{ATP}</i>	201
6.4.3.1.	<i>Antibody validation</i>	203
6.4.4.	EXPRESSION OF K2P CHANNELS	207
6.4.4.1.	<i>Expression of TASK-1</i>	207
6.4.4.2.	<i>Expression of TASK-3</i>	210
6.4.4.3.	<i>Expression of TRAAK</i>	213
6.4.4.4.	<i>Expression of TREK-1</i>	216
6.4.4.5.	<i>Expression of TREK-2</i>	219
6.4.4.6.	<i>Expression of TWIK-2</i>	222
6.4.5.	<i>Confocal analysis of CPA and SVA SMC</i>	224
6.4.5.1.	<i>Subcellular localisation of Ca_v1.2</i>	224
6.4.5.2.	<i>Subcellular localisation of TASK 1</i>	226
6.4.5.3.	<i>Subcellular localisation of TASK-3</i>	229
6.4.5.3.1.	<i>TASK-3 co-localisation with related K2P channel members</i>	229
6.4.5.4.	<i>Subcellular localisation of TREK-1</i>	236
6.4.5.5.	<i>Subcellular localisation of TWIK-2</i>	240
6.5.	DISCUSSION	244
6.5.1.	<i>Ca_v1.2 channels</i>	245
6.5.2.	<i>BK_{Ca} channels</i>	246
6.5.3.	<i>K_{ATP} channels</i>	248
6.5.4.	<i>K2P channels</i>	249
6.5.4.1.	<i>TASK 1/3 channels</i>	250
6.5.4.2.	<i>TRAAK channels</i>	253
6.5.4.3.	<i>TREK 1/2 channels</i>	255
6.5.4.4.	<i>TWIK-2 channels</i>	261
6.5.5.	<i>Future research</i>	263
6.5.6.	<i>Conclusion</i>	267
7.	FUNCTIONAL INVESTIGATIONS OF ION CHANNELS IN CPA	268
7.1.	INTRODUCTION	268
7.2.	OBJECTIVES.....	268
7.3.	MATERIALS AND METHODS	268

7.4. RESULTS	269
7.4.1. <i>Effect of ion channel blockers on the U46619 contraction</i>	269
7.4.2. <i>Response of ion channel activators</i>	276
7.4.2.1. <i>NS1619</i>	276
7.4.2.2. <i>Response to RIL in the presence of ion channel blockers at 20% pO₂</i>	278
7.4.3. <i>Response to H₂O₂ in the presence of ion channel blockers at 20% pO₂</i>	281
7.4.4. <i>Response to acidic pH in the presence of ion channel blockers at 20% pO₂</i>	285
7.4.4.1. <i>Response to acidic pH response in the presence of ion channel blockers at 5% pO₂</i> ...	293
7.5. DISCUSSION	297
7.5.1. <i>Alterations to the baseline resting tension</i>	297
7.5.2. <i>Modulation of the U46619 response</i>	298
7.5.3. <i>Modulation of the response to NS1619</i>	304
7.5.4. <i>Modulation of the response to RIL</i>	305
7.5.5. <i>Modulation of the response to H₂O₂</i>	307
7.5.5.1. <i>Modulation of the H₂O₂ mediated contraction</i>	307
7.5.5.2. <i>Modulation of the H₂O₂ mediated relaxation</i>	308
7.5.6. <i>Modulation of the response to acidic pH</i>	310
7.5.7. <i>Future research</i>	316
7.5.8. <i>Conclusion</i>	319
8. DISCUSSION	320
8.1. <i>Comparing placental vessels</i>	322
8.2. <i>Importance of pH in other systems</i>	325
8.3. <i>The biphasic response to acidic pH</i>	327
8.4. <i>Proton sensing ion channels</i>	329
8.5. <i>The placenta as a diagnostic tool</i>	332
8.6. <i>Future research</i>	333
9. CONCLUSION	339
10. BIBLIOGRAPHY	340
APPENDIX	363
I. SOLUTION COMPOSITIONS.....	363
II. WORKING DILUTIONS OF ANTIBODIES	366
III. ANTIBODY AMINO ACID TARGET SITES AND PREDICTED MOLECULAR WEIGHT (MW).	368
IV. SUPPLIERS.....	370
V. PATIENT INFORMATION SHEET & CONSENT FORMS	373
VI. TRANSMISSION ELECTRON MICROSCOPY (TEM) IMAGING OF CPA AND SVA	374

Declaration

I declare that this thesis is the result of my own work based on research that was undertaken at the Academic division of Obstetrics and Gynaecology, Derby Medical School, University of Nottingham during the period of October 2007 to October 2010.

Tayyba Ali

March 2012

Acknowledgements

My most sincere thanks are to my supervisors Dr Raheela Khan and Professor Fiona Broughton Pipkin. Your kind support and guidance along the way helped to steer the research in the right direction. I am grateful to you both for your patience and invaluable support over these years particularly with the preparation of this thesis. Your enthusiastic interest helped to make sense of all the data and I will always be indebted to you for showing confidence in me. I would never have made it this far if it was not for your wise words and encouragement over the years.

I would also like to thank Mrs Averill Warren for all your generous support and training over the years. The data presented here would not have materialised if it was not for your knowledge and insight with the experimental techniques.

A very special thank you to Dr Susan Anderson who helped me with the immunohistochemistry and microscopy analysis. Your input and advice was always greatly appreciated.

I am very grateful for all the administrative support provided by Miss Tanya Fletcher. Thank you for always making an exception for me when ordering those last minute things.

I would also like to express my deepest thanks to Mrs Hilary Glanowski who made it possible to follow up on the patient's notes. I greatly appreciate your input in helping to make sense of all the information available.

I would also like to thank Dr Suraj Patel for who had an influential role in my training in the laboratory. His initial experiments and invaluable experience with the Western blotting technique helped me to avoid the same setbacks that he had to endure.

I am also grateful to Dr Chris Towlson and Dave Cadagan. Your help and guidance on the preparation of this thesis has also been very much appreciated.

I would also like to thank all the patients who agreed to take part in this study along with the labour ward staff at the Royal Derby hospital who were always willing to help with the collection of samples.

I am deeply indebted to the support and encouragement provided to me by my ever-suffering family. I know that my parents will now take comfort in knowing that I may now have finally finished my studies and can no longer call myself a student! Your patience and guidance has always been an important bedrock for me and helped bring me to where I am now.

Finally I would like to thank my fellow research colleagues who were always there to provide help and support with the day to day problems that frequently arose.

This study was funded by the British Heart foundation and the School of Graduate Entry Medicine and Health.

Publications

Abstracts

Ali, T. Broughton Pipkin, F. Khan, R. N. 2008 Expression of BK_{Ca} in arteries isolated from the maternal-fetal interface of the placenta. *British Journal of Surgery* Volume 95 Issue S3.

Ali, T. Broughton Pipkin, F. Khan, R. N. 2008 Expression of two-pore domain potassium channels (K2P) in the placenta. *J Physiol Proc Physiol Soc* 13 C5.

Ali, T. Broughton Pipkin, F. Khan, R. N. 2009 Expression of Two Pore Domain Potassium Channels (K2P) in the Placenta. *Reproductive Sciences* 16(3) Suppl 595.

Ali, T. Warren, A.Y. Broughton Pipkin, F. Khan, R. N. 2009 Activation of Two Pore Domain Potassium Channels (K2P) in Arteries Isolated from the Placenta and Myometrium. *Reproductive Sciences* 16(3) Suppl 594.

Ali, T. Broughton Pipkin, F. Khan, R. N. 2011 Investigating the effect of acidic pH on placental resistance arteries. *British Journal of Obstetrics and Gynaecology* 118(8) p1008.

Abstract

Chorionic plate (CPA) and stem villous (SVA) arteries located at the fetal and maternal interface of the placenta respond to stimuli including hypoxia and acidic pH which can be the result of an intermittent blood supply. Unlike other vascular tissue the placenta lacks nervous control so any response to such stimuli will be autoregulated by ion channels. Members of the two pore domain potassium channel family (K2P) the Tandem of P domains in a weak inward rectifying (TWIK) related potassium channel (TREK-1) and the TWIK Related acid sensitive K⁺ channel (TASK-1/3) have been shown to respond to both intracellular and extracellular pH. The hypothesis that there is differential expression and modulation of these candidate ion channels in normal pregnancy was tested. Placentae (N) were collected with written informed consent from healthy patients undergoing elective Caesarean section at term (≥ 37 weeks). The functional responses of resistance sized arteries ($\leq 500\mu\text{m}$) (n) taken from the SVA and the CPA were characterised using wire myography. Vessels were pre-contracted with U46619 and the effect of extracellular pH was studied using 1M lactic acid to produce falls of 0.2 pH units over a range of pH 7.4-6.4. The effects of a variety of ion channel modulators along with tissue oxygenation (20%, 5% and 2% O₂) were also investigated on the vascular response of CPA and SVA. Western blot analysis was performed on crude CPA and SVA tissue homogenates with separation by 12% SDS-PAGE to quantify expression of TASK-1/3 and TREK-1. The subcellular localisation of each ion channel was also examined with smooth muscle cells (SMC) cultured from the CPA and SVA by confocal immunofluorescence. CPA and SVA were equally positive for TASK 1/3 (N=31) and TREK 1 (N=40) at the protein level. SMC from CPA and SVA showed expression for TASK 1/3 (N=8) with an increased fluorescence stain around the peri nuclear region. TREK-1 (N=12) expression showed a linear organisation that closely overlapped with α actin IF stain. The acidic pH stimulation triggered a biphasic relaxation that was repeated with each subsequent pH insult. A change from pH 7.4-7.2 produced a $29 \pm 3\%$ (n=9) relaxation of CPA which increased to $61 \pm 4\%$ at the lowest pH of 6.4 in 20% pO₂. Similarly, altering the pH of pre-constricted SVA caused a $21 \pm 2\%$ (n=6) fall at pH 7.2 with a maximum relaxation of $69 \pm 2\%$ at pH 6.4 (p<0.01). Lowering pO₂ from 20% to 5% inhibited the relaxation response seen with CPA ($45 \pm 3\%$, n=8) and SVA ($34 \pm 3\%$, n=6) at pH 6.4. CPA were also treated with the TREK-1 blocker L-methionine (1mM) which increased the relaxation to $67 \pm 7\%$ (n=6 p<0.001) at pH 6.4. Similarly the TASK 1/3 blocker ZnCl₂ (1mM) gave a maximum relaxation of $72 \pm 5\%$ (n=8 p<0.01) in 20% pO₂. The TREK-1 opener riluzole demonstrated a potent relaxation with both CPA ($75 \pm 5\%$, n=6) and SVA ($78 \pm 5\%$, n=6) in 20% pO₂. Our data has shown that tissue oxygenation and extracellular pH within the physiological range has an important role in controlling vasodilatation in the placenta. Protons are readily transported across the cell membrane and can activate a range of targets including the K2P channels. The relaxation by riluzole has not been previously reported and implicates a direct role for TREK-1 in controlling placental vessel function. However, when TREK-1 and TASK-3 channels were blocked, the response by CPA to lower pH was exaggerated, and reflects the complex pharmacology of pH on vascular function. This also suggests that K2P channel activity can be compensated for by other pH sensitive channels and work is currently underway to identify the role of other potential ion channels that may be involved in this pathway.

Abbreviations

- 2-βME-2-β mercaptoethanol
- 4-AP-4-aminopyridine
- 5-HT-5-hydroxytryptamine
- AA-Arachidonic acid
- ACE-Angiotensin converting enzyme
- ACh-Acetylcholine
- ADI-ADI Instruments
- Ang-Angiotensin
- ANOVA-Analysis of variance
- AMIL-Amiloride hydrochloride
- AP-Alkaline Phosphatase
- APA-Apamin
- ASICs-Acid sensitive ion channels
- ATP-Adenosine trisphosphate
- AVP-Arginine vasopressin
- BaCl₂-Barium Chloride
- BCA-Bicinchoninic Acid
- BK-Bradykinin
- BK_{Ca}-Calcium activated large conductance potassium channel
- BP-Blood pressure
- BSA-Bovine serum albumin
- BUP-Bupivacaine
- Ca²⁺-Calcium ion
- CAT-Catalase
- Ca_v1.2-Voltage gated L type calcium channel
- CGRP-Calcitonin gene-related peptide
- Choline Cl-Choline Chloride (C₅H₁₄ClNO)
- Cl⁻-Chloride ion
- CO₂-Carbon dioxide
- COS-Chinese hamster ovary cells
- COX-Cyclooxygenase
- CPA-Chorionic plate arteries
- CPV-Chorionic plate veins
- CRH-Corticotrophin releasing hormone
- Cs-Caesarean section
- Cu²⁺-Copper ion
- CuCl₂-Copper chloride
- CURC-Curcumin
- Cyclic AMP-Cyclic adenosine 3'5' monophosphate
- Cyclic GMP-Cyclic guanosine 3'5' monophosphate
- DAB-3,3' Diaminobenzidine
- DMEM-Dulbecco's modified eagle medium
- DMSO-Dimethyl sulfoxide
- DMT-Danish MyoTechnologies

- DNP-2,4-Dinitrophenol
- EC-Endothelial cell
- EC₅₀-50% maximal effective concentration
- EC₈₀-80% maximal effective concentration
- ECM-Extra cellular matrix
- EDHF-Endothelium-dependent hyperpolarising factor
- EDTA-Ethylenediaminetetraacetic acid
- EL-Elastic lamina
- ELLSCS-Elective lower segment Caesarean section
- eNOS-endothelial nitric oxide synthase
- ER-endoplasmic reticulum
- Et-1-Endothelin-1
- EtOH-Ethanol
- FBS-Fetal bovine serum
- FITC-Fluorescein Isohiocynate
- GLB-Glibenclamide
- GPx-Glutathione peroxidase
- H⁺-Hydrogen ion
- HCO₃⁻-Bicarbonate ion
- H&E-Haematoxylin & Eosin
- H₂O₂-Hydrogen peroxide
- HBSS-Hank's Balanced Salt Solution
- HCl-Hydrochloric acid
- HEK-Human embryonic kidney cells 293
- HEPES-(4-(2-hydroxyethyl)-1-piperazineethanesulphonic acid
- HETE-Hydroxyeicosatetraenoic acid
- HFPV-Hypoxic fetoplacental vasoconstriction
- HPV-Hypoxic pulmonary vasoconstriction
- HUVECs-Human umbilical vein endothelial cells
- IBTX-Iberiotoxin
- IF-Immunofluorescence
- IHC-Immunohistochemistry
- IK_{Ca}-Calcium activated intermediate conductance potassium channel
- IQR-Interquartile range
- I/R-Ischaemia/reperfusion
- IUGR-Intrauterine growth restriction
- IVS-Intervillous space
- K⁺-Potassium ion
- K2P-Two pore domain potassium channels
- K_{ATP}-ATP activated potassium channel
- K_{ir}-Inward rectifier potassium channel
- kDa-KiloDalton
- kPa-KiloPascal
- KPSS-High potassium physiological salt solution
- K_V-Voltage activated potassium channel
- LA-Linoleic acid

- LIDO-Lidocaine
- L-METH-L-Methionine
- L-NAME-L-NG-nitro-arginine methyl ester
- L-NNA-L-NG-nitro-Arginine
- M.ANAN-Methanandamide
- MB-Methylene blue
- MEM-Minimum essential media
- MMP-Matrix metalloproteinases
- mN-Millinewton
- mRNA-Messenger ribonucleic acid
- M-WU test-Mann Whitney U test
- MYO-Myometrium
- Na⁺-Sodium ion
- NaCl-Sodium chloride
- NaCN-Sodium cyanide
- NAD-Nicotinamide adenine dinucleotide
- Na_v-Voltage gated sodium channels
- NHE-Sodium/hydrogen exchanger
- NIFED-Nifedipine
- NO-Nitric Oxide
- NORM-Normal
- NOS-Nitric oxide synthase
- ns-not significant
- OCT-Optimal cutting temperature embedding medium
- OMP-Omeprazole
- OUAB-Ouabain
- PBS-Phosphate buffered saline
- pCO₂-Partial pressure of Carbon Dioxide
- PE-Pre-eclampsia
- PFA-Paraformaldehyde
- PG-Prostaglandin
- PGI₂-Prostacyclin
- P_i-Effective pressure
- PKA-Protein kinase A
- PlGF-Placental like growth factor
- pO₂-Partial pressure of Oxygen
- PSS-Physiological salt solution
- QUIN-Quinidine
- RAS-Renin angiotensin system
- RB-Rat brain
- RIL-Riluzole
- RM-ANOVA-Repeat measures ANOVA
- ROI-Region Of interest
- ROS-Reactive oxygen species
- R.RED-Ruthenium red
- RT-Room temperature

- RT-PCR-Reverse transcription polymerase chain reaction
- SA-Spiral arteries
- SD-Standard deviation
- SDS-PAGE- Sodium Dodecyl Sulphate Polyacrylamide Gel Electrophoresis
- SEM-Standard error of the mean
- sFlt-Soluble fetal liver tyrosine like
- SH SY57-rat neuroblastoma cell line
- SK_{Ca}-Calcium activated small conductance potassium channel
- SNP-Sodium Nitroprusside
- SMC-Smooth muscle cell
- SOD-Superoxide dismutase
- SVA-Stem villous arteries
- TASK-TWIK related acid sensitive potassium channel
- TBS-Tris Buffered Saline
- TBS-T-Tris buffered saline + Tween
- TEA-Tetraethylammonium
- TEM-Transmission Electron Microscopy
- TRAAK- TWIK-related arachidonic acid-stimulated potassium channel
- TRAM-34- Triarylmethane-34
- TREK-TWIK related potassium channel
- TRITC-Tetramethyl Rhodamine Iso-Thiocyanate
- TWIK-Tandem of P domains in Weak Inward rectifier potassium channel
- Tx-Thromboxane
- U46619-Thromboxane mimetic (9,11-dideoxy-11 α ,9 α epoxymethanoprostaglandin F(2 α))
- VEGF-Vascular endothelial growth factor
- VGCC-Voltage gated calcium channel
- WB-Western blotting
- Zn²⁺-Zinc ion
- ZnCl₂-Zinc chloride

1. Introduction

The profound changes that occur during pregnancy are aimed at optimising the physiological adaptations required for a successful pregnancy. The normal increase in blood flow throughout gestation is the combined result of altered vascular anatomy along with changes in the perfusion of both the maternal and placental circulations to maintain fetal growth. During pregnancy, the peripheral resistance decreases while the maternal cardiac output increases and the processes that bring about the changes are not fully understood. Crucially, it has been shown that impaired blood flow may be associated with placental and fetal growth dysfunction. Gaining a better insight into the precise nature of the external factors that can influence vascular tone may help towards an improved understanding of the placental vascular function and is the focus of my study.

1.1. Maternal adaptations to pregnancy

Haemodynamic changes within the maternal circulation during pregnancy has revealed a series of coordinated adaptations take place to accommodate the demands of the growing placenta and fetus. **Figure 1.1-1** shows the gradual increase in blood plasma volume which eventually reaches a maximal increase in intravascular volume of 40-45% when compared to the non-pregnant state (Poston, McCarthy et al., 1995, Chamberlain and Broughton Pipkin, 1998). An increase in cardiac output, plasma

volume and erythrocyte mass are also observed which help to promote a fall in the haematocrit (Kaufmann, Mayhew et al., 2004). The heart rate also progressively increases and along with the greater stroke volume to contribute to the increased cardiac output also seen (Conclin, 1994, Poston, McCarthy et al., 1995, Pijnenborg, Vercruysse et al., 2006, Blackburn, 2007).

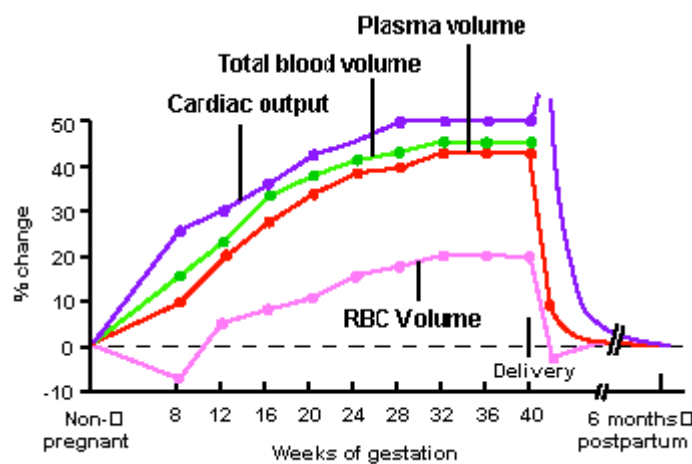


Figure 1.1-1 showing the main changes in haemodynamic and blood volume that occur in the human maternal circulation during pregnancy. The blood volume peaks at around 34 weeks and the levels return close to non-pregnant levels post-delivery (Image obtained from Conclin, 1994).

Although the cardiac output increases, a bigger proportionate fall in peripheral resistance contributes to the overall fall in blood pressure (BP). These changes are also brought about via the widespread release of vasodilators (see [Chapter 1.6](#)) in response to increased flow. The changes to peripheral resistance are most striking in the renal and uterine circulations which act as vital shunts to help cope with the increased blood volumes as 10-20% of the total cardiac output is directed to these vascular regions. The two main hormones oestrogen and progesterone are important for maintaining a successful pregnancy and have been implicated in promoting

changes in blood volume due to their ability to regulate the renin-angiotensin system (RAS). Oestrogen can increase the circulating levels of angiotensin (Ang), while progesterone driven sodium (Na^+) loss detected at the macula densa increases renin synthesis and release. This results in an increase in Ang II concentrations which in turn stimulate aldosterone synthesis and release. This physiological change would increase the salt/water reabsorption within the renal circulation and in support of this view the RAS has been shown to be stimulated during the luteal phase of the menstrual cycle and is maintained for the duration of pregnancy (Broughton Pipkin, Craven et al., 1981, Symonds, 1981, Walsh, 1985). The RAS system is important for facilitating the retention of Na^+ to meet the growth demands of the placenta and fetus as well as maintaining maternal blood volume. The placenta has also been shown to contribute to this process and is a crucial source for progesterone release (Symonds, 1981). These separate changes all help to compensate for the rise in blood volume by bringing about an overall fall in peripheral resistance so as not to place huge demands on the maternal circulation.

1.2. Maternal vascular remodelling

Vascular remodelling is a process that involves structural changes to existing vessels and occurs amongst other states, in pregnancy. Remodelling is evident in a range of vascular beds but is most dramatic in the maternal uterine spiral arteries (SA). The process involves removal of the endothelium, disorganising the smooth muscle cell layer and vasodilatation. The SA with a narrow lumen are converted into

large vessels as the endothelium and internal elastic lamina are eventually replaced by placental trophoblast cells (**Figure 1.2-1**). In the non-pregnant state, the normal function of the SA is to contract during menstrual bleeding to limit the loss of blood. Following pregnancy, this function is altered to convert the SVA into conduit-like low resistance vessels to optimise the flow of blood towards the placental membranes (Robertson, Brosens et al., 1973, Roberts, Taylor et al., 1989, Babawale, Mobberley et al., 2002). Remodelling is the result of combined maternal and placental factors and the alteration in SA physiology seen during pregnancy, helps to bring about dilation and reduced contractile activity of the uterine vessels aiding the reduction in BP seen during pregnancy (Pijnenborg, Anthony et al., 1991, Arribas, Hillier et al., 1997).

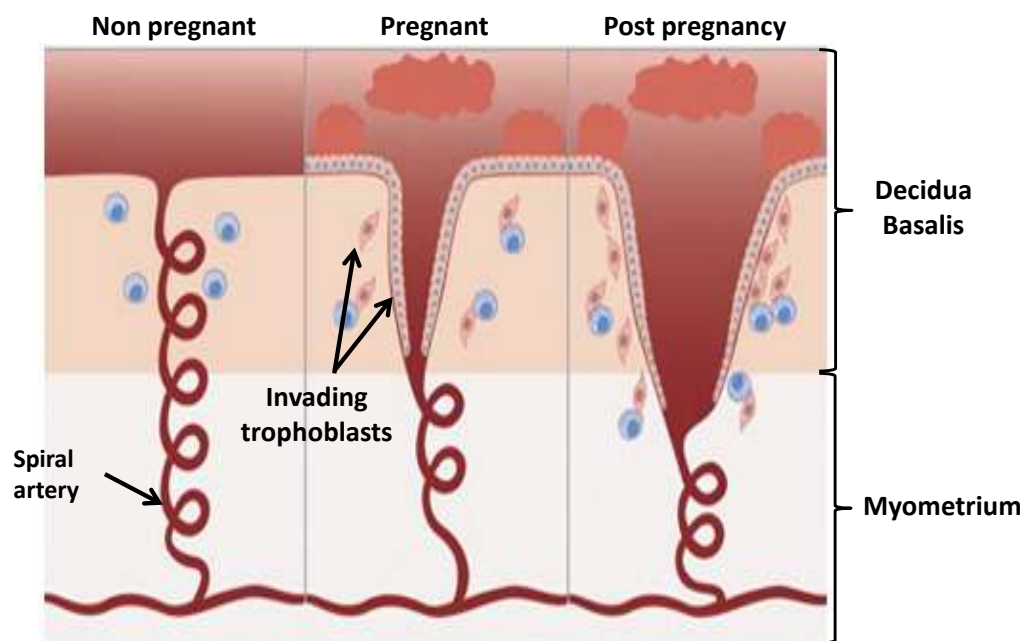


Figure 1.2-1 shows the structural transformation that occurs in the maternal uterine SA in response to pregnancy. The SA are a target for the invading placental trophoblast cells which increase the diameter of the SA by invasion and create a low resistance to blood flow (Image adapted from Maynard, Epstein et al., 2007).

Remodelling is a complex mechanism involving key factors that bring about the eventual disorganisation of the smooth muscle cells (SMC) and endothelium cells (EC) along with degradation of the extracellular matrix (ECM) by proteinases such as matrix metalloproteinases (MMP) (Baker and Kingdom, 2004). A key component identified with this process is the carefully timed increase in circulating growth factors including the vascular endothelial growth factor (VEGF) along with its receptor soluble forms like tyrosine kinase-1 (sFlt-1) (Maynard, Min et al., 2003). Studies have shown that circulating levels of such angiogenic factors increase during the first trimester at the time of SA remodelling and the significance of this lies at the centre of understanding the consequences of an angiogenic imbalance. Functional investigations have also shown that SA during pregnancy have an altered response to circulating contractile agents such as Ang II when compared to non-pregnant tissue and this change is thought to be a direct consequence of successful remodelling (Kaufmann, 1982, Pijnenborg, Anthony et al., 1991, Kublickiene, Kublickas et al., 1997). This adaptation would also ensure increased volumes of blood could be shunted by these transformed vascular beds towards the placental structures which have a high demand for blood to ensure the exchange of crucial substances (Poston, McCarthy et al., 1995, Huppertz, 2007, Huppertz, Abe et al., 2007). The structural changes of the vascular bed evidently occur before implantation and are complete within 6-12 weeks (wks) of gestation. This adaptation is also designed to keep the amount of blood flowing into the uterine arteries constant regardless of changes in maternal blood pressure (Brosens, Robertson et al., 1972, Pijnenborg, Robertson et al., 1981). Interestingly only SA closest to the centre of the placental blastocyst disc

are altered while neighbouring vessels appear to remain unaffected. This may be explained by the controlled targeting of the trophoblast cells (**Chapter 1.3**) that target blood vessels in the area of the myometrium adjacent to the placental bed to possibly ensure maternal blood will enter the placental membranes at a high velocity (Robertson, Brosens et al., 1973, Pijnenborg, Anthony et al., 1991).

1.3. Early placental development

The maternal and fetal circulations are closely associated and early development of the placenta is aimed at establishing a highly vascularised tissue that provides a vital barrier separating the two systems (Kaufmann, 1982, Huppertz, 2007). The two main processes that are involved include vasculogenesis, where new vessels are formed, and angiogenesis, which involves the branching of established vessels. The maternal adaptations to pregnancy are almost complete by the end of the 1st trimester at which point maternal blood will enter the placental intervillous spaces (IVS) via the SA which initially begins at 8-9 wks and increases at 12wks (Brosens, Robertson et al., 1972, Pijnenborg, Anthony et al., 1991, Lyall, 2005, Huppertz, 2007). Post fertilisation, the rapidly dividing ovum forms a blastocyst that becomes implanted into the maternal endometrial stroma (**Figure 1.3-1**). The outer layer of the blastocyst will go on to form the placental precursor cells, the trophoblast cells, which come into direct contact with the endometrium. The trophoblast cells form plugs to prevent the premature entry of highly oxygenated maternal blood, which is postulated to be a risk factor for early pregnancy loss (Jauniaux, Watson et al., 2000, Blackburn,

2007). The invasion of the trophoblast cells has been shown to trigger the remodelling and structural changes of SA to convert the vessels to a low resistance and high flow vascular region.

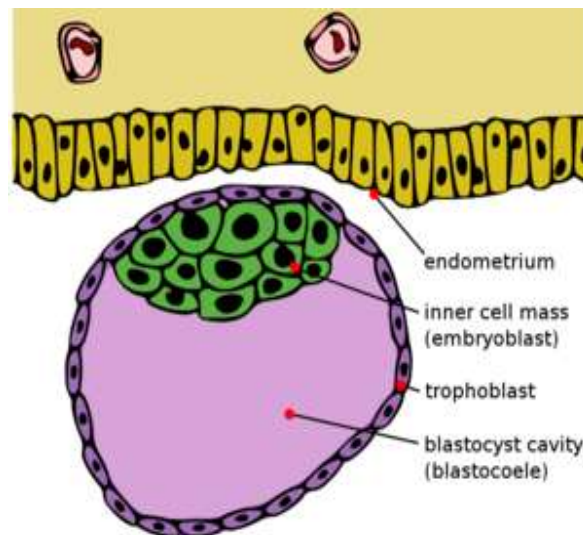


Figure 1.3-1 shows the rapidly dividing ovum rapidly which forms different populations of trophoblast cells. The blastocyst forms the outer cell mass that comes into direct contact with the maternal endometrium. Image obtained from <http://stages-of-pregnancy-development.com/pregnancy-week-2/>

By 7-8 days the blastocyst proliferates and shows polar growth at the point of implantation and two important cell layers can be distinguished at this point;

- The large cytotrophoblasts with single nuclei
- Multi nucleated syncytiotrophoblasts which are formed from fusion of cytotrophoblast cells

The developmental changes from these early cell growths to a fully functioning villous structure have been summarised in **Figure 1.3-2** with a focus on the maternal interface of the placenta.

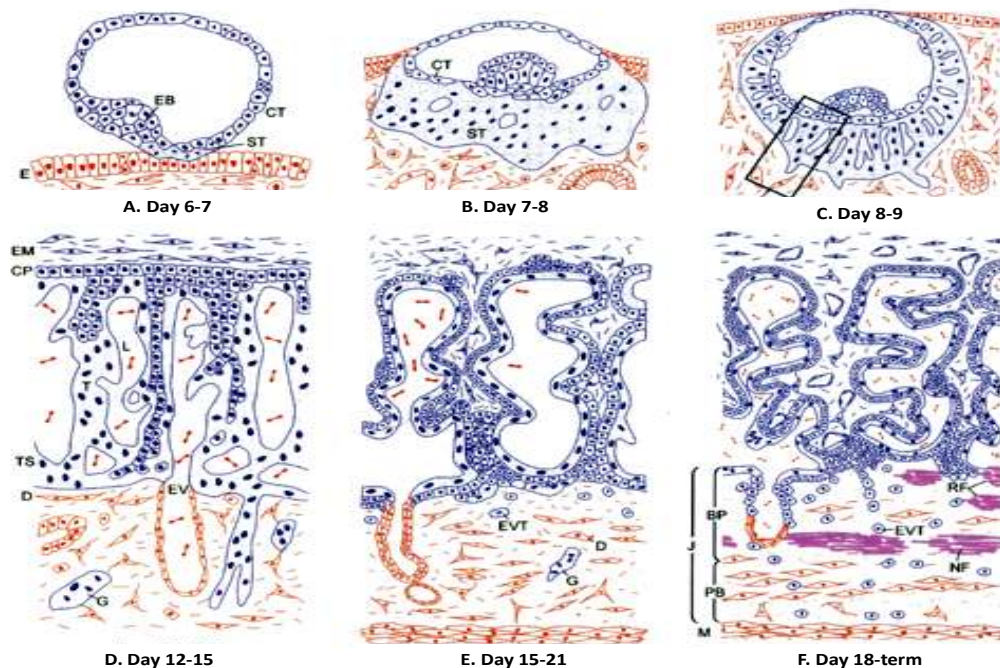


Figure 1.3-2 summarising the development of the human villous tree during gestation. A, B & C show the lacunar stage. D, E&F shows the transition from lacunar to primary, secondary and finally tertiary villi. The trophoblast grows in cell columns to form the basal segments that help to anchor the placenta. Maternal tissue has been shown in red and fetal tissue is blue. *Endometrial endothelium (E), embryo blast (EB), cytotrophoblast (CT), syncytiotrophoblast (ST), extra-embryonic mesoderm (EM), chorionic plate (CP), trabeculae (T), maternal blood lacunae (L), trophoblast shell (TS), endometrial vessel (EV), decidua (D), Rohr's fibrinoid (RF), Nitabuch's fibrinoid (NF), trophoblast giant cell (G), extravillous cytotrophoblast (EVT), basal plate (BP), placental bed (PB), junctional zone (J), myometrium (M).* (Image obtained from Benirschke, Kaufmann et al., 2006).

Placental villous development is supported by a range of angiogenic growth factors found in both the placental and maternal circulations which are carefully balanced at key stages. VEGF and placental like growth factor (PLGF) can be detected in maternal plasma at around 6wks and remain high until term (Maynard, Min et al., 2003, Demir, Kayisli et al., 2004). The growth factors, along with the relatively hypoxic environment are needed for angiogenesis to drive an increase in trophoblast cell populations to form highly vascularised villi. The growing trophoblast cells take

on the phenotype of villous trees and stems that will eventually form a complex network of blood vessels that begin to transport blood (Kaufmann, Sen et al., 1979, Pijnenborg, Robertson et al., 1981, Roberts, Taylor et al., 1989, Huppertz, Abe et al., 2007). These early outgrowths undergo extensive angiogenesis, which involves the branching of existing vessels, to eventually form well defined arteries, veins and arterioles (Huppertz, Abe et al., 2007) which carry oxygenated and deoxygenated blood and exchange nutrients with the maternal blood which flows in close proximity (Robertson, Brosens et al., 1973, Pijnenborg, Robertson et al., 1981, Roberts, Taylor et al., 1989, Fox, 1997, Lyall, 2006).

The placenta is described as a low resistance system (Myatt, 1992) where blood pressure varies significantly and ensures a stable volume of blood is continually transported to the fetus (McCarthy, Woolfson et al., 1994). Pressure differences exist along the vascular connections and drive blood from the basal plate towards the chorionic plate and down the umbilical cord (Brosens, Robertson et al., 1972, Pijnenborg, Robertson et al., 1981, Roberts, Taylor et al., 1989, Goldenberg, Iams et al., 1996). The early villous trees develop to form fully functioning vessels that lack autonomic control and help to keep the fetus constantly perfused. At 20wks no new vessels are formed and instead the villi form multiple branches of mature villi which are continually replaced with intermediate villi for the remainder of the gestation period (**Figure 1.3-3**) (Fox, 1997, Kaufmann, Mayhew et al., 2004).

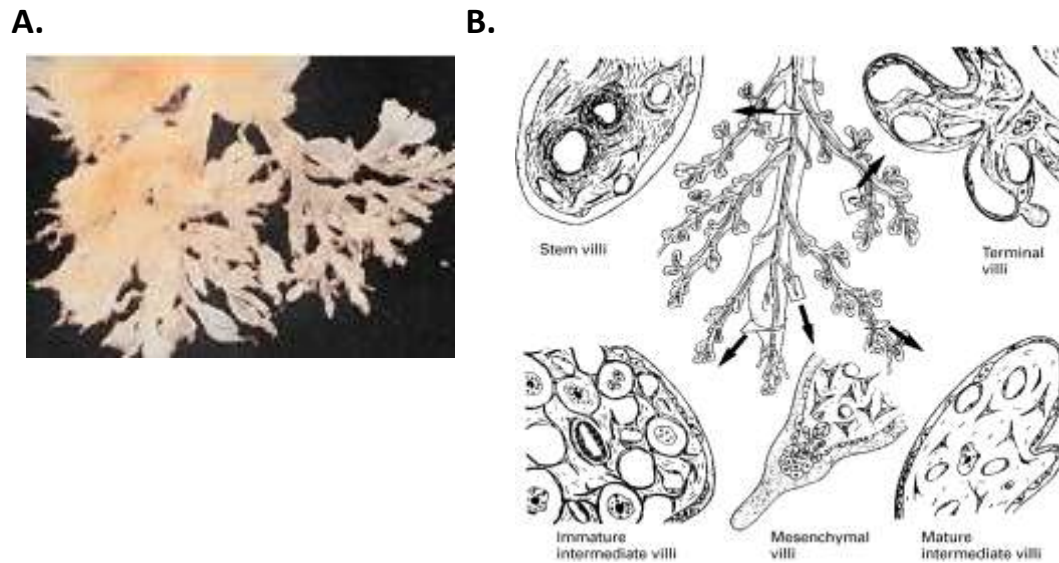


Figure 1.3-3 showing the villous core in more detail. **A** shows an actual image of a villous tree like structure that has been freshly isolated from the placenta. **B** shows the multiple branching villi that comprise a single villous tree. The branches can be classified according to their size and structure. The large central villous core (stem villi) branches laterally to form the intermediate villi from which the terminal villi are protruding from (Image obtained from Benirschke, Kaufmann et al., 2006).

1.4. The term placenta

The human placenta is a key component for successful mammalian reproduction and phylogenetic evidence has revealed that a carefully programmed development of different tissue layers has to occur for the tissue to perform its intended function during gestation (Wildman, Chen et al., 2006). During the first 12wks the trophoblast cell mass increases to increase the surface area of the villous from 0.3m^2 to 12.5m^2 at term (Jauniaux, Watson et al., 2000, Hampl, Bibova et al., 2002, Yung, Calabrese et al., 2008). The human placenta is classified as a

hemochorial, discoid placenta (Wildman, Chen et al., 2006) and weighs $480 \pm 135\text{g}$ at term, with a diameter of 18cm and 2.5cm in thickness (Benirschke, Kaufmann et al., 2006). The placenta is a highly active tissue, with its own oxygen and glucose demands, and these are met as a result of the carefully matched flow with the maternal circulation flow. As the placenta ages, signs of calcification, increased fibrin deposits, infarcts and syncytial knots at the branching villi are observed. This is due to the preparation of placental separation whereby the placenta is expelled from the uterus and involves shearing of the placental membranes and occurs during the third and final stage of delivery (Blackburn, 2007). The placenta is adapted to perform a wide range of physiological functions that would be fulfilled by the kidneys, lungs, endocrine glands as well as the gastrointestinal tracts of the fetus. A clear boundary can be identified within the placenta with multiple lobes on the maternal portion of the placenta that contain the vital villous structures. In contrast the fetal portion contains the large chorionic vessels which carry blood to the fetus via the umbilical cord (**Figure 1.4-1**).

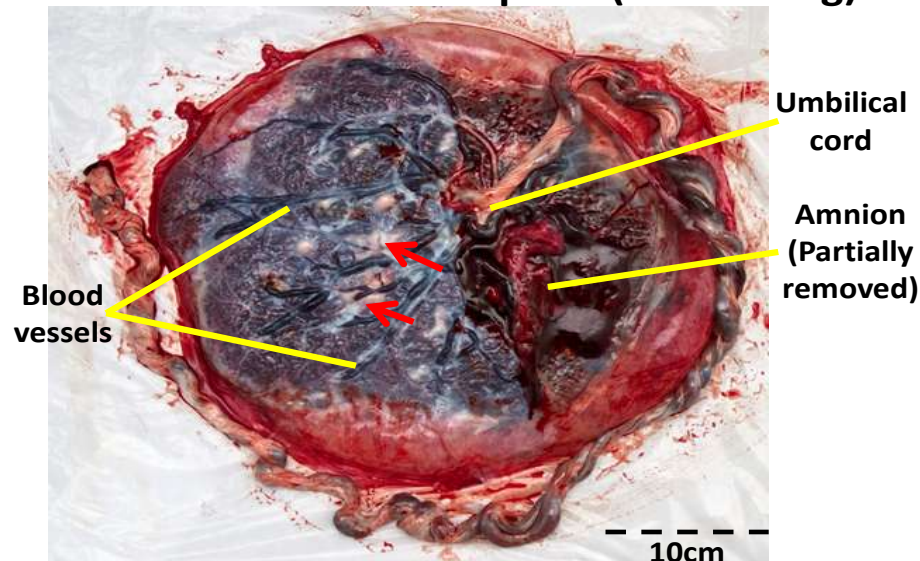
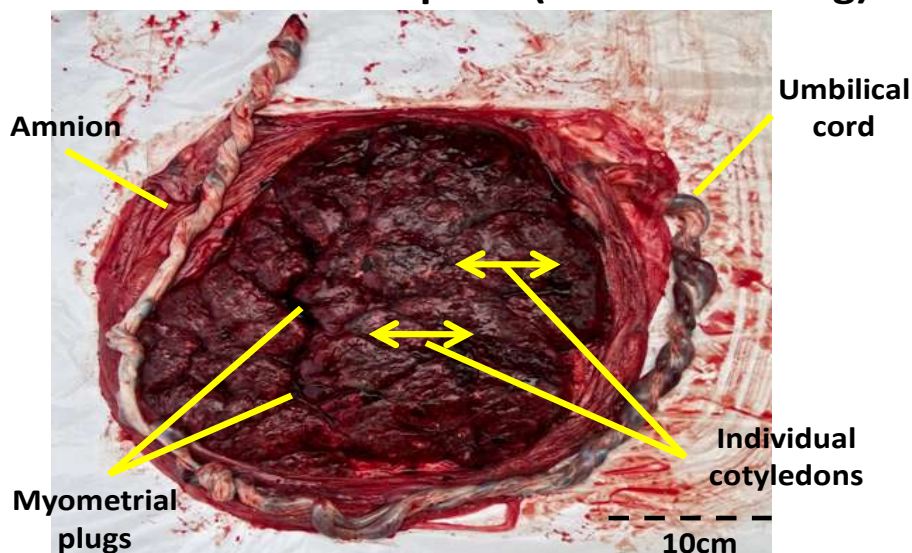
A. View of the chorionic plate (fetal facing)**B. View of the basal plate (maternal facing).**

Figure 1.4-1 shows a freshly isolated human term placenta. A shows the chorionic plate. The amnion layer has been partially peeled back to reveal the vast network of arteries and veins which converge towards the umbilical cord. This sample is a full term placenta (37wks) and areas of calcification (red arrow) can be seen which is common for a fully developed placenta. **B** shows the same placenta viewed from the basal plate. Individual cotyledons can be seen which encase bundles of stem villous arteries and the myometrial plugs mark the point where the placenta was implanted within the uterus. An intact umbilical cord along with the amniotic sac which once encased the fetus during pregnancy is also observed.

1.5. Transport across the placenta

As the placenta lacks any form of autonomic control, vessel diameter is believed to be controlled by locally released signalling molecules that alter the action of cells (see **Chapter 1.6.1**) that make up a blood vessel (Kaufmann, 1982, Fitzgerald, Mayo et al., 1987, Benirschke, 1998). The placenta is well adapted for this function as villous trees are designed to increase the surface area for diffusion of key substances and the multiple branching brings the fetal vessels in close proximity to the oxygen rich maternal blood. Maternal blood enters the IVS at high pressure and is the main junction for exchange of key molecules such as hormones, growth factors, and antibodies, while toxins such as urea are excreted in the opposite direction (**Figure 1.5-1**) (Ramsey, 1962, Pijnenborg, Robertson et al., 1981, Huppertz, 2007).

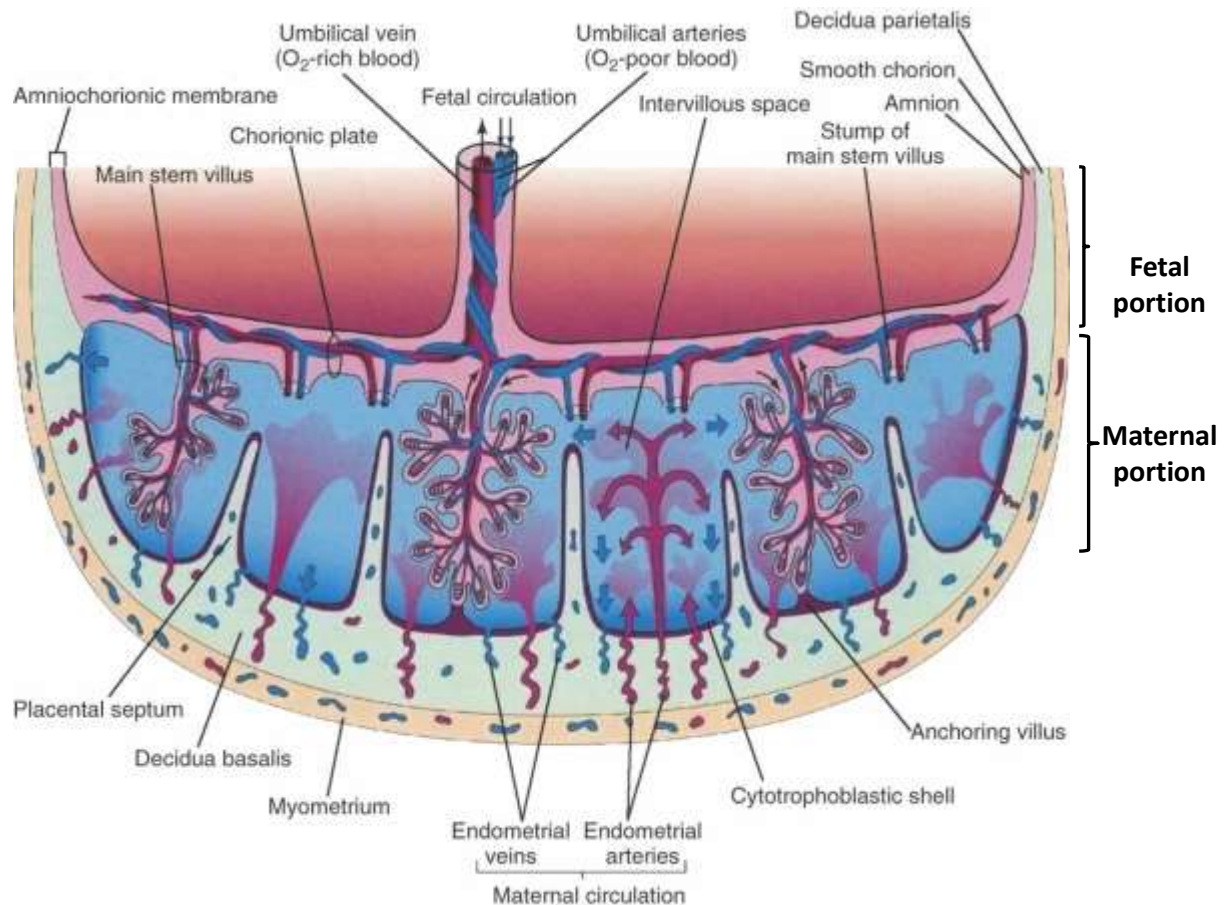
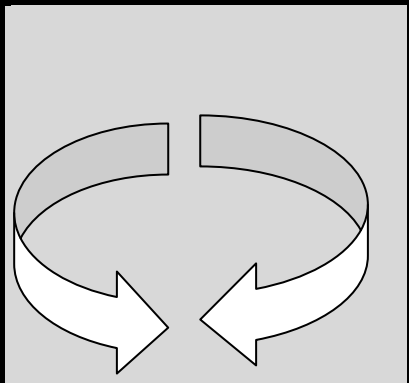


Figure 1.5-1 showing the cross sectional structure of the human term placenta. The placenta can be separated into the fetal and maternal portions which represent the different vascular sections of the placenta. The direction of the maternal blood as it enters the IVS is also shown. (Image adapted from Saunders, 2009).

The placenta functions as a complete transport system where the oxygen rich blood is transported by the placental veins and deoxygenated blood along with waste by-products from the fetus are transported towards the maternal circulation, with a much higher oxygen content, via the arteries. The molecules that are transported from the rich maternal SA blood to the fetus have been summarised in **Table 1.5-1**. The main transport molecules include oxygen (O₂), water (H₂O), electrolytes, carbohydrates, lipids, peptides, vitamins, hormones, pathogens including viruses and

any circulating drugs. In the opposite direction, carbon dioxide (CO₂), H₂O, urea and other metabolic waste products as well as hormones synthesised by the fetal and placental circulations are transported from the placenta to the uterine veins.

Table 1.5-1 summarising the exchange of substances across the three main transport systems that are established during pregnancy (Adapted from Blackburn, 2007).

Maternal circulation	Placental circulation	Fetal circulation
Amino acids Antibodies Cholesterol Drugs Fatty acids/lipids Glucose Hormones O ₂ Viruses Vitamins (fat & water soluble) Water		Bilirubin CO ₂ Urea Uric acid Water

The main exchange processes involve passive and energy requiring active transport mechanisms to successfully exchange key substances and can be summarised by the equation below;

$$\text{Diffusion} = \frac{\text{substance characteristics} \times \text{surface area} \times \text{concentration gradient}}{\text{distance}}$$

Exchange of substances occurs at the placental barrier which is made up of 5 key cell populations (**Figure 1.5-2**). The placental and maternal circulations come into close proximity and form the main point of exchange with the maternal circulations but are prevented from mixing by a thin layer of syncytiotrophoblast

cells and the basement membrane (Kaufmann, Mayhew et al., 2004, Polin, Fox et al., 2004). The placental exchange surface is enlarged from 5 m² at 28wks to 12.5 m² shortly before delivery (Nicolaidis, Economides et al., 1989, Blechner, 1993, Benirschke, 1998, Blackburn, 2007). Exchange of substances is mediated by flow while glucose is transported using active transport through specialised transporters found in the basement plasma membrane. Any potential disruptions in the flow of blood in the placenta can have adverse consequences for the circulatory system and limit the O₂ supply to the fetus (Schneider, Danko et al., 1984, Blechner, 1993, Polin, Fox et al., 2004).

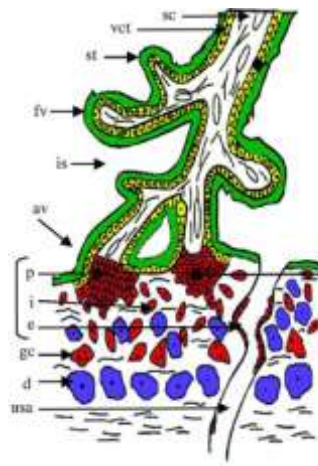


Figure 1.5-2 showing the placental barrier which prevents the direct mixing of the two circulations. Any substance transferred from the maternal circulation will cross each cell layer before reaching the placental blood vessel. *Sc*, Stromal core; *vct*, villous cytotrophoblast; *st*, syncytiotrophoblast; *fv*, floating villi; *is*, intervillous space; *av*, anchoring villi; *p*, proliferative extravillous cytotrophoblast (EVCT); *i*, invasive EVCT; *e*, endovascular EVCT; *gc*, giant cells; *d*, decidua; *usa*, uterine spiral artery. (Image adapted from Handschuh et al., 2007).

1.6. Control of vascular tone in the placenta

The placenta is devoid of neuronal connections (Prystowsky, 1961, McCarthy, Woolfson et al., 1994) and yet maintains the ability to regulate its own blood flow which remains the focus of many research studies. A range of mechanical and molecular factors influence the control of vessel tone for a blood vessel. In the placenta, a careful balance of vasoconstrictors and vasodilators work to control the overall perfusion pressure of the tissues (Myatt, 1992, Poston, McCarthy et al., 1995, Sweeney, Jones et al., 2006). Isolated blood vessels have demonstrated the ability to alter their diameter to respond to acute changes in the volume of blood flow (**Figure 1.6-1**). This is possible as blood vessels have “mechanosensors” which detect physical changes (*shear stress*) or increasing transmural pressure (*wall stress*) placed on the vessel wall (Bayliss, 1902, Bevan and Osher, 1972, Mulvany and Aalkjaer, 1990). *Vascular tone* is described as the event which brings about a random contraction which narrows the lumen diameter. The increase in physical stress on EC, either due to an increase in blood flow or circulating autocooids, will trigger a calcium (Ca^{2+}) influx into the EC, to alter vessel tone (shown in **Figure 1.6-2**) (Halpern, Mulvany et al., 1978, Jovanovic, Grbovic et al., 1994c, Sweeney, Jones et al., 2006).

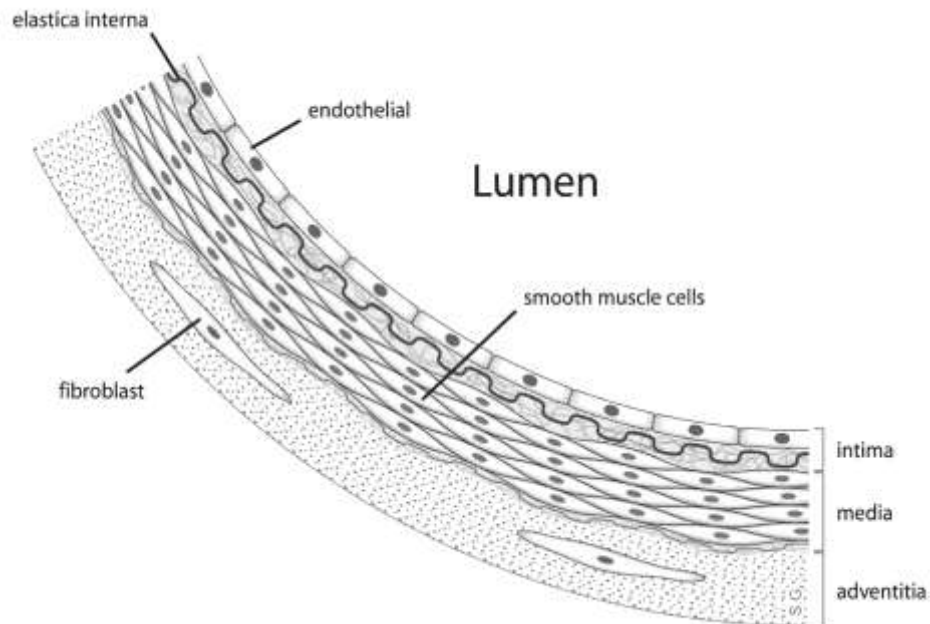


Figure 1.6-1 showing the structure of a generalised artery. The one cell thick EC layer is typically surrounded by several layers of SMC separated only by the elastic interna. The whole vessel is held together by the adventia which contains a mixture of connective tissue proteins including collagen, elastin, and glycoproteins (Image obtained from Baker and Kingdom, 2004).

The EC is a single cell thick layer which lines the lumen of blood vessels and is responsible for increasing the vessel diameter and reducing the resistance to the flow of blood (Robertson, Schubert et al., 1993, Smit and Iyengar, 1998, Parkington, Tonta et al., 1999). The EC is receptive to changes in humoral and haemodynamic changes to release a range of factors that can influence the function of cells within the blood vessel (**Figure 1.6-2**). Contraction of a cell is the result of second messenger signalling cascades which respond to the entry of Ca^{2+} . Nitric oxide (NO) released from the EC can diffuse to the SMC to oppose contractions via activation of adenylate cyclase to increase cyclic guanosine 3'5' monophosphate (cGMP). Similarly the

prostaglandin (PG), prostacyclin (PGI₂) can increase the production of cyclic adenosine 3'5 monophosphate (cAMP) (King, Gude et al., 1995, Boura, Leitch et al., 1998, Smit and Iyengar, 1998).

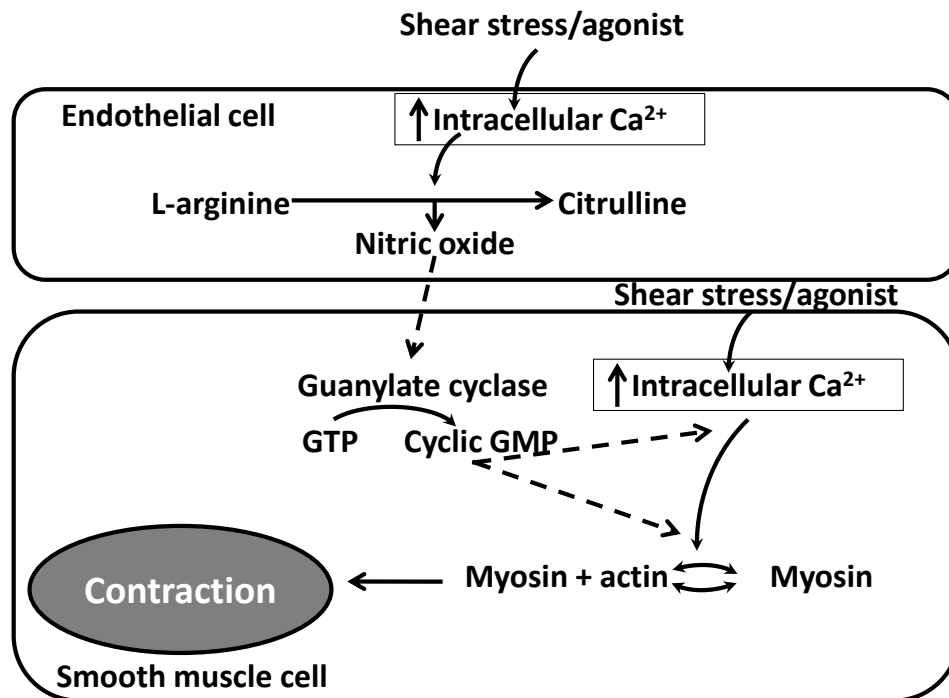


Figure 1.6-2 showing the cell signalling events that determine the overall contraction and relaxation of blood vessel SMC. NO can promote relaxation of SMC via the release of diffusible molecules that originate from the endothelial cell. In this instance cGMP reduces the intracellular Ca²⁺ to uncouple the myosin-actin complex. Image adapted from (Baker and Kingdom, 2004).

The placenta has shown to possess some important differences in the vascular anatomy and is comprised of three main vessel types (**Figure 1.6-3**);

1. Umbilical vessels –which consist of a single large vein and two arteries which separate to supply each half of the placenta,
2. Chorionic plate arteries (CPA) and veins (CPV)–radially branched at the surface and run in parallel to the stem villous arteries (SVA),

3. Multiple dividing villi- which are bathed in maternal blood and anchor the placenta into the basal plate.

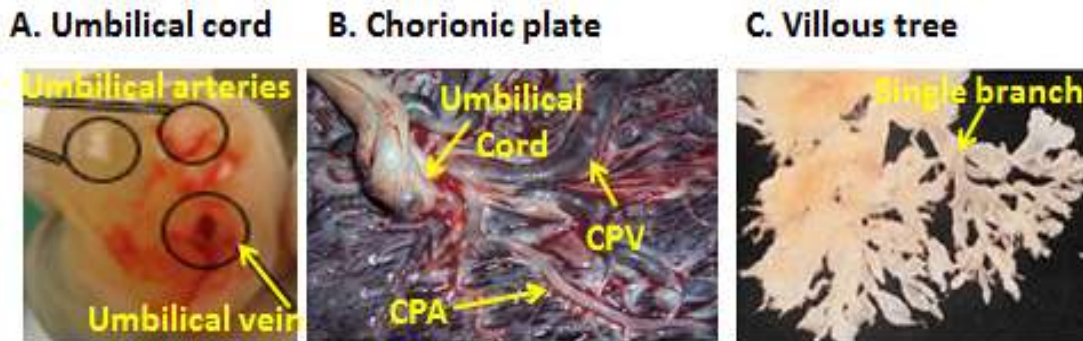
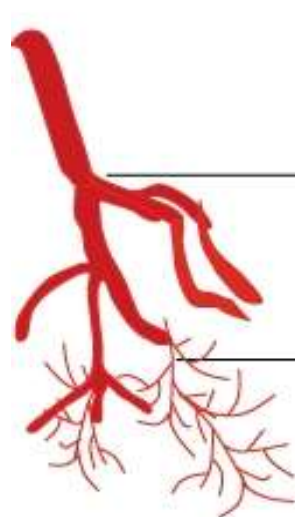


Figure 1.6-3 showing the main class of vessels found within the placenta. **A** shows the cross sectional structure of the umbilical cord which contains two arteries that spiral around a central vein. The umbilical cord forms the vital link between the fetus and the placenta. **B** shows the point of cord insertion in the chorionic plate where the CPA and CPV branch out across the surface of the basal plate and are clearly visible. **C** shows a villous tree that has been cleaned away from its surrounding tissue. The multiple branches increase the surface area for exchange with the maternal circulation.

Deoxygenated blood from the fetus is transported in the two umbilical arteries which connect to the chorionic plate and spread out radially. The chorionic vessels branch extensively into the multiple small villous trees. The veins carry oxygenated blood back towards the fetus and the rate of flow is estimated to be 500 ml/min and is dependent upon the fetal heart rate. The branches of terminal villi represent the site of exchange for O_2 and nutrients. There is an important arterial gradient that exists across the different vascular regions which help to maintain a low pressure system that offers little resistance. The most important placental vascular response is at the maternal facing villous arteries and veins which need to cope with the different blood pressure and O_2 tensions of maternal blood (Myatt, 1992, Poston, McCarthy et al., 1995, Pijnenborg, Vercruyssen et al., 2006, Sweeney, Jones et al., 2006).

The presence of SMC within the villous tree implicates these vessels in setting the peripheral resistance across the placenta (Kaufmann, 1982, Tanaka, Kuwabara et al., 1999). The placental circulation is dependent upon adequate matching of the placental and uterine blood flow and it has been shown that key adaptations are made to achieve this. The ever importance of this process has been demonstrated with diseased states (see [Chapter 1.7](#)).

The placenta lacks any form of autonomic regulation and instead the vascular function is under the direct influence of locally released hormonal factors and mechanisms (Kingdom and Kaufmann, 1999, Kaufmann, Mayhew et al., 2004). This has stimulated a focus into the role of agonists that control vascular tone in the maternal circulation during pregnancy. Due to the low resistance within the placenta, a range of vasoconstrictors (**Figure 1.6-4**) at a sub maximal dose have been applied to stimulate the vessels (Chaudhuri and Furuya, 1991, Myatt, 1992, McCarthy, Woolfson et al., 1994, Granger, Alexander et al., 2002, Wang and Zhao, 2010). Isolated vessels have shown to be responsive to a range of agonists including to serotonin, PGI₂, NO and endothelin-1(Et-1) and will be detailed in the following sections.



	Vasoconstrictors	Vasodilators
Umbilical vessels	Ang II ET-1(ETRA) TXA ₂ BK 5-HT AVP	PGI ₂ NO AM (ET-1/ETR ₂)
Chorionic plate vessels	Ang II ET-1 TXA ₂ 5-HT	NO PGI ₂ AM
Villous tree	Ang II ET-1 TXA ₂ BK 5-HT LTs ROS	NO ANP PGI ₂ AM

Figure 1.6-4 showing the variation in sensitivity to agonists across the placental vessels. Each agonist is listed in order of potency. (Image obtained from Myatt, 1992).

1.6.1. Vasoconstrictors

The placenta is an example of a low resistance circulation (Myatt, 1992) and unsurprisingly, a very limited number of contractile agents can stimulate the placental vessels to produce a potent vasoconstriction response. There is also evidence of regional variations in the response produced which may reflect the varying distribution of receptors that are found to be expressed across the vascular tissue of the placenta.

Ang II: Ang II can bind to its two main receptors AT1 and AT2 and its ability to constrict vessels is determined by which receptor is expressed in the tissue effected. The placenta expresses the high affinity Ang II receptors and the Ang converting

enzyme (ACE) is found in abundance within the placental plasma (Myatt, Brewer et al., 1992, Myatt and Webster, 2009, Wang and Zhao, 2010).

Et-1: Et-1 is a powerful vasoconstrictor released from the EC to initiate long lasting contractions of SMC. It is found across the placenta and is most abundant within the amniotic fluid and umbilical vessels (Chaudhuri and Furuya, 1991, McCarthy, Woolfson et al., 1994, Khalil and Granger, 2002).

5-hydroxytryptamine (5-HT): 5-HT is an amine which is also a potent vasoconstrictor of umbilical arteries and is taken up and stored by circulating platelets (Maigaard, Forman et al., 1986, Allen, Skajaa et al., 1991).

Thromboxane (Tx): the main source of Tx is within platelets where it is synthesised and released to promote aggregation of platelets at the site of injury. Tx itself is synthesised via the arachidonic acid (AA) eicosanoid pathway (**Figure 1.6.1-1**). In the placenta, Tx is produced by the umbilical vein which is a major source of the agonist and suggests Tx may have a role at the time of placental separation (FitzGerald, Fitzgerald et al., 1987). The placental decidua, trophoblast and amniotic tissue are also important sources of Tx within the placenta. While lower concentrations of Tx are found within the stem villi and trophoblast cells (Maigaard, Forman et al., 1986, Fitzgerald, Mayo et al., 1987, McCarthy, Taylor et al., 1994).

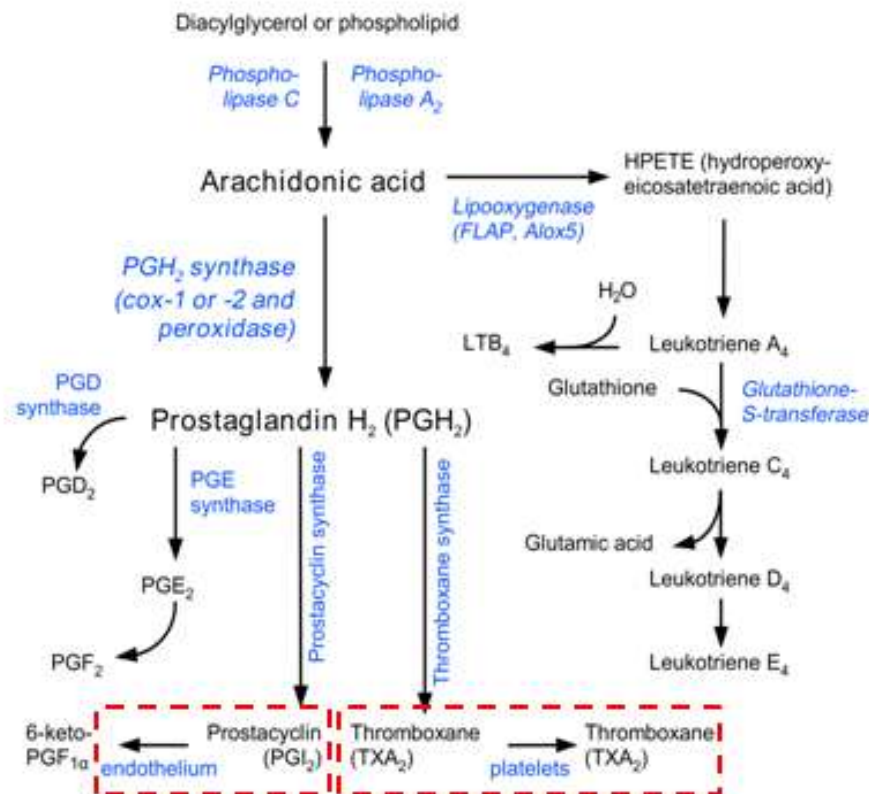


Figure 1.6.1-1 summarising the AA pathway to result in the biosynthesis of both TxA₂ and PGI₂ (red box). The opposing contractile or relaxation response is the result of TxA₂ binding its TP receptor or PGI₂ binding its IP receptor within the same cell. Image adapted from (Myatt and Webster, 2009).

1.6.2. Vasodilators

The physical stress placed upon a vessel will be immediately met with a physiological response and the EC is ideally placed to detect acute changes in flow and pressure. The EC can influence vascular resistance via the release of important factors that can influence the neighbouring cells within the blood vessel. A range of vasodilators which have been reported to have an effect on placental vessels include the calcitonin gene related peptide (CGRP) which relaxed CPA *in vitro* (Firth and Broughton Pipkin, 1989, Dong, Vegiraju et al., 2004, Dong, Green et al., 2005) while

substance P has shown to dilate villous vessels (Benirschke and Kaufmann, 1995, Dong, Green et al., 2005). However the predominant vasodilators that have generated most interest when understanding the physiology of placental vascular resistance will be highlighted in this section.

PG: PGI₂ and PGE₂ are potent relaxing agents of placental vessels and are synthesised by the AA pathway that also gives rise to circulating Tx. High levels of circulating AA help maintain levels of PGI₂ which influences SMC via activation of cAMP (Allen, Skajaa et al., 1991). PGI₂ has a powerful influence on the function of chorionic plate and stem villous and it has also been shown that an imbalance of PGI₂ and Tx may lead to increased resistance in the placenta (Walsh, 1985).

NO: O₂ and the NO precursor L-arginine are important stimulants for the release of NO. High levels of NO can inhibit corticotrophin releasing hormone (CRH), which is found in syncytiotrophoblasts and to forms a negative feedback loop. CRH is activated at the time of parturition and placental separation and may be crucial in determining the length of gestation (King, Gude et al., 1995). Reductions in tissue oxygenation can inhibit the NO converting enzyme NO synthase (NOS) and has been linked with an increase in vascular resistance when tissue perfusion is reduced.

Endothelium derived hyperpolarising factor (EDHF): Inhibition of both endothelium derived NO and PGI₂ lead to the identification of an additional and highly significant vasodilator, EDHF (Boura, Leitch et al., 1998, Yamanaka, Ishikawa et al., 1998). EDHF is most important in small vessels where NO and PGI₂ release is reduced. Relaxation is produced by hyperpolarisation of the cell membrane and

EDHF has shown to be important when NO and PGI₂ release is reduced (Boura, Leitch et al., 1998, Coleman, Tare et al., 2004).

1.6.3. Biophysical factors

Little is known about the influence of biophysical factors such as pO₂ which alters at key stages of placental development, on vascular tone in the placenta. Any increase in vascular resistance will reduce flow mediated responses such as the effective transfer of nutrients across the placental membranes. The placenta needs to maintain a constant supply of oxygenated blood and any fluctuations in the blood pH, glucose, and gases (including O₂ and CO₂) will alter the functioning of the umbilical vessels which could be potentially disastrous for the fetus (Nicolaidis, Economides et al., 1989, Kingdom, Macara et al., 1994).

1.6.3.1. Tissue oxygenation

The placenta works at a multi organ level providing gas exchange, excreting waste products and controlling endocrine function all at the same time. The nutrient supply is a major factor for determining the full growth potential of the fetus. Stress or insults that occur during the early stages of development can severely disrupt the ability of the placenta in performing this function. The pO₂ within the placenta has shown to alter at key stages of development. Maternal blood entering the IVS spaces

at 12wks of gestation causes a significant shift in the pO_2 for the from 20mmHg to 60mmHg (Nicolaidis, Economides et al., 1989). The placenta still maintains a low partial pressure of O_2 (pO_2) when compared to adult tissue, to minimise oxidative stress which results from an imbalance of the cells production of reactive oxygen species (ROS) and the cell's antioxidant capacity.

The relatively low pO_2 environment in the early stages of development has the advantage that it keeps oxidative stress to a minimum and promotes cell proliferation. Entry of maternal blood at high pO_2 has the potential to overwhelm the antioxidant capacity of the placenta (Burton, 2008). The second major challenge for the placenta is the change in pO_2 during delivery of the placenta and even this short exposure to oxidative stress has shown to introduce important cellular differences within the placental tissue (Cindrova-Davies, Yung et al., 2007). It was shown that the extent of oxidative damage was dependent on the duration of labour with potentially adverse effects on the normal functioning of placental vessels.

Changes in O_2 supply will affect the mitochondria, endoplasmic reticulum (ER) and cell membrane potential of excitable cells. Reduced pO_2 can lead to hypoxia and the placenta has demonstrated the ability to alter vessel tone in response to hypoxic insults. The study by Hampl (et al., 2002) showed that the placental vessels could constrict in response to hypoxia to redirect blood flow, termed hypoxic fetoplacental vasoconstriction (HFPV), and has important parallels with the response seen in the pulmonary circulation. pO_2 can also regulate cell growth as low pO_2 promotes cell proliferation while high pO_2 is needed to allow cell differentiation. During the initial stages of pregnancy the placenta is poorly perfused as the vascular

connections are not complete. As a result low pO_2 helps to drive the rapid increase in cytotrophoblast population (Kingdom and Kaufmann, 1999, Huppertz, Kingdom et al., 2003). As the trophoblast cells reach the proximity of the IVS the pO_2 increases, to trigger a switch from proliferation to differentiation of the invading trophoblast cells. This suggests hypoxia may have a role in regulating the long term adaptations made in the flow of blood in the placenta possibly via the generation of ROS (Jakoubek, Bibova et al., 2006). The main ROS identified in the placenta include superoxide anions, hydroxyl radicals, hydrogen peroxide (H_2O_2), and the toxic peroxynitrite ($ONOO^-$). ROS can alter vessel function, cellular processes, and cell cycle regulation. They also have the capacity to cause lipid peroxidation and long term protein damage and crucially can alter vascular tone due to the effects on EC as illustrated in **Figure 1.6.3.1-1**.

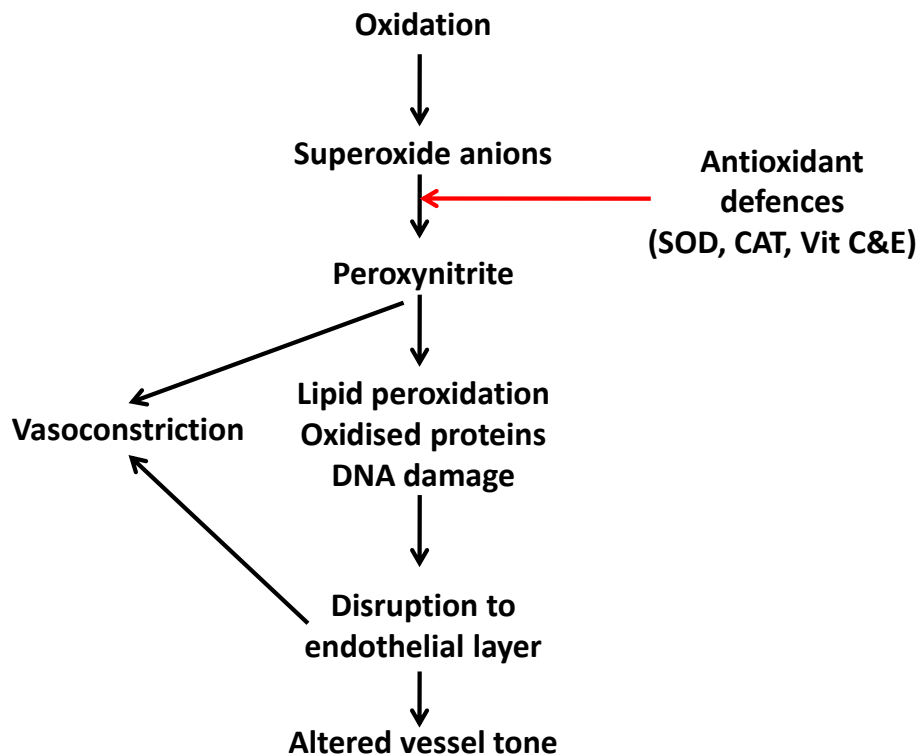


Figure 1.6.3.1-1 shows how reduced perfusion can lead to oxidative stress. ROS can target the EC to alter the control of vessel tone and may have a role in control of placental vascular function. (Image adapted from Baker and Kingdom, 2004).

ROS increase during pregnancy and can target ion channels and alter the physiology of vascular smooth muscle (Brainard, Korovkina et al., 2007, Garovic and Hayman, 2007, Maynard, Epstein et al., 2007). Current understanding suggests that the placenta may potentially divert blood flow away from O₂ deficient areas towards highly perfused areas to increase the pO₂ (Hampl, Bibova et al., 2002). Oxidative stress increases during pregnancy and lipid peroxidation can further complicate the condition. This carries a risk for both the mother and the fetus and fetal haemoglobin is much more vulnerable to the effects of ROS. Normally the level of ROS produced is carefully balanced but this balance changes during pregnancy and lipid peroxides

increase while ROS scavengers fall (Huppertz, 2007). This allows ROS and free radicals to increase which can be lethal to cells as they cause extensive damage to surrounding tissues as well as disrupting the control of Ca^{2+} movements.

1.6.3.2. Acid base homeostasis

Tissue acidosis can be detrimental for normal tissue function and low pO_2 can lead to the production of metabolic acids which have shown the ability to alter ion channel activity (Holzer, 2009). Hydrogen ions (H^+) are highly permeable and can freely cross the cell membrane to bind to ion channels such as potassium channels (Chapter 1.7.2). There is growing evidence to show changes in intracellular pH $[\text{pH}]_i$ can influence the cellular function in a number of vascular beds. Alterations in pH can be the result of changes in ventilation or metabolic dysfunctions all of which alter the balance of acid-base ratio which can be rapidly restored through the action of many metabolic buffers (Aalkjaer, 1990, Holzer, 2009). The placenta also needs to remove excess hydrogen ions (H^+) that build up from the high metabolic turnover of the growing fetus and presents a unique challenge for the placenta in maintaining its acid base balance. Haemoglobin and bicarbonate ions (HCO_3^-) are the most important cellular buffers that work to maintain the resting pH and the Henderson-Hasselbalch equation shown below summarises the role of HCO_3^- in removing H^+ with the equation below (Canzanelli, Greenblatt et al., 1939, Blechner, 1993).



In low O_2 environments, the energy currency molecule adenosine 5' triphosphate (ATP) can still be produced via anaerobic glycolysis as carbohydrates can be broken down to produce pyruvic acid and H^+ ions. The excess H^+ ions are removed by nicotinamide adenine dinucleotide (NAD^+) which forms NADH. The extra H^+ can be combined with O_2 in the mitochondria to form a water molecule however when O_2 is not available the H^+ can be accepted by pyruvic acid to form lactate which disassociates to form lactic acid. Lactic acid diffuses freely into the blood stream and can alter the pH of blood if buffering systems are not functioning normally as free H^+ ions accumulate (Schneider, Danko et al., 1984).

H^+ ions present a unique challenge for any tissue. H^+ can be removed from the cell via the Na^+-H^+ exchanger (NHE) and Na^+ can in turn be removed by HCO_3^- but this can reduce the amount of free H_2CO_3 molecules outside the cells to alter the $CO_2:H_2CO_3$ ratio. The rate limiting step can result in cell pH levels remaining low for long periods of time depending upon cell potential (contracting or relaxed) and H_2CO_3 availability. This shift in ion balance can alter vasoreactivity and has been studied with a view to understand hypertension where patients can have low pH in their blood plasma (Canzanelli, Greenblatt et al., 1939, Aalkjaer, 1990, Smith, Austin et al., 1998). Under hypoxic conditions, the rate of ATP production will fall and consequently Na^+/K^+ pumps cannot maintain the ionic gradients across membranes allowing Ca^{2+} to move freely across the cell to eventually cause cell swelling and widespread tissue damage (Schneider, Danko et al., 1984).

The balance of pH is also important in the placenta and both the metabolically demanding fetus and placenta rely on the maternal circulation to buffer the pH of placental blood. The typical pH values for healthy patients have been summarised in **Table 1.6.3.2-1** pH values also vary with gestational age as shown by samples of amniotic fluid which become more acidic in the third trimester as this is the time the fetal kidneys mature and begin to excrete waste substances to remove the pH load (Serr, Czaczkes et al., 1963, Wilson, Hunter et al., 1977). The rise in uric acid reflects the key change in development as the fetus reaches its maximum growth potential and also a time when its metabolism will also be increasing exponentially (Schneider, Danko et al., 1984, Burton, Jauniaux et al., 2009).

Table 1.6.3.2-1 summarising the relative values of key substances measured in blood samples from both maternal and fetal umbilical vessels from healthy samples.

Substance	Maternal	Umbilical Cord		References
		Artery	Venous	
pCO ₂ (kPa)	4.8 ± 0.5	49 ± 1.6	38 ± 1.4	(Blechner, 1993, Westgren, Divon et al., 1995, Shirey, St Pierre et al., 1996, Loh, Woodworth et al., 1998, Martin, Gaillard et al., 2003)
pO ₂ (kPa)	12.35 ± 2	18 ± 0.6	29 ± 0.1	(Nicolaidis, Economides et al., 1989, Blechner, 1993, Westgren, Divon et al., 1995, Loh, Woodworth et al., 1998)
Bicarbonate (mmol/l)	26 ± 4	22 ± 0.2	20 ± 0.3	(Economides and Nicolaidis, 1989, Blechner, 1993, Westgren, Divon et al., 1995)
Lactate (mmol/l)	1 ± 0.5	2.98 ± 1.40	2.80 ± 1.4	(Blechner, 1993, Martin, Gaillard et al., 2003)
pH	7.53 ± 0.6	7.28 ± 0.13	7.35 ± 0.5	(Nicolaidis, Economides et al., 1989, Blechner, 1993, Westgren, Divon et al., 1995, Martin, Gaillard et al., 2003)

A recent publication (Bainbridge, Roberts et al., 2009) investigated the link with poor blood supply and placental development. This study used cultured trophoblast cells that were grown in the presence or absence of uric acid (10mg). Hyperuricemia can be detected in comprised pregnancies and raised levels can be detected as early as 10wks of gestation. The exact role of uric acid on placental growth and development has yet to be established. This study showed that uric acid could inhibit trophoblast integration into uterine microvascular EC monolayers which

is a key feature of invading trophoblast cells in normal culture conditions. Uric acid accumulation can potentially alter the normal function of invading trophoblast and could explain the poor remodelling of SA. An increase in uric acid can induce inflammation and has been linked to renal disease and increased hypertension. However the effect on vessel remodelling is not yet fully known and this study provides an important insight in to how metabolic acids can alter the normal working of vascular tissue. The concentration of uric acid used (10mg) was similar to the levels detected at 9-15wks gestation. This time point is significant as it marks the time the cytotrophoblasts will need to migrate and invade the decidual layer of the myometrium and any acid base imbalance may have severe consequences for the normal development of the placenta (Roberts and Lain, 2002).

1.7. The role of Ion channels

The vascular tone in organs such as the heart or kidneys can be controlled by either the nervous system or circulating factors released in the blood or locally produced signals. The placenta stands apart from other vascular tissues as it lacks autonomic control nerve supply which draws focus on the specific ion channels that may be involved with bringing about a vascular response. There is a need to understand the profile of ion channels that may be involved in controlling vascular tone in the placenta due to the link with poor placental perfusion common to compromised pregnancies which may originate from impaired vascular control.

The four main ion channel families listed in **Table 1.7-1** have been implicated in a range of cellular functions and movement of ions across the cell membrane can alter the membrane potential of the cell. Vascular tissue is rich in expression of ion channels that can directly influence SMC to control the vessel tone. The activity and conductance of each ion channels is closely linked with the cells metabolic status and hypoxia and pH can alter cellular activity by targeting such ion channels. Vascular SMC can respond to changes in the flow of blood by contracting. The contraction is mediated by the movement of ions across the cell membrane and changes the size of the lumen. The resting membrane potential is normally held at -70mV and this can increase to -55mV upon stimulation. Depolarising the membrane allows Ca^{2+} to enter the cell through voltage gated Ca^{2+} channels (VGCC) while Ca^{2+} can also be released from intracellular stores such as the ER.

Table 1.7-1 showing the 4 main class of ion channels families (transmembrane domain (TM). Pore (P)).

Calcium channels (Ca^{2+})	Chloride channels (Cl^-)	Sodium Channels (Na^+)	Potassium Channels (K^+)
P/Q Type	CIC1-CIC7	Amiloride sensitive	Voltage gated
R Type	CIC Ka-Kb	Voltage sensitive	Ligand gated
L Type			Inward rectifiers
T Type			Two pore domain
N Type			

1.7.1. L Type calcium channel (Ca_v1.2)

Ca²⁺ is an important intracellular messenger that governs a wide range of cell activities ranging from cell excitation to regulation of gene expression. Ca²⁺ enters the cell membrane through one of four identified L (Long lasting) Type Ca²⁺ channels (Ca_v1.1-4). Ca²⁺ channels are found on the cell membrane and on internal membranes of cell organelles including the ER, nucleus and mitochondria (Striessnig, 1999, Korovkina and England, 2002). The concentration of Ca²⁺ is kept low in the cytoplasm during cell rest when Ca²⁺ is taken up into internal stores mainly the ER, where it is important for protein synthesis. During cell excitation, Ca²⁺ levels will rise in the cytoplasm to depolarise the membrane potential and in vascular tissue this will contract SMC. The main influx of Ca²⁺ is through the Ca_v1.2 channel which was first identified in cardiomyocytes (Mikami et al., 1989). The ion channel is a large 210-240 kDa sized protein which comprises a voltage sensor and conducting pore and is the target for a wide range of second messenger molecules. Nifedipine (NIFED) is a potent blocker of Ca_v1.2 and is commonly administered as a treatment for pregnancy induced hypertension. The channel blocker was investigated to demonstrate the importance of Ca²⁺ currents in controlling the vasoaction of placental vessels. Cooper (et al., 2006) demonstrated that the contraction in response to U46619 was significantly inhibited (67% inhibition) in the presence of NIFED which provides indirect evidence for the expression of Ca_v1.2 in the placental arteries.

1.7.2. Potassium channels (K^+)

The rise in intracellular $[Ca^{2+}]_i$ can activate Ca^{2+} sensitive K^+ channels which are the largest family of ion channels (**Table 1.7-1**). K^+ ions are very important to cells as they have the primary function of generating a membrane potential. There are four main categories of pore forming K^+ ion channels including the voltage gated channels, Ca^{2+} activated and inward rectifier channels. These have been identified in a variety of vascular beds and investigations have also shown that their altered expression can be linked to various disease phenotypes including hypertension, ischaemia and diabetes.

The membrane potential of a cell is defined as the electrical potential inside the cell measured relative to the electrical potential outside of the cell (Perney and Kaczmarek, 1991, Blaustein, 2004, Brainard, Korovkina et al., 2007). The resting membrane potential is generated by the unequal distribution of ions in the extracellular and intracellular fluid and is determined largely by the concentrations of K^+ , Ca^{2+} , Na^+ , and Chloride (Cl^-) ions (Khan, Smith et al., 1997). As the K^+ ion has a positive charge, differences in the concentration between the cells intracellular and the extracellular fluid will generate a voltage membrane (V_m) potential at the membrane interface (Hodgkin and Huxley, 1952). The imbalance of K^+ ions is also actively maintained by cellular transporters including the Na^+/K^+ ATPase (Blaustein, Kao et al., 2004) which have greatest influence on V_m when the cell is at rest. At the resting membrane potential of both excitable and non-excitable cells, the concentration of K^+ ions outside the cell membrane is 3-5mM and inside the cell is 130-160mM, giving a

25-fold difference in concentrations and leads to a net negative membrane potential at rest (**Figure 1.7.2-1**) (Lawson, 1996, Lodish, Berk et al., 2000, Blaustein, Kao et al., 2004).

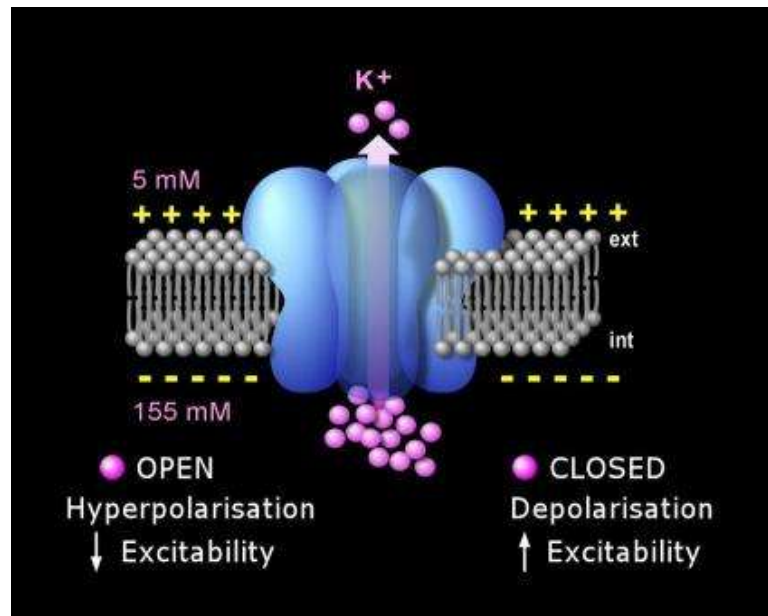


Figure 1.7.2-1 shows how the cell excitability can be influenced by the movement of K⁺ across the cell membrane. Inhibition of K⁺ channels will increase the cell excitability as K⁺ can no longer move out of the cell. (Image obtained from Sandoz, Douguet et al., 2009).

1.7.2.1. Large conductance potassium channel (BK_{Ca})

Ca²⁺ activated K⁺ channels (**Table 1.7.2.1-1**) are important for SMC function and have a central role in regulating vascular tone. The channels are made up of three sub families and include the small conductance (SK_{Ca}), the intermediate (IK_{Ca}) and the BK_{Ca}. The different channels are identified by the size of their conduction and the BK_{Ca} in particular has been implicated in regulating active tone (Khan, Smith et al., 1993, Parkinson, Tonta et al., 1999, Korovkina and England, 2002). BK_{Ca} channels

form intrinsic sensors which respond to changes in Ca^{2+} , membrane depolarisation and vasoconstriction and maintain Ca^{2+} homeostasis.

Table 1.7.2.1-1 listing the main pharmacological agents that can be used to target the each type of Calcium activated potassium channels

Ca^{2+} activated K^+ channels		
	Inhibitors	Activators
BK, maxi ($\text{K}_{\text{Ca}1.1}$)	Charybdotoxin, Iberiotoxin, paxilline, TEA	NS1610, NS1619, Resveratrol
Intermediate ($\text{K}_{\text{Ca}3.1}$) (IK_{Ca})	Charybdotoxin, TRAM-34, Maurotoxin, Clotrimazole.	EB10, NS309
Small (SK_{Ca}) ($\text{K}_{\text{Ca} 2.1-2.3}$)	Apamin (APA)	EB10, NS309

At rest the intracellular concentration of Ca^{2+} is normally kept low but following depolarisation, the voltage activated Ca^{2+} channels permit the entry of the ion in to the cell to cause contraction. In blood vessels, the increase in Ca^{2+} causes vasoconstriction of SMC to decrease the blood vessels diameter. This in turn activates BK_{Ca} which makes it an ideal mechanosensor that links vasoconstriction and membrane depolarisation closely together (Khan, Smith et al., 1993). The ion channel is responsible for increasing the movement of K^+ out of the cell to hyperpolarise the membrane potential. The cell cannot therefore respond to further electrical stimulation. BK_{Ca} can also trigger the release of vasodilators from the EC and are becoming more widely studied for their potential role in endothelial dysfunction linked with hypertension. Animal models which do not have functioning BK_{Ca} channels (knockdown of the $\beta 1$ subunit in male adult mice models) were resistant to

Ca²⁺ sparks and developed pulmonary hypertension (Brenner, Perez et al., 2000), and it would be interesting to determine how this knockdown affected the fetal and/or placental development in female pups. This finding further supports the view that BK_{Ca} channels are important in regulating vascular homeostasis and may have a role in controlling placental vascular function (Parkington, Tonta et al., 1999, Scotland, Chauhan et al., 2001, Eichhorn and Dobrev, 2007) .

1.7.2.2. ATP sensitive potassium channel (K_{ATP})

The K_{ATP} channel is part of the inward rectifier family of K⁺ channels (K_{ir} 6.1 or 6.2). It was first identified in cardiac muscle tissue but is also found in vascular SMC and EC (Noma et al., 1983, Gutterman, Miura et al., 2005). It is composed of four pore forming subunits and four sulphonylurea receptors (SUR) which are the ATP binding proteins. The channel activity is determined by the ratio of ADP to ATP as high metabolic activity will trigger a fall in the ADP:ATP ratio and this would increase the channel opening (**Figure 1.7.2.2-1**). In vascular tissue this would cause SMC membrane hyperpolarisation and induce vasodilatation to perfuse the surrounding tissue with more blood. The K_{ATP} is an important O₂ sensor as ATP levels are closely linked to the oxidative state of the cell and oxidative stress will reduce K_{ATP} activity (Duprat, Guillemare et al., 1995, Seino and Miki, 2003). Studies have shown that channel activity can be recovered with the administration of antioxidant based therapies (Pasquali et al., 2006, Brakemeier, Eichler et al., 2003, Ko, Han et

al., 2008) while the most effective blocker is glibenclamide (GLB) (Brakemeier, Eichler et al., 2003, Ko, Han et al., 2008, Feletou, 2009).

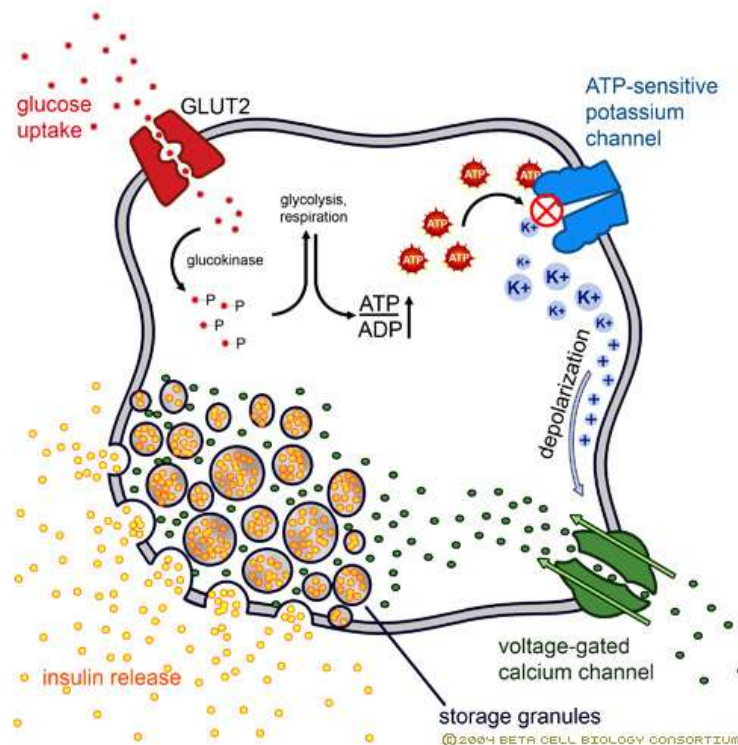


Figure 1.7.2.2-1 illustrating how K_{ATP} channels in pancreatic β cells regulate secretions of insulin. The gating of K_{ATP} is closely linked to the metabolic status. Glucose taken up by the cell through the glucose transporter (GLUT2) will alter the level of ATP within the cell which inhibits K_{ATP}. Image obtained from www.betacell.org/content/articles/print.php?aid=1.

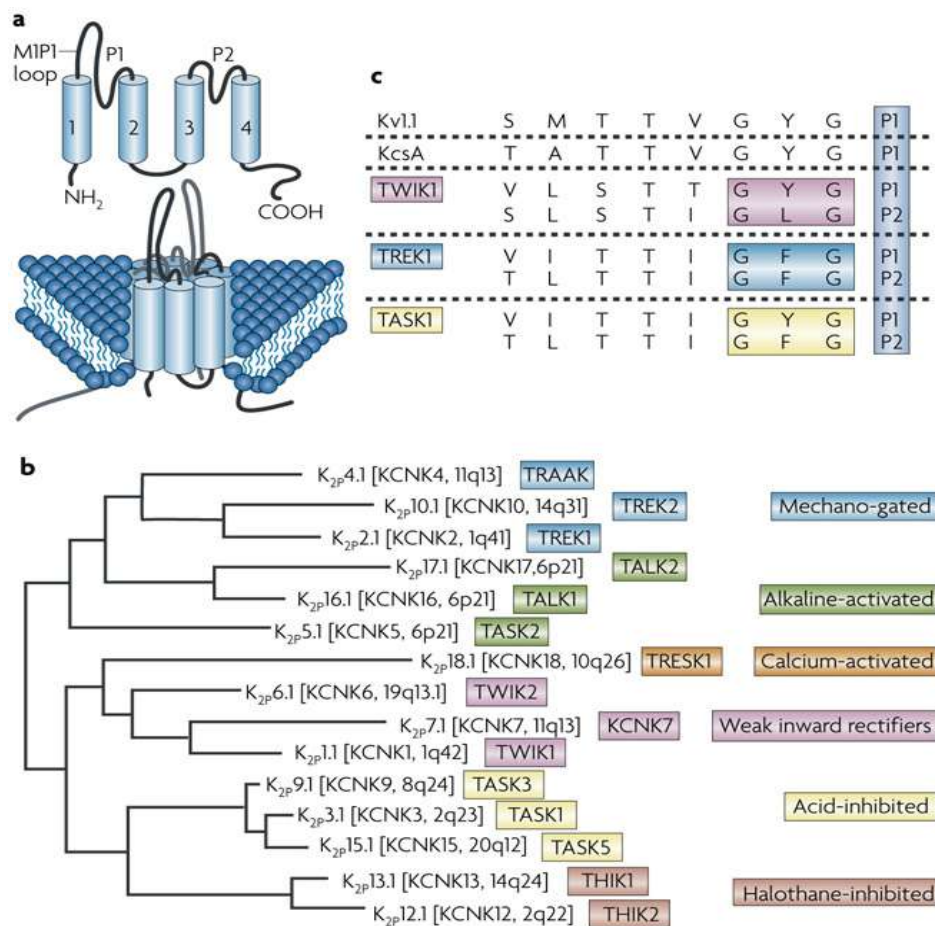
K_{ATP} channels may also have a role in the control of placental vascular function. Recent work by Jewsbury (et al., 2007) investigated the effect of specific K_{ATP} blockers on isolated CPA and CPV. The advantage of using pharmacological agents that are specific for K_{ATP} channels activity is that this would provide a way to target SMC function in blood vessels as patch clamp work has previously shown that placental vascular SMC but not EC were sensitive to the K_{ATP} antagonist GLB. The K_{ATP} opener pinacidil, but neither cromakalim nor nicorandil could relax CPA in a

dose dependant manner when studying isolated vessels with wire myography. More interestingly CPV also produced a similar relaxation to pinacidil suggesting that both vessel types have the same sensitivity for the K_{ATP} agonist. This provides indirect evidence for the presence of K_{ATP} mRNA in placental vessels from IUGR samples (Corcoran, Lacey et al., 2008). The close association with a cells' metabolic status and K_{ATP} activation may have important consequences for the highly active placenta (Guet-Bara, Ibrahim et al., 1999, Hussain and Cosgrove, 2005, Wareing, Bai et al., 2006, Jewsbury, Baker et al., 2007, Feletou, 2009) and there is a need to study expression of the ion channel at the protein level.

1.7.3. The two pore domain family of potassium channels (K2P)

The K2P channels are a new family of K^+ channels and since the first member was identified (tandem of P domains in weak inward rectifier K^+ , **TWIK-1**) (see Ketchum, Joiner et al., 1995, Lesage, Guillemare et al., 1996), the numbers have rapidly grown and currently 15 members have been identified (**Figure 1.7.3-1**). The K2P channels are distinguished by the presence of four transmembrane segments and two pore forming domains. Their pharmacological properties vary greatly and recent work has shown that they have very different mechanisms of modulation. For example TWIK and the TWIK related K^+ channel (**TREK**), demonstrate sensitivity to acidic pH conditions inside the cell while TWIK related acid sensitive K^+ (**TASK**) is stimulated by weak changes in extracellular pH (Duprat, Lesage et al., 1997, Lesage, Lauritzen et al., 1997, Chavez, Gray et al., 1999, Richter, Dvoryanchikov et al.,

2004). The ion channel family are widely expressed particularly in the central nervous system and studies using knockout animal models have shown they may have a role in depression and pain sensation. They can function in both excitable and non-excitable cells and are crucial for maintaining the resting membrane potential (Duprat, Guillemare et al., 1995, Lesage, Guillemare et al., 1996, Reyes, Duprat et al., 1998, Gruss, Mathie et al., 2004).



Nature Reviews | Neuroscience

Figure 1.7.3-1 showing the phylogeny tree of the 15 K2P family members identified. showing the topology of the K2P channel (Image obtained from Honore, 2007).

TWIK-1 has been located in heart, brain, placenta, lung, liver, kidney, pancreas (Lesage, Guillemare et al., 1996), stomach, prostate & uterus (Medhurst, Rennie et al., 2001). Medhurst (et al., 2001) also showed that TWIK-1 mRNA expression was highest in human central nervous tissue than in peripheral tissues, with the cerebellum giving the highest expression. TWIK-2 (**Table 1.7.3-1**) is another K2P which is 313 amino acids long, its chromosomal location is 19q13 and it has 53.8% sequence similarity along with 72 and 88% amino acid similarity between the 1st and 2nd pore respectively to TWIK-1 (Chavez, Gray et al., 1999, Medhurst, Rennie et al., 2001).

Table 1.7.3-1

TWIK-2 (KCNK6)	
Current	Open rectifier
Amino acid	313
Activators	AA
Blockers	Barium (Ba^{2+}), quinine, quinidine, volatile anaesthetics
Distribution (highest)	Placenta , heart, colon, spleen, lung, liver, kidney, thymus, stomach, prostate, & small intestine
Key references	(Lesage, Guillemare et al., 1996, Patel, Honore et al., 1998, Chavez, Gray et al., 1999, Patel, Maingret et al., 2000, Goldstein, Bayliss et al., 2005)

TREK-1 (**Table 1.7.3-2**), TREK-2 (**Table 1.7.3-3**) and the TWIK Related Arachidonic Acid K^+ channel (TRAAK) (**Table 1.7.3-4**) are part of the mechano-gated members of K2P K^+ channels. Both TREK and TRAAK are activated by stress,

cell swelling and membrane stretching which is mostly dependant on the osmolarity of the fluid rather than changes to the cytoskeleton (Patel and Honore, 2001). Another potent stimulant is AA and polyunsaturated fatty acids such as linoleic acids and docosahexaenoic acids, however they are unaffected by saturated fatty acids (Maingret, Fosset et al., 1999). An additional modulator of TREK is pH particularly in the acidic pH range inside the cell cytosol. If the intracellular fluid becomes slightly acidic this will cause a shift in the pressure activity curve towards positive and as a result will lead to channel opening at atmospheric pressure (Maingret, Fosset et al., 1999). TREK-1 can also respond to cell swelling by opening its channels to cause a large efflux of K^+ ions which will then change the osmotic potential of the extracellular fluid and as a result drive water out to consequently reduce cell swelling. TREK-1 and TREK-2 are sensitive to volatile anaesthetics like chloroform, diethylether, halothane and isoflurane, while TRAAK is insensitive (Maingret, Patel et al., 1999, Patel, Honore et al., 1999, Lesage, Terrenoire et al., 2000). TREK-1 is also known to be temperature sensitive in neurons of the hypothalamus and dorsal root ganglion and there is a possibility that it could be involved with body temperature regulation, but this is not fully supported in the literature (Maingret, Patel et al., 2000).

Table 1.7.3-2

TREK-1 (KCNK2)	
Current	Open or voltage dependent
Amino acid	426
Activators	AA, unsaturated fatty acids, lysophospholipids, volatile anaesthetics, mechanical stress, & riluzole
Blockers	Ba ²⁺ , Zinc (Zn ²⁺), caffeine, curcumin, internal acidification, PKA, PKC, & quinidine.
Distribution (highest)	Foetal brain , spinal cord, thalamus, putamen, cavdate nucleus, stomach, small intestine, lung, heart, & brain.
Key references	(Fink, Lesage et al., 1998, Maingret, Lauritzen et al., 2000, Maingret, Patel et al., 2000, Goldstein, Bayliss et al., 2005, Lauritzen, Chemin et al., 2005, Chemin, Patel et al., 2007)

Table 1.7.3-3

TREK-2 (KCNK10)	
Current	Open rectifier
Amino acid	538
Activators	AA, riluzole, isoflurane, halothane, volatile anaesthetics, linoleic acid, & intracellular acidification
Blockers	PKA, PKC & quinidine
Distribution (highest)	Cerebellum , spleen, testes, kidneys & small intestine
Key references	(Lesage, 2003, Goldstein, Bayliss et al., 2005)

Table 1.7.3-4

TRAAK (KCNK4)	
Current	Open rectifier
Amino acid	393
Activators	AA, riluzole, heat, stretch, & lysophospholipids,
Blockers	Gadolinium (Gd ³⁺) & sipatrigine
Distribution (highest)	Brain , retina & spinal cord, amygdale, caudate nucleus, temporal cortex, hippocampus & placenta
Key references	(Maingret, Patel et al., 2000, Reyes, Lauritzen et al., 2000, Goldstein, Bayliss et al., 2005, Andresen, Lloyd et al., 2007)

Another member of the K2Ps is TASK which has the main characteristic of being sensitive to change in extracellular pH (**Table 1.7.3-5**). TASK-1 has a chromosome location of 2p23 and is a 394 amino acid that produces an outward rectification of 14pS (Lesage and Lazdunski, 2000). TASK channels are very sensitive to changes in pH with 90% channel activity for TASK-1 at pH 7.7 but only 10% at pH 6.7, with a 50% inhibition at pH 7.3 (Lesage and Lazdunski, 2000) which makes TASK-1 very sensitive as that is only a 0.4 unit increase in acidity. TASK-1 is inhibited by local anaesthetics such as lidocaine and bupivacaine and it is opened by volatile general anaesthetics such as halothane, and isoflurane at the concentration used in general anaesthesia. TASK-1 is most abundantly expressed in the pancreas and placenta, as well as the peripheral and CNS tissue (Medhurst, Rennie et al., 2001). The general role of TASK-1 seems to be helping to maintain the resting potential along with the closely related channel TASK-3 (**Table 1.7.3-6**) (Ketchum, Joiner et al., 1995, Lesage, Guillemare et al., 1996, Patel, Maingret et al., 2000).

Table 1.7.3-5
TASK-1 (KCNK3)

Current	Open rectifier
Amino acids	394
Activators	Halothane, volatile anaesthetics & isoflurane
Blockers	Ba ²⁺ , Zn ²⁺ , external acidification, quinidine, anandamide, & AA
Distribution (highest)	Pancreas , placenta, brain, lung, prostate, heart, kidney, uterus, stomach, small intestine & colon
Key references	(Duprat, Lesage et al., 1997, Goldstein, Bayliss et al., 2005, Duprat, Lauritzen et al., 2007)

Table 1.7.3-6
TASK-3 (KCNK9)

Current	Not determined
Amino acid	374
Activators	Halothane
Blockers	External acidification, lidocaine, bupivacaine, Zn ²⁺ , Copper (Cu ²⁺) & ruthenium red
Distribution (highest)	Brain , testis, & stomach
Key references	(Bayliss, Sirois et al., 2003, Goldstein, Bayliss et al., 2005, Duprat, Lauritzen et al., 2007)

K2P channels expressed in the taste receptors has shown that these channels produce the reflex response seen with bitter acidic foods as the channels are activated (Medhurst, Rennie et al., 2001, Bayliss, Sirois et al., 2003, Beckett, Han et al., 2008, Meuth, Bittner et al., 2008). In other tissues the leak channels have shown to increase tissue oxygenation by regulating the diameter of blood vessels and in particular

TREK-1 is shown to function in SMC and is stimulated during cell stretch (Reyes, Duprat et al., 1998, Richter, Dvoryanchikov et al., 2004, Xian Tao, Dyachenko et al., 2006). More recently research in to respiratory ventilation during sleep showed that the reduction in breathing and consequent increase in pCO₂ will trigger a decrease in the pH. A reflex response (“waking reflex”) in the brain responds to this by increasing the respiratory output inducing behavioural arousal to reduce the pCO₂ (Czirjak, Fischer et al., 2000, Bayliss, Sirois et al., 2003, Bryan, You et al., 2006). Many groups are studying the role of K2P channels in this mechanism to better understand sleep disturbances and unexplained infant deaths which occur during sleep (Cluzeaud, Reyes et al., 1998, Chavez, Gray et al., 1999, Pountney, Gulkarov et al., 1999, Patel, Maingret et al., 2000, Feletou, 2009).

There is an increasing body of evidence to show that K2P channels are expressed in the placenta and suggest the K⁺ channel family may have a role in controlling vessel function. Recent work (Bai, Bugg et al., 2005, Wareing, Bai et al., 2006) has identified the expression of TASK -1 and TREK- 1 in specific regions of the placenta including the trophoblast layer but the functional role of the ion channel family within the placenta is incomplete. The TASK channel modulator Anandamide, was reported to produce a marginal effect on the vasoactivity of placental CP vessels (Wareing, Bai et al., 2006). The detection of K2P channels in the trophoblast also suggests a potential role for other K2P channels in the regulation of blood flow in the placenta and potentially in the regulation of the acid base balance and provides an exciting new insight into how this pathway can be targeted.

1.8. Vascular dysfunctions linked with the placenta

The importance of adequate maternal adaptations to pregnancy has been demonstrated with complicated pregnancies which show evidence of placental insufficiency. Studying abnormalities from diseased tissue has also shown that vascular function may hinder the normal growth and development of the fetus especially if the insult occurs during the early trimester (Robertson, Brosens et al., 1973, Ashworth, 1997, Kublickiene, Kublickas et al., 1997, Baker and Kingdom, 2004, Chaddha, Viero et al., 2004). The adequate growth and development of the fetus is only achieved through the carefully timed adaptations to pregnancy that results in the efficient exchange of nutrients and gases across the maternal and fetal circulations through the placenta. Placental insufficiency is a major risk factor for the onset of disease and is believed to be the origins for conditions that result in compromised pregnancies such as hypertension linked pregnancy and the most fatal pre-eclampsia (PE) and intrauterine growth restriction (IUGR) which will be detailed in this section. In cases of PE and IUGR quite often the SA are narrow as they fail to remodel in this way and blood flow is restricted. The normal remodelling of the SA ensures that there is a constant flow of blood which limits the production of ROS. In PE it would seem that narrow arteries cause the blood to pass in pulses which favours the production of ROS and gives one possible pathway for the development of the adverse condition (Blechner, 1970, Moll, 2001, Lyall, 2005, Pijnenborg, Vercruysse et al., 2006).

1.8.1. PE

PE is a condition that is only seen spontaneously in humans and is described as a multisystem condition for which there is currently no cure. PE incidence is estimated to account for 4-7% of pregnancies worldwide and is a leading cause neonatal and maternal morbidity and mortality. In the UK this accounts for on average 5/1000 pregnancies per year and 60,000 of maternal deaths are associated with PE (Tuffnell, Jankowicz et al., 2005). In addition, a further 20% of those diagnosed with PE are thought to be at a greater risk of developing heart disease compared to 2% in the wider population (Goldenberg, Culhane et al., 2008). Some cases of heart abnormalities following pregnancy have been reported as early as seven years after the original diagnosis of PE. This suggests the condition is either causing permanent alterations in the vascular system or instead exposing those individuals who are already have a risk of heart disease to develop it earlier. The symptoms of PE can vary from a mild increase in blood pressure to severe oedema, seizures, liver and renal abnormalities. The symptoms commonly occur in the second or third trimester when the condition is most difficult to treat due to the risk it places on the fetus (Roberts, Taylor et al., 1989, Pijnenborg, Anthony et al., 1991, Goldenberg, Iams et al., 1996, Fox, 1997, Bolte, van Geijn et al., 2001, Goldenberg, Culhane et al., 2008). The clinical features of PE as defined by the International Society of Hypertension (ISH) often present after 20wks and include hypertension (BP >140/90), proteinuria (>0.5g/L), edema and if untreated will progress to elcamptic convulsions and

pulmonary edema (Roberts and Lain, 2002, Baker and Kingdom, 2004, Garovic and Hayman, 2007).

At the physiological level it has been shown that PE is associated with widespread vasoconstriction of the maternal circulation particularly affecting the renal, uterine, cerebral and hepatic circulations and increased platelet activation. PE is now widely understood to be a disease of the endothelium and evidence has come from specific markers as well as functional studies (Roberts, Taylor et al., 1989, McCarthy, Taylor et al., 1994, Ashworth, 1997, Maynard, Epstein et al., 2007). The second wave of trophoblast invasion is flawed in PE cases (**Figure 1.8.1-1**) and the maternal SA retain their contractile activities. This disorganised vascular remodelling will lead to an interrupted blood supply to the placenta and therefore restrict growth of the fetus.

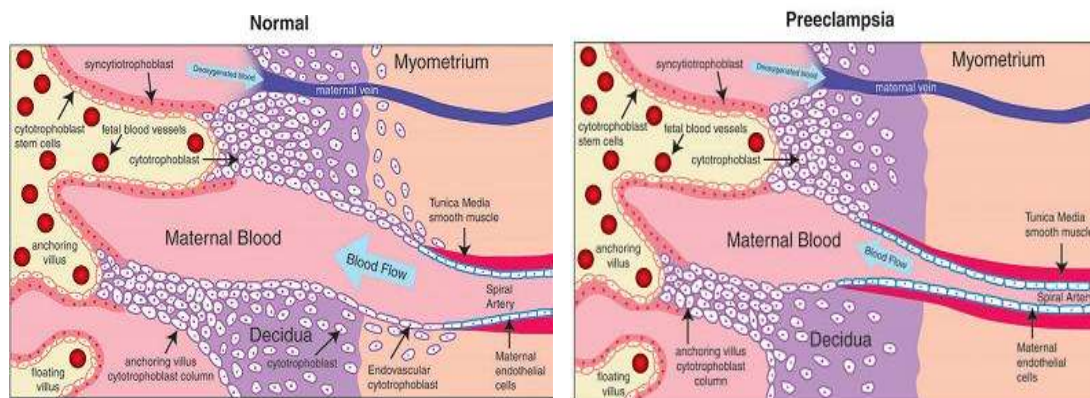


Figure 1.8.1-1 shows the key difference in maternal SA between normal and PE samples. The invasion of SA in PE is shallow leaving the SA relatively untransformed and the trophoblast cells fail to reach the myometrium. (Image obtained from Maynard, Epstein et al., 2007).

In PE, it has been shown that placental perfusion is greatly reduced. The placenta is the main target organ for PE related pathology (Kelly, Stone et al., 2000). This may disrupt the carefully balanced oxidative capacity of the low pO_2 placenta to

increase oxidative stress. The placenta also has a further role in PE and it is now understood that a yet to be identified factor may be released from the placenta into the maternal circulation marking the second stage of the disease. PE shows remission following delivery of the placenta and PE is found in cases of hydatidiform where the fetus is absent (Roberts and Lain, 2002, Baker and Kingdom, 2004).

1.8.2. IUGR

In common with PE, IUGR has been linked with reduced placental perfusion. IUGR is used to describe babies that fail to reach their full growth potential after correcting for maternal weight and ethnicity (Gardosi, Chang et al., 1992). In the clinical setting this is defined as birth weights that fall below the 10th centile of the expected growth for that specific gestation and accounts for 3-7% of all pregnancies (Goldenberg, Culhane et al., 2008, Romo, Carceller et al., 2009). The fetus triples in weight during the final trimester and is the point where IUGR can be diagnosed and often the clinical intervention is to deliver the baby often occurring before term (Gardosi, Mongelli et al., 1995, Baker and Kingdom, 2004).

Examinations of IUGR effected placenta has shown some anatomical differences in the structure and number of terminal villi compared to normal healthy samples. This would greatly reduce the transport capacity of the placenta and it has been shown that expression of key transporters for nutrients exchange are reduced along the basement membrane from IUGR samples (Jansson and Powell, 2007). IUGR also has important parallels to PE with placental insufficiency being at the

centre of both conditions. This also suggests that a similar pathophysiology may be involved in disrupting the normal functioning of the placenta (Burton, Yung et al., 2008, Scifres and Nelson, 2009, Scifres, Stamilio et al., 2009). Patients diagnosed with IUGR and PE have shown to have increased risk of developing PE in subsequent pregnancies, along with an increased risk in developing diabetes, renal disease and obesity. Put together with the extra cost of neonatal specialist care required at the time of birth and throughout life PE is costing healthcare providers millions each year. The increase in mortality is more significant in developing countries which cannot provide the adequate health care that is needed to deal with pre term deliveries (Brosens, Robertson et al., 1972, Roberts, Taylor et al., 1989, Goldenberg, Iams et al., 1996, Goldenberg, Culhane et al., 2008).

At present the most effective treatment is delivery of the fetus and placenta however this may occur before term and contributes to the increasing pre-term delivery linked complications seen worldwide costing health providers millions each year with neonatal care (Goldenberg, Iams et al., 1996, Fox, 1997, Moutquin, 2003, Garovic and Hayman, 2007, Goldenberg, Culhane et al., 2008).

1.9. Methods used to study the placenta

Blood flow is a good clinical marker of how well the placental unit is functioning and has advanced the diagnosis of placental abnormalities *in vivo* (Pijnenborg, Dixon et al., 1980, Fox, 1997, Soares and Hunt, 2006, Deurloo, Spreeuwenberg et al., 2007). The reduction in blood flow to the placenta observed

with IUGR and PE predisposes to impaired fetal growth and development and more evidence is needed to understand how vascular tone is controlled across the placenta.

1.9.1. Whole placentae

In vivo methods such as Doppler ultrasounds and echocardiographs have been employed to measure changes in feto-placental blood flow and provide a measure of blood flow (Fairlie, Moretti et al., 1991, Deurloo, Spreeuwenberg et al., 2007, Moore, Ong et al., 2007). They have increasingly been used to provide a measure of fetal well-being and give a measure of how the fetal cardiac output changes at different stages of pregnancy. Examining Doppler waveforms gives information of the widespread resistance as the systolic and diastolic flow can be quantified. Doppler ultrasound has been used to measure blood flow velocities to provide clinical markers of poor perfusion. In normal pregnancies umbilical end diastolic velocity should increase and fetal placental resistance should steadily decrease with gestation (Fairlie, Moretti et al., 1991, Myatt, 1992, Soares and Hunt, 2006, Deurloo, Spreeuwenberg et al., 2007). This method of studying blood flow gives information in the general hemodynamic changes that need to occur and provide a method for detecting increased resistance to flow in the venous circulations.

1.9.2. Resistance vessels

Doppler waveforms measure changes in large vessels such as the umbilical vein but gives limited information on the flow of blood in the peripheral vessels. The small diameter vessels in the range of 50-500 μ m offer the most resistance to flow and therefore determine the widespread resistance to flow and need to be studied to better understand the regulation of vascular resistance (Mulvany and Aalkjaer, 1990). The amount of resistance is proportional to the vessel length while the radius has an inverse relationship to the amount of flow. When studying vessels the pressure, flow, and radius need to be taken into consideration and small changes in either parameter will have a profound effect on intraluminal flow. The main control over flow is by the radius of the vessel which can be altered by basal and agonist induced mechanisms. The diameter is itself under the influence of the cell layers that comprise the vascular wall to generate a force and the amount of force is a measure of tone or active tension whereby SMC are activated and can be measured using isolated vessel (Mulvany and Halpern, 1977, Halpern, Mulvany et al., 1978). Changes in pressure, flow and resistance have been measured using two main techniques, namely perfusion myography and wire myography (**Figure 1.9.2-1**).

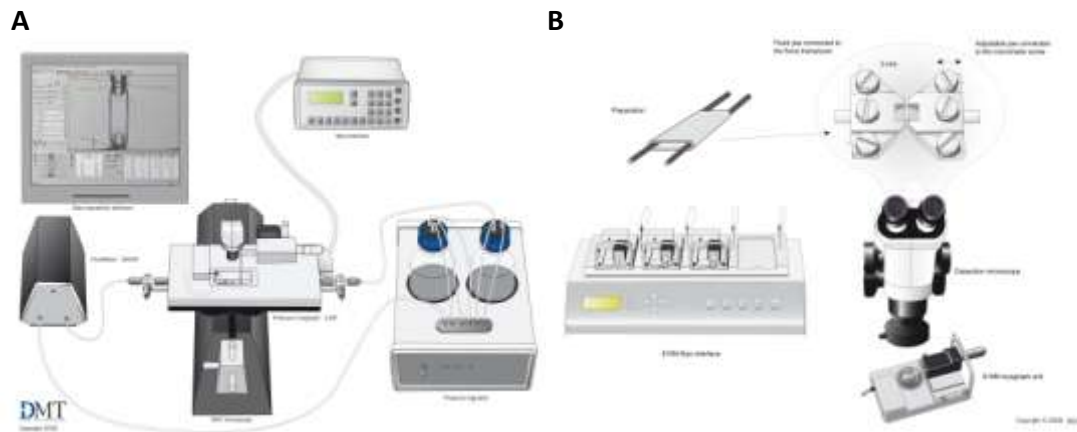


Figure 1.9.2-1 showing the experimental setup for the perfusion (A) and wire (B) myograph apparatus. The pressure myograph requires the constant monitoring of the vessel diameter using a video display. In contrast wire based myography involves threading the vessel on to two stainless steel jaws using two parallel wires which stretch the vessel into a flat parallel sheet. The changes in force on the wires as a result of the vessel contracting can be recorded by the highly sensitive force transducers. Images obtained from www.dmt.dk.

The perfusion myograph: Increases in shear stress as a result of increased flow will induce dilation (Halpern, Mulvany et al., 1978, Spiers and Padmanabhan, 2005). The perfusion myograph measures vessel diameter in response to changes in flow. With this method, the vessel can be perfused to different pressures and the lumen diameter is measured by viewing the vessels with an inverted microscope. The vessel is mounted between two glass microcannulae and is perfused with normal saline which is passed through the lumen using a flow pump. Pressure transducers are attached to the opposite side to record the intraluminal pressure and the system is closed (Halpern, Mulvany et al., 1978, Halpern, Osol et al., 1984, Mulvany and Aalkjaer, 1990). The main advantage is that the vessel is held in a cylindrical shape, like that found *in vivo*, and the shear stress applied can be manipulated along with the amount of flow (Dunn, Wellman et al., 1994). However the difficulty with this

method is that the direction of flow applied must match the direction of flow *in vivo* to limit the damage to EC (Sen and Semenza, 2004).

The Wire myograph: In contrast to perfusion myography, the wire myograph adapted by Mulvany (et al 1977) uses two fine wires and is useful for measuring force generation as well as vessel dimensions of small arteries. The isometric study of vessels uses two parallel tungsten wires which are passed through the lumen of the vessel. The vessel is then mounted onto two jaws where one is connected to a force transducer and the other to a micrometer screw. The jaws are adjustable and allow the measurement of blood vessel diameter and wall tension to calculate contractility of the vessels. The vessel has to firstly be normalised in order to accurately match the conditions the vessel would be held in *in vivo* and to gain the most active tension. The internal circumference (L_{100}) can be adjusted to reflect the conditions found within the tissue and 100mmHg (13.1 kPa) which is the internal pressure for rat adult small vessels, is commonly used (Mulvany and Aalkjaer, 1990, McPherson, 1992). This can be calculated using the Laplace equation which takes the vessel length and circumference into account;

$$\text{Effective pressure } (P_i) = \text{wall tension} / (\text{internal circumference} / 2\pi)$$

Small resistance arteries have shown the ability of regulating vessel tone and isolated blood vessels can spontaneously contract upon stretch (Bevan and Osher, 1972, Mulvany and Halpern, 1977, Halpern, Mulvany et al., 1978). Two main forces apply pressure on the blood vessel, this first being fluid stress which is caused by the

volume of blood flowing. While the second is applied along the vessel wall as the cross sectional area changes (shear stress). The size of active tone increases with smaller vessel sizes and arteries <500µm provide the highest level of resistance. The development of active tone controls peripheral resistance and allows vessels to respond to changes in the external environment even when vessels are isolated from the vascular tissue. This also has an important implication for understanding how the vascular system reacts to external stimuli and makes small arteries an important target for agonists that can relax vascular SMC (Sen and Semenza, 2004).

1.10. Background to the study

The placenta needs to maintain a low resistance system to deliver sufficient O₂ and nutrients to the fetus. Blood vessels within the placenta respond to challenges in maternal blood supply by altering the vessel diameter but the exact nature of the ion channels involved in this response are not known. Chronic hypoxia will lower the pH and present a unique challenge for the placenta. If the vessels in the placenta fail to respond to changes in pH then the tissue will continue to fluctuate. Recent studies have shown that the pH sensitive K₂P channels are highly expressed in the placental trophoblast cells and in the myometrium (Bai, Greenwood et al., 2005) which supplies the placenta with its oxygen and nutrient requirements. These findings raise the possibility that these ion channels could also provide an important therapeutic target for regulating pH within the placental *in vivo* and requires further investigation.

The precise role of K^+ in controlling the basal tone across the placental vasculature is not fully understood. Moreover it is not clear how hypoxic insults alter the physiology of K^+ channels. Hampl (et al 2002) has provided an insight into how O_2 can alter placental vessel function of resistance arteries. My study aims to examine further stress by studying the role of pH on CPA and crucially SVA from normal samples which are at the maternal facing boundary of the placenta. This is particularly important as poor perfusion can limit the normal growth development of the fetus and has been linked to the onset of IUGR and PE both of which are leading causes of fetal and maternal morbidity.

The aims of the study were to firstly compare the two types of human placental vessels namely the CPA and SVA to examine the characteristic of vessels from across the fetomaternal interface of the placenta from normal pregnancies. The second aim was to characterise the key O_2 and pH sensitive ion channels to identify which ion channel(s) have a role in mediating the vascular response of the placenta to stress.

2. Hypothesis

The study hypothesis states that expression of O₂ and pH sensing ion channels including the K2P family varies across the placental maternal facing SVA and fetal facing CPA, and such ion channels have a role in controlling the response to pH stress.

2.1. Objectives

The objectives of this study were to;

- Identify expression of the Ca_v1.2, BK_{Ca} and K_{ATP} channel along with the K2P members TWIK-2, TREK-1/2, TRAAK, and TASK-1/3 in normal human placental blood vessels by Western blotting analysis.
- Investigate any differences in ion channel expression between PE and normal non-labouring placental vessels using Western blotting analysis.
- Determine the cellular distribution of ion channels within cultured myocytes from CPA and SVA using confocal immunofluorescence.
- Examine the functional responses of both CPA and SVA in response to hypoxia and pH stress along with ion channel modulators using wire myography.

3. Materials and methods

3.1. Patient recruitment

Whole placentae and myometrial (MYO) biopsies were obtained from the Department of Obstetrics and Gynaecology at the Royal Derby Hospital. Ethical approval was obtained from the Derbyshire Ethics Committee. Tissue was collected from fully informed patients who had given written consent prior to elective lower segment Caesarean section (ELLSCS). The information included in the patient information sheet (See [Appendix V](#)) was also explained to ensure the patients knew and understood what would happen with the samples once they were collected and answer any questions the recruit may have. Once consent was obtained three copies of the consent forms ([Appendix V](#)) were obtained with original signatures, for the patient's own personal records, for our secure files and for inclusion the patient's medical notes to inform the labour ward staff that consent had been taken. All consent forms and sample information was then logged and kept in secure files. Each sample was assigned a unique identification code to ensure anonymity and this code was then used to follow up the patient information using the medical notes.

3.2. Tissue collection

Two main cohorts of patients, firstly normal (NORM) were recruited to the study with full informed written consent. All samples were from singleton

pregnancies and delivered by ELLSCS at term gestation (≥ 37 wks). The reasons for ELLSCS included maternal requests, previous ELLSCS or breech presentation while diabetics, smokers and women with high blood pressure were excluded. Any patients with a history of cardiac or renal disease, or patients receiving pharmacological treatment other than iron supplementation were also excluded. Our second group consisted of patients diagnosed with PE which was defined as a BP recording of $\geq 140/90$ mmHg after 20 wks gestation and 24hr proteinuria of ≥ 0.5 g/L in the absence of urinary tract infection.

Women undergoing ELLSCS at full term (≥ 37 wks) were approached and myometrial (MYO) biopsies of approximately 2x2x1.5cm were taken from the upper region of the transverse incision made at the time of ELLSCS (**Figure 3.2-1**). MYO biopsies were transported in chilled Physiological salt solution (PSS, see [Appendix I](#) for composition) and aerated with 95% O₂/5% CO₂ before using in experiments. The details of the compositions of all the different buffers used along with the suppliers and their addresses have been listed in the appendices ([Appendix I-IV](#)).

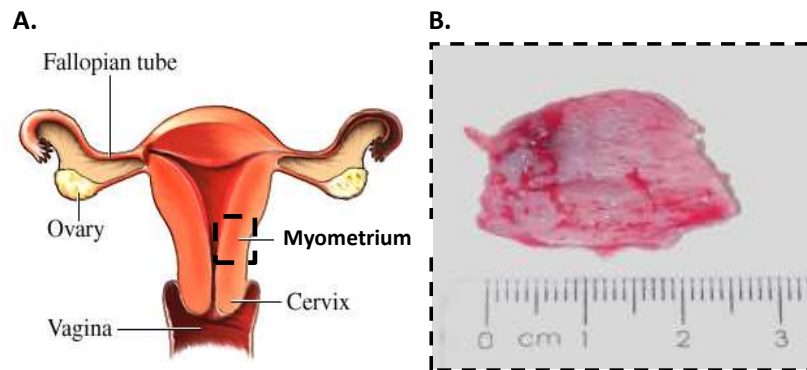


Figure 3.2-1 shows the source of the MYO biopsy that was obtained at ELLSCS. A shows the structural arrangement of a human female reproductive tract and the location of the myometrium. (Image obtained from www.lab.anhb.uwa.edu.au/mb140/CorePages/FemaleRepro/htm).

B shows a freshly collected MYO biopsy that has been obtained at ELLSCS.

3.2.1. Isolation of placental arteries

Placentae were collected within 20mins of delivery and transported to the Medical School Clinical Sciences laboratory. The amnion was firstly peeled away by hand to reveal a vast network of arteries and veins running along the chorionic surface. An artery in isolation from a neighbouring vein was identified by following that point of cord insertion and was used to identify the smaller resistance sized branches that divided further along the tissue. The 4th order branch of the CPA was selected (**Figure 3.2.1-1**) and an incision was made into the tissue to dissect the vessel away with its surrounding tissue intact. Three separate samples from each placenta were taken in this way and the method of storage for both tissue samples was determined by the type of experiment that would be undertaken. Following fine dissection to remove any connective tissue, CPA were transferred to room temperature PSS and used immediately for wire myography (**Chapter 3.7**). The CPA

branching into the maternal portion of the placenta was also used to identify the matched SVA. SVA were removed by scraping away trophoblast tissue using the blunt end of a pair of forceps to leave the villous arteries which were dissected away from the placenta. In addition non-pressurised CPA and SVA rings were placed in fixative for immunohistochemistry (IHC) analysis (Chapter 3.3). For cell culture experiments isolated samples were placed in Hanks Balanced Salt Solution (HBSS) and cultured within 4hrs of collection (Chapter 3.5), while for Western blotting (Chapter 3.4) the isolated arteries were firstly washed in homogenising buffer to remove traces of blood before being labelled, dated and then snap frozen in liquid nitrogen (N₂) then stored at -80°C.

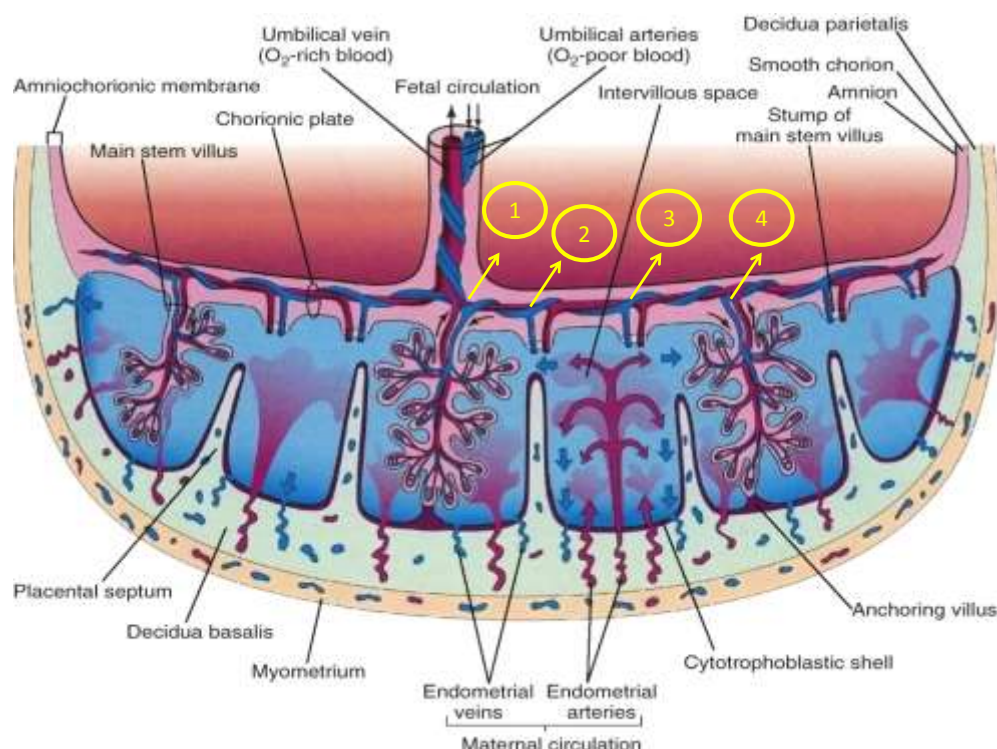


Figure 3.2.1-1 illustrating how the placental arteries were identified in the placenta. The 4th branch (numbered in image) of the CPA was routinely identified following the point of cord insertion. A large section was removed that contained both the CPA and SVA (Image adapted from Saunders, 2009).

3.3. IHC

1mm long non-pressurised CPA and SVA rings (described in [Chapter 3.2.1](#)) were firstly cleaned of any surrounding connective tissue and immediately placed in Bouin's solution (see [Appendix I](#) for composition) which is a fixative that has the added advantage that it stains tissue yellow so it can be viewed more easily. The samples were stored in 5ml Bijou tubes at 4°C before being transported to the Advanced Microscopy Unit based at the Queens Medical Centre, Nottingham, for sectioning.

The samples were removed from the Bouin's solution, transferred to a clean 35mm petri-dish and a small drop of distilled H₂O was added to wash off any excess fixative solution. At the same time a small amount of Optimum Cutting Temperature (OCT) embedding medium (Tissue Tek) was placed onto a cork disc ready for the sample to be added. Using a dissecting microscope (Olympus SZ51), the tissue was cut in half using a 22 size scalpel blade to give 0.5mm cross sectional segments which could then be transferred to the OCT using fine forceps. The tissue was then orientated so the lumen was facing up and the OCT coated disk was immersed face up into liquid N₂ cooled isopentane allowing for the rapid freezing of tissue specimens. This was achieved by placing the isopentane liquid into a plastic pot which fits over the liquid N₂ container. The isopentane freezes immediately but thaws slowly as it was left at room temperature (RT) to give the desired temperature of -116°C for freezing tissue samples. This was then repeated for each sample to be analysed. The freshly frozen samples were then transferred to a cryostat shown in **Figure 3.3.1-1** (Leica CM1900). OCT was added to a cryostat chuck before the cork discs were

quickly removed from the isopentane and glued on to the cryostat chuck. The samples were then left in the cryostat which was maintained at -18°C for 15mins to allow them to adjust to the temperature difference at which point the samples were then ready for cutting.

3.3.1. Cryostat tissue sectioning

The cryostat has two temperature settings one for the knife blade and the second for the anti roll plate (**Figure 3.3.1-1**). For our blood vessels, the cutting blade was set to -20°C while the anti roll plate was adjusted to -18°C . This was the optimum temperature that prevented the tissue slices from rolling up after each cut was made. The OCT was firstly trimmed by sectioning with a fresh knife blade until a complete tissue section could be seen.

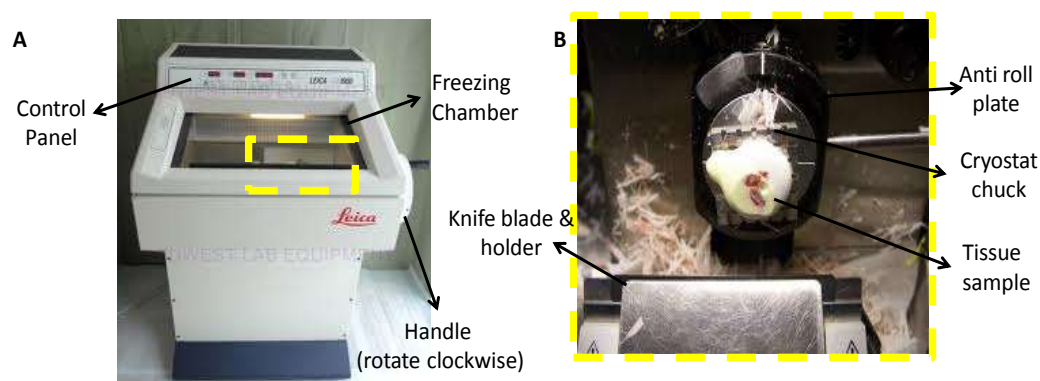


Figure 3.3.1-1 showing the Leica CM1900 that was used to prepare the tissue sections. **A** shows the large chamber which maintains the different temperatures for the knife blade and the anti-roll plate. **B** shows the knife blade in more detail. The handle is used to slowly move the anti-roll plate and bring the sample into close contact with the knife blade. The thin sections can be collected directly onto glass slides which have been kept at RT.

The instrument parameters were set to give 5µm thick slices. The section was then picked up using a gelatine coated slide (76 x 26 x 1.2mm, VWR). This was done by holding the slide using a thumb and forefinger and the slide was carefully lowered through the open cryostat window and was held over the slice for a few seconds. This adhered the sample on to the slide which was then viewed using an inverted microscope (Olympus GX41) to ensure a complete vessel cross section had been cut and check that no folding had occurred. The slides were allowed to dry at RT and the tissue block was wiped clean with 100% acetone and a small brush to clear away any tissue debris ready for more samples to then be collected. The knife blade was then moved along horizontally to use a fresh cutting edge after each set of slices had been taken. 20 slices were taken from each vessel sample and stored in slide trays at RT.

3.3.2. Haematoxylin and eosin (H&E) staining

The H&E technique was used to stain vessels taken from CPA and SVA tissue. The slides were placed in a slide rack that can hold up to 10 slides so multiple slides can be treated at the same time. The slides were washed in running tap water for 5mins before placing them in 500ml glass jar that contained Mayer's Haematoxylin for 10minutes. The samples were then washed again in running tap water before washing them in Scott's tap water (see [Appendix I](#) for composition) for 2mins to stain the nuclear chromatin and nuclear membranes blue. The samples were washed again in running water for 5mins before placing them in 1% eosin for 3mins.

After a brief wash in running water the slides were dehydrated using increasing concentrations of alcohol (70%, 90% and 100%) for 2mins each. The samples were then cleared using xylene for 5mins before mounting the slides with glass coverslips which had been freshly coated in DPX mounting medium and the sections were then ready for viewing. A light microscope (Zeiss Axiovert 25) was used to visualise the sections and images were captured using an Olympus DP70 camera and Cell[^]F software (version 2.8). The Cell[^]F software programme also allows for measurements of the vessels including the wall thickness using the software programme for further analysis.

3.3.3. IHC staining for vascular SMC

IHC was performed to localise key proteins of interest in CPA and SVA samples. The frozen sections were placed on a slide rack and immersed in a 500ml glass staining dish with running tap water for 7mins. The slides were then transferred to a glass coplin jar which has been filled with chilled acetone to fix the samples for 10mins. The slides were then washed in 0.1M PBS (see [Appendix I](#) for composition) for 5mins to remove any excess fixative. After air drying the slides each sample was ringed with a DAKO fine wax pen. This ensured that any antibody added would be concentrated over a small surface area while also allowing more than one antibody to be added to the same slide without contaminating neighbouring samples as well as reducing the volume of antibody preparation that was needed to immerse each sample. The slides were firstly blocked with 0.3% H₂O₂ for 20mins to block

endogenous peroxidase activity. After a 5min PBS wash the second blocking agent, 20% horse serum in PBS, was applied for 30mins to block non-specific antibody binding. Following the blocking steps the slides were again washed for 5mins in PBS and placed face up onto a flat tray that was kept moist to prevent sample dehydration. Primary antibody (see [Appendix II](#) for dilutions) was placed on each sample for 2hrs at RT without any shaking. One sample of CPA and SVA was also incubated with multi link control IgG (1:100 dilution) as a negative control and the tray was encased in cling film to ensure the samples did not dry out. Following this, the slides were again washed in PBS for 5minutes, before the samples were developed using the Vectorstain Elite Kit (Universal) (Vector laboratories) following the manufacturer's instructions. This method uses a three stage avidin-biotin complex (ABC) where the avidin has four biotin binding pockets (**Figure 3.3.3-1**). This has the added advantage that the same secondary antibody can recognise both monoclonal and polyclonal primary antibodies raised in mouse, rabbit and goat species. Briefly 100µl of biotinylated secondary antibody was diluted in 5ml 20% horse serum in PBS and one drop was added to the samples and left at RT for 30mins. During this time the streptadavin-biotin complex was prepared by mixing 100µl of solution A to 100µL of solution B and diluted with 5ml PBS. This was left to stand for 30mins in which time the slides were then washed in PBS for 5mins before applying the ABC reagent for a further 30mins.

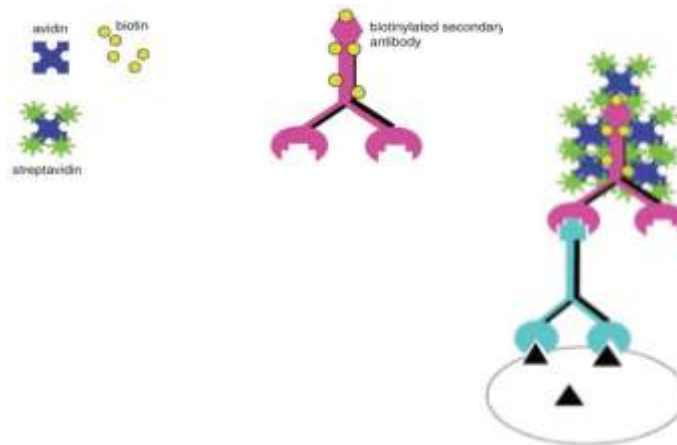


Figure 3.3.3-1 showing the principle behind the ABC complex. The method uses the ABC complex to amplify the signal of the bound secondary antibody. (Image adapted from Hoffman, Le et al., 2008).

After a 5min wash in PBS, fresh 3,3' Diaminobenzidine (DAB) was added to each sample to localise the antigens. 20µl of DAB chromogen was mixed with 1ml buffer substrate and left on the samples for 5mins. Positive immunoreactivity with DAB caused the samples to develop to a brown colour. Following a 5min wash in PBS the slides were counterstained with Mayer's Haematoxylin for 1min which stained any tissue that did not react with the DAB blue. The samples were then washed thoroughly in running tap water for 5mins. The samples were then ready for the final dehydration steps in graded alcohols (70%, 90%, and 100%) for 1min each. The slides were then cleared using xylene before finally mounted using Dpex mounting medium. A glass cover slip (number 1 thickness, 22x50mm, VWR) was placed over the slides which were then left to dry overnight at RT before being imaged. This was repeated at least three times for each sample to confirm the results. A light microscope (Zeiss Axiovert 25) was used to visualise the sections and images were captured using an Olympus DP70 camera and Cell[^]F software (version 2.8).

3.4. Western blotting

3.4.1. Tissue collection

Paired samples of CPA and SVA were collected in order to make direct comparisons of protein expression within the same patient. The matched arteries were then washed in chilled homogenising buffer to remove any traces of blood before snap freezing in liquid nitrogen and storing at -80°C (described in [Chapter 3.2.1](#)).

3.4.2. Control tissue

Women undergoing ELLSCS were also consented for a MYO biopsy (described in [Chapter 3.2](#)). MYO biopsies were transported to the laboratory in chilled PSS and washed thoroughly in homogenising buffer before snap freezing in liquid nitrogen and storing at -80°C. Whole female non pregnant rat brain (RB) tissue was used as a further positive control tissue and was obtained from the Institute of Cell signalling at the University of Nottingham. Briefly adult Sprague Dawley rats were decapitated following the Animal Experimentation Act (1986), and the freshly removed brain was immediately frozen in liquid N₂ and kept at -80°C.

3.4.3. Tissue homogenisation

Samples were removed from cold storage and kept chilled on ice while each buffer was also prepared and kept chilled on ice at all times. Mechanical homogenisation was the best method for turgid muscle tissue such as the MYO which is much tougher to get into suspension when using chopping alone. However a lot of heat is generated with this method which can denature the protein structures that we were interested in separating. As a result it was imperative to keep all the buffers along with the tissue samples chilled at all times. The method involved homogenising the tissue for short spurts and then immediately returning the sample to ice to keep the sample chilled. The first step of tissue homogenisation was to remove the tissue from the storage tubes and place on a glass petri dish placed over an ice bucket to keep the samples chilled. Using a 22 gauge scalpel blade that was kept on ice was used to chop the tissue into small pieces in homogenisation buffer (HB). To further maintain protein integrity the HB was supplemented with protease and phosphatase inhibitors added to fresh HB (see [Appendix I](#) for composition). As a general guide 1ml of buffer was added for every 0.5g of tissue used. The freshly chopped tissue was aspirated using sterile 3ml Pasteur pipette to a 14ml BD Falcon round bottom tube. The advantage of using a round bottom tube was that all the tissue can come into close contact with the homogeniser. The Heidolph DIAX 900 (Heidolph instruments, Schwabach, Germany) hand held homogeniser was then introduced into the tube and switched on for bursts of 1min followed by returning the tube to ice to allow the sample to cool before repeating the homogenisation. This was done until all the

clumps of tissue were in suspension and any tissue that still remained was discarded. Each sample was carefully prepared in this way after which each sample was then passed through a 21 gauge fine needle several times to break down any cells that remained in suspension.

Following the physical breakdown of the protein structures that hold cells together we then used a series of centrifugal spins to separate the cell suspension. The first spin involved a crude spin to remove tissue clumps centrifuging at 1,000g for 10mins at 4°C. The resulting supernatant (supernatant 1) was collected and separated from pellet 1 and transferred to a clean 2ml eppendorf tube, before being centrifuged again at 15,000g (EBA 12R Hettich) for 90mins at 4°C to pellet the cell membranes (pellet 2) and the cytosol (supernatant 2). Pellet 1 was discarded and 200µl of Solubilisation buffer was added to pellet 2 which was also vortexed and sonicated using an Ultra-Turrax sonicator (VWR) for 15mins on ice before being centrifuged again at 1000g, 10mins at 4°C and stored at -80°C. The supernatants 1&2 along with pellet 2 would contain a mixture of crude cell pellets and the preliminary data showed that supernatant 2 produced the best isolation of cell fractions with the least red blood cell (RBC) contamination and was used for all of our subsequent experiments.

3.4.4. Protein determination

The bicinchoninic acid (BCA) assay was chosen and relies upon a change in colour on a reduction of Copper (Cu^{2+}) to Cu^+ in the presence of proteins. Proteins react with alkaline Cu^{2+} to produce a cuprous cation which in turn reacts with BCA to

produce an intense purple pigment. The intensity of the coloured product will be directly linked with the concentration of the protein and can be measured using spectrometry at a peak absorbance of 562nm. A standard curve was then generated based on a known concentration of protein. In the BCA assay the values for the bovine serum albumin (BSA) standards were used to produce a calibration graph and the straight line equation was used to determine the concentration of protein in the test samples (**Figure 3.4.4-1**).

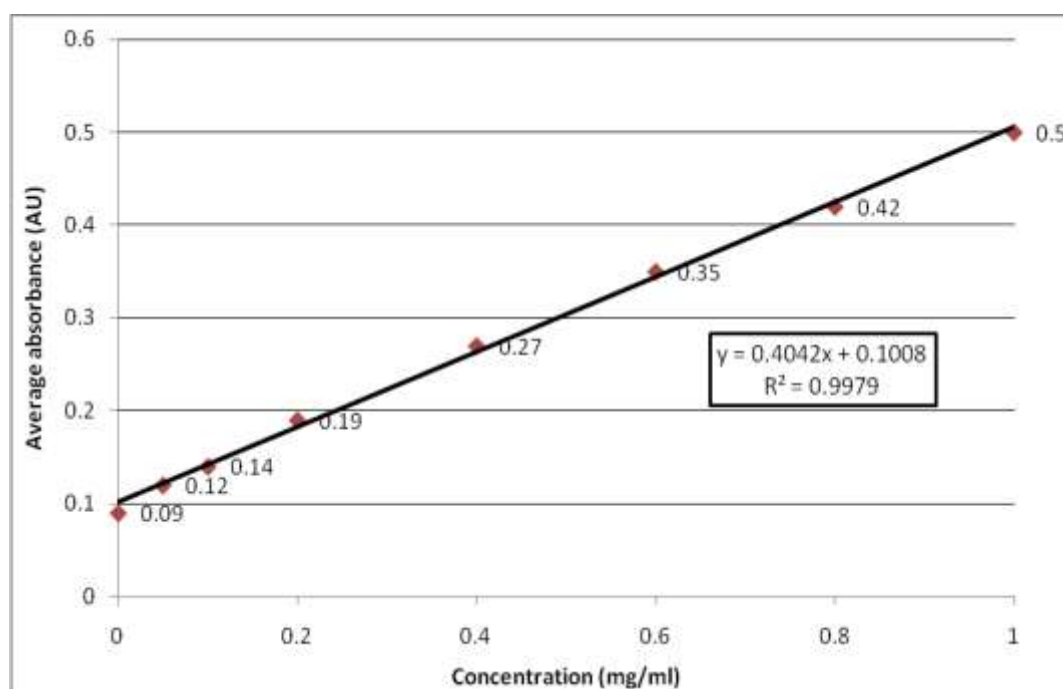


Figure 3.4.4-1 showing the standard curve obtained from BSA controls. This was used to calculate protein concentration of our unknown CPA and SVA samples.

BSA protein standards were firstly prepared at concentrations of 0, 0.05, 0.1, 0.2, 0.4, 0.6, 0.8, and 1 mg/ml from a stock solution of 10 mg/ml of BSA prepared in 0.9% NaCl. A small aliquot of crude cell pellets (pellet 2, and supernatant 1&2) were diluted to 1 in 10 in 0.9% NaCl. 10µl of each sample was added in duplicate to a 96-

well plate along with 200µl of freshly prepared BCA working reagent (BCA with 2% Copper Sulphate (CuSO₄)) was also added to each well. The plate was then left at 37°C with gentle agitation for 30mins. The absorbance was subsequently read at 562nm using a Thermo plate reader (MultiSkan ® Spectrum and Skanlt ® software version 2.2) and the final concentration of samples (mg/ml) was determined.

The final step in preparing samples prior to Western blotting was the addition of a denaturing sample buffer. The bonds that hold the subunits together such as disulphide bridges common to K2P ion channels form large protein structures and need to be disrupted to obtain a quality separation with electrophoresis. This also has the advantage that the buffer protects the proteins from further degradation and further adds colour to the colourless samples to trace their progression on a gel. Samples were diluted in Laemmli loading buffer (see [Appendix I](#) for composition) with the reducing agent 2% 2-β mercaptoethanol (2-βME) (50µl for every 950µl of sample buffer) to achieve a final concentration of 30µg/10µl. 100µl aliquots of each sample were prepared to be used for each experiment to avoid repeated freeze-thaw cycles and stored at -80°C.

3.4.5. SDS PAGE Electrophoresis

The first step in Western blotting is to separate the mixture of proteins within the tissue lysate according to the molecular weight of the proteins. Sodium Dodecyl Sulphate Polyacrylamide Gel Electrophoresis (SDS-PAGE) was developed as a method to separate proteins according to their size and charge (Tiselius, 1937,

Towbin, Staehelin et al., 1979). The Bio-Rad mini-protein II electrophoresis unit was used and the resolving gel (see [Appendix I](#)) was freshly prepared and poured in between two glass plates and left to polymerise for 30-40mins. For the present study a 10% polyacrylamide resolving gel (30% Bis-acrylamide stock solution) was prepared to get a better separation of the larger sized proteins (100-150 kDa) using the method originally described by Laemmli (1970). Hydrated isobutanol was added to the gel to reduce any drying and to prevent any contamination entering from the atmosphere. Once the gel had set, the isobutanol was washed off and a 4% stacking gel (see [Appendix I](#)) was poured directly over the resolving gel and a 10-lane comb was carefully slotted in. The placental CPA and SVA samples along with MYO and RB were removed from -80°C storage and denatured by boiling the samples at 95°C for 5mins before transferring to ice ready for electrophoresis. Kaleidoscope pre stained molecular weight markers (BioRad) were loaded with each gel to monitor the migration of proteins. Equal amounts of tissue lysate were added to each lane and then resolved by electrophoresis on a 10% (w/v) polyacrylamide resolving gel and 4% stacking gel immersed in running buffer (see [Appendix I](#)) for 1hour at 40mA (20 mA for each gel) and has been shown in **Figure 3.4.5-1**.

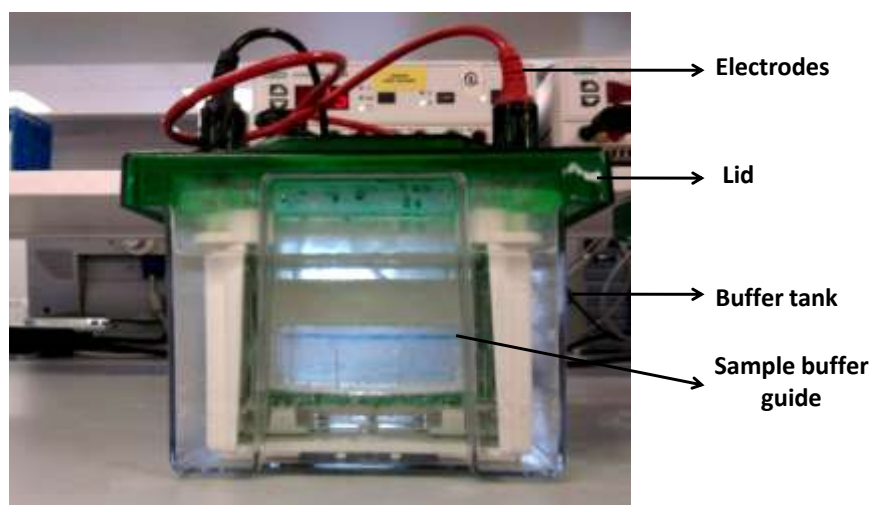


Figure 3.4.5-1 showing the Bio-Rad mini-protein II electrophoresis unit. Each sample was carefully loaded into separate lanes. The blue dye front line shows the migration of the samples and the run was stopped when the dye front reached the bottom of the gel.

3.4.6. Electrophoresis

The next stage required the transfer of separated proteins from the acrylamide gel to a nitrocellulose membrane so that the target proteins can be probed. The method involves using pressure to drive proteins from the negative electrode towards a membrane (nitrocellulose or PVDF) at the positive electrode (**Figure 3.4.6-1**). At this point it was vital to prevent protein damage as the high pressure used generates heat as a waste product and this could damage the protein structures and reduce the quality of the transfer. As a result all transfer buffers were kept chilled, the ice cooling unit was stored at -80°C prior to use and the whole transfer was carried out inside a cold room (4°C). The resolved gels were removed from the glass plate and placed in the middle of a sandwich of filter pads, filter paper along with a nitrocellulose membrane (Geneflow, $0.2\mu\text{M}$ pore size) ready to be electroblotted onto. The

sandwich was then tightly secured inside a cassette and the whole component was held in an electrode module (**Figure 3.4.6-1**) and filled with ice cold transfer buffer (**Appendix I**). This wet transfer prevents the gel from shrinking under the high temperatures that are generated as the voltage is held constant. The electroblotting was carried out using a BioRad wet blot system for 2hrs at 100V constant in a cold room. As the transfer buffer was prone to heating up at this high voltage setting it was replaced with fresh chilled buffer after 1hr. After electroblotting was completed the membrane was removed from the cassette and the proteins could be visualised using non-specific Ponceau S red solution (0.1% Ponceau, 5% acetic acid v/v). The solution was poured over the entire membrane and was used to assess the success of the transfer. The Ponceau S stain was washed out with Tris Buffered Saline (TBS) (pH 7.4) with 0.1% v/v Tween (TBS-T) for 5mins and the blots were then ready for blocking.

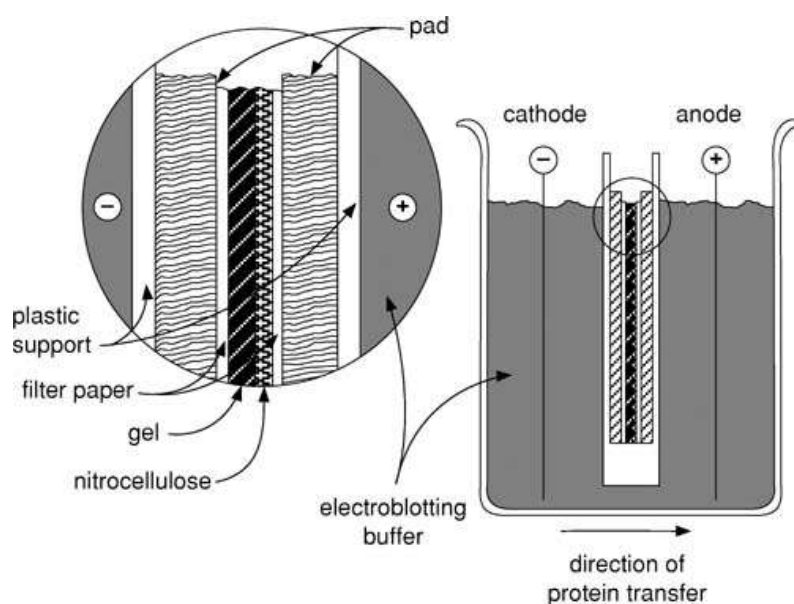


Figure 3.4.6-1 showing the assembly of the transfer sandwich. The entire transfer apparatus was placed in a chilled room to minimise the build-up of heat during the transfer. Image obtained from <http://www.currentprotocols.com/protocol/ns0519>

3.4.7. Blocking & antibody application

Before the proteins could be probed with specific antibodies non-specific binding was blocked. The nitrocellulose membranes have a high affinity for proteins so it was vital to firstly block any unbound regions of the blot with a large protein such as BSA or the equally effective Marvel non fat milk solution. Previous work in the lab has shown that the ideal concentration to use was 7% w/v non fat dry milk (Marvel milk) in TBS-T for 1h at RT with gentle agitation by hand every 10mins. The blots were then washed twice with TBS-T for 1min each before application of the primary antibodies (see [Appendix II](#) for dilutions) prepared in 3% w/v marvel milk/TBS overnight on a gentle shaker at 4°C.

3.4.8. Control peptide blocking

The primary antibodies for each ion channel of interest (Alomone) were each supplied with a control peptide which is designed to validate the specificity of the antibody. The peptide was prepared using the manufacturer's instructions where the peptide was added to an antibody preparation in excess. The peptide will competitively bind to the antibody and as a result prevent the antibody from binding to the target epitope. This should then prevent the detection of the target band in each sample when the secondary antibody is applied. If control peptide was not available, the primary antibody was replaced with control IgG (1:1000) instead.

3.4.9. β actin measurement

Each Western blotting experiment is prone to fluctuations which may be caused by the inconsistent transfer of protein, or protein degradation due to heating. To ensure consistency in the data analysis the total protein content of each sample needed to be quantified. After each target protein was detected the same nitrocellulose membrane was used to detect the house keeping protein β actin (Ferguson, Carroll et al., 2005). The blot was stripped of any bound antibody using a mild alkaline based stripping solution (ReBlot Plus, Chemicon International) for 20mins. The solution was then removed and the blot was once again washed in TBS-T and blocked using 5% marvel milk solution in TBS-T for 90mins at RT. The blots were then washed

twice with TBS-T for 1min each before application of the β actin (1:8000 antibody dilution) prepared in 3% w/v marvel milk/TBS overnight on a gentle shaker at 4°C.

3.4.10. Secondary antibody & data analysis

Secondary antibodies conjugated to an enzyme will initiate a chemical reaction to emit chemiluminescence that can be visualised at a specific wavelength. The alkaline phosphatase (AP) method uses a hydrolase enzyme that removes phosphate groups to initiate a colour change that can be viewed directly using chemiluminescence. The advantage of AP conjugated antibodies is that the enzyme reaction is stable allowing for the blot to be exposed for longer without any loss of the signal intensity. During the course of our studies, the secondary antibody supplied from Dako was withdrawn from production. As a result we obtained an alternative AP conjugated antibody obtained from Sigma used at a dilution of 1:30,000. Each sample was then re-analysed using the new secondary antibody to ensure the accuracy of our initial observations.

After removing any unbound primary antibody with six 5mins washes in TBS-T the blots were incubated with either goat anti mouse or goat anti rabbit AP conjugated secondary antibodies in 3% w/v marvel milk protein/ TBS for 2h at room temperature. The blots were then washed again in TBS-T (6x 5mins washes) and 2x 5mins washes in TBS. The blots were then ready for developing using the nonisotopic chemiluminescent detection system Immuno-Star-AP kit (BioRad). The enhancer and substrate were combined according to the manufacturer's instructions and added

evenly to the nitrocellulose membrane which was then protected from direct light. After 10mins the excess solution was removed and the blot was viewed using a Chemi-Doc imaging system and images were analysed with the BioRad Quantity one software (Version 4.5.1 Build 059). Control blots were analysed alongside and each membrane was exposed for ≤ 5 mins each. The auto expose option stopped the exposure at the same saturation level (315 pixels) after which the background intensity would begin to distort the image and prevent any valid analysis to be completed. Both the average and total band intensities were measured after removing the background intensity levels using the rolling disc option. This was done for each individual lane. The software was also used to approximate the molecular weight of the proteins identified using the pre-stained molecular markers as a general guide. The pre-stained markers were used to primarily assess the efficiency of the transfer, and the different coloured bands provide a rough guide for sizing the different protein bands on the gel. All Western blotting experiments were repeated at least three times for each patient (N) sample and both the mean \pm SEM along with median \pm interquartile range (IQR) were recorded. Protein expression of the ion channels of interest were compared with the Shapiro-Wilk normality test. Multiple means for unpaired samples were compared using two way Analysis of variance (ANOVA) (non-parametric) with *Bonferroni* post hoc test while paired observations were analysed using two tailed students' *t* test (parametric). p values < 0.05 caused rejection of the null hypothesis.

3.5. Culturing SMC

3.5.1. Culturing SMC from CPA and SVA explants

All work was carried out in a sterile Class II bio safety cabinet using aseptic techniques. SMC were cultured using explants of CPA and SVA based on the methodology of Leik (et al., 2004). The isolated tissue segments (described in [Chapter 3.2.1](#)) were placed in warm Hanks Balanced Salt Solution (HBSS) (See [Appendix I](#) for composition). The freshly dissected vessels were then cut down the length of the artery to expose the lumen and 1mm² square pieces were placed with the endothelium facing down on to a 12-well plate. After a period of 2-4mins sufficient Dulbecco's Modified Eagle Medium (DMEM) (See [Appendix I](#) for composition), tissue culture medium supplemented with 10% (v/v) heat inactivated fetal bovine serum (FBS), 100 units/ml penicillin and 100µg/ml streptomycin was added to each well. The culture plates were then left overnight in a 37°C incubator supplied with 5%CO₂/95% air. The media was removed after 24hrs and replaced with 2ml of fresh DMEM added slowly so as not to dislodge the explant. This allowed the explants to adhere to the culture plate and prevent the tissue piece from floating in the medium. Explants that attached immediately showed signs of cell growth in the shortest space of time and gave the highest yield of cells from a single explant (**Figure 3.5.1-1A&B**). Following this initial media change the media was then replaced every 2-3days.

After a period of 3-4wks the growing cells could be sub-cultured by simply removing the explant and detaching the cells to transfer them into a T-25 tissue culture flask. Firstly cells were serum starved overnight to remove any endothelial and fibroblast cells which may be contaminating the population of smooth muscle cells. The cells were then washed twice in HBSS to remove any serum followed by incubation in 0.125% Trypsin-ethylenediaminetetraacetic acid (Trypsin-EDTA) for no more than 3mins. The cells were encouraged to disperse by gently scraping the bottom of the plate with a broad tipped sterile Pasteur pipette in a circular motion. The detached cells were supplemented with FBS and transferred to a 15ml universal and centrifuged at 125g 21°C for 5mins. The resulting pellet was washed for a second time in HBSS to remove any traces of Trypsin-EDTA and finally re-suspended in complete DMEM media and seeded in a new T-25 flask to use in further experiments. Following this first passage further subcultures were restricted to only two further passages.

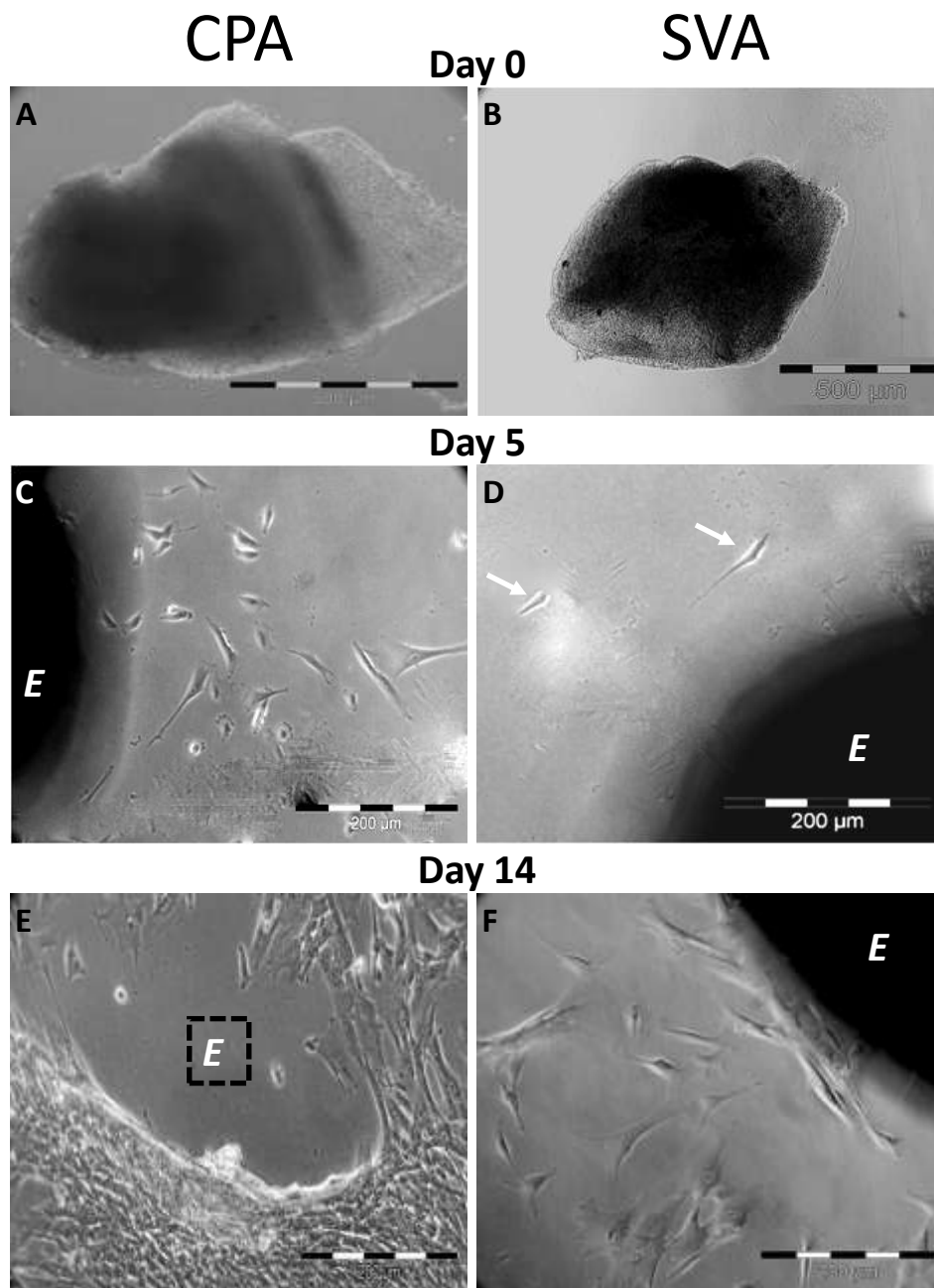


Figure 3.5.1-1 shows culture of SMC from tissue explants of CPA (A) and SVA (B). Cells from CPA explants can be seen after 5 days (C) and reach confluency after 14 days (E). E also shows cells growing in sheets and the clear space in the centre represents the area where the explant (E) once was. In contrast SVA took a lot longer to show signs of cell growth. At the same time point (D) a few isolated cells can be seen (white arrows) around the explant and a smaller population of cells can be seen after 14 days in culture (F). Scale bar 500 μm A&B. 200 μm C-E.

3.5.2. Culturing SMC from MYO

MYO tissue from non labouring patients (described in [Chapter 3.2](#)) was used to isolate SMC to be used as a positive control for the antibodies to be tested. The freshly collected tissue was immediately washed twice in HBSS and transferred to a 60mm petri dish and finely minced in 10ml collagenase A (2mg/ml) in HBSS using a sterile size 22 scalpel blade. The tissue suspension was then incubated with the enzyme solution for 1 hour at 37°C with gentle trituration every 20mins. The cell suspension was then diluted in 5ml HBSS and centrifuged at 100g for 5mins. The resulting pellet was washed and centrifuged again twice in HBSS to remove any cell debris and finally re-suspended in 5ml of DMEM in a T-25 flask. The media was firstly refreshed after 18h and then replaced every 3 days. The cells became confluent after 5 days at which point they were ready for fixation ([Chapter 3.6.1](#)).

3.5.3. SH SY57 cells

The K2P class of ion channels are reported to be highly expressed in mammalian brain tissue (Ketchum, Joiner et al., 1995). As a result further positive control of rat brain cells in culture were also included. SH SY57 cells are a commercially available neuroblastoma cell line originally cultured from human neural tissue and were cultured from frozen cell suspensions that were stored in liquid N₂. The growth media used was Eagle's minimum essential medium (MEM) (supplemented with 1% essential amino acids and 0.5% sodium pyruvate) mixed with

equal amounts of F-12 Ham nutrient mixture (1:1). To prepare the working solution of growth media for the cells MEM/F-12 was supplemented with 15% (v/v) FBS and 100 units/ml penicillin and 100µg/ml streptomycin. Frozen cell pellets were removed from storage (liquid N₂) and thawed immediately before being transferred to a T-25 flask with 5ml growth media. Once the cells reached confluence they were then transferred to a new culture flask (described in [Chapter 3.5.1](#)) and used immediately. The cells used were limited to passages 35-40 and were not re-frozen after the final passage.

3.6. Immunofluorescence (IF) of SMC

In order to confirm the identity of the freshly cultured CPA and SVA explants, cells were stained for markers found specifically in SMC. This included α actin which is expressed by smooth muscle cells while vimentin is expressed in cells of mesenchymal origin and as a result would be predicted to be positive across a range of placental cells. Cells were also stained for markers of the endothelium (von Willebrand factor & CD31), Fibroblast and leukocytes (CD45) to evaluate the purity of our culture population (not shown). In addition to identifying the presence of the key cell markers a range of antibodies raised against the Ca_v1.2, BK_{Ca}, K_{ATP}, and the K2P family of ion channels (TASK 1/3, TRAAK, TREK 1/2 and TWIK-2) were included to determine their expression in placental vascular SMC and a full antibody list along with working dilutions have been summarised in [Appendix II](#).

3.6.1. Fixation of cells

Fixation is the first step that aims to preserve all the cell components and prevent cell damage from cell swelling. For our investigation we sought to examine membrane bound antibodies so it was imperative that this was not damaged during this process. As a result we chose to use paraformaldehyde (PFA) which is the preferred method for examining sensitive proteins that may be susceptible to damage when using more harsh alcohol based fixatives such as acetone/methanol (Ryter, 1988). Briefly cells were seeded at a density of 4×10^5 onto sterile round glass slides (35mm; VWR) which were placed in a 24 well plate in advance. Cells were allowed to reach confluence (usually 1-2days) before being placed in low serum media (2% FBS) and used for fixation. The media was then aspirated off and the cells were washed twice in HBSS followed by two gentle 5min washes in ice cold PBS (pH 7.4, Sigma). Each well was then incubated with 4% PFA w/v (see [Appendix I](#) for composition) for 20mins and any unattached cells were washed off using three short PBS washes. A further permeabilisation step was introduced by treating the cells with 0.5% v/v Igepal in PBS for 15mins at 4°C which helps to aid antibody penetration into the cell body. The detergent introduces small punctate holes into the cell membrane to enable the epitope to cross the cell boundary (Ryter, 1988).

3.6.2. Blocking of non-specific binding sites

Once the cells were fixed they were ready for the blocking stage which is important for preventing any non-specific antibody binding. In the first instance the fixed cells were blocked for the primary antibody with 3% bovine serum albumin (BSA)/1% glycine in PBS for 15mins and then blocked with a mixture of 10% goat and 10% chick serum in PBS. After 1h the blocking solution was aspirated and either a single antibody (either mouse monoclonal or rabbit polyclonal) (see [Appendix II](#) for dilutions) or a cocktail mixture of two different primary antibodies such as α actin & TREK-1 (for dual staining) were freshly prepared in 10% goat serum/10% chick serum in PBS and were added to each well (200 μ l) and left overnight at 4°C with gentle shaking. A negative control was also used where primary antibody was replaced with either control IgG or peptide that had been incubated with the respective ion channel antibody following the manufacturer's instructions (described in [Chapter 3.4.8](#)). On the following morning, excess primary antibody was removed in three 5min washes with chilled PBS.

3.6.3. Secondary antibody application & evaluation

Fluorescent tagged secondary antibodies were used to reveal the location of bound primary antibody. The advantage of this method is that the sample will only fluoresce when an external light source is introduced to excite the electrons (excitation). As the electrons lose this energy they return to the ground state and emit

the gained energy in the form of light which can be imaged using a microscope (emission). Once the light source is removed the sample will return to its unexcited state and for this reason the sample was wrapped in foil to protect it from any direct light in between viewings (Paddock, 2000). The culture plate was wrapped in foil to protect it from direct light and each well was incubated with a cocktail of both anti mouse fluorescein-5-isothiocyanate (FITC) and anti rabbit Tetramethyl Rhodamine Iso-Thiocyanate (TRITC) conjugated secondary antibodies (see [Appendix II](#) for dilutions) in 10% goat and 10% chick serum in PBS for 1.5h in the dark with gentle shaking. The wells were then washed three times in PBS for 5mins each. At this point the nucleus was also stained using fresh DAPI (1:5000 working dilution in PBS). This was added to each well after the final PBS wash for 10mins and then washed repeatedly again with PBS. After the final PBS wash the samples were then left in PBS: glycerol (1:1 v/v) and were then ready for mounting.

3.6.4. Slide preparation

The cells were viewed using a confocal microscope. In preparation for this stage the round glass slides were removed from the 24-well plate using fine forceps and placed face up onto a clean glass slide (76x26x1.2mm VWR). This was then coated with a drop of PBS: glycerol before a second glass coverslip (22x50mm VWR) was carefully placed on top avoiding any air drops that may form. The slides were stored in a slide box at 4°C ready for viewing.

3.6.5. Confocal IF

Confocal microscopy is an advancement of IF and has allowed the generation of 3D images of cells with much higher resolution. The main difference is that light emitted from the specimen is reflected back through a pinhole greatly reducing the background light that can distort images when using IF alone (**Figure 3.6.5-1**). The further advantage with this method is that the microscope gives a much more shallow depth of field and the ability to collect serial optical sections to form a detailed image. The serial sections or Z stacks can then be used to reconstruct the image using image software to reconstruct a 3D image of the tissue or cell (Sheppard and Wilson, 1981, Paddock, 2000). A further benefit for our investigations is that more than one laser can be used simultaneously making it possible to view two differently labelled proteins within the same focal plane.

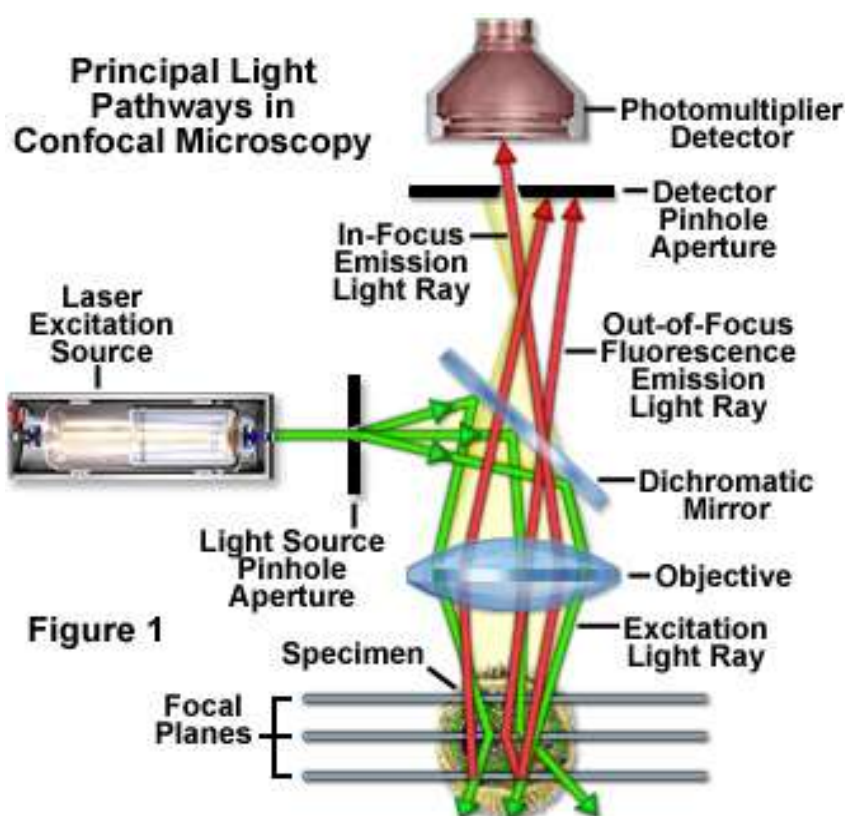


Figure 1

Figure 3.6.5-1 showing how a confocal microscope captures images. The important difference with confocal IF imaging is that a pin hole restricts the amount of background haze that can distort the image and results in a higher resolution image which can be viewed at higher magnifications. Image obtained from <http://www.microscopyu.com/articles/confocal/confocalintrobasics.html>.

Mounted slides were placed face down on the slide stage and viewed using a Leica TCS SP2 confocal microscope with Acousto-Optical Beam Splitter (AOBS) scan head and a 63x glycerol immersion objective lens. Images were captured using three laser lines in single scans to eliminate any overlap between the channels. DAPI IF was viewed using an Ultraviolet laser (372 nm excitation and 385nm emission). FITC was viewed using 488 nm excitation with 505-530 emission (Argon laser) and TRITC was viewed with 546nm excitation and 560nm emission (Helium//Neon laser) (**Figure 3.6.5-2**). Each slide was viewed at 3 different magnifications to focus on a cluster of cells and then narrow down the field of view to then magnify a single cell.

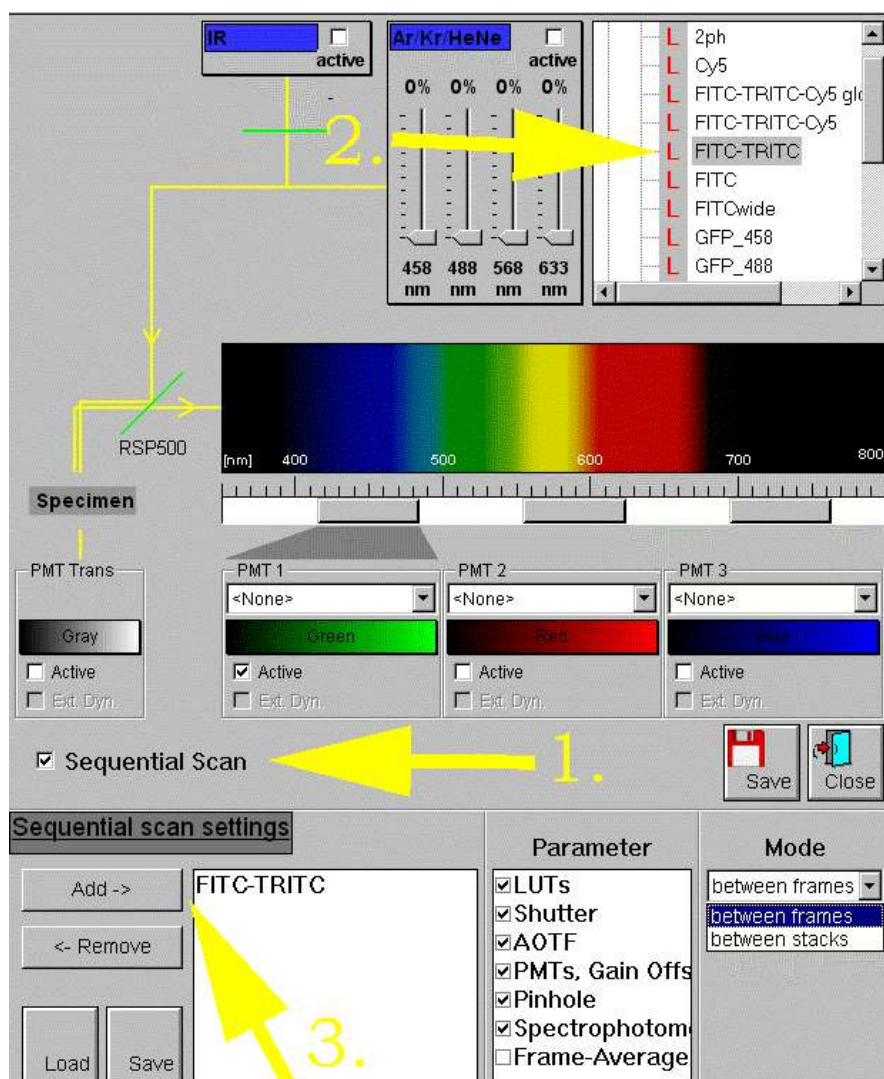


Figure 3.6.5-2 showing the stages involved in capturing the confocal IF image. Once the field of view had been selected a range of options needed to be inputted into the software. **1.** Shows the option for sequential scan as selected. **2.** Shows the filters that have been selected (FITC and TRITC) The wavelength to be examined can be defined to ensure there is no overlap between different lasers. **3.** Shows the order in which the microscope will capture each image between frames so that a FITC and then a TRITC image was taken across the same focal point.

3.6.6. 3D images

Following IF staining using SMC specific markers, we were next interested in investigating the expression of key ion channels that may be involved in the control of placental vascular tone. This was performed using confocal microscopy in order to capture high resolution images of each cell population. A Z stack was taken across the cell at changing depths which can be merged in to a maximal projection to show the cell in its entirety. The separate stacks were also used to create a 3D image of the cell for further analysis. This also allows for high resolution images to be taken of intracellular structures and more importantly to identify the precise location of our ion channels of interest within SMC.

3.6.7. Confocal image analysis

Three representative pictures were taken of each SMC population and Z stacks were collected by taking images at every 2-5 μ m to form a complete image. The separate stacks were then merged to form a single 3D projection and subsequent analysis of the individual distribution pattern for each channel was analysed using Leica Microsystems software (LCS 2.5 1347). Co-localisation of a chosen protein was investigated to determine the interaction with a second protein of interest. This was performed by examining the pixel distribution of the merged images and quantify the amount of yellow colour which represents areas of co-expression. A region of interest (ROI), such as the nucleus, was selected using the Leica software (Leica

Microsystems LCS 2.5 1347) to examine the linear distribution of the stain across the complete image. This was done to help to identify the peak intensities of the IF stain as the objective lens was moved through the cell.

3.6.8. Method optimisation

Two different markers were applied to the same cell to stain for expression of α actin confirming the SMC identity along with the ion channel of interest. This was possible through the use of different fluorescently tagged antibodies that recognise mouse monoclonal (α actin) and rabbit polyclonal primary antibodies (ion channels). The different excitation wavelengths required for each respective fluorescent tagged secondary antibody meant that two different proteins could be localised within the same cell. The nucleus was also labelled using DAPI (blue) in addition to identifying our proteins of interest. However this introduced an additional problem as α actin was also now positive within the nucleus which had not previously been seen when using single IF staining (**Figure 3.6.8-1**) and could not be resolved altering the balance of the filters intensity. One explanation for this may be due to the fact that DAPI is a strong staining molecule and some excess secondary FITC and/or TRITC conjugated antibody has bound to the DAPI molecule. As a result we opted to firstly reduce the concentration of the secondary antibodies (**Appendix II**) and the DAPI step was removed.

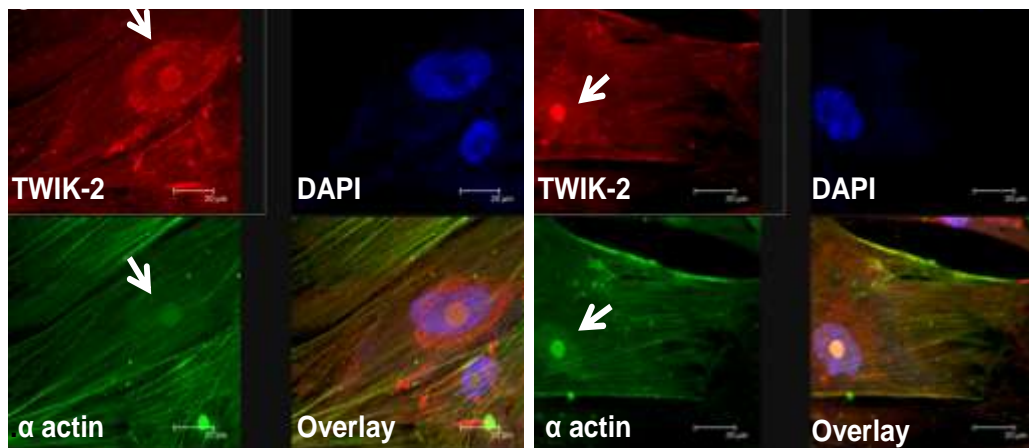


Figure 3.6.8-1 showing confocal microscopy of IF staining along with DAPI to stain the nucleus. The main problem encountered was that both α actin and in this instance TWIK-2 were appearing positive inside the nucleus (white arrows) which had not been seen prior to DAPI staining. As a result this step was removed from the specimen preparation.

3.7. Wire myography

Small vessels (200-500 μ m) offer the most resistance to the flow of blood and set the overall peripheral resistance (Bevan and Osher, 1972, Mulvany and Aalkjaer, 1990). Peripheral resistance will determine the cardiac output, maintain systemic blood flow and regulate organ blood flow. Wire based myography uses ring preparations to observe the mechanical properties of vessels *in vitro* (described in [Chapter 1.9.2](#)). The method involves recording the amount of force (millinewtons (mN)) generated on two parallel wires that have been introduced inside the lumen of the blood vessel. The force generated by the contracting vessel is then translated into isometric tension recordings which can then be analysed (Mulvany and Halpern, 1977, Halpern, Mulvany et al., 1978, Davis and Gore, 1989). The main advantage of this technique is that vessel function can be studied in isolation. This is due to the intrinsic nature of vessels that develop basal and myogenic tone in addition to responding to external factors such as contractile agonists. The method involves dissection of the vessel from its surrounding tissue, before a defined segment is mounted onto two parallel wires that are connected to two jaws.

An important first step with this protocol was to determine the experimental settings for the vessels. Each vessel within the vascular tissue will have its own optimum wall tension, termed passive tension, and increasing the amount of distension on the vessel will increase this tension. The internal vessel circumference has a positive relationship with the passive tension and for our studies the internal circumference needed to be set to a value (defined as L_{100}) to accurately reflect the

circumference of the vessel at which the most active tension is produced while maintaining the conditions the vessel would be exposed to *in vivo*. This is primarily determined by the pressure of blood flowing which for example in adult rat arteries is 100mmHg (13.3 kPa) (Mulvany and Halpern, 1977, Halpern, Mulvany et al., 1978).

3.7.1. Artery preparation

The CPA and SVA were dissected from the whole placenta as described in [Chapter 3.2.1](#). The freshly cut tissue segments were immediately placed in warm PSS bubbled with O₂ (see **Table 3.7.7-1** for the different gas mixtures used). Starting at the chorionic plate, the tissue was then secured onto a 14cm petri dish filled with sylgard, using 25gauge needles, and then gently washed to remove any excess blood. The tissue was then stretched to reveal the translucent connective tissue and white dense arterial matter. The vessel was carefully dissected away from the surrounding tissue using a pair of Dumont microforceps (size 5, WPI) and mini vannas dissection scissors with superfine tips and viewed under a stereomicroscope (Olympus SZ60, Japan) with a fibre optic light source.

The artery sample was then transferred to a 5cm sylgard petri dish and again secured using 25gauge (g) surgical needles. The connective tissue was dissected away from the arterial wall working along the vessel length in a clockwise direction. A small amount of connective was left in place to allow the vessel to be handled during the mounting procedure (described in [Chapter 3.7.2](#)). The clean vessel was cut in to

four 2mm segments using an eyepiece graticule as a guide and transferred to the myograph chamber.

The SVA were identified by continuing the dissection from the CPA. The SVA were then prepared in the same manner as CPA but a slightly different technique was employed to clean the vessel branches. The maternal portion of the placental tissue could be easily cleaned away from the vessels using the blunt end of a pair of dissection forceps to reveal a clean blood vessel. The sample was then transferred to the myograph chamber ready for mounting. The SVA required very little fine dissection and care was taken as to not to make contact with the arterial wall as this often caused an immediate clamping of the vessel lumen. The lumen could not then be manipulated in order to introduce the two fine wires and such vessels were not used for further analysis.

3.7.2. Wire mounted arteries

5ml of warm PSS was added to each chamber of the multi myograph system (Danish MyoTechnologies (DMT) myograph interface 610M version 2.2, Aarhus, Denmark). A 50µm tungsten wire was secured at one end of the jaw with the fixing screws (**Figure 3.7.2-1B**). The vessel was fed on the free end of the wire and positioned in the space between the two jaws before securing the wire with a second fixing screw. Care was taken to avoid any damage or stretching of the vessels to minimise the damage to the endothelium or artery by limiting the amount of vessel handling. A second wire was passed through the lumen and fixed to the opposite jaw

so that the two wires were in parallel and any remaining connective tissue is removed. Both wires were made taut to ensure the vessel segment was fixed in place within the myograph jaw. The remaining vessel segments were mounted in the same way and the myograph and one vessel was used as a time/vehicle control (described in [Chapter 3.7.10](#)). The chamber was continually bubbled with O₂ and the PSS was replenished every 15mins using vacuum suction (**Figure 3.7.2-1A**). The vessel was left to equilibrate for 1hr in oxygenated PSS and gradually heated to 37°C. The temperature of the myograph was continuously monitored with a temperature probe and PSS was replaced each time with equally warm bubbled PSS heated to 37°C using a water bath (SUB6, Grant instruments, Cambridge).

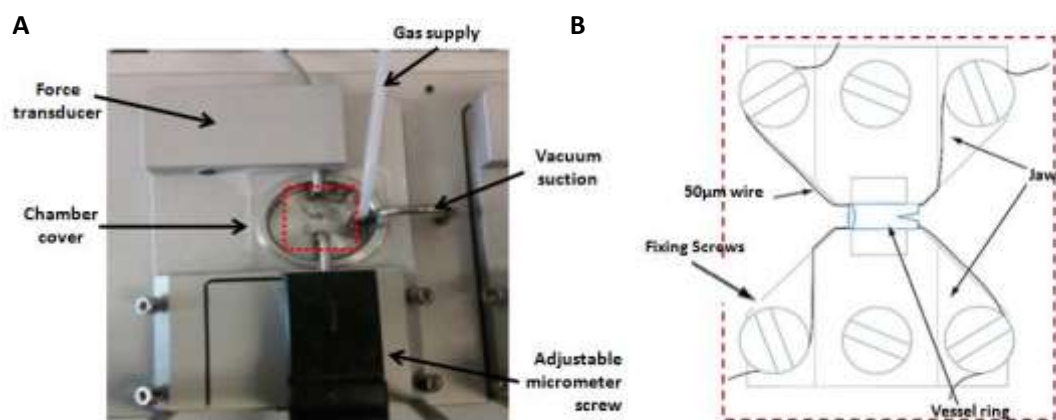


Figure 3.7.2-1 showing an individual myograph chamber. **A** shows the different components that comprise the complete myograph unit. The adjustable jaw is connected to a micrometer which can be used to distend the vessel. The second jaw is connected to a calibrated force transducer to measure the amount of force (mN) generated. **B** shows a vessel segment that has been mounted using two parallel wires. The vessel is positioned within the gap of the jaws and secured in place using the fixing screws (image adapted from www.dmt.dk).

An adjustable micrometer screw was used to separate the jaws and stretch the vessel between the two parallel wires. The calibrated force transducer (see Chapter 3.7.3) measured forces between 0 and 30 mN. The force output was digitized with a PowerLab 8/30 (ADInstruments (ADI)) and LabChart software (ADI, Version 6.0) connected to a PC and data was collected at 10 Hz (Figure 3.7.2-2).

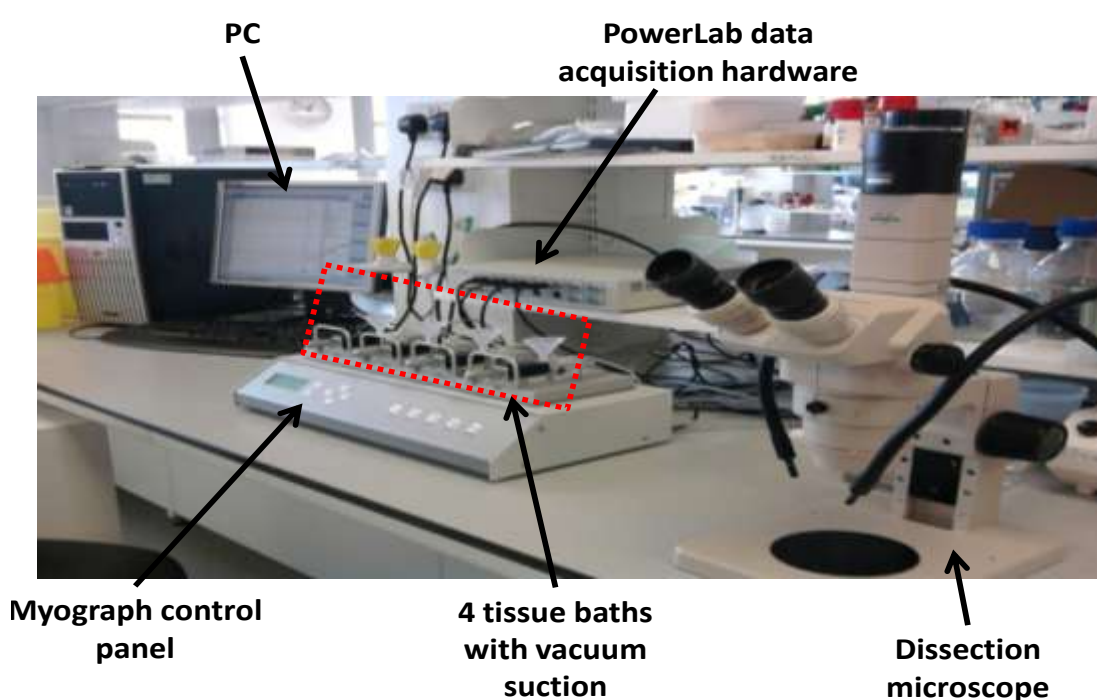


Figure 3.7.2-2 shows wire myograph set-up which consisted of the dissection microscope and multi myograph system (DMT). Drugs and solutions were added directly to each bath and force generated was displayed on the control panel. The PC connected to the PowerLab recorder enabled viewing of the chart recordings in real time as well as storing of the data for further analysis.

3.7.3. Calibration of force transducers

The myography transducers were regularly checked and calibrated on a monthly basis using a myograph calibration kit (ADI). This involved tightly securing

a single wire to the jaw connected to the force transducer and the chamber was filled with warm PSS. The balance needle was secured in between the wire and the jaw and positioned into place over the myograph chamber using the bridge provided. A 2g weight was added to the balance which displayed the predicted force of 9.81mN. This was repeated for each chamber and the calibration was saved as a reference within the LabChart settings file.

3.7.4. Normalisation procedure

Following mounting of the arteries, the next step was to normalise the experimental conditions was undertaken. The aim of this procedure was to firstly standardise the vessels by applying the same target resting pressures and secondly to record the internal circumference of the artery at the set target pressure (see [Chapter 3.7.5.1](#)). The pressure applied refers to the hydrostatic pressures found *in vivo* is referred to as L_{100} . The optimum setting for L_{100} was calculated for placental vessels and have been described in [Chapter 3.7.5](#). The individual internal circumference and segment length were measured in order to calculate the effective pressure (P_i). The segment length was measured using an eye piece graticule and the internal circumference was calculated by measuring the distance between the two parallel wires using a calibrated micrometer screw (**Figure 3.7.4-1**). These readings were then used to calculate the P_i using the Laplace equation (Mulvany and Halpern, 1977).

$$\text{Effective pressure } (P_i) = \text{wall tension} / (\text{internal circumference} / 2\pi)$$

$$\text{Wall tension (mN/mm)} = \text{measured force (mN)} / 2 \times \text{segment length}$$

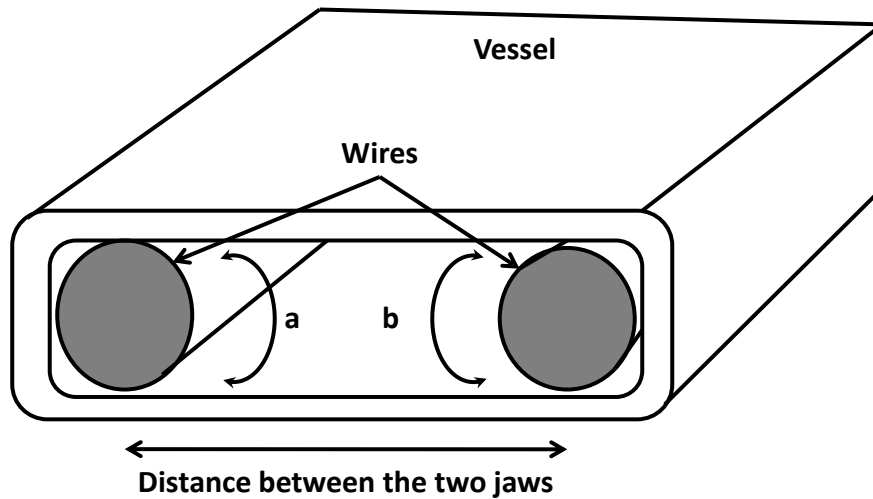


Figure 3.7.4-1 illustrating the parallel sheet that forms when the mounted vessel is gradually distended. Measurements of the circumference of the two wires (a&b) and secondly the distance between the two jaws (determined by the micrometer screw) were needed to calculate the internal circumference.

Gradually distending the vessels increased the internal circumference and resulted in the wall tension also increasing. **Figure 3.7.4-2** shows an original trace recording in real time of the step wise distension of the vessel which gradually increases the wall tension (mN). This was recorded following a 60sec delay and along with the vessel length measurement was then used to determine the effective pressure (kPa) value using the Laplace equation described above.

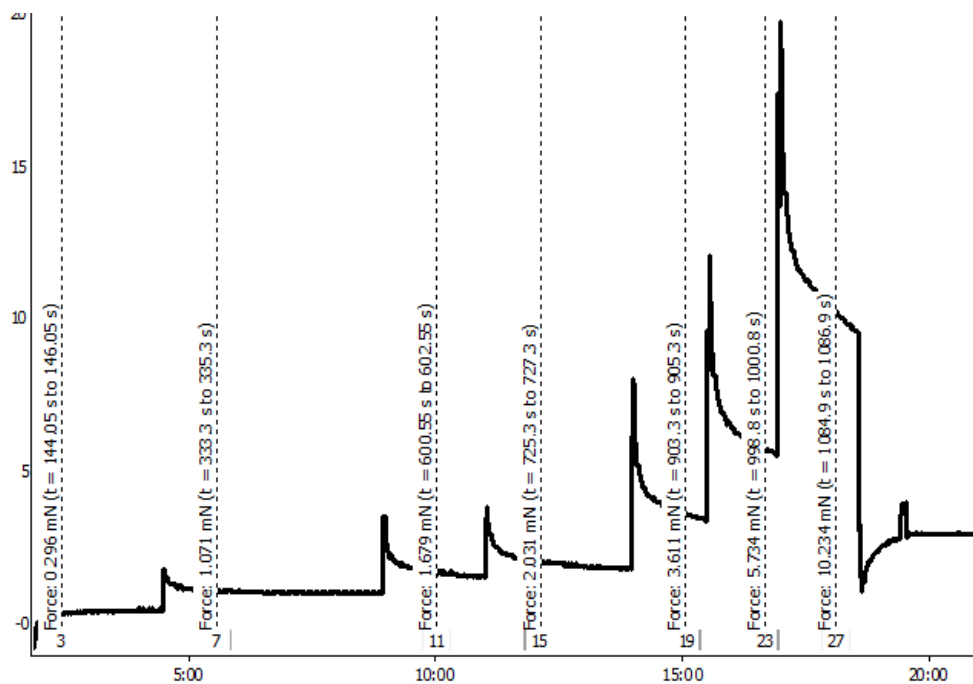


Figure 3.7.4-2 showing an original trace recording as the vessel was subjected to increasing stretch. Each mounted vessel was gradually distended using the adjustable micrometer screw and the force generated was recorded after a 60sec delay. The x axis shows time (mins) and the y axis measures force (mN).

The effective pressure was determined for each distension step using LabChart software. The calibration factors (segment length and wire diameters) were firstly entered along with the micrometer reading. The effective tension was then calculated based on the force generated by the vessel at each step. This was repeated until the target effective pressure was exceeded and an exponential curve was then plotted. The point on the curve that corresponded to our set target pressure was then used to adjust the micrometer screw. The vessel circumference at rest (IC1) and normalised (IC100) were also determined and our target vessel diameters were between 200-500 μ m. Any vessel outside this range were excluded from further analysis. Following normalisation, the vessels were then left to equilibrate for a further 15mins.

3.7.5. Initial experiment settings

3.7.5.1. Determining the ideal resting tension

The resting tension of any vessel is dependent upon the type of artery and the specific tissue from which the vessel has been isolated. At the same time, the physiological responses should closely reflect the conditions found *in vivo* (Mulvany and Aalkjaer, 1990, McPherson, 1992). As a result the first objective was to define a resting tension to ensure our experiments were all standardised to allow for comparisons to be made between groups. The traditional resting tension of **13.3 kPa** (100mmHg) has been described with wire myography studies that have utilised resistance sized adult blood vessels (Mulvany and Halpern, 1977, Mulvany and Warshaw, 1979). However **5.1 kPa** represents the transluminal pressure recorded across the IVS of the placenta and had been used in the literature for examination of placental vessels (Kleiner-Assaf, Jaffa et al., 1999, Wareing, Crocker et al., 2002). As a result we chose to validate the importance of the different resting tensions on CPA responsiveness at the two normalisation values (both at $0.9L_{100}$ see [Chapter 3.7.5.2](#)). The baseline tension at 13.3 kPa was 2.23 ± 0.4 kPa which was significantly higher than the 5.1 kPa baseline pressure of 0.06 ± 0.08 kPa ($p < 0.05$). The passive wall tension contributed to 23% and 7% of the total wall tension generated at 13.3 kPa and 5.1 kPa respectively. The normalised internal diameter of the vessels at 13.3 kPa was $626 \pm 13 \mu\text{m}$ while at 5.1 kPa the internal diameter was $485 \pm 9 \mu\text{m}$ ($p < 0.001$).

A cumulative dose-response curve has been shown in **Figure 3.7.5.1-1** as CPA were stimulated with increasing doses of the agonist U46619 (10nM-1 μ M). A classic sigmoidal dose-response curve was produced under both experimental settings with a dose dependent exponential increase in active effective pressure (kPa) followed by a plateau phase as the vessel reached its maximal response. Altering the normalisation pressure to 5.1 kPa resulted in a significant decrease in the maximal contraction to U46619 and (RM-ANOVA, $p < 0.05$) when compared to each dose of U46619 applied at 13.3kPa. The half maximal (EC_{50}) and sub-maximal concentrations (EC_{80}) of the agonist across the two resting tension settings were compared and found not to be significantly different (**Table 3.7.5.1-1**). The signal to noise ratio was calculated at the two resting tension settings where the active tension (signal (S)) was divided by its standard deviation (SD) (noise (N)). This was found to be greater when vessels were stretched to the 13.3 kPa ($S/N=5.2$) compared with $S/N=2.9$ ($p < 0.05$) at 5.1 kPa. As a result of these combined differences, for the present study CPA and SVA were set to the target transluminal pressure of 5.1kPa for all subsequent experiments. This enabled the maximal response to be observed from the isolated vessels whilst also closely matching the conditions found *in vivo* (Kaufmann, 1982, McPherson, 1992, Wareing, Crocker et al., 2002, Wareing, Greenwood et al., 2003).

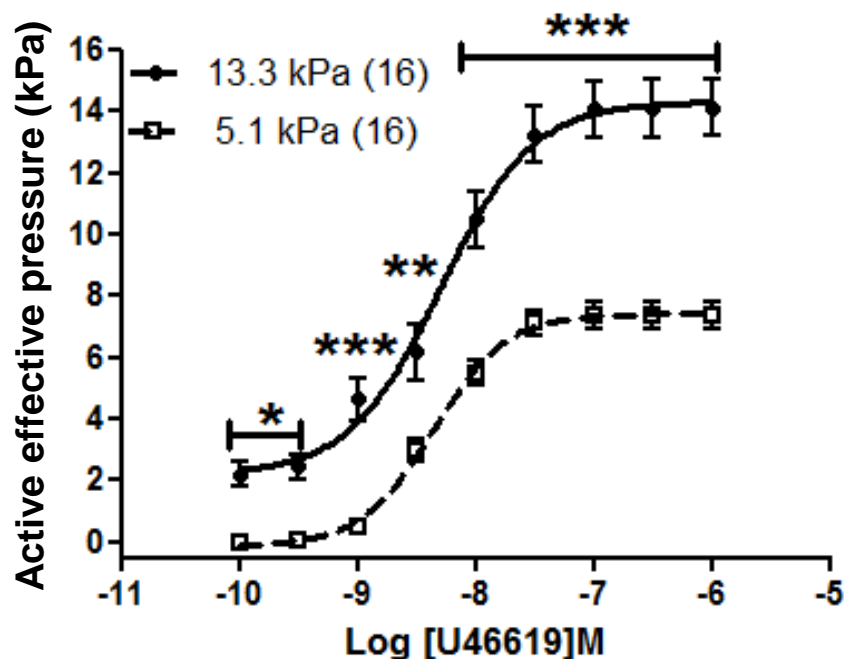


Figure 3.7.5.1-1 shows the dose-response for CPA (N=16) which have been stimulated with increasing doses of U46619. Lowering the resting tension to 5.1 kPa (open squares) caused a downward shift in the dose-response curve. Data points are expressed as mean \pm SEM along with vessels treated (n) from placentae (N). * $p < 0.05$, ** $p < 0.01$, *** $p < 0.001$.

Table 3.7.5.1-1 showing the two resting tension setting and the respective LogEC_{50} and LogEC_{80} values calculated from the U46619 dose-response curve for CPA.

Normalisation pressure kPa (n)	$\text{LogEC}_{50}(\text{M}) \pm \text{SEM}$	p	$\text{LogEC}_{80}(\text{M}) \pm \text{SEM}$	p
13.3 (16)	-8.3 ± 0.2	ns	-7.9 ± 0.3	ns
5.1 (16)	-8.4 ± 0.1		-8.1 ± 0.2	

3.7.5.2. Optimal working diameter (L_{100})

In addition to the resting pressures, the optimum internal diameter settings needed to be determined in order to observe the most active tension of the vessel segments. The optimal working diameter was determined experimentally for both

CPA and SVA in order to find the balance between applying stretch to the vessel and obtaining the maximum reactivity. The extent of stretch applied will determine the active tension that is generated when the vessel is stimulated with an agonist. A series of incremental steps were used to increase the vessel diameter from $0.5\text{-}1.0L_{100}$ (Figure 3.7.5.2-1) (L_{100} representing the circumference of the vessel at rest and exposed to a transmural pressure of 5.1 kPa). At each proportion of L_{100} , the passive tension was recorded after which the vessel was stimulated with a single maximal dose of the agonist U46619 ($1\mu\text{M}$) to measure the total tension generated by the vessel.

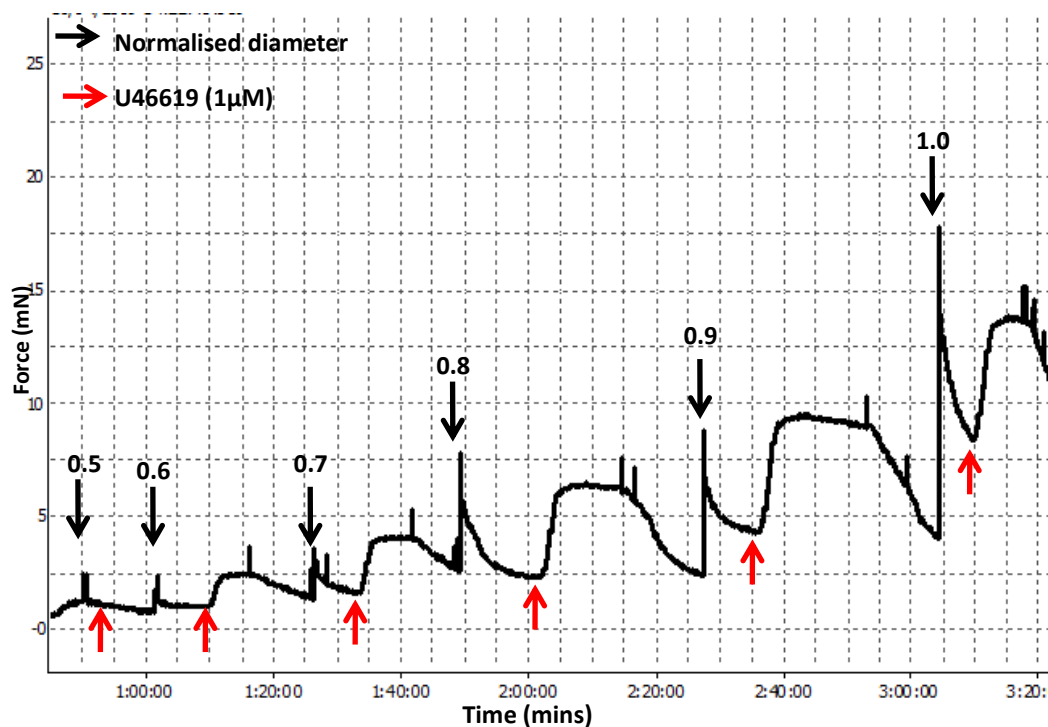


Figure 3.7.5.2-1 showing the experimental protocol for determining the optimum working diameter. The original trace shows each incremental step that was used to adjust the vessel diameters. The black arrows indicate the different IC1 settings. The vessel was stimulated with a single dose of U46619 ($1\mu\text{M}$) (red arrows) and the maximum response was then recorded for each setting. The vessel was allowed to recover before the protocol was repeated at the next normalisation setting which ranged from $0.5\text{-}1.0L_{100}$.

The exponential plots of total and passive wall tensions for CPA and SVA under increasing vessel circumference have been shown in **Figure 3.7.5.2-2**. The difference between the total tension and the passive tension gives a measurement of the active wall tensions generated at each diameter setting. It was found that the active wall tension peaked at $0.9L_{100}$ with both CPA and SVA and further stretching of the vessel caused a decline in the active wall tension. At $1.1L_{100}$ the average active tension was -0.07 mN/mm and 0.03 mN/mm for CPA and SVA respectively. The internal normalised diameter (IC100) also increased exponentially with increasing L_{100} settings and CPA were found to exceed the $500\mu\text{m}$ mark (dotted line) when the internal circumference was adjusted to $\geq 0.9L_{100}$. In contrast the SVA, which also showed a linear increase in vessel diameter peaked at $378 \pm 13.7\mu\text{m}$ with the highest setting. Based on this evidence the vessel circumference was adjusted to $0.9L_{100}$ for both CPA and SVA. At this experimental setting the internal normalised diameter (IC100) was $524 \pm 0.84\mu\text{m}$ for CPA and $329 \pm 13.7\mu\text{m}$ for SVA which was significantly lower ($p < 0.05$).

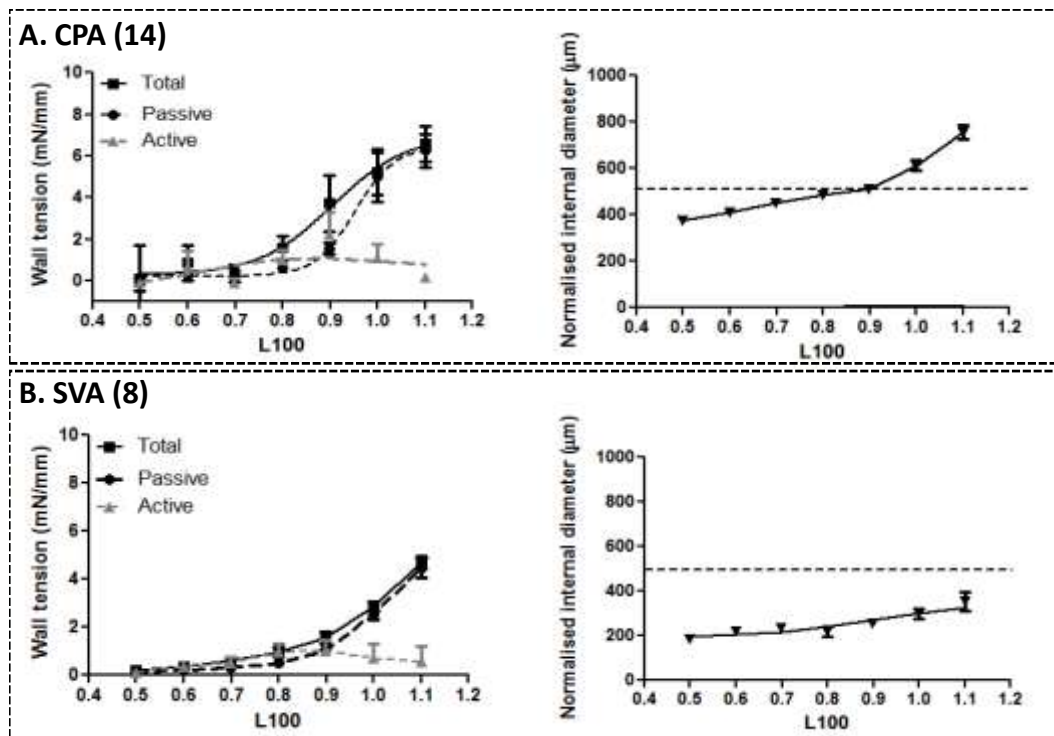


Figure 3.7.5.2-2 shows how the optimal working diameter for CPA (A) (N=14) and SVA (B) (N=8) were determined. The respective total (closed squares + solid black line), passive (closed circles + dotted black line) and active wall tensions (closed triangle + dotted grey line) generated with increasing vessel diameter settings are shown. The exponential curves showed that wall tension increases as the vessel is placed under more stretch and peaks at 0.9_{L100} with both CPA and SVA vessels. The effect of increasing stretch on the normalised internal diameter has also been shown (right panel) where the dotted line represents $500\mu\text{m}$. Data are expressed as mean \pm SEM along with vessels treated (n) from placentae (N).

3.7.6. Assessment of vessel viability

The first contraction to U46619 was used as an internal standard for that individual vessel. The target maximal active effective pressure was $\geq 6\text{kPa}$ with the highest dose of U46619 and was set as the target P_i for all subsequent experiments (Halpern, Mulvany et al., 1978). Any vessel which did not achieve this P_i was excluded from our studies and any vessel which exhibited a 10% loss in contractile activity during the duration of the experiment was also removed from further analysis.

60mM of high K^+ PSS (KPSS) (see [Appendix I](#) for composition) was used to assess the vessel viability at the end of each experiment and has been shown in **Figure 3.7.6-1**. An immediate response was produced as the vessel contracts; however this response was short-lived and the vessel returned to its resting tension. The vessel did not also return to the original baseline and required several washes with fresh PSS to replenish the resting ion gradients. As the KPSS response could potentially alter the K^+ ion concentration within the cells, the KPSS stimulation was used as the final step of each experiment to measure the level of vessel activity that remained intact and any vessel which failed to respond to KPSS stimulation was also omitted from the study.

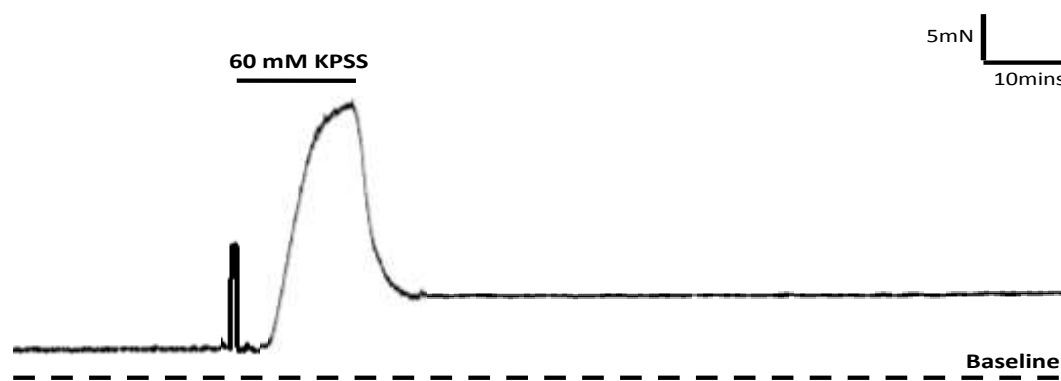


Figure 3.7.6-1 shows the immediate contraction that follows stimulation with 60mM KPSS. The response was short lived as the vessel returns close to its baseline tension. The KPSS stimulation was used at the end of the experiment to assess viability.

3.7.7. Effect of pO_2

The effect of altered partial pressures of O_2 (pO_2) on the responses of placental vessels was also investigated using three different gas mixtures (British Oxygen Company, (BOC) UK) to perfuse the myograph chambers (**Table 3.7.7-1**). At the

lower O₂ settings (5% and 2%) the PSS was replaced each time with warm PSS that had not been freshly bubbled.

Table 3.7.7-1 summarising the different pO₂ settings that were used and the corresponding calculated partial pressures of O₂ (pO₂).

O ₂ (%)	Gas mixture	pO ₂ (mmHg)
20	95% O ₂ /5% CO ₂	156
5	90% N ₂ /5% O ₂ /5% CO ₂	38
2	93% N ₂ /2% O ₂ /5% CO ₂	16

3.7.8. Drugs and solutions

Cumulative dose-response curves were completed using the agonists listed in **Table 3.7.8-1** in 2min increments with a 5min plateau. Drug compounds added to the chamber were made up in stock solutions daily. The total additions of each compound made up <1% of the total chamber volume. Time controls or vehicle controls (diluent only) were also included in each experiment.

Table 3.7.8-1 summarising the different agonists that were used to stimulate placental vessels along with the concentrations applied.

Drug	Diluent	Concentration range applied
1M D-Lactic acid	PSS	pH 7.4, 7.2, 7.0, 6.8, 6.6, 6.4.
1M Sodium Bicarbonate (NaHCO ₃)	PSS	pH 7.4, 7.5, 7.6, 7.7, 7.8, 7.9, 8.0.
Acetylcholine (ACh)	PSS	10 ⁻¹⁰ , 10 ⁻⁹ , 10 ⁻⁸ , 10 ⁻⁷ , 10 ⁻⁶ , 10 ⁻⁵ M.
Arginine vasopressin (AVP)	PSS	10 ⁻¹⁰ , 10 ^{-9.5} , 10 ⁻⁹ , 10 ^{-8.5} , 10 ⁻⁸ , 10 ^{-7.5} , 10 ⁻⁷ , 10 ^{-6.5} , 10 ⁻⁶ M.
Bradykinin (BK)	PSS	10 ⁻¹⁰ , 10 ⁻⁹ , 10 ⁻⁸ , 10 ⁻⁷ , 10 ⁻⁶ , 10 ⁻⁵ M.
Hydrogen peroxide (H ₂ O ₂)	PSS	10 ⁻¹⁰ , 10 ⁻⁹ , 10 ⁻⁸ , 10 ⁻⁷ , 10 ⁻⁶ , 10 ⁻⁵ M.
1M Hydrochloric acid (HCl)	PSS	pH 7.4, 7.2, 7.0, 6.8, 6.6, 6.4.
Linoleic acid (LA)	PSS	10 ⁻⁹ , 10 ^{-8.5} , 10 ⁻⁸ , 10 ^{-7.5} , 10 ⁻⁷ , 10 ^{-6.5} , 10 ⁻⁶ M.
Riluzole (2-amino-6-trifluoromethoxy benzothiazole) (RIL)	Dimethyl sulfoxide (DMSO)	10 ⁻⁹ , 10 ^{-8.5} , 10 ⁻⁸ , 10 ^{-7.5} , 10 ⁻⁷ , 10 ^{-6.5} , 10 ⁻⁶ M.
NS1619	PSS	10 ⁻¹⁰ , 10 ⁻⁹ , 10 ⁻⁸ , 10 ⁻⁷ , 10 ⁻⁶ , 10 ⁻⁵ M
Sodium Nitroprusside (SNP)	PSS	10 ⁻¹⁰ , 10 ⁻⁹ , 10 ⁻⁸ , 10 ⁻⁷ , 10 ⁻⁶ , 10 ⁻⁵ M
U46619 (9,11-dideoxy-11alpha,9alpha-epoxymethanoprostaglandin F(2α))	PSS	10 ⁻¹⁰ , 10 ^{-9.5} , 10 ⁻⁹ , 10 ^{-8.5} , 10 ⁻⁸ , 10 ^{-7.5} , 10 ⁻⁷ , 10 ^{-6.5} , 10 ⁻⁶ M

3.7.9. Measurement of vasoconstriction and vasodilatation

The first contractile response produced by each vessel to a specific stimulus was used to calculate the maximum constriction and normalised to 100%. **Figure 3.7.9-1** demonstrates how the maximum and minimum recordings were taken from the original trace. This was converted to the maximum constriction (100%) using the equation (max-min) and all subsequent responses were measured against the first contraction and expressed as a %.

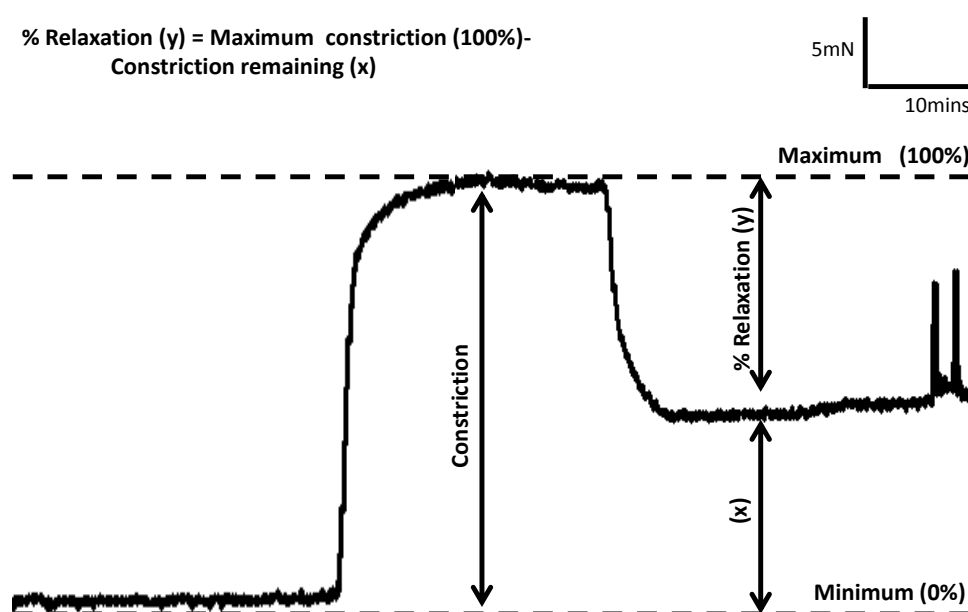


Figure 3.7.9-1 showing how the maximum constriction was measured using the original trace recordings. The maximum tension was subtracted from the minimum/baseline tension and represents 100% constriction. All subsequent contractions were then normalised to this value. For vasodilatation, the % of the contraction that remained was used to give a measure of the total % relaxation across each dose applied (equation).

Relaxation was then measured as the % loss in maximum constriction when a specific vasodilator was applied to the pre-constricted vessels. This measurement was

deduced from the difference between the maximum constriction (100%) and the contraction which remains and has been shown in **Figure 3.7.9-1**.

3.7.10. Drug assessment

A range of ion channel modulators and control blockers were used in our study and have been summarised in **Table 3.7.11-1**. Each compound was added directly to the chamber 20mins prior to stimulation and diffused into the tissue bath. The baseline tension was assessed pre and 5mins post addition of each pharmacological agent. One vessel was used a time control where no further drugs were added to the tissue bath or as a vehicle control where the solvent alone was added. Concentrations applied were based on experiments performed in our lab along with published literature.

3.7.11. Data analysis

The concentration response curves were analysed by fitting the data to the four parameter logistic equation;

$$y = (y \text{ min}) + (y \text{ max} - y \text{ min}) / (1 + 10^{(\log EC_{50} - x)})$$

Where y max is the maximum contraction achieved, y min is the minimum contraction achieved and y is the response. Data were presented as mean \pm SEM with

the number of vessels (n) treated from number of placentae (N). Each separate experimental observation was made using a single patient sample without any duplication, and the former was used for statistical analysis. Retrospective power calculations at 80% difference were performed using the Altman Nomogram (Whitley and Ball, 2002) and a minimum of six independent experimental observations from six different patients were required in order to have sufficient data to observe a significant trend. Normal distribution of the data sets were initially determined using the Shapiro–Wilk normality test. The concentration response curves were plotted and compared using global curve fitting using GraphPad Prism version 5 (GraphPad Software Inc, San Diego, CA, USA). The top and bottom plateaus were constrained and shared and the logEC₅₀ values were compared between groups. Analysis of the pilot data revealed that the fitting of a sigmoidal dose response (variable slope) was the most appropriate choice for constructing a dose response curve and this method was applied for all the subsequent data. Statistical significance between the values was calculated using a one-way ANOVA and the appropriate post hoc test for multiple comparisons was chosen (Dunnett's for the comparison against the time control and Bonferroni comparison for multiple pairs) at each individual concentration of the agonists used. A p value of <0.05 was considered to be statistically significant.

Table 3.7.11-1 summarising the different ion channels blockers that have been used along with the main ion channel that will be inhibited. L-NAME was used to block release of EC dependent vasodilators while NaCl and Choline Cl was used to control for Cl^- and Na^+ ions respectively. The optimised concentrations were based on preliminary experiments.

Drug (Blocker of)	Abbreviation	Concentration	Diluent
4-aminopyridine (K_v)	4-AP	1mM	PSS
Amiloride hydrochloride (NHE)	AMIL	10 μM	PSS
Apamin (SK_{Ca})	APA	10 μM	PSS
Barium chloride (TWIK-2)	BaCl_2	1mM	PSS
Bupivacaine (TASK 1/3)	BUP	200 μM	PSS
Catalase (H_2O_2)	CAT	200U/ml	PSS
Choline chloride ($\text{C}_5\text{H}_{14}\text{ClNO}$)	Choline Cl	125mM	PSS
Copper chloride (TASK)	CuCl_2	1mM	PSS
Curcumin (TREK)	CURC	10 μM	Ethanol (EtOH)
Glibenclamide (K_{ATP})	GLB	50 μM	DMSO
Iberiotoxin (BK_{Ca})	IBTX	200nM	PSS
Lidocaine (TASK)	LIDO	100 μM	PSS
L-Methionine (TREK)	L-METH	1mM	PSS
L-NG-nitro-arginine methyl ester (NOS)	L-NAME	100 μM	PSS
Methanandamide (TASK)	M.ANAN	100 μM	EtOH
Nifedipine (Ca_v)	NIFED	10 μM	PSS
Omeprazole (H^+/K^+ ATPase)	OMP	10 μM	PSS
Ouabain (Na^+/K^+ ATPase)	OUAB	50 μM	PSS
Quinidine (TWIK)	QUIN	200 μM	DMSO
Ruthenium red (TREK)	R.RED	10 μM	EtOH
Sodium chloride	NaCl	1mM	PSS
Tetraethylammonium (K^+)	TEA	5mM	PSS
Zinc chloride (TASK)	ZnCl_2	1mM	PSS

4. Comparing the structure of CPA and SVA

4.1. Introduction

The structure of a blood vessel can reveal important information about its function and the relative distribution of SMC around the lumen can help in understanding the vasoactive responses produced by such vessels. The vessels across the maternal and fetal interface of the placenta will be subject to very different conditions and this may influence the structural development of the vessels. This in turn may have important consequences for vessel function. We hypothesise that CPA and SVA from term placentae have a different cross sectional structure.

4.2. Objectives

- To compare the size and relative wall thickness of CPA and SVA transverse sections.
- Use IHC to examine the distribution of SMC and EC in each vessel type.

4.3. Materials and methods

Freshly obtained samples of CPA and SVA were fixed and prepared for cryostat sectioning using the method described in [Chapter 3.3](#). H&E staining was used

to measure the general structural anatomy of each vessel cross sectional area. IHC was used to examine the mixed cell populations found within each vessel wall. TEM ([Appendix V](#)) was also undertaken to image the vessel cross sections for ultrastructural details.

4.4.Results

4.4.1. H&E of CPA and SVA

A single CPA surrounded by connective tissue has been shown in **Figure 4.4.1-1A** while the SVA image shows two arteries that have been isolated from a single villous branch imaged at the same magnification (**Figure 4.4.1-1B**). H&E staining of CPA revealed the anterior portion bulges out of the chorionic plate. The most striking difference was that the SVA were smaller both in diameter and size in comparison to the CPA when imaged at the same magnifications. The stem villous (SV) veins could be visually distinguished by their larger sized lumens (not shown). Two adjacent SVA along with a single SV vein were consistently found in close proximity to each other which made it difficult to isolate one completely free SVA. **Figure 4.4.1-1C&D** shows the images under higher magnification and the differences in the CPA and SVA lumens can be visualised. SVA appear to have a smaller diameter which was further investigated (see [Chapter 4.4](#)). The EC can be identified

Comparing the structure of CPA and SVA

by a dense stain around the lumen which represents the one cell thick layer of EC and was seen with both CPA and SVA (**Figure 4.4.1-1E&F**).

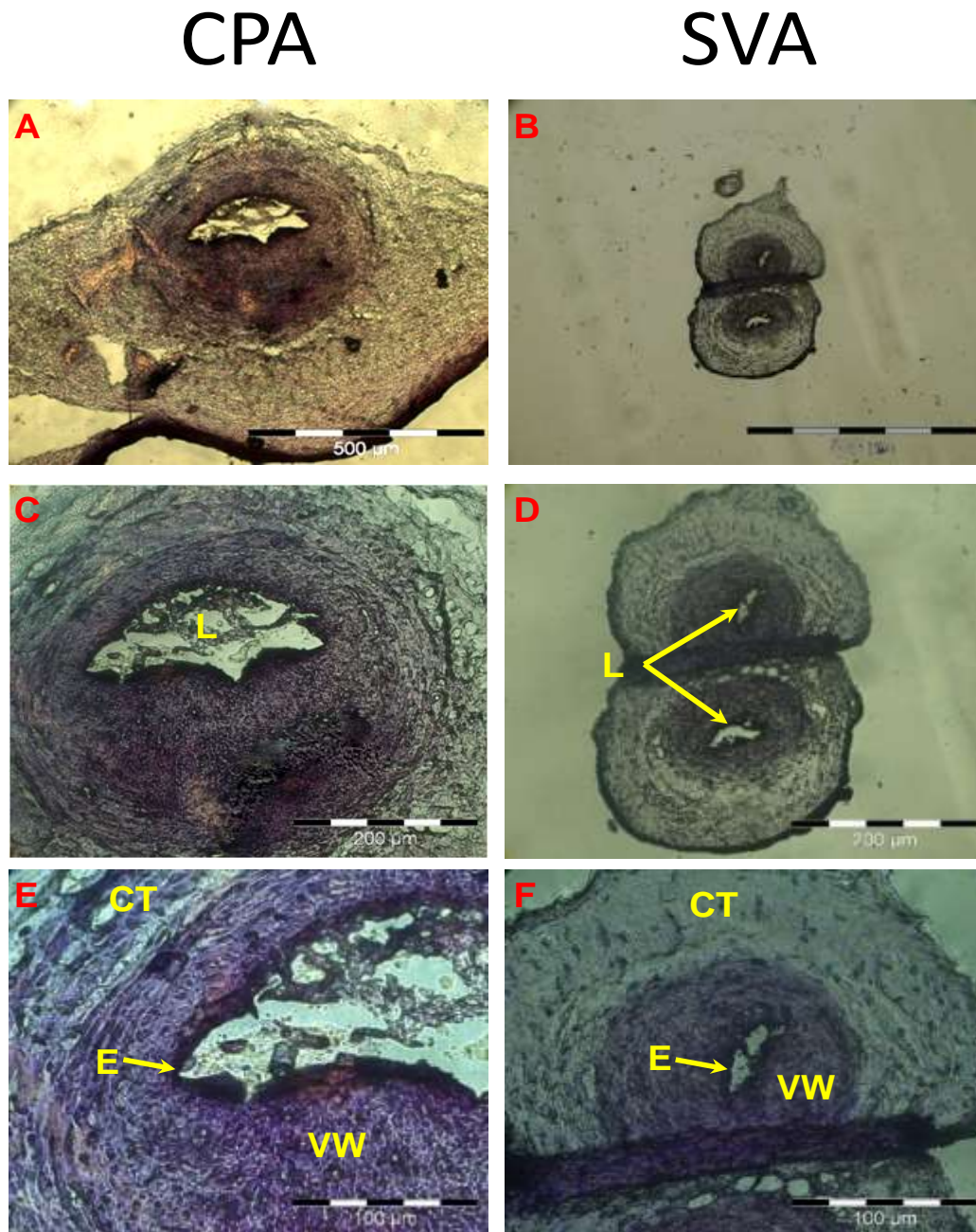


Figure 4.4.1-1 representative H&E staining of paired CPA and SVA 5 μ m thick vessel cross sections (N=12) are shown. A&B show the contrasting size of SVA compared to CPA vessels. C&D show the same cross section viewed at higher magnification. The lumen (L) can be identified in each artery. E&F show the endothelium layer, which can be distinguished as the dense coat at the margin of the vessel lumen, is intact in both vessels (arrow). Connective tissue (CT), Endothelial layer (E), Lumen (L), Vessel wall (VW). Scale bar 500 μ m A&B, 200 μ m C&D, 100 μ m E&F.

The H&E images showed an uneven distribution of cells in the CPA wall. The wall thickness of CPA and SVA was calculated using the Cell[^]F software programme (Chapter 3.3.2). CPA were orientated so that the anterior section (the fetal facing portion) was compared to the posterior portion, representing the part of the vessel that is embedded inside the chorion (Figure 4.4.1-2). Figure 4.4.1-3A shows the contrasting size and structure of CPA and SVA which represent the different regions of the placenta the vessels were taken from. Comparing the wall thickness showed that the posterior section of CPA, but not SVA, was significantly thicker ($p < 0.001$, $N = 10$) when compared to the anterior portion (Figure 4.4.1-3B). The ratio of wall thickness in CPA anterior to posterior portions was 1:5 while in SVA tissue the ratio was 1:1 as an even distribution of cells around the vessel lumen was observed with SVA, regardless of vessel orientation.

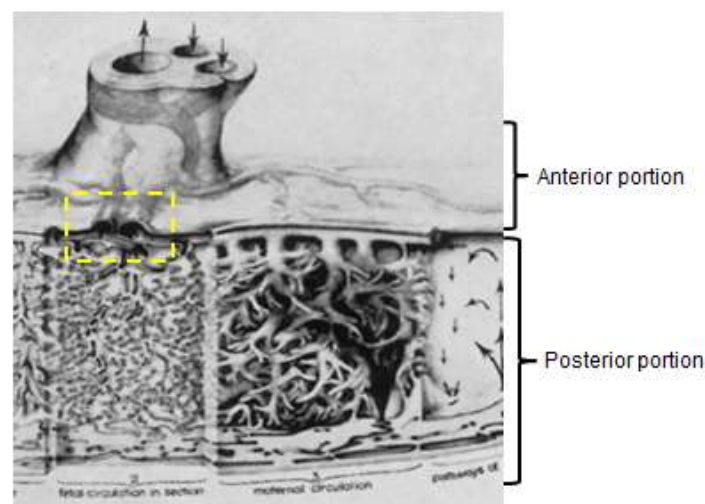


Figure 4.4.1-2 showing the orientation that was used of CPA as found within the placental bed (yellow box). The anterior portion can distinguished from the posterior portion which is embedded within the basal plate. (Image adapted from Benirschke, Kaufmann et al., 2006).

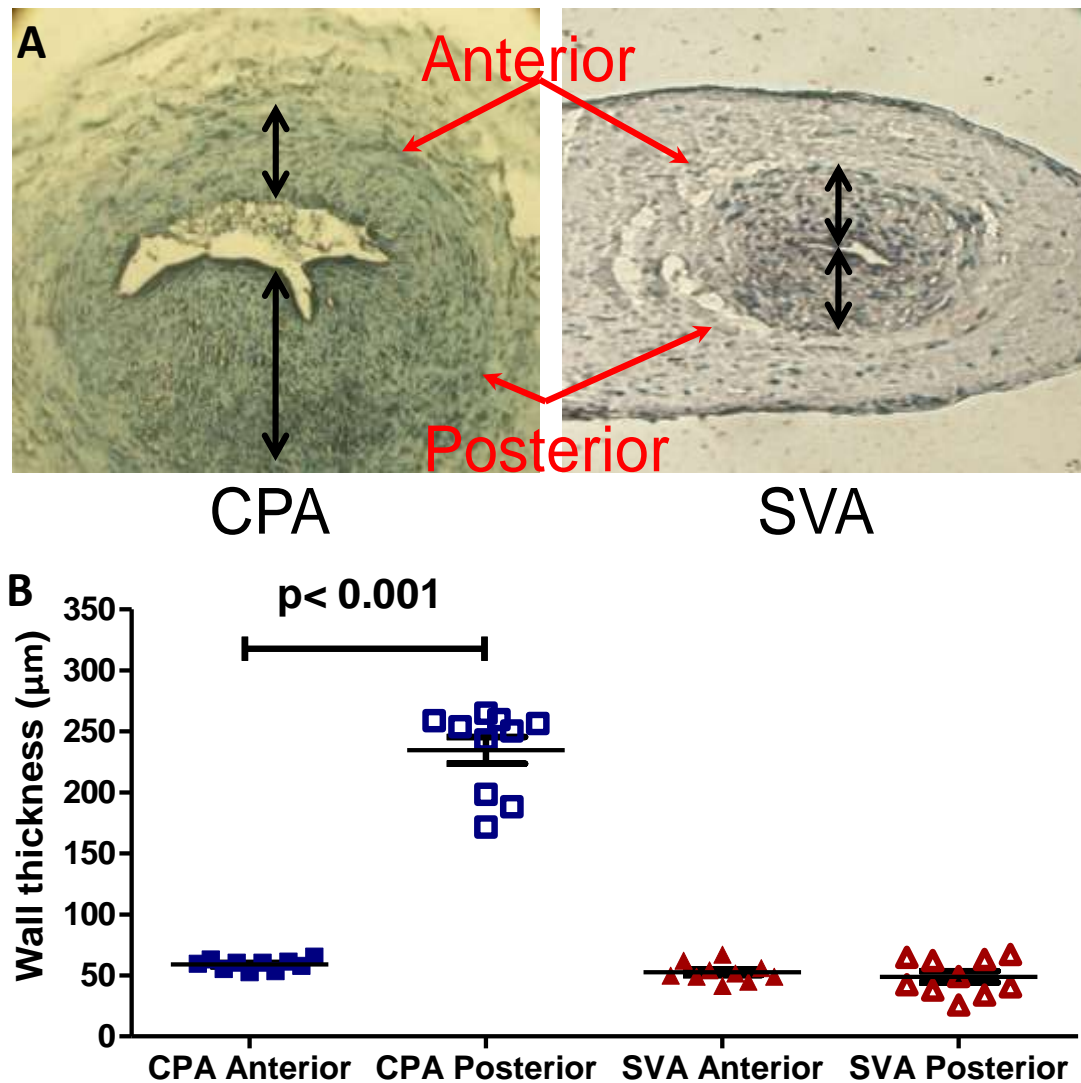


Figure 4.4.1-3 A shows from where the wall thickness measurements were taken to compare the anterior (fetal facing) to posterior (maternal facing) sections of the artery for each matched sample. B shows the scatter graph of wall thickness recordings for CPA and SVA paired samples (N=10). The CPA showed a significant thickening of the posterior section of the blood vessel ($p < 0.001$) and this was not seen with SVA.

4.4.2. IHC to identify SMC

Following H&E staining of isolated CPA and SVA the individual cell layers that comprise each vessel type using specific cell markers were identified. Immunostained frozen CPA and SVA tissue slices were positive for the SMC marker α actin (**Figure**

4.4.2-1). Immunoreactivity was localised to the vessel wall while the surrounding adventitia remained unstained. The blood vessels consisted mostly of SMC as cytokeratin, vimentin and fibroblast markers were all negative in both CPA and SVA (not shown). The endothelial markers CD31 and Von Willebrand also failed to produce a positive stain (not shown) which was unexpected as the H&E imaging shows the EC is present. As a result the vessels were imaged under higher magnification using TEM ([Appendix VI](#)) in order to determine if the EC layer was intact in both CPA and SVA.

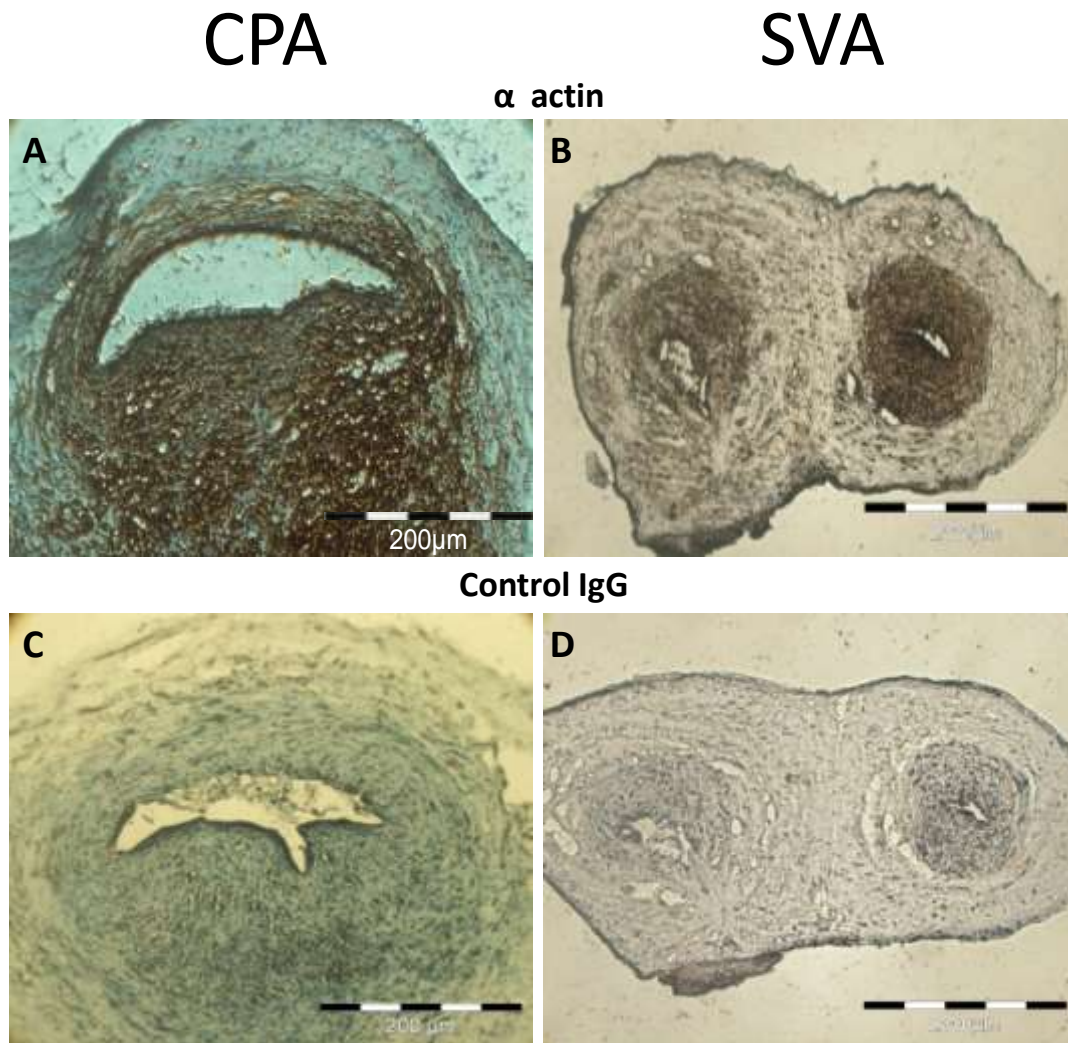


Figure 4.4.2-1 showing positive staining (brown) of CPA (A) and SVA (B) with α actin (N=8). The stain is produced predominately in the vessel wall and the surrounding connective tissue remains unstained. Substituting primary antibody with control IgG (C&D) produced no stain confirming the specificity of the antibody used. *Scale bar 200 μ m A-D.*

4.5. Discussion

The data presented in this chapter has shown that important structural differences exist between the small arteries of the placenta which may depend upon the region of the placenta that is sampled. Importantly, very few studies have made direct comparisons with paired patient samples which are important for understanding

patient specific differences that may exist in placental function and to which the placenta adapts differently. H&E staining of CPA and SVA cross sections showed differences in the structural make up of each vessel which can be explained by the very different functions served by the different vascular beds. CPA found at the fetal interface of the placenta, emerging from the umbilical cord, are required to cope with the transfer of large volumes of blood. As a result they require a large lumen that is supported by a thick layer of SMC to help keep the vessel diameter constant. This was confirmed in every one of the 10 paired samples that were analysed and is consistent with features described in other studies (Fujikura and Carleton, 1968, Weser and Kaufmann, 1978, Kaufmann, Sen et al., 1979). In contrast, SVA are found at the maternal barrier and require thin vessel walls to increase the surface area for exchange when they come into close contact with maternal blood which is at a higher pO_2 . It was found that each villous branch contained vessels that were in very close proximity to each other and thus made it difficult to isolate a single artery cleanly. This was in contrast to CPA and shows how the placenta can regulate the growth and differentiation of different vascular beds according to the function that is required in that specific tissue layer (Robertson, Brosens et al., 1973, Benirschke and Kaufmann, 1995, Poston, McCarthy et al., 1995, Benirschke, 1998, Nikkels, 2007). IHC showed that vessels were negative for markers of cytokeratin and fibroblast while the two EC markers Von Willebrand and CD31 were also negative which was unexpected. This could reflect the rigorous cutting process used to prepare the vessels for staining (discussed in [Chapter 4.5](#)). The CPA wall thickness was dependent upon the orientation of the vessel within the chorionic plate bed as the fetal facing wall of the

CPA was significantly thinner compared to the maternal facing posterior section of the vessel and agrees with the findings of Fujikura (et al., 1968). In this study, IHC staining showed that the vessels were rich in SMC which was confirmed by the positive staining for α -actin. Evidence of atherosclerosis and hyperplasia were also observed, which would be expected as full term tissue that has reached its full growth potential was being examined. The structural make up of a blood vessel will have important consequences for vessel function. Our data has shown that vessels at the fetal maternal interface of the placenta can be histologically distinguished as the CPA and SVA have distinct phenotypes. These differences may reflect different blood pressures, blood flow, hormones or local factors experienced by the very different vascular beds across the fetoplacental cross sections (Sweeney, Jones et al., 2006). For example the thin walled part of CPA may be stressed more by blood flow and amniotic fluid pressure and presents another challenge for the vessels to adapt to. In contrast the posterior portion of the vessel will be more stable and may be the main regulator of the vessel diameter. This flexibility in vessels is also seen in arteries from joints and muscles, both of which are examples of tissue that require flexible movement (Fujikura and Carleton, 1968, Mulvany and Aalkjaer, 1990, Benirschke and Kaufmann, 1995, Benirschke, Kaufmann et al., 2006, Cindrova-Davies, Yung et al., 2007, Mulvany, 2007) .

It has previously been reported that CPA from healthy pregnancies, have a distinct phenotype with thickening of the SMC layer only at the maternal facing portion of the vessel. This was first reported in CPA by Fujikura (et al., 1968) and later in CPV also by Fujikura (et al., 1990). Their data showed that the uneven

distribution of tissue around the lumen was a normal feature of placental surface vessels and not associated with a pathological condition. The important observation made was that this feature was present in all of the 110 samples analysed and appears after 17wks of gestation. The uneven spread of SMC around the lumen was only reported in arteries and veins <300µm in diameter, as chorionic plate vessels that branched further into the placenta did not carry this phenotype. Furthermore, the explanation put forward was that the asymmetrical pattern of cell layers around the lumen is the result of vessel thinning through cell shedding on one side of the blood vessel (Fujikura and Carleton, 1968, Fujikura and Hosoda, 1990, Nikkels, 2007). This histological feature is only seen with vessels immediately beneath the amnion and may actually help to anchor the vessels onto the basal plate as they are vulnerable to damage from fetal movements. It may also explain why this feature is only seen after 17wks as this is the time when the fetus is growing rapidly in size and will inevitably press against the placenta (Fujikura and Hosoda, 1990, Benirschke and Kaufmann, 1995, Babawale, Mobberley et al., 2002).

SVA set the resistance for the rest of the fetal placental vessels and come into closest contact with maternal blood to exchange vital growth products for the placenta and fetus (Kaufmann, Mayhew et al., 2004). IHC examination of SVA has been carried out by Tanka (et al., 1999) who showed that SVA are very different from SV veins. Both SV vessels had circular SMC that were surrounded by longitudinal collagen fibrils, with the crucial difference that the SMC population was greater in the SV veins compared with the SVA. This difference in vessel structure would favour blood to flow towards the baby and the dense collagen layers may function to keep

the vessel length constant when the SMC contracts. There were also local differences in the phenotype of both arteries and veins and this could be attributed to the release of different local factors such as hormones, endothelial factors, pH, and lactate or CO₂ levels. Blood flow varies greatly within the placenta and presents different challenges to the blood vessels which need to autoregulate the vessel diameter in response to these different insults (Robertson, Brosens et al., 1973, Kaufmann, Sen et al., 1979, Tanaka, Kuwabara et al., 1999).

It is important for maternal and fetal blood products to be kept apart to avoid an immune response while at the same time the barrier between the two circulatory systems needs to be thin enough to allow exchange to occur. At term the syncytiotrophoblast can be as much as 2µm thin and any stress to the cell layers could damage this and rupture the barrier which is a risk linked to PE (Brosens, Robertson et al., 1972, Myatt, 2002, Baker and Kingdom, 2004, de Luca Brunori, Battini et al., 2005). It would be interesting to see if there are any structural differences in samples from stressed pregnancies as Cindrova-Davies (et al., 2007) has shown that labouring and non labouring placenta have different markers for oxidative stress. Furthermore, Stanek (2009) also described evidence of hypoxic lesions in placental samples from diabetic, PE and still birth pregnancies. There is also evidence of tissue distortion that is age dependant as the placenta grows and matures. By its very nature the placenta has a high metabolic rate and there is supporting evidence of oxidative stress occurring in healthy placental tissue samples (Zhou, Fisher et al., 1997, Jauniaux, Watson et al., 2000, Burton, Jauniaux et al., 2009).

These studies demonstrate the importance of studying normal tissue to then have a basis with which to compare compromised pregnancy samples. However, there is a need to further develop the methods used in this study. The vessels used in this analysis were fixed immediately following tissue isolation. However the vessels should have been placed under pressurised conditions, before fixation, to allow the vessel wall thickness to be accurately measured. The observation that CPA had an uneven wall thickness could be due to loss of tissue structure as the vessel has been removed from its supporting connective tissue, which can be elucidated to by using pressurised vessels instead. In addition CD31 and Von Willebrand which are both EC markers, failed to produce a positive stain which suggests that there was a problem with antigen retrieval method. This issue would need to be resolved successfully before we could consider moving on ion channel antibodies. One alternative is to use a heat based antigen retrieval instead of the enzyme digestion method that we used. This involves heating the samples to promote cross linked epitopes to unfold and has been shown to improve IHC staining (Shi, Key et al., 1991). In this method the samples would require paraffin fixation instead of freezing which would help the samples to retain their structure. However, the drawback of high intensity heating of small structures like blood vessels is that the samples melt off the glass slides. This could be resolved by taking square blocks of tissue to examine a group of vessels rather than focussing on one isolated vessel. A further extension to the data presented in this thesis, is to show histologically, arteries from veins, which were easily distinguished by their differences in structure wall thickness. The makers Von

Willebrand, CD34 and CD31 should also be explored further to support this observation.

4.5.1. Conclusion

In summary our data has shown important morphological differences between CPA and SVA which help to understand the different responses produced by the vessels to different stimulants. Furthermore we observed that CPA have a distinct phenotype with vessel wall thickening restricted to the posterior portion of the vessel wall and supports our hypothesis. In contrast, SVA have a tubular appearance with an even distribution of SMC around the lumen. IHC staining showed that the vessels are rich in smooth muscle α actin and H&E imaging showed the presence of intact EC which will be important for our functional studies (see [Chapter 5](#)).

5. Assessing the functional characteristics of CPA and SVA

5.1. Introduction

The placenta needs to maintain a low resistance system to deliver sufficient O₂ and nutrients to the fetus. Blood vessels within the placenta respond to challenges in maternal blood supply by altering the vessel diameter. There is also evidence to show that the response in particular of the CPA and CPV is dependent upon the level of oxygenation (Hampl, Bibova et al., 2002, Wareing, Greenwood et al., 2006a) but this has yet to be determined with SVA. The hypothesis to be tested is that CPA and SVA from across the fetomaternal interface of the placenta will respond differently upon stimulation with the same agonists and this response is influenced by pO₂.

5.2. Objectives

- Define the optimal conditions required to study the functional response of placental resistance arteries.
- Assess the vasoconstriction and vasodilatation properties of arteries sampled from the CPA and SVA.
- Determine the influence of pO₂ in mediating the responses to various stimuli.
- Investigate the effect of ROS and pH stress in CPA and SVA.

5.3. Materials and methods

Arteries from the CPA and SVA were prepared for wire myography ([Chapter 3.7](#)) in order to gain functional information, at the normalisation setting of 0.9_{L5.1kPa}. Dose-response experiments were performed using the agonists listed in **Table 3.7.8-1** under changing pO₂ settings (**Table 3.7.7-1**).

5.4. Results

5.4.1. Sample number

A total of 508 CPA (n) from 134 placentae (N) were included in our functional studies and displayed a 95% viability rate (described in [Chapter 3.7.6](#)). A further 27 placentae (N) were used to isolate SVA and from the 105 SVA (n) that were successfully mounted only 46 (44%) proved to be viable for use in wire myography analysis.

5.4.2. Vessel size

The internal diameter when vessels were maximally relaxed (IC1) was $418 \pm 12.3\mu\text{m}$ for CPA (n=96) and $261 \pm 9.6\mu\text{m}$ for SVA (n=46, $p < 0.001$, Mann Whitney U test (MW-U)). **Figure 5.4.2-1** shows the scatter plot of the spread of vessel sizes

included in our study. CPA were taken from the 4th branch following the umbilical cord artery branching and consistently had a diameter within the 200-500 μ m range for resistance sized vessels. The SVA had a significantly smaller diameter ($p<0.001$) and had a narrower IQR when compared to the CPA population.

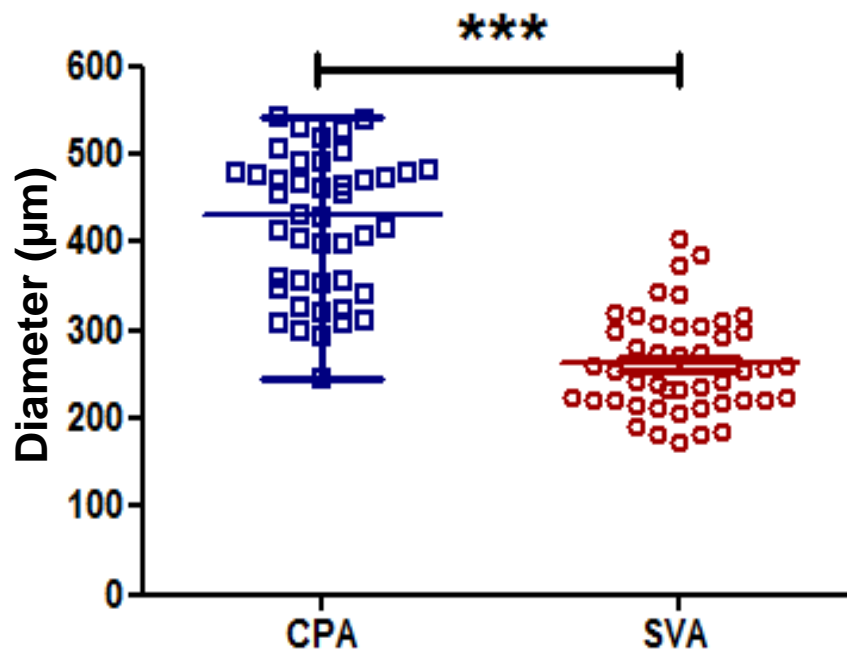


Figure 5.4.2-1 Showing the scatter graph for the internal diameter (μ m) values for CPA (N=96) and SVA (N=46) at rest (IC1). Data are shown as median \pm IQR *** $p<0.001$.

5.5. Pharmacological investigations with CPA

5.5.1. Response to contractile agonists

5.5.1.1. AVP

The first contractile agent investigated was AVP which triggered a dose dependent response with a maximal response ($101 \pm 5\%$ of the KPSS contraction) at the highest dose tested. However there was a partial loss in the maximum constriction as the response did not stabilise (not shown). The contraction was not sustained nor reproducible with each subsequent stimulation so an alternative contractile agent was investigated.

5.5.1.2. Thromboxane mimetic U46619

Administration of the thromboxane mimetic U46619 produced a potent contraction ($145 \pm 2\%$ of the KPSS contraction) that was stable for prolonged periods of time with no evidence of a loss in contraction. This desired stable contraction made U46619 our agonist of choice for use in our time controlled experiments when studying the vasodilatation responses. The dose-response curves for AVP and U46619 have been summarised in **Figure 5.5.1.2-1**. The contractile response was immediate in

response to U46619 and achieved significance at $10^{-7.5}$ M and 10^{-7} M. The EC_{50} values for the two agonists have been summarised in **Table 5.5.1.2-1** and a lower concentration of U46619 was required to gain 50% of the maximum contractile activity of CPA although this was not significant.

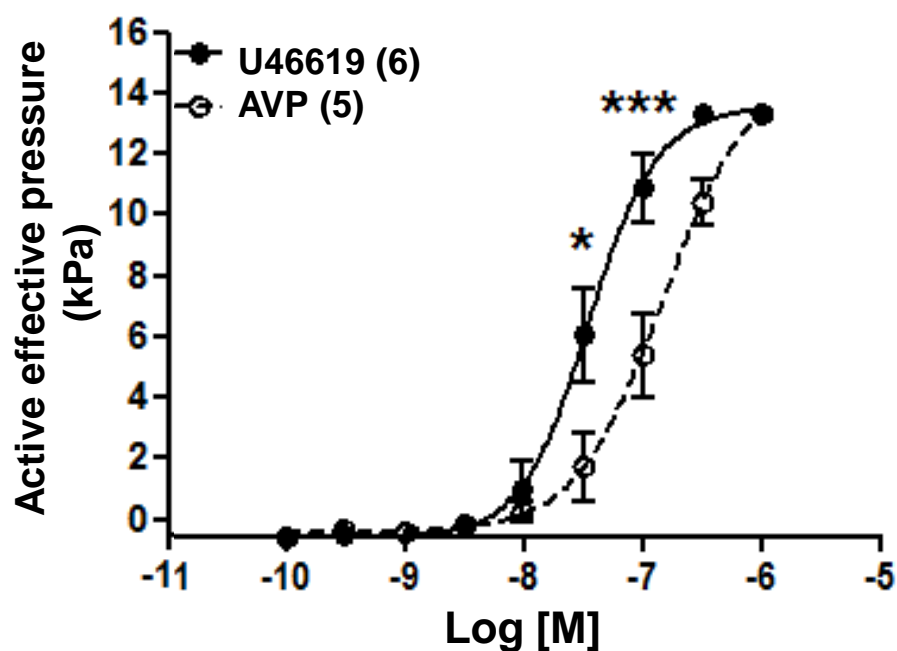


Figure 5.5.1.2-1 showing the dose-response curve with the contractile agents U46619 (N=6) (closed circles) and AVP (N=5) (open circles). U46619 produced a significant shift in the dose-response as the response was more potent. Data are presented as mean \pm SEM along with vessels treated (n). * $p < 0.05$, *** $p < 0.001$.

Table 5.5.1.2-1 summarising the EC_{50} values for U46619 and AVP.

Vessels (n)	Log EC_{50} (M) \pm SEM	p
U46619 (6)	-7.5 ± 0.1	ns
AVP (5)	-6.8 ± 0.3	

5.5.2. Response to endothelium-dependent vasodilators

5.5.2.1. ACh

Following pre constriction with U46619 (1 μ M) CPA were exposed to incremental doses of ACh (10⁻¹⁰-10⁻⁵M). **Figure 5.5.2.1-1** shows the original trace recording representing the dose dependant relaxation produced by CPA in response to ACh. A maximal relaxation response of 24 \pm 5% was achieved at highest dose of ACh and was reduced to 21 \pm 8% in the presence of L-NAME (p>0.05, n=5). The logEC₅₀ values extrapolated for each treatment has been summarised in **Table 5.5.2.1-1**.

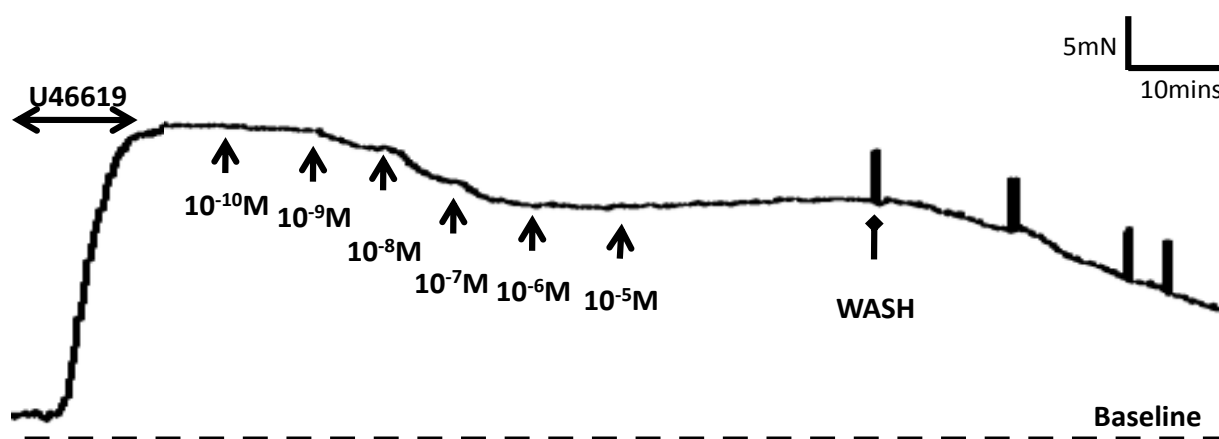


Figure 5.5.2.1-1 showing an original trace with application of ACh in pre-constricted CPA. The vessel was then washed with fresh PSS to allow for recovery of the baseline.

Table 5.5.2.1-1 summarising the EC₅₀ values which have been obtained with ACh in the presence and absence of L-NAME.

Vessels (n)	LogEC ₅₀ (ACh)M \pm SEM	Maximum Relaxation (%) \pm SEM
ACh (6)	-7.4 \pm 0.6	24 \pm 5
ACh + L-NAME (5)	-7.1 \pm 0.7	21 \pm 8

5.5.2.2. BK

CPA pre-contracted with U46619 were exposed to stepwise increasing concentrations of BK (10^{-10} - 10^{-5} M) and has been shown in **Figure 5.5.2.2-1**. A marginal relaxation response was produced by the placental vessels reaching a maximum relaxation of 13% (**Table 5.5.3.1-1**).

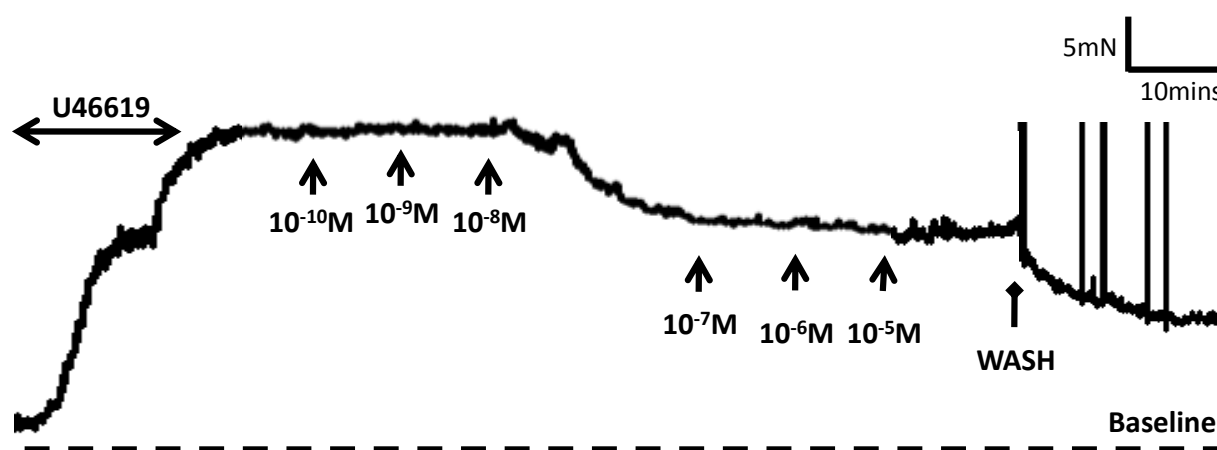


Figure 5.5.2.2-1 showing an original trace with application of BK with pre-constricted CPA vessels. The vessel was then washed with fresh PSS to allow for recovery.

5.5.3. Response to endothelium-independent vasodilators

5.5.3.1. SNP

SNP is an example of an endothelium-independent vasodilator and application of increasing concentrations of SNP (10^{-10} - 10^{-5} M) again produced a steep relaxation with CPA between 10^{-9} - 10^{-8} M (**Figure 5.5.3.1-1**). Directly comparing the

response with both ACh and BK shows that SNP causes a downward shift in the dose-response curve and achieves significance at $\geq 10^{-8}\text{M}$ (**Figure 5.5.3.1-2**). **Table 5.5.3.1-1** summarises the EC_{50} values obtained with both endothelium-dependent and independent vasodilators using CPA.

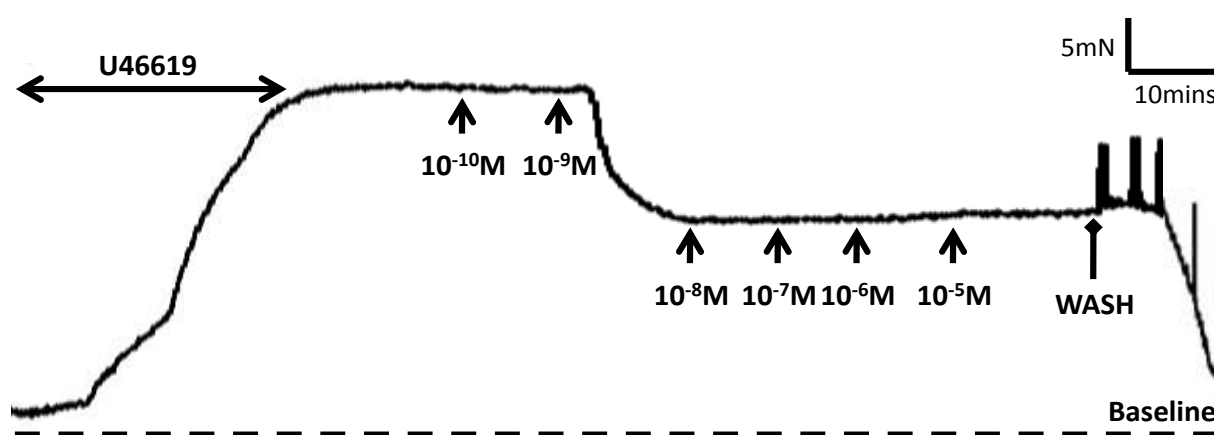


Figure 5.5.3.1-1 showing an original trace with application of SNP with pre-constricted CPA. A steep relaxation response was observed with low dose application of the agonist.

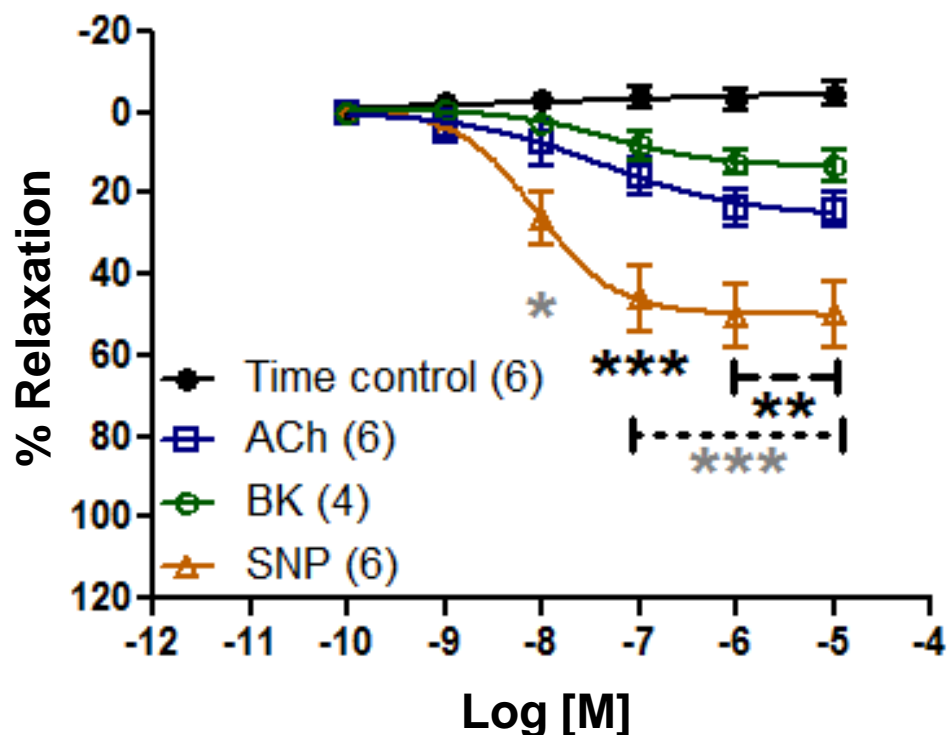


Figure 5.5.3.1-2 summarising the dose-response curves for ACh (N=6), BK (N=4), and SNP (N=6). The SNP response (orange) was markedly greater when compared with BK (green line with grey *) and ACh (blue line with black *). Time control responses did not show any significant loss in the contraction. Data are presented as mean \pm SEM along with vessels treated (n) from placentae (N). * $p < 0.05$, ** $p < 0.01$, *** $p < 0.001$.

Table 5.5.3.1-1 summarising the EC_{50} values for both endothelium dependant and independent vasodilators with CPA.

Vessels (n)	Log EC_{50} (M) \pm SEM	Maximum Relaxation (%) \pm SEM
ACh (6)	-7.4 \pm 0.8	24 \pm 4
BK (4)	-7.3 \pm 0.4	13 \pm 2
SNP (6)	-8.1 \pm 0.6	50 \pm 8

5.6. Comparing CPA to SVA

5.6.1. Effect of changing pO₂

A pO₂ of 20% (156mmHg) is normally used for wire myography experiments to ensure the vessel is continually perfused with sufficient O₂. This optimised the viability of the vessel for the duration of the experiments to be performed which can last ≥ 6 hours (Mulvany and Warshaw, 1979). However a pO₂ of 5% (39mmHg) closely reflects the physiological O₂ concentrations found within the placenta *in vivo* (Wareing, Crocker et al., 2002, Wareing, Greenwood et al., 2006a). Furthermore pO₂ of 2% (16mmHg) represents the pathophysiological levels of tissue oxygenation that have been observed with IUGR affected pregnancies (Economides and Nicolaides, 1989). As a result the importance of altering pO₂ was investigated to examine both the physiological and pathophysiological responses from the vessels. **Table 5.6.1-1** summarises the baseline tension recording in each vessel type across the three different pO₂ settings (each at 0.9L_{5.1kPa}). No significant change was seen in the baseline tension across CPA and SVA perfused with changing pO₂. The pH of the saline was also recorded and found not to be significantly altered across the different pO₂ settings (IQR [7.42-7.45], $p > 0.05$, $n = 14$).

Table 5.6.1-1 Summarising the baseline tension in different pO₂. There was no significant difference in the baseline passive tension when the O₂ content was lowered across both CPA and SVA.

pO ₂ (%)	Vessels (n)	Baseline tension (kPa) ± SEM	p
20	CPA (12)	0.16 ± 0.01	ns
	SVA (10)	0.14 ± 0.02	
5	CPA (16)	0.11 ± 0.03	ns
	SVA (13)	0.08 ± 0.03	
2	CPA (12)	0.12 ± 0.05	ns
	SVA (10)	0.09 ± 0.03	

5.6.2. Contractile responses

The response to U46619 in both CPA and SVA was compared at different O₂ tensions. **Figure 5.6.2-1** shows the vessels do remain viable across the differing pO₂ concentrations. The response to U46619 in CPA (**Figure 5.6.2-1A**) shows an initial increase in the contractile response with both 5% and 2% pO₂ achieving significance at 10⁻⁸M (p<0.01). Further stimulation with U46619 fails to increase the active tension produced by the vessels. The maximum contraction to U46619 was significantly lower when compared with the contraction produced at 20% pO₂ (p<0.001). The active pressure generated by CPA at 20% pO₂ continued to increase exponentially and failed to reach a plateau with the highest concentrations of U46619 applied (10⁻⁶M). The dose-response at 5% and 2% overlap and showed no significant difference when directly compared across the dose-response curve. In contrast SVA displayed minimal contractions with U46619 at 20% and 5% (**Figure 5.6.2-1 B**) However the response to U46619 significantly increased when the pO₂ was lowered to 2%

Assessing the functional characteristics of CPA and SVA

($p < 0.001$ at 10^{-8} - 10^{-6} M). **Table 5.6.2-1** summarises the LogEC_{50} values for U46619 across the different pO_2 settings. Comparing the response between CPA and SVA, it was interesting to note that the response at 2% pO_2 was not significantly different as the SVA could display similar reactivity to U46619 displayed by CPA at this low pO_2 setting. In contrast contractility with both the 20% and 5% pO_2 treatments were significantly higher in CPA ($p < 0.001$). Finally, it was shown that the response by CPA at 5% was matched by the response to U46619 at 2% pO_2 .

Table 5.6.2-1 Summarising the EC_{50} values which have been obtained with U46619 across the different pO_2 conditions.

pO_2 (%)	Vessels (n)	LogEC_{50} (U46619)M \pm SEM	p
20	CPA (12)	-7.5 ± 0.1	*** -8 - -6M
	SVA (10)	-7.0 ± 0.5	
5	CPA (16)	-8.4 ± 0.1	*** -8.5 - -6M
	SVA (13)	-8.3 ± 0.1	
2	CPA (12)	-8.4 ± 0.1	ns
	SVA (10)	-8.1 ± 0.3	

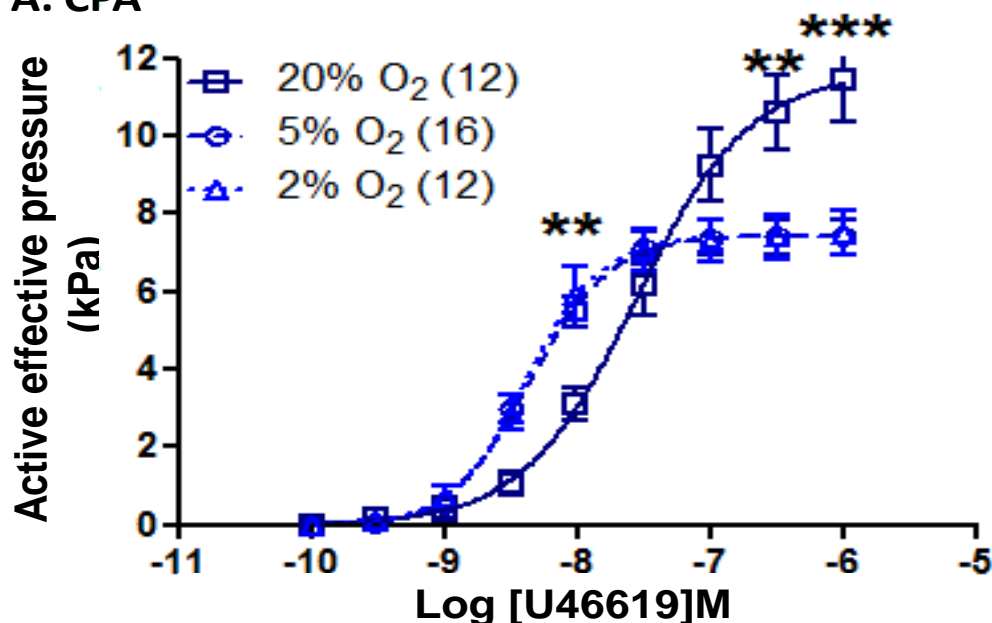
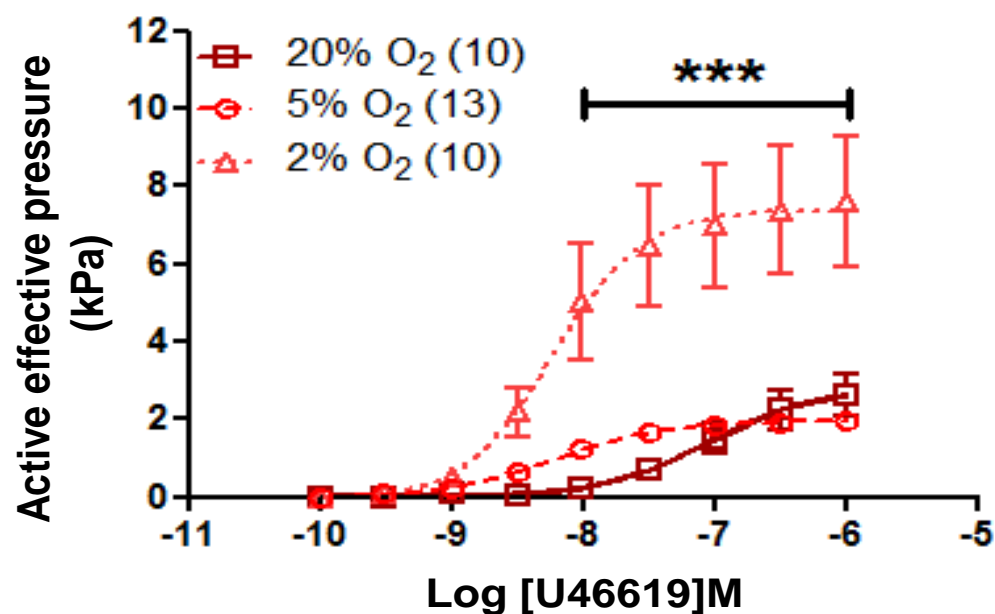
A. CPA**B. SVA**

Figure 5.6.2-1 summarising the dose-response curves with U46619 at different pO₂ concentrations. A shows the response of CPA. Lowering the pO₂ to 5% (N=16) and 2% (N=12) caused a leftward shift in the dose-response which was significantly at the lower doses (10⁻⁸M). Vessels at 20% pO₂ (N=12) continue to increase exponentially and fail to reach a plateau with the highest concentrations of U46619. B shows the dose-response curves for U46619 with SVA. The vessels show minimal contractility at 5% (N=13) and 20% O₂ (N=10) while the response at 2% (N=10) is significantly higher $\geq 10^{-8}$ M. Data are presented as mean \pm SEM along with vessels treated (n) from placentae (N). **p<0.01, ***p<0.001.

5.6.3. Vasodilatation responses

The next objective was to compare the vasodilatation responses across CPA and SVA vessel with lowering pO₂ conditions and has been illustrated in **Figure 5.6.3-1**. The maximal relaxation to SNP at 20% O₂ was 30% and 4% in CPA and SVA respectively (p<0.001) (**Table 5.6.3-1**). Surprisingly, the SNP induced relaxation was enhanced as pO₂ was lowered (**Figure 5.6.3-2**). CPA produced the highest relaxation at 5% while 2% pO₂ caused the dose-response to shift upwards but each treatment did not achieve significance across the SNP concentrations applied (**Figure 5.6.3-2A**). It was found that lowering the pO₂ improved the response produced and 2% pO₂ appeared to evoke the maximum relaxation response in SVA (**Figure 5.6.3-2B**). **Table 3.2-1** summarises the LogEC₅₀ values for SNP across the different pO₂ settings.

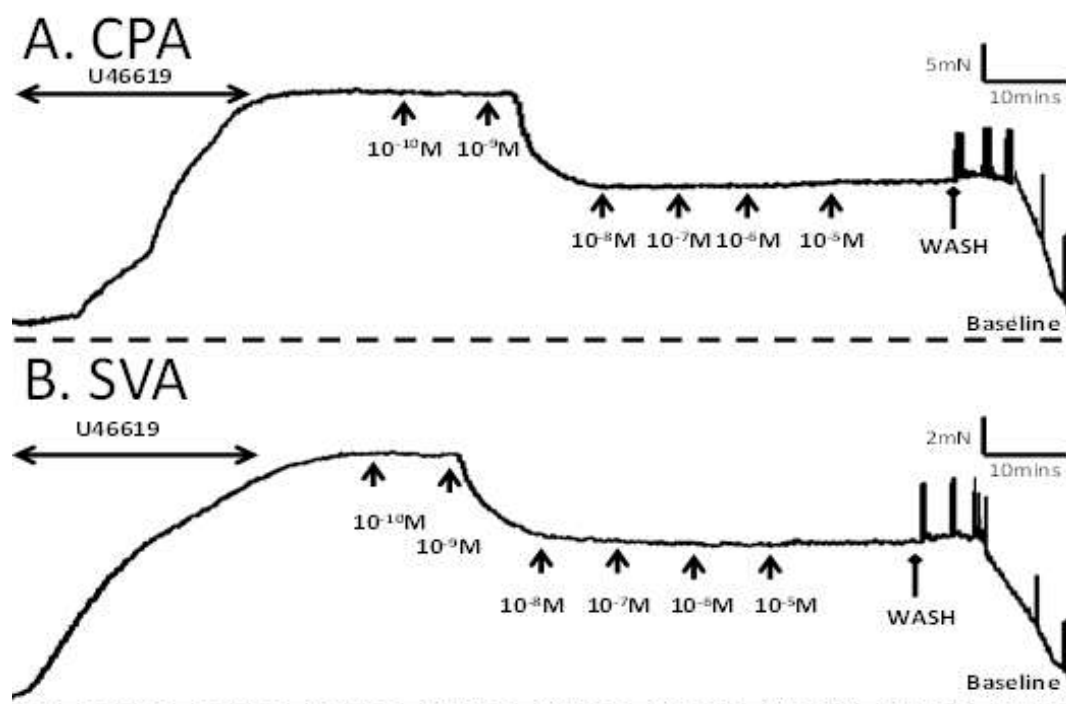


Figure 5.6.3-1 shows the SNP response with CPA and SVA in 5% pO₂. The representative trace shows the step wise relaxation to SNP with U46619 pre-contracted vessels. The response is immediate as the vessel reaches it maximum relaxation with the low doses of SNP and was seen with both vessels types. Further addition of SNP fails to enhance the relaxation seen.

Table 5.6.3-1 summarising the EC₅₀ values which have been obtained with SNP across the different pO₂ conditions.

pO ₂ (%)	Vessels (n)	LogEC ₅₀ (M) ± SEM	p	Maximum Relaxation (%) ± SEM
20	CPA (9)	-8 ± 0.2	***-8 - -5M	30 ± 8
	SVA (6)	-6.0 ± 0.3		4 ± 2
5	CPA (8)	-8 ± 0.5	*** -7- -5M	55 ± 11
	SVA (6)	-7 ± 0.2		27 ± 3
2	CPA (5)	-6.9 ± 0.2	ns	40 ± 4
	SVA (6)	-6.4 ± 0.2		52 ± 8

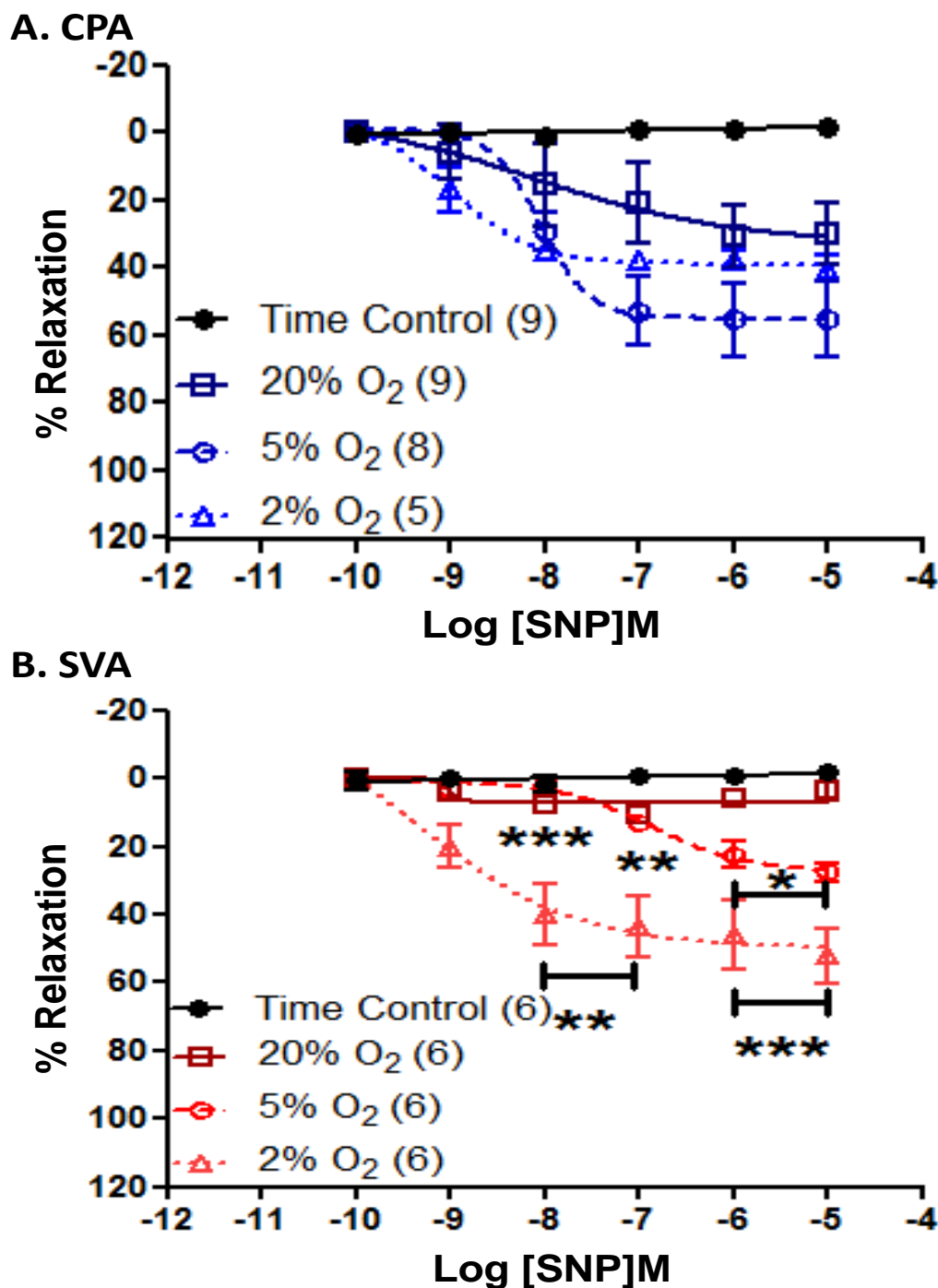


Figure 5.6.3-2 summarising the concentration dependant dose-response curves to SNP across different pO_2 . **A** shows the response with CPA which showed the most relaxation at 2% (N=5) and 5% pO_2 (N=8) when compared to the response at 20% pO_2 (N=9). **B** shows the responses to SNP with SVA. Lowering the pO_2 improved the response produced with cumulative additions of SNP and was significantly different at 2% pO_2 (N=6) when directly compared to the 5% (N=6) and 20% (N=6) responses. Data are presented as mean \pm SEM along with vessels treated (n) from placentae (N). * $p < 0.05$, ** $p < 0.01$, *** $p < 0.001$.

5.6.4. Response to RIL

The response to the TREK channel opener RIL was investigated with CPA and SVA to determine if the vessels could produce a response across the different pO₂ treatments. **Figure 5.6.4-1** shows the original trace recording of RIL application. A potent relaxation that was concentration dependant was seen with both CPA and SVA. Comparing the dose-response curves (**Figure 5.6.4-2**) showed that lowering the pO₂ induced a downward shift in the dose-response with both the 5% and 2% responses but this only achieved significance with CPA at 2% pO₂ with application of 10^{-7.5}M (p<0.001). The SVA response does not display such a change to the RIL relaxation under different pO₂ settings and only the 5% treatment showed significantly more relaxation when compared to the 2% treatment (10⁻⁷M (p<0.05). **Table 5.6.4-1** summarises the LogEC₅₀ values for RIL across the different pO₂ settings.

Table 5.6.4-1 summarising the EC₅₀ values which have been obtained with RIL across the different pO₂ conditions. No significant difference was observed across the different pO₂ settings

pO ₂ (%)	Vessels (n)	LogEC ₅₀ (RIL) M ± SEM	p	Maximum Relaxation (%) ± SEM
20	CPA (6)	-7.2 ± 0.06	ns	75 ± 5
	SVA (6)	-7.1 ± 0.2		78 ± 5
5	CPA (6)	-7.5 ± 0.1	ns	73 ± 6
	SVA (4)	-7.4 ± 0.05		75 ± 4
2	CPA (6)	-7.5 ± 0.1	ns	76 ± 6
	SVA (4)	-7.3 ± 0.03		74 ± 4

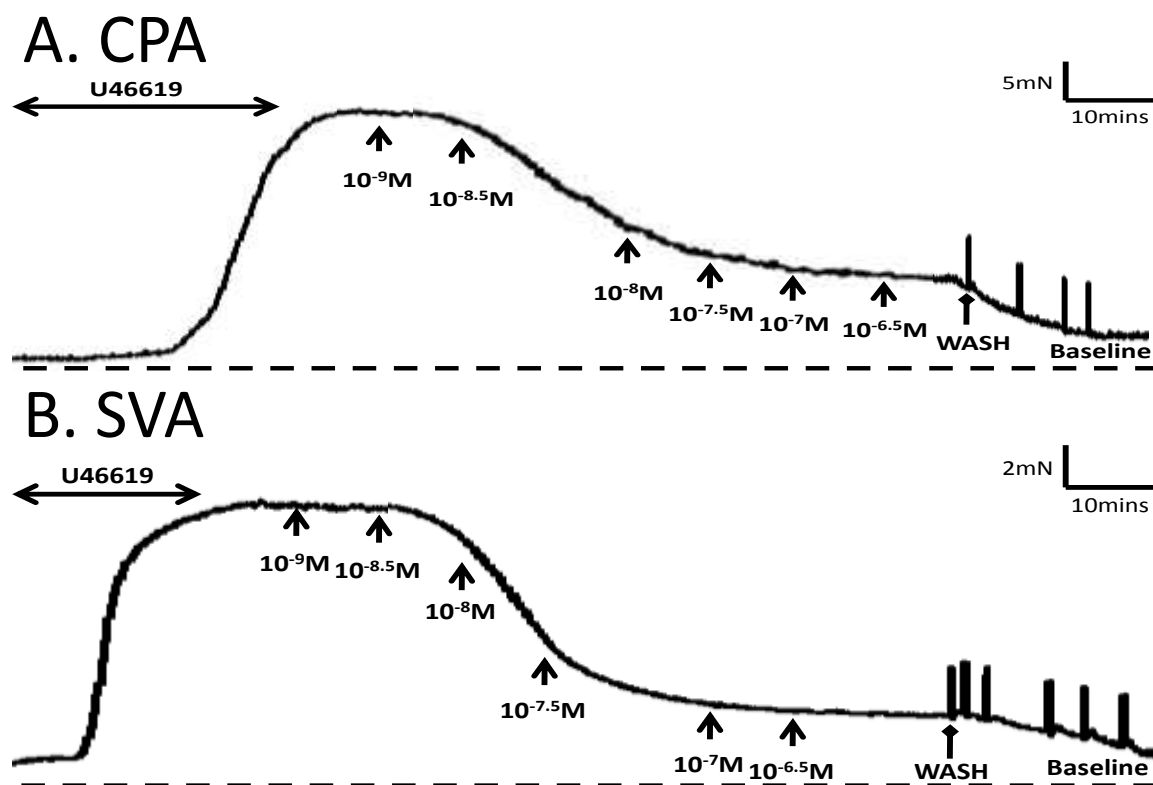


Figure 5.6.4-1 showing the original trace recording representing the RIL dose-response in CPA and SVA in 5% O_2 perfusion. The representative trace shows the step wise relaxation to RIL in U46619 pre-contracted vessels. The potent response almost reaches the baseline tension with both SVA and CPA.

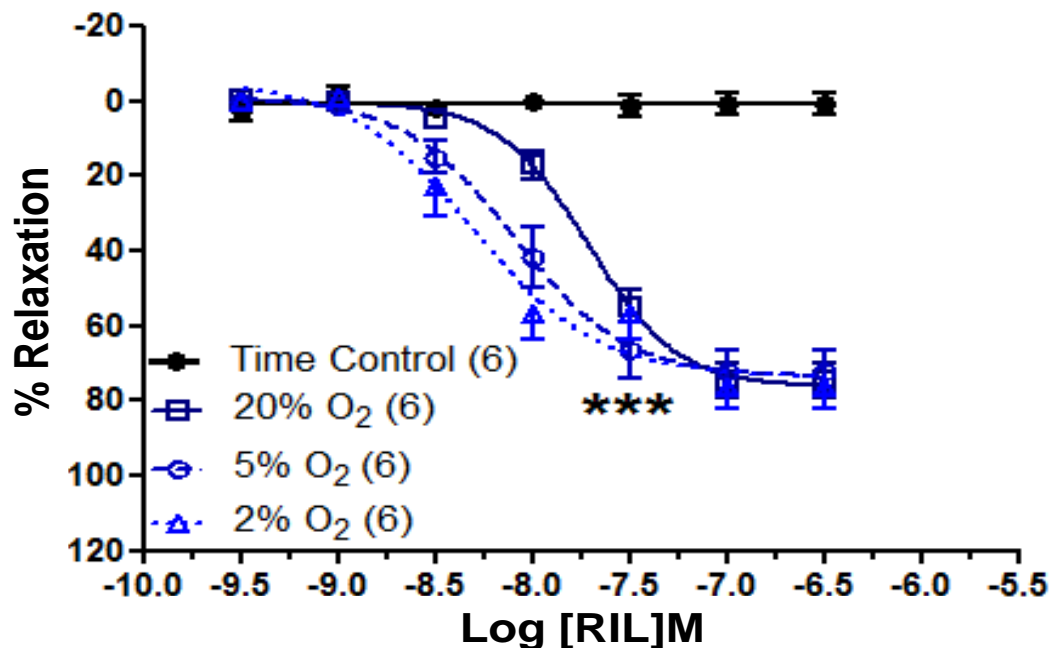
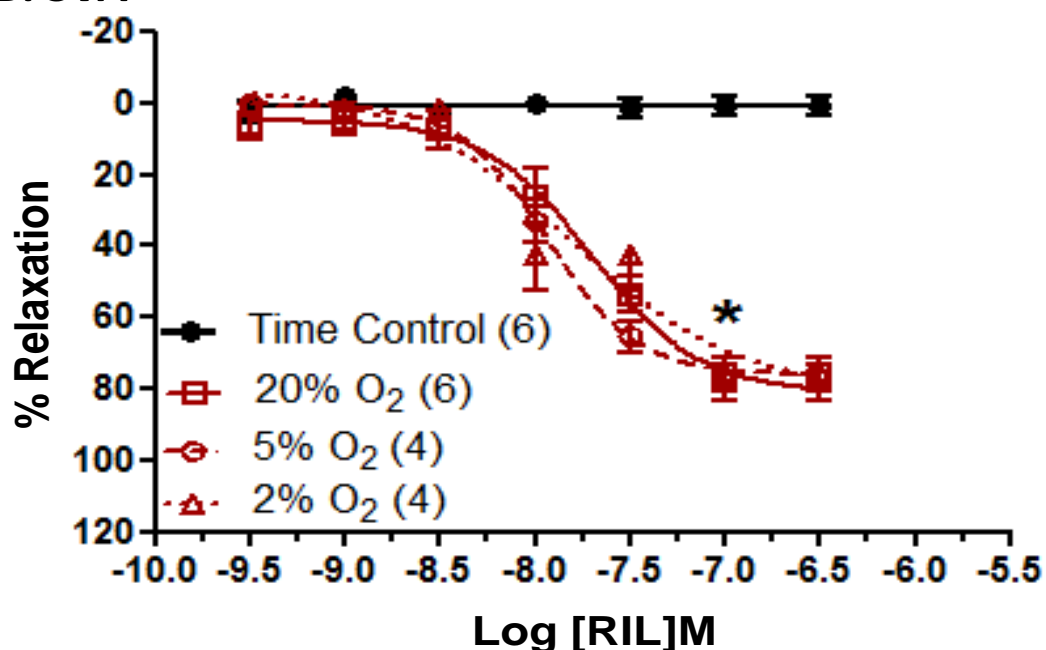
A. CPA**B. SVA**

Figure 5.6.4-2 summarising the concentration response curves with RIL. A shows the dose response curve to RIL with CPA under the different pO₂. At 5% (N=6) and 2% (N=6) pO₂, the curve shifts to the left but only the 2% treatment was significantly different to 20% (N=6) at 10^{-7.5}M. B shows the dose-response to RIL in SVA (N=6). Lowering the pO₂ treatments showed that only 2% (N=4) was significantly different when compared with the 5% (N=4) response at 10⁻⁷M. Data are presented as mean ± SEM along with vessels treated (n) from placentae (N). *p<0.05, ***p<0.001.

5.6.5. Response to H₂O₂

Blood vessels from a range of vascular tissues can respond to ROS by altering their vessel diameters to produce a cellular response. The aim of this series of experiments was to investigate the response of placental vessels to the ROS H₂O₂. **Figure 5.6.5-1** shows the effect of increasing doses of H₂O₂ addition to pre-contracted CPA and SVA with 5% O₂ perfusion. The representative trace shows a concentration dependent relaxation produced by each vessel type which went beyond the baseline tension at the highest doses used. This was due to the fact that the treatment proved to be toxic for both the CPA and SVA as the vessels were unable to respond to further contractile stimuli (both with U46619 and KPSS) post washout. The importance of varying pO₂ on the response to H₂O₂ was also compared. The dose-response curves were shown to be altered with both CPA and SVA as the pO₂ was lowered from 20% to 5% and 2% (**Figure 5.6.5-2**). The response in CPA appeared to be biphasic and the greatest relaxation occurred at 5% pO₂. While perfusion of SVA at 2% resulted in a small blunting of responses to H₂O₂. **Table 5.6.5-1** summarises the EC₅₀ values for H₂O₂ across the different pO₂ settings and direct comparisons of the CPA and SVA responses showed that the 5% and 2% response was significantly different between the two placental vessels at 10⁻⁸M.

The role of H₂O₂ as a vasoconstrictor has also been demonstrated in **Figure 5.6.5-3** which shows the original response of CPA stimulated with H₂O₂ at rest with 20% pO₂. Both CPA and SVA produced a similar response with an immediate contraction that was short lived as the vessel begins to return to its resting tension. The response was not reproducible with each subsequent stimulation (**Figure 5.6.5-4**) with the agonist and this experiment again

proved to be toxic for both CPA and SVA which could no longer produce a response to a stimulant post washout. This was also the case when each concentration dose was applied in a random order.

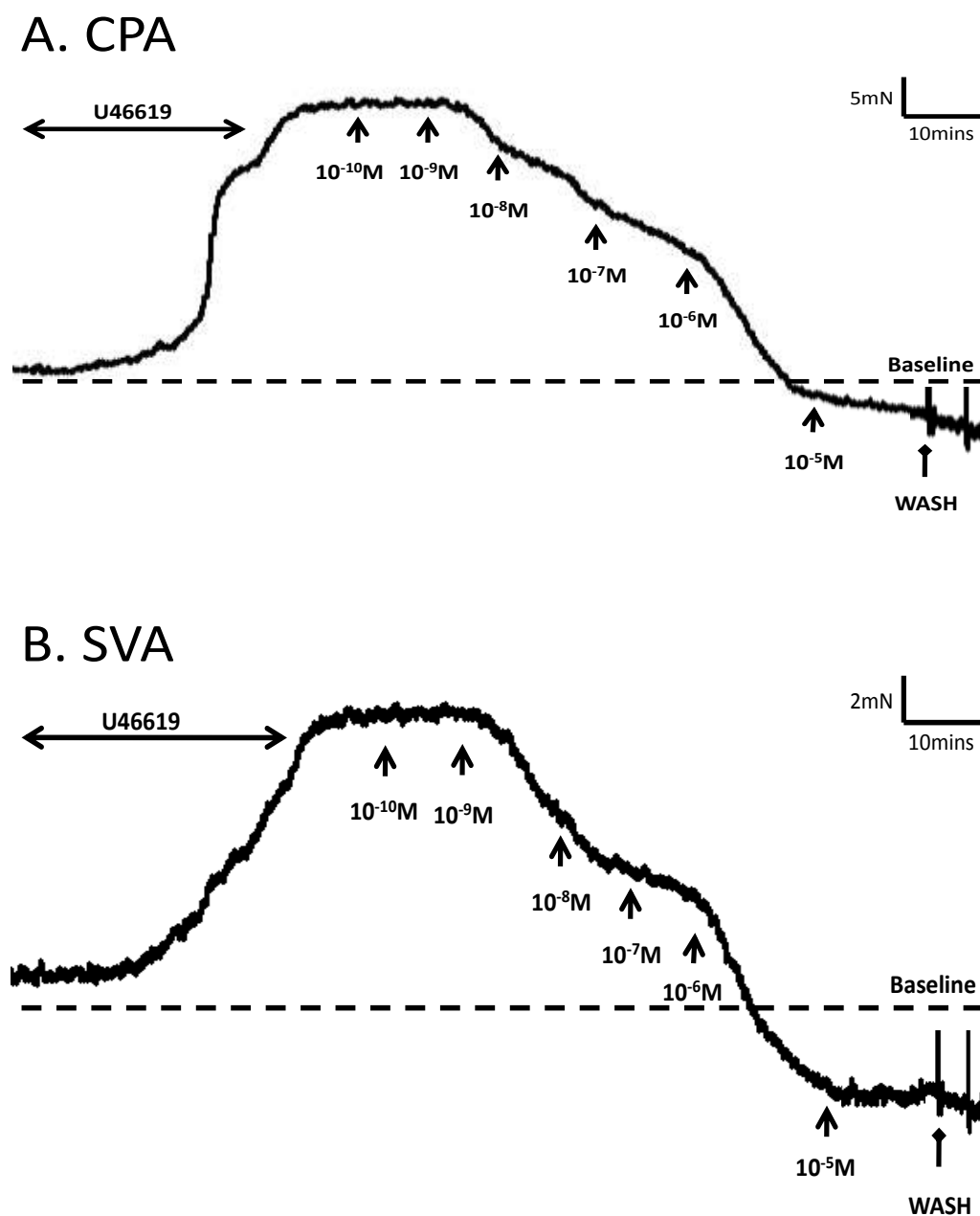


Figure 5.6.5-1 illustrates the effects of H_2O_2 addition in pre-contracted CPA (A) and SVA (B) vessels with 5% O_2 perfusion. The representative traces show a concentration dependent relaxation which exceeded the baseline tension.

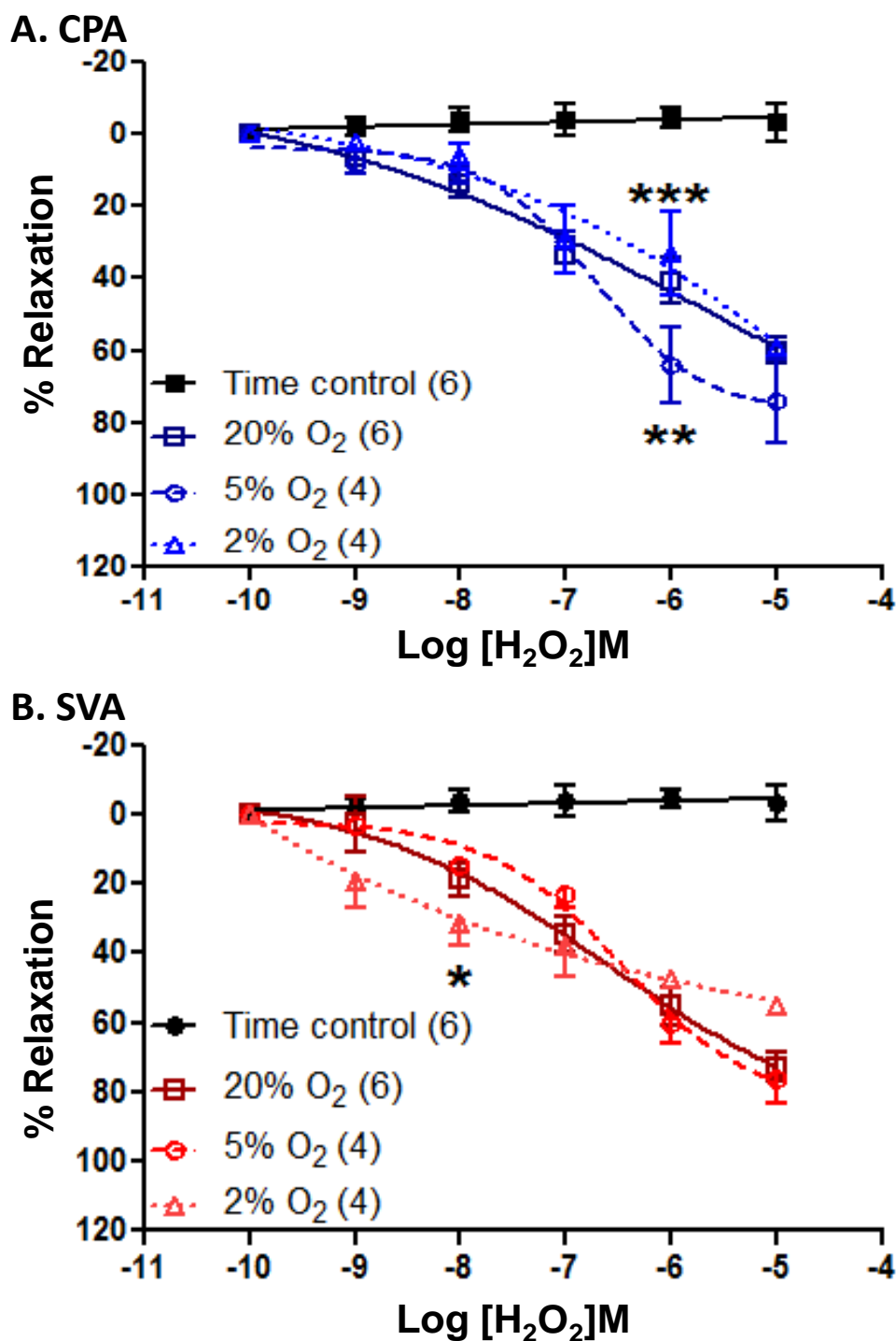


Figure 5.6.5-2 summarising the response to H_2O_2 across different pO_2 settings. **A** shows the response with CPA. The 5% pO_2 (N=4) response at 10^{-6}M was significantly different to both the 20% (N=6) and 2% (N=4) response curves. **B** shows the dose-response curves for SVA (N=6). The 5% (N=4) response was significantly different to the response at produced at 2% pO_2 (N=4) at 10^{-8}M . Data are presented as mean \pm SEM along with vessels treated (n) from placentae (N). * $p<0.05$, ** $p<0.01$, *** $p<0.001$.

Assessing the functional characteristics of CPA and SVA

Table 5.6.5-1 summarising the EC_{50} values obtained with H_2O_2 across the different pO_2 conditions. The 5% & 2% pO_2 treatment showed a significant difference between CPA and SVA both at $10^{-8}M$.

pO_2 (%)	Vessel (n)	$LogEC_{50} (H_2O_2)M \pm SEM$	p	Maximum Relaxation (%) $\pm SEM$
20	CPA (6)	-5.5 ± 0.1	ns	60 ± 4
	SVA (6)	-6.6 ± 0.1		73 ± 4
5	CPA (4)	-6.7 ± 0.4	* -8M	74 ± 11
	SVA (4)	-6.4 ± 0.2		76 ± 7
2	CPA (4)	-5.1 ± 0.2	* -8M	59 ± 3
	SVA (4)	-5.0 ± 0.3		54 ± 7

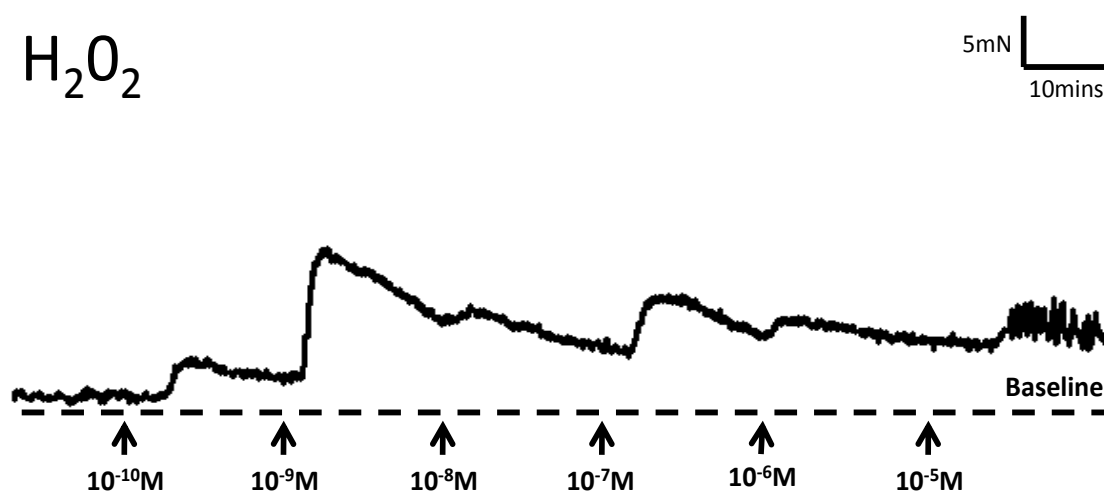


Figure 5.6.5-3 showing an original trace with application of H_2O_2 (10^{-10} - $10^{-5}M$) to CPA in 20% pO_2 . The recording shows the response with un-stimulated vessels. Both CPA and SVA produced a biphasic contraction that was short lived and could return to its resting tension.

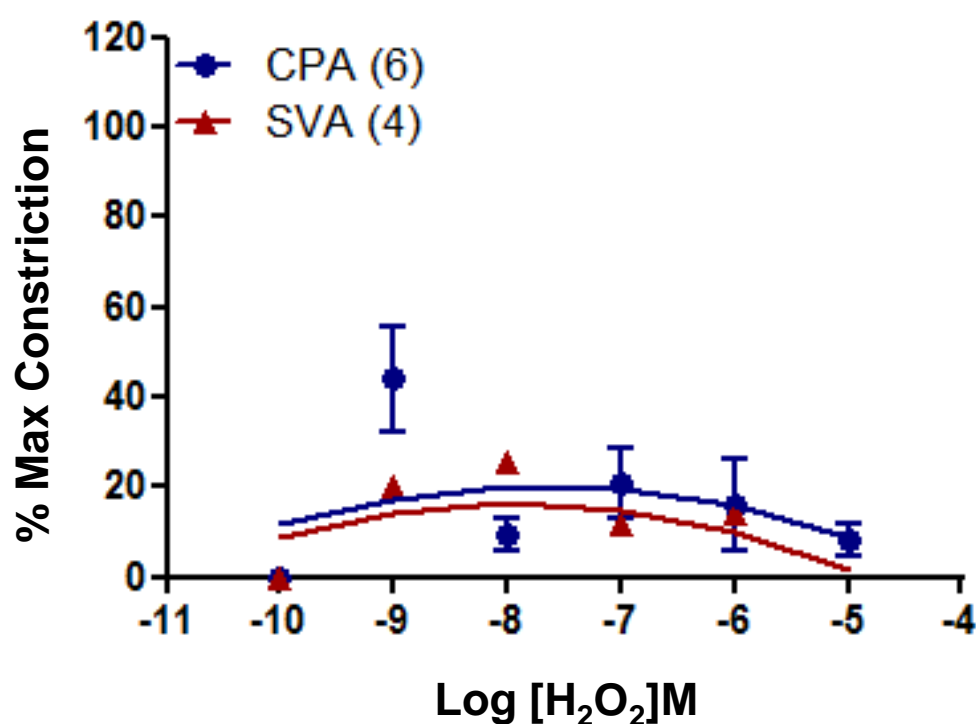


Figure 5.6.5-4 showing the smooth curve graph summarising the contractile response to H_2O_2 . CPA (N=6) and SVA (N=4) displayed a similar response to H_2O_2 application at rest. The response failed to achieve 50% of the maximum constriction produced with U46619. Data are presented as mean \pm SEM along with vessels treated (n) from placentae (N).

5.6.6. Effect of alkaline pH at 20% pO₂

The pH of the PSS buffer was increased using 1M NaHCO₃. Cumulative addition of the alkali resulted in a concentration dependent contraction which was seen with both SVA and CPA (**Figure 5.6.6-1**). The dose-response curves showed that CPA produce a contraction that peaked at 41% of the original U46619 constriction at pH 8.0 (**Figure 5.6.6-2**). This was significantly higher than the response produced by SVA which only achieved 3% of the maximal U46619 contraction ($p < 0.001$ pH 7.7-8.0). The EC₅₀ values extrapolated from the best fit curve have been summarised in **Table 5.6.6-1**.

Table 5.6.6-1 summarising the EC₅₀ values which have been obtained with NaCHO₃ with CPA and SVA.

Vessels (n)	EC ₅₀ ± SEM	p
CPA (6)	7.6 ± 0.3	ns
SVA (4)	7.9 ± 0.2	

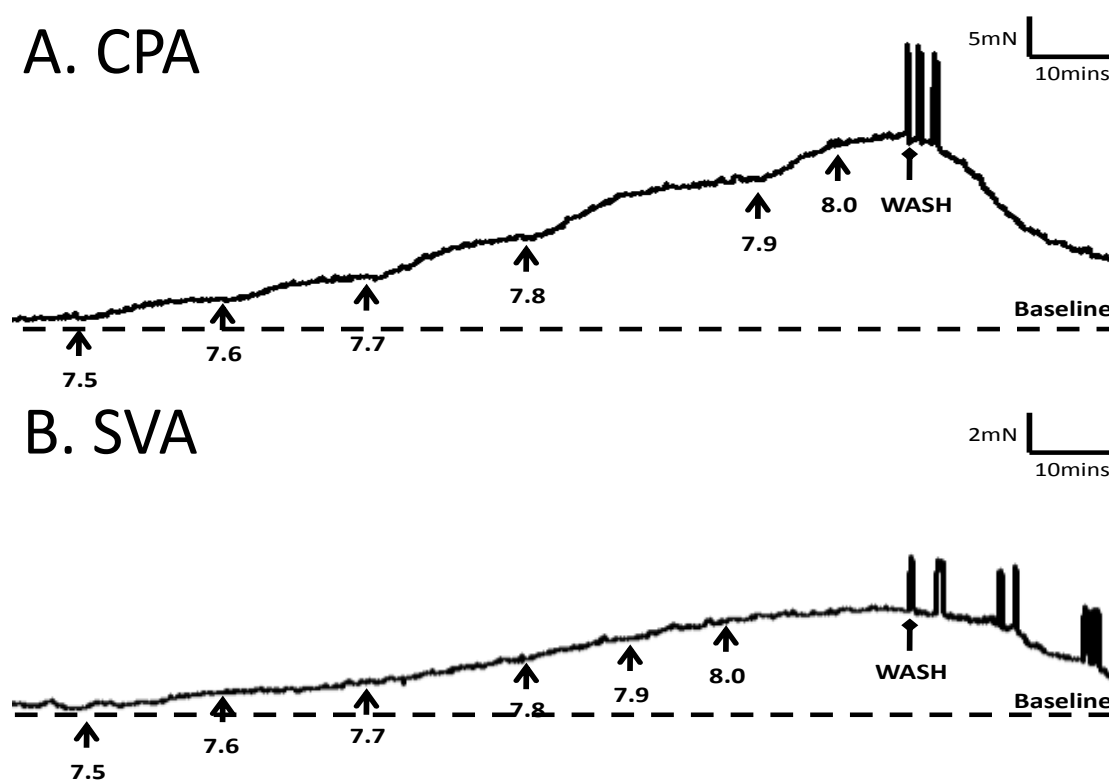


Figure 5.6.6-1 showing the representative trace recordings of NaHCO_3 induced contractions in CPA (A) and to a lesser extent with SVA (B).

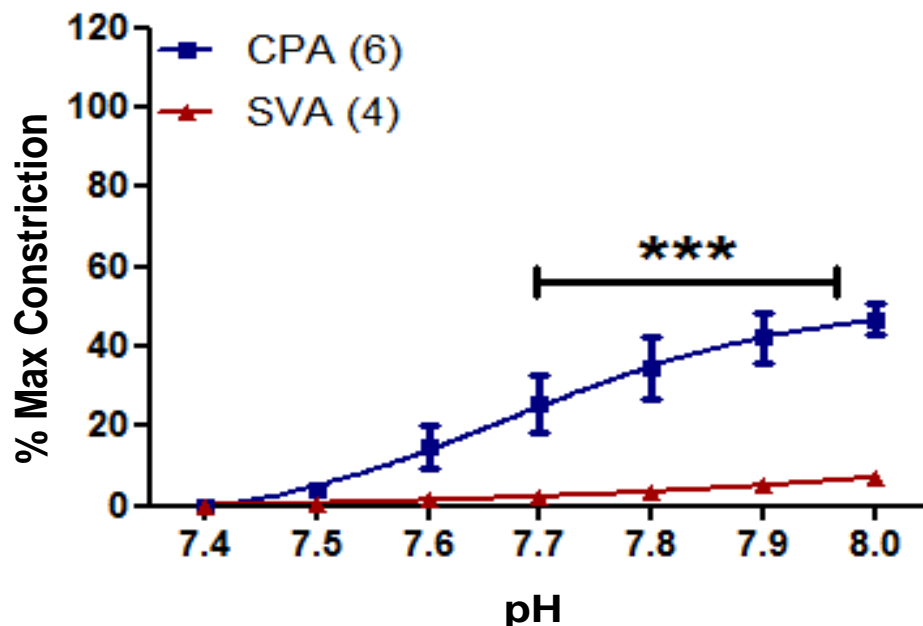


Figure 5.6.6-2 showing the concentration response curves for the effect of increasing the pH of the bathing saline at 20% pO_2 . The response with CPA (N=6) was significantly more potent when compared to SVA (N=4) but both responses did not match the maximal constriction achievable with the vessels. Data are presented as mean \pm SEM along with vessels treated (n) from placentae (N). *** $p < 0.001$.

5.6.7. Effect of acidic pH

The pH of the bathing saline was lowered to investigate the effect of acidic pH stress on both CPA and SVA. Early work with hydrochloric acid (HCl) showed the response was immediate with a 0.2 change in pH (**Figure 5.6.7-1**). The acidic pH treatment produced no change in the vessel activity at rest but vessels pre-contracted with U46619 relaxed in response to incremental acidic pH changes to give a maximum relaxation of $59 \pm 1.5\%$ at pH 6.4 in 20% pO₂.

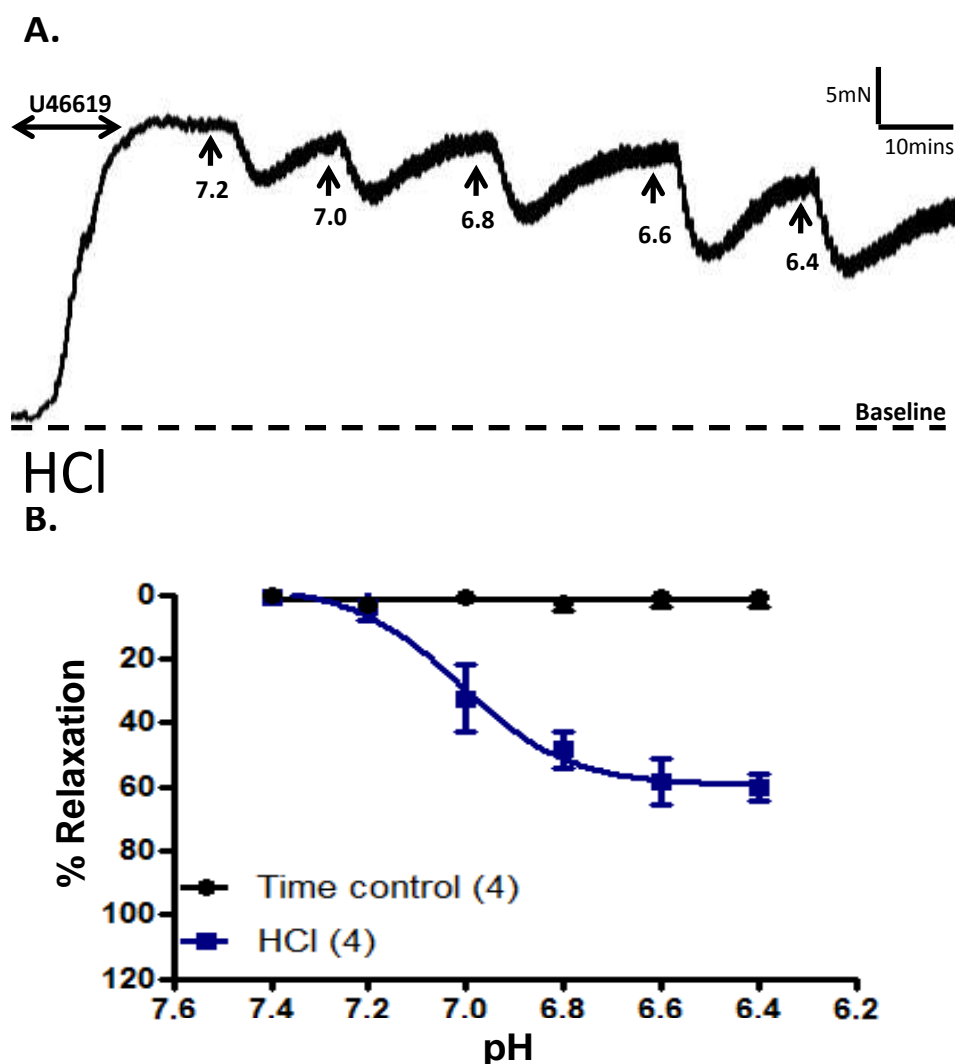


Figure 5.6.7-1 shows the response to HCl stimulation in CPA (N=4). A biphasic response was observed with an immediate loss in contraction that was followed by a slower recovery of the original contractile force. **B** shows the dose-response curve to low pH and values are shown as mean \pm SEM along with vessels treated (n) from placentae (N).

The response to lactic acid, which is endogenously found within circulations such as the placenta (Nicolaidis, Economides et al., 1989) was then explored. Repeated application (20 μ l) of 1M lactic acid was added to the PSS buffer over 2min increments. The response to low pH was biphasic as the relaxation produced at each addition was reversible and the vessel could gradually return its maximum constriction. As a result the pH stimuli was instead added over increments of 10mins to ensure that we were able to observe the complete

response each time. **Figure 5.6.7-2** shows the original trace recording for both CPA and SVA which produce a markedly similar biphasic response with both vessel types. A single response has been shown in **Figure 5.6.7-2C** to demonstrate the response when the pH is lowered from pH 7.4 to pH 7.2. The response is biphasic with an initial immediate loss in vessel tone (phase I) followed by the gradual reversal (phase II) as the vessel regains its original constriction level. This was repeated with each pH stimulus that is added. It was also found that washout of the vessel with fresh PSS alone produced a rapid increase in vessel tone as the pH was switched from pH 6.4 to the original at rest state of pH 7.4 (**Figure 5.6.7-2** red box).

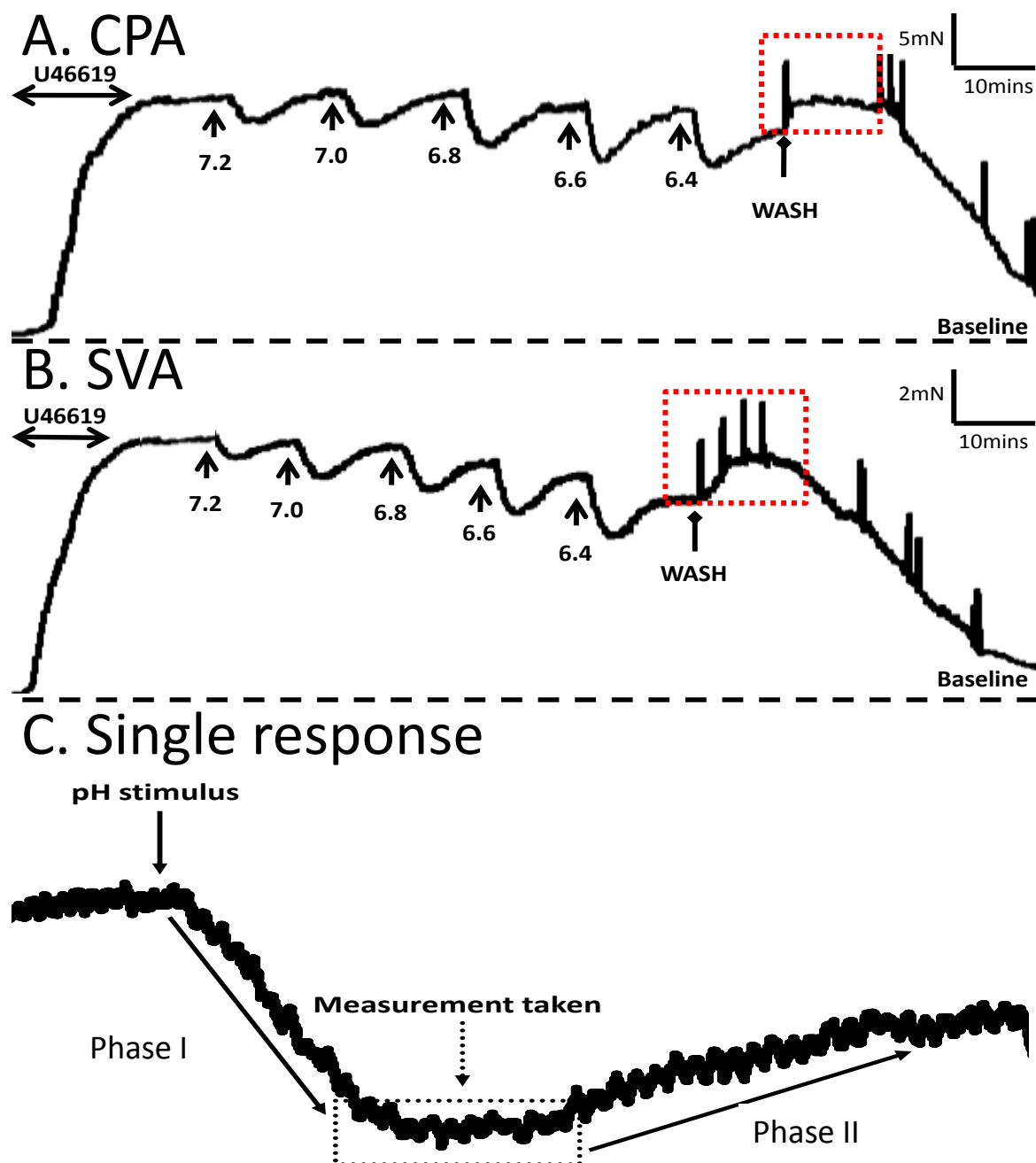


Figure 5.6.7-2 showing representative trace recordings of the lactic acid induced relaxation in CPA (A) and SVA (B). Repeated doses of the acid lowered the pH by 0.2 units every 10mins and ranged from 7.2-6.4. The bathing saline was then replaced with fresh PSS which caused an immediate increase in the vessel tone (red box) as the pH level switched from pH 6.4 to 7.4. **C** shows the biphasic response to 1M lactic acid. Lowering the pH by 0.2units produced a rapid relaxation (Phase I) which was reversible. Phase II represents the period of recovery as the vessel can return to its maximum constriction. The relaxation produced with each pH stimulus was recorded at the peak relaxation produced (boxed).

Figure 5.6.7-3 summarises the dose-response curves with increasing concentrations of lactic acid across both CPA and SVA. The same pH stress was applied to vessels perfused with 20%, 5% and 2% O₂ and reducing the pH from 7.4 to 6.4 caused a dose-dependent relaxation in both vessel types across each pO₂ setting. However the steepest increase in relaxation was produced at 20% across CPA and SVA both of which also produced a linear dose-response curve at this pO₂ setting. Reducing the pO₂ to 5% causes an upward shift in the dose-response and the response was significantly lower when compared with the relaxation seen at 20% (p<0.01). Furthermore, reducing the O₂ levels to 2% also attenuated the relaxation to acidic pH but this was significant (p<0.05) with SVA only at pH 6.8-6.4. **Table 5.6.7-1** summarises the EC₅₀ values which have been obtained with 1M lactic acid across CPA and SVA. The upward shift in the relaxation was most evident for the 5% treatment in both CPA and SVA. Directly comparing the pH stress responses at each pO₂ setting showed that the most significant difference was between the responses produced at 5% pO₂.

Assessing the functional characteristics of CPA and SVA

Table 5.6.7-1 summarising the EC₅₀ values which have been obtained with 1M lactic acid across CPA and SVA. *p<0.5, **p<0.01.

pO ₂ (%)	Vessels (n)	LogEC ₅₀ (M) ± SEM	p	Maximum Relaxation (%) ± SEM
20	CPA (9)	6.9 ± 1.3	ns	61 ± 4
	SVA (6)	6.8 ± 0.5		69 ± 2
5	CPA (8)	6.5 ± 1.3	** pH 6.8 *pH 7, 6.6	45 ± 3
	SVA (6)	6.6 ± 0.7		34 ± 3
2	CPA (5)	6.9 ± 1.2	ns	53 ± 3
	SVA (6)	6.8 ± 0.3		39 ± 7

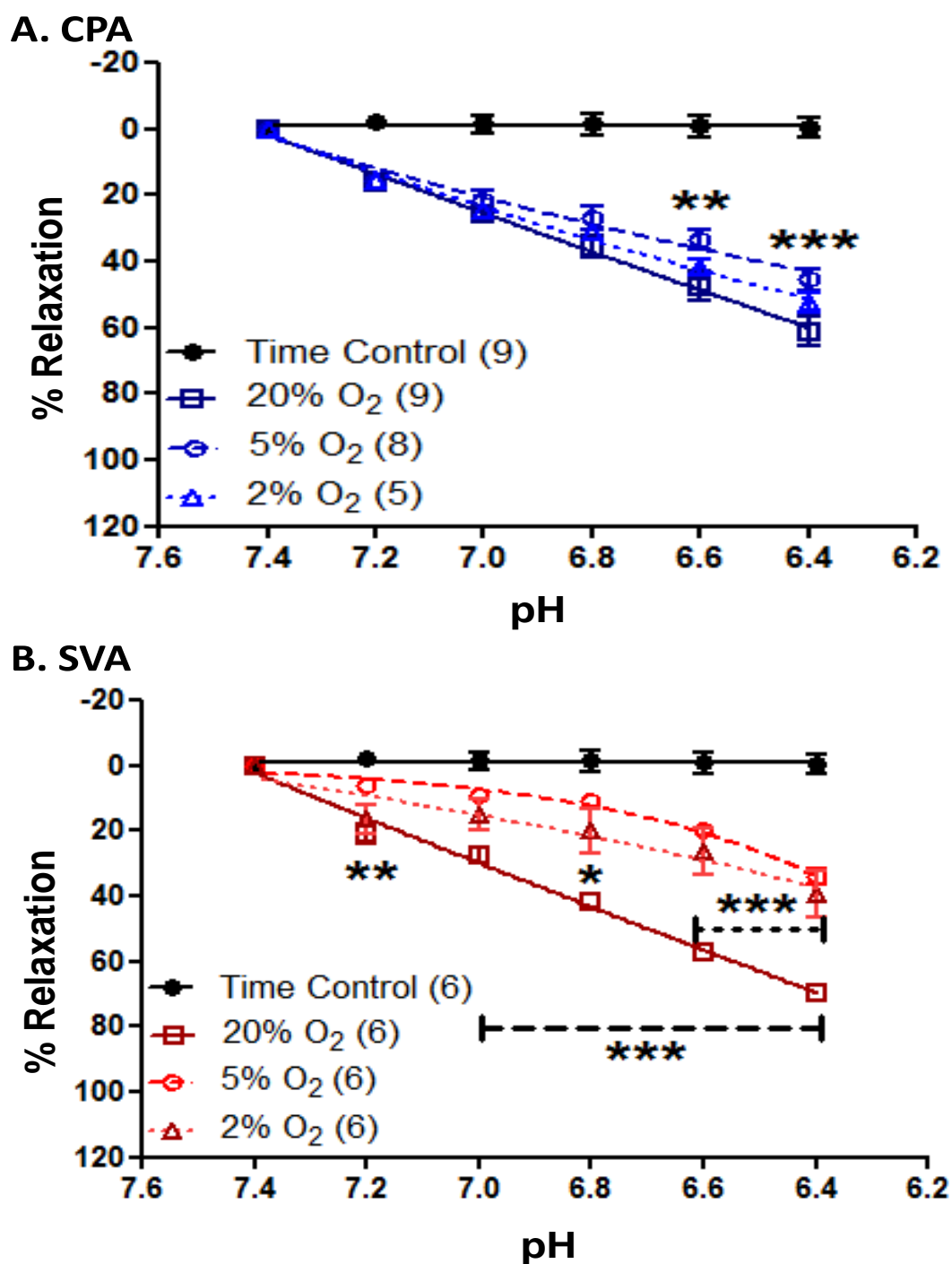


Figure 5.6.7-3 showing the concentration response curves for the effect of increasing lactic acid concentrations. **A** summarises the pH dose-response in CPA across the three different pO_2 conditions ($N=9$). Lowering pO_2 to 5% ($N=8$) and 2% ($N=5$) caused an upward shift in the dose-response curve which was only significant at 5% O_2 . **B** summarises the response with SVA to pH ($N=6$). Lowering the pO_2 produced a significant reduction in the maximum relaxation at both 5% ($N=6$) and 2% ($N=6$) pO_2 . Data are presented as mean \pm SEM long with vessels treated (n) from placentae (N). * $p<0.05$, ** $p<0.01$, *** $p<0.001$.

5.7. Response of PE-CPA at 20% pO₂

CPA from PE patients (N=4) (See **Table 6.4.1-1** for patient details) obtained at ELLSCS (**Chapter 3.2**) were also included in our functional studies. **Figure 5.7-1A** summarises the scatter plot graph to show the variation in vessel diameters within each patient group. Isolating the same 4th branch of the CPA from PE placental samples was not found to be significantly different to NORM CPA. **Figure 5.7-1B** also shows the dose-response curves which summarise the response to U46619 stimulation of CPA and the PE vessels demonstrated a greater contractile activity when examining the active effective pressure generated by the blood vessels. The increase in contractile activity was significantly greater with application of the higher doses of the vasoconstrictor ($<10^{-7.5}$ M). **Table 5.7-1** summarises the EC₅₀ values obtained with U46619.

Table 5.7-1 summarising the EC₅₀ values obtained with U46619 stimulation of CPA across each patient group.

Vessels (n)	LogEC ₅₀ (U46619)M ± SEM	p
NORM (14)	-7.9 ± 0.1] ns
PE (4)	-8.2 ± 0.2	

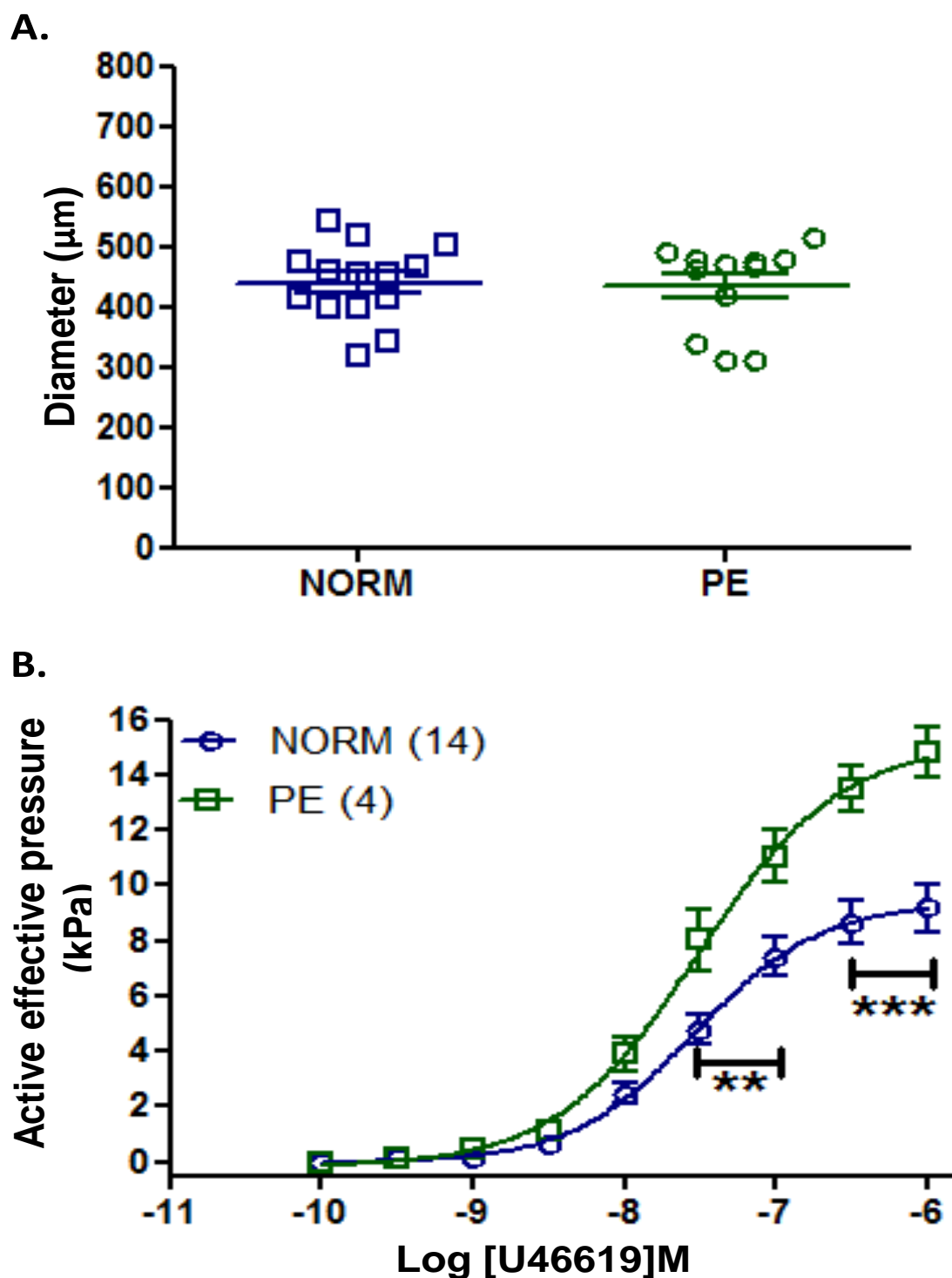


Figure 5.7-1 summarising the contractile properties of vessels from NORM (N=14) and PE CPA (N=4). **A** shows the scatter plot of vessel diameters and no difference was observed in the two groups. Data are presented as median \pm IQR. **B** summarises the dose-response curves with U46619 stimulation which showed a significant difference in the response of PE-CPA with the higher doses of U46619. Data are presented as mean \pm SEM along with vessels treated (n) from placentae (N). ** $p < 0.01$, *** $p < 0.001$.

5.7.1. Response of PE CPA to SNP

The relaxation response to SNP was examined using CPA from each patient and has been shown in **Figure 5.7.1-1**. **Table 5.7.1-1** summarises the EC_{50} values which have been obtained with SNP using CPA and no significant difference in response to SNP was found when comparing PE to NORM samples.

Table 5.7.1-1 summarises the extrapolated $LogEC_{50}$ data for SNP along with the maximum relaxation produced by each different sample.

Vessels (n)	$LogEC_{50}(SNP)M \pm SEM$	p	Maximum relaxation $\pm SEM$
NORM (14)	-5.5 ± 0.1] ns]	63 ± 3
PE (4)	-5.7 ± 0.1		49 ± 7

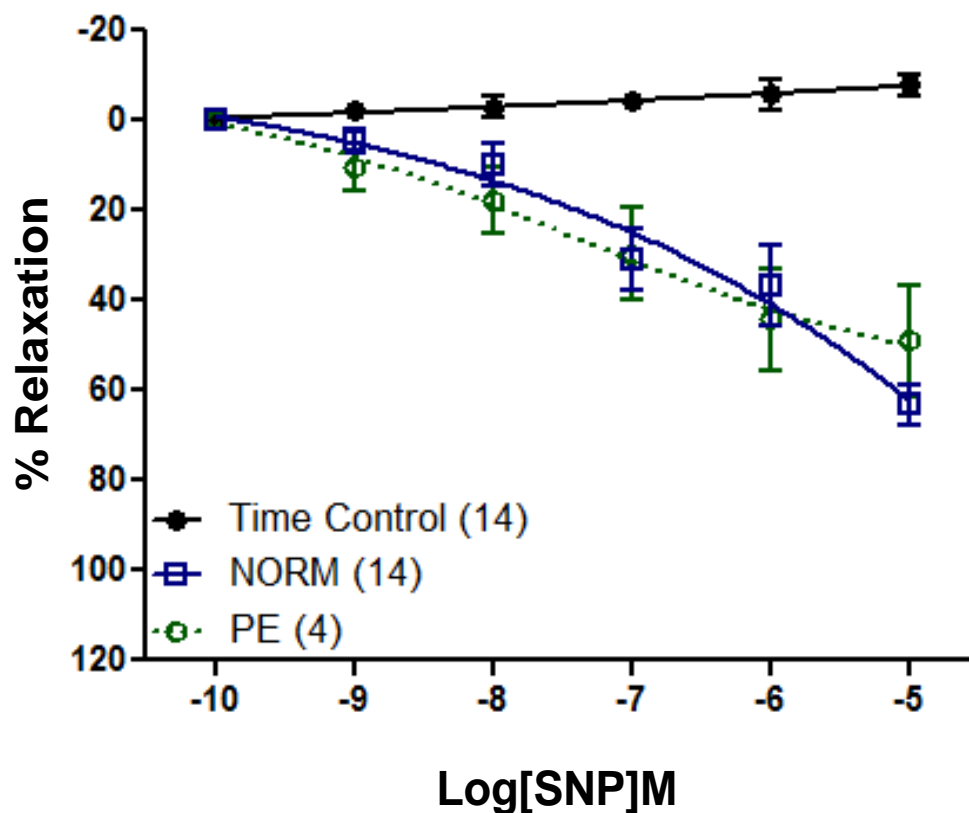


Figure 5.7.1-1 showing the response to SNP. PE-CPA (N=4) could produce a response to SNP and this was not significantly different to the NORM (N=14) response across each dose applied. Data are presented as mean \pm SEM along with vessel treated (n) from placentae (N).

5.7.2. Response of PE CPA to RIL

CPA from the PE group also demonstrated the ability to respond to the TREK opener RIL which again produced a potent relaxation that was dose dependant. The dose-response curve for each different sample have been summarised in **Figure 5.7.2-1** and no significant change was seen with the response to RIL when comparing the response of NORM and PE CPA (**Table 5.7.2-1**).

Table 5.7.2-1 summarises the extrapolated LogEC_{50} data for RIL along with the maximum relaxation produced by each different sample.

Vessels (n)	$\text{LogEC}_{50}(\text{RIL})\text{M} \pm \text{SEM}$	p	Maximum relaxation $\pm \text{SEM}$
NORM (14)	-6.6 ± 0.1	ns	81 ± 5
PE (4)	-6.7 ± 0.1		84 ± 5

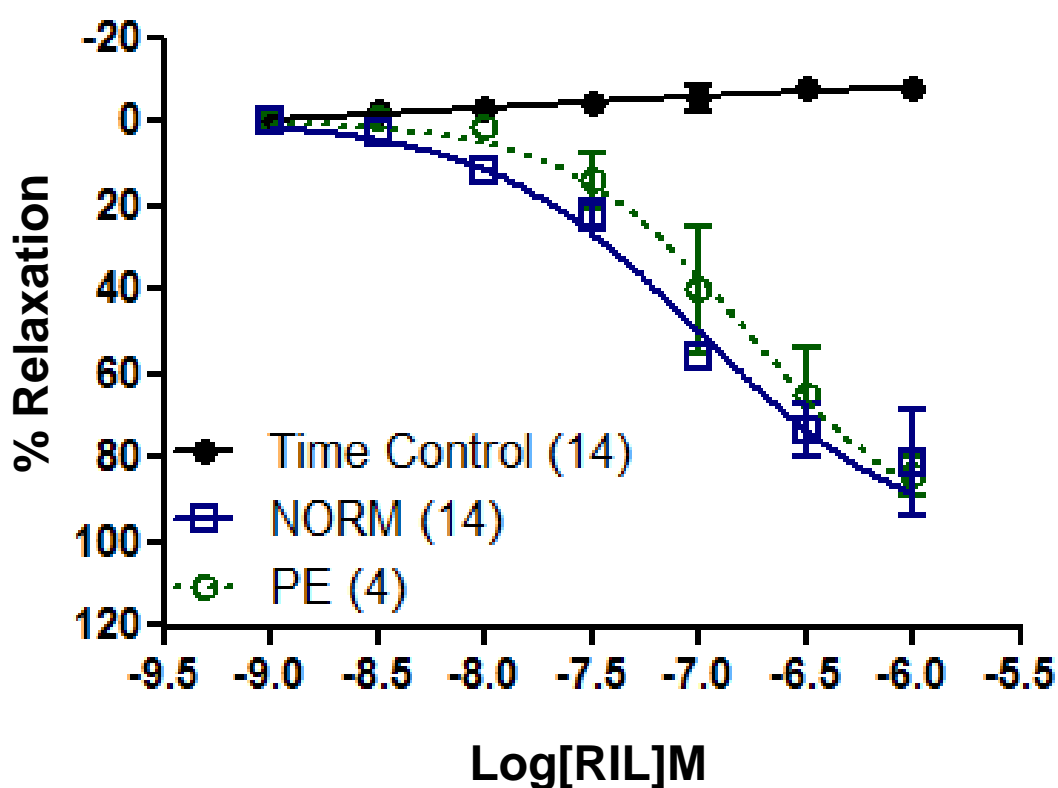


Figure 5.7.2-1 response to RIL across different patient groups. No significant change was found in the response of PE-CPA (N=4) when compared with NORM (N=14). Data are presented as mean \pm SEM along with vessels treated (n) from placentae (N).

5.7.3. Response of PE CPA to stress

5.7.3.1. Response of PE CPA to H₂O₂

H₂O₂ was applied to examine the response to ROS with PE CPA perfused with 20% pO₂. PE CPA reach 100% relaxation as the vessel tone rapidly declined with application of H₂O₂ (**Figure 5.7.3.1-1**). There is also evidence of a biphasic response to H₂O₂ with the presence of small contractile oscillations in the vessels following the addition of the smaller doses of H₂O₂ only (red box). The relaxation response by PE CPA was shown to be significantly greater than the response of NORM CPA (**Figure 5.7.3.1-2**). **Table 5.7.3.1-1** summarises the extrapolated EC₅₀ recordings in response to H₂O₂ application NORM and PE CPA.

Table 5.7.3.1-1 summarising the LogEC₅₀ values for H₂O₂ application which was found to be significantly different with PE-CPA.

Vessels (n)	LogEC ₅₀ (H ₂ O ₂)M ± SEM	p	Maximum relaxation ± SEM
NORM (14)	-5.5 ± 0.1] *<0.05	60 ± 5
PE (4)	-6.8 ± 0.1		75 ± 5

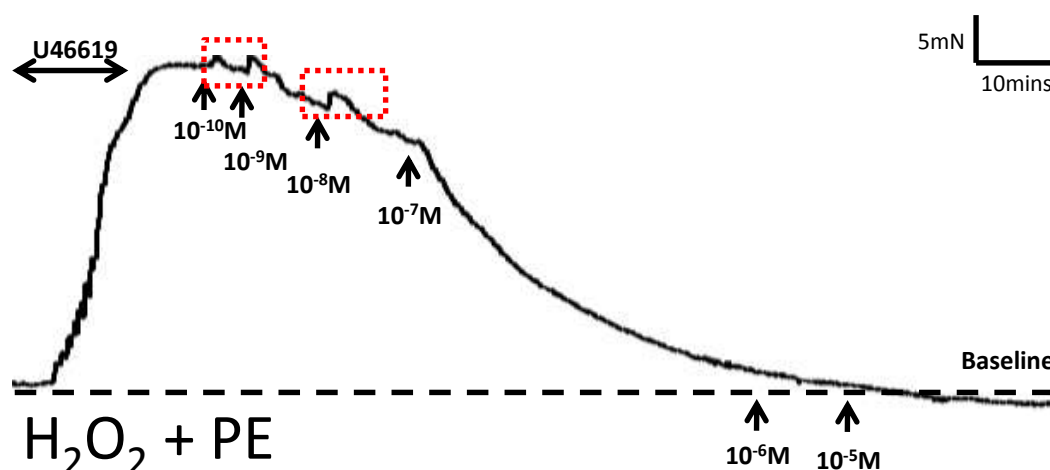


Figure 5.7.3.1-1 showing the effect of H_2O_2 on pre-constricted PE CPA. A biphasic response was observed with H_2O_2 application with an initial increase in vessel contraction that was followed by an immediate relaxation. This was overcome with higher doses of H_2O_2 ($\geq 10^{-7}M$) to result in a potent relaxation response.

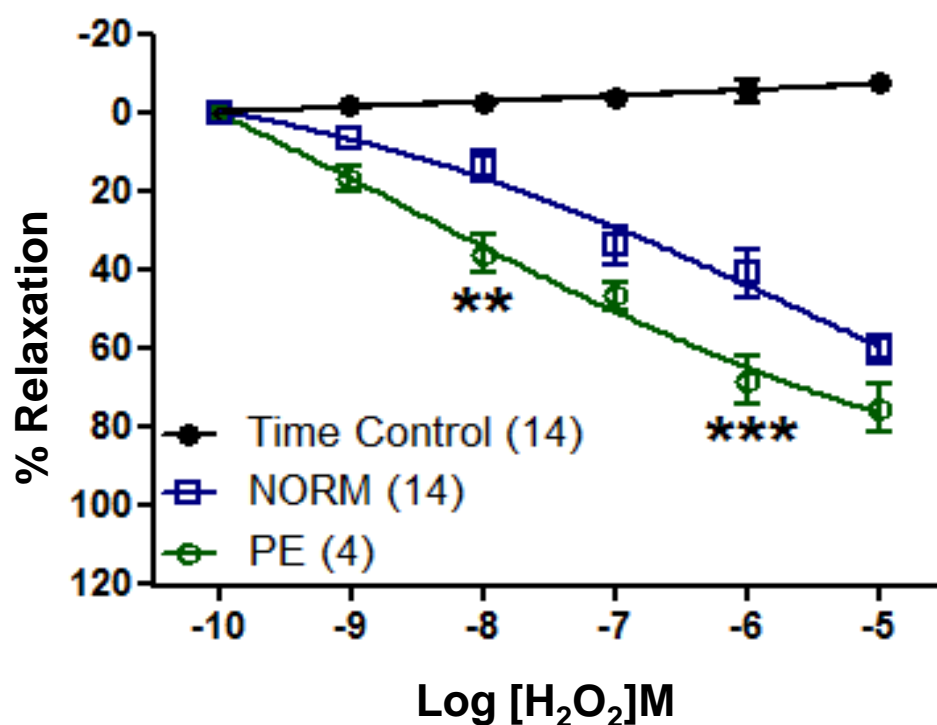


Figure 5.7.3.1-2 dose-response curves showing the response of CPA to H_2O_2 application. PE-CPA (N=4) demonstrated a significant downward shift in the dose-response when compared with NORM (N=14) as the relaxation was elevated. Data are presented as mean \pm SEM along with vessels treated (n) from placentae (N). ** $p < 0.01$, *** $p < 0.001$.

5.7.3.2. Response of PE CPA to acidic pH

The response of CPA to application of lactic acid experiments was performed across each different CPA sample population. **Figure 5.7.3.2-1** shows an original recording from the CPA as the pH was lowered. The vessels show evidence of a smaller loss in tone which was quickly recovered before the next insult was introduced. **Figure 5.7.3.2-2** summarises the dose-response curves with the application of lactic acid and PE showed significant inhibition from pH 7.0-6.4. **Table 5.7.3.2-1** summarises the EC₅₀ in response to increasing doses of lactic acid using CPA from a range of placental samples. The PE vessels produced the lowest relaxation in response to pH (37 ± 5 %) compared with NORM CPA (60 ± 5 %, $p < 0.01$). The post wash out induced rapid contraction of the CPA was also seen with the PE samples (not shown).

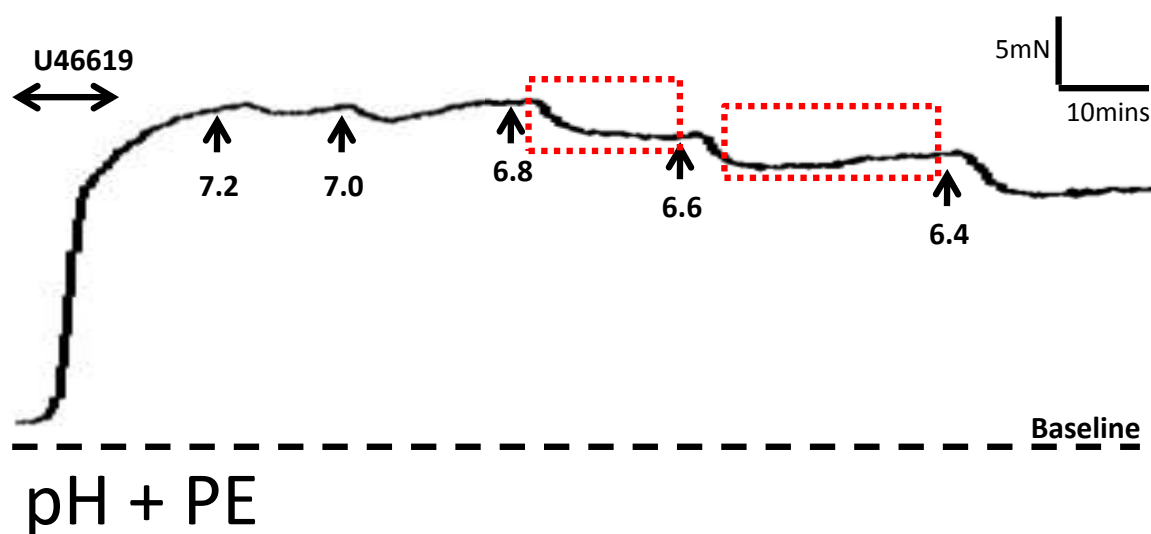


Figure 5.7.3.2-1 showing the response to pH in CPA from a PE samples. An attenuated response to pH was observed as the initial loss of vessel tone (phase I) was reduced which also allowed for the recovery of vessel contraction (phase II) to be achieved sooner (red box).

Table 5.7.3.2-1 summarising the dose-response data for acidic pH across different patient groups.

Vessels (n)	EC ₅₀ ± SEM	p	Maximum relaxation ± SEM
NORM (14)	6.9 ± 0.1	} <0.01	60 ± 5
PE (4)	6.8 ± 0.1		37 ± 5

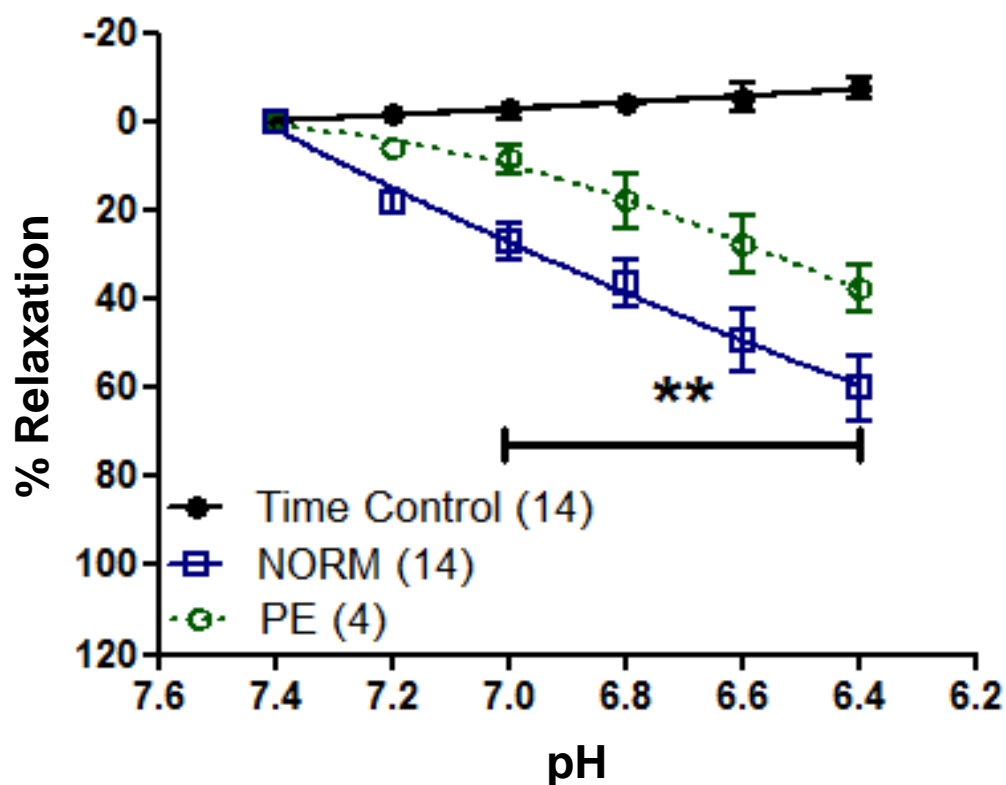


Figure 5.7.3.2-2 summarising the effect of changing pH with NORM (N=14) and PE-CPA (N=4). A significant inhibition in the relaxation response to pH was seen with PE-CPA samples across the high pH range (pH 7.0-6.4). Data are presented as mean \pm SEM along with vessels treated (n) from placentae (N). **p<0.01.

5.8. Discussion

5.8.1. Comparing CPA to SVA

The CPA and SVA represent very distinct regions of the placenta and will experience very different vascular challenges. Examining the cryosection preparations of CPA revealed a polarised phenotype with an uneven distribution of SMC around the lumen (Chapter 4.4.1). Further to this, SVA had a significantly small vessel diameter when compared to CPA. This difference in structure will have important consequences for the response of each vessel type to the flow of blood. Resistance arteries and arterioles have less SMC to surround the endothelial layer and the wall: lumen ratio will be an important determining factor in the final response of vessels (Mulvany and Warshaw, 1979, Mulvany and Aalkjaer, 1990, McPherson, 1992). The wire myography has been developed as a research tool to provide an *in situ* model for studying isolated vessels. The widely applied transluminal pressure for adult vessels within the range of 200-500µm is 13.3 kPa (Mulvany and Aalkjaer, 1990) which is higher than that found in the placental IVS, which is reported to be in the range of 2-5 kPa (Rodesch, Simon et al., 1992, Mawissa, Jauniaux et al., 1993, Kleiner-Assaf, Jaffa et al., 1999, Kaufmann, Mayhew et al., 2004). In order for our data to be relevant it was imperative to match the conditions found *in vivo* and thus chose to apply a transluminal pressure of 5.1 kPa with both CPA and SVA. The significance of this lower pressure setting has previously been shown by Wareing (et al., 2002, Wareing, Greenwood et al., 2003).

Using the same experimental parameters allowed for direct comparisons to be made between each vessel. Upon stimulation with U46619 the CPA could generate significantly more active tension with 20% perfusion. The SVA produced a small contraction with the higher doses of U46619 and the dose-response curve failed to reach plateau suggesting that a much higher concentration of U46619 was required to obtain the maximum vessel response. However when considering both the wall thickness of SVA along with the smaller diameter, it could be possible that the transluminal pressure of 5.1kPa was beyond the stretch capability of the resistance vessel and may have restricted the response to U46619 stimulation. The contractile response of SVA increased when the pO_2 was reduced from 20% (156mmHg) to 5% (38mmHg) with the lowest pO_2 setting of 2% (15mmHg) producing the most significant increase in active tension which could match the response produced by CPA at 2% pO_2 . When the pO_2 was lowered to relative hypoxic levels (2%) the SVA responded with increased vasoconstriction. This suggests the SVA may need to maintain low pO_2 to optimise the uptake of O_2 maternal circulation and provides more evidence to suggest that the placental vessels can respond to changes in their microenvironment to effectively alter their vessel physiology.

In contrast the SVA, CPA with a greater wall: lumen ratio produced the greatest response to U46619 stimulation. Lowering pO_2 with CPA reduced contractile activity as the active tension produced at both 5% and 2% was significantly lower than that observed at 20% pO_2 . This suggests that CPA need to maintain their optimal vessel tone with high stretch and the apparent elasticity provided by the vessel wall is an adaptation to the large volumes of blood that flow through this transport system (Kaufmann, Sen et al., 1979, Mulvany and Aalkjaer, 1990, McPherson, 1992, Kaufmann, Mayhew et al., 2004, Wareing, Greenwood et

al., 2006a). The very nature of the placenta as an intermediary between the fetal and maternal circulations means the pO_2 will significantly vary between each separate vascular region at crucial stages. Fetal pO_2 levels are very different to adult pO_2 levels, as shown by fetal haemoglobin which binds O_2 with a higher affinity (Barker, Gluckman et al., 1993). It was interesting to see how altering the pO_2 along with transluminal pressures could dramatically alter the contractile properties of the vessels which is an important factor to take into consideration when interpreting results. The fetal and placental pO_2 levels vary at different stages of placental development, and at the time of parturition, the pO_2 can increase from in the umbilical arteries, at a time when the fetus will be taking its first breaths. This event could also impact upon our experimental analysis, as we are utilising end state tissue that has been collected post-delivery, during which time, the placenta has also been exposed to the ambient environment (Economides and Nicolaides, 1989).

5.8.2. Contractile responses

Differences in the functional activity of a blood vessel allude to the tissue specific adaptations by each vessel to perform the different roles across the placenta. The early work with CPA made significant progress in understanding the response of vessels to contractile agents, changing pO_2 and stress. The choice of the correct contractile agent was crucial for our functional studies. U46619 gave an immediate and potent response that was stable for long enough to allow for our time controlled experiments. Vasoconstriction is produced when TxA_2 binds directly to its receptor in SMC which are expressed across the placental vascular system (Catella, Lawson et al., 1987, Howard, 1987, Hall, Han et al., 1989, Hedberg, Mento

et al., 1989, Myatt, 1992). U46619 is a thromboxane mimetic that has been widely used in placental studies as it gives both potent and reproducible contractions in isolated blood vessels. SVA could produce a response to U46619 but was significantly lower when compared to the response produced by CPA at the same pO_2 settings. An important difference was found with SVA during the dissection and mounting procedure. The SVA were highly sensitive to touch as the lumen would immediately clamp shut upon contact and further manipulation with the dissection apparatus could not reverse this change. This highlights the very different nature of vessels from the placenta which are capable of regulating their own vessel tone without the need for external stimuli. It would also suggest that SVA may have responded differently with an alternative contractile agent such as Et-1 (Allen, Skajaa et al., 1991, McCarthy, Woolfson et al., 1994, Sabry, Mondon et al., 1995a, Kingdom, Huppertz et al., 2000) or 20-Hydroxyeicosatetraenoic acid (20-HETE) which is powerful vasoconstrictor implicated in the control of blood flow and like Tx is synthesised via the AA pathway (Schwartzman, Falck et al., 1989, Gebremedhin, Lange et al., 2000).

5.8.3. Vasodilatation in the placenta

A wide range of vasoactive substances are found within the placental circulation but there is a poor understanding as to which factor is key for mediating relaxation of specific placental vessels. There is also evidence of local differences existing within the placenta which have been attributed to the different functions performed by the distinct vessels (Chaudhuri and Furuya, 1991, Cipolla, Smith et al., 2009).

The role of the EC layer in mediating vessel activity was investigated using BK and ACh both of which promote the release of NO from EC which could not demonstrate a significant relaxation response both in the presence and absence of L-NAME. It is worth noting that L-NAME requires an additional hydrolysis step to improve its solubility in *in vitro* preparations which may explain why we only observed a small inhibition with the ACh response (Gardiner, Compton et al., 1991, Jovanovic, Grbovic et al., 1994c, Griffith and Kilbourn, 1996). An alternative competitive inhibitor of NO is L-NG-nitro-Arginine (L-NNA) which is closely related to L-NAME and can easily permeate the cell membrane and along with methylene blue (MB) have shown to produce specific inhibitors of NO production and release (Griffith and Kilbourn, 1996, Sand, Andersson et al., 2006).

A recent study (Sweeney, Wareing et al., 2008) reported a relaxation response to BK by placental vessels. The crucial between this and my study was the addition of a sub-maximal dose ($<1\mu\text{M}$) of U46619 (EC_{80} dose) and vessels were allowed to stabilise for longer (10mins instead of 5mins in our study) prior to addition of BK. U46619 is potent vasoconstrictor which has the advantage that the contractile response stabilises which was in direct contrast to AVP which showed evidence of a loss in pre-tone. However the concentration used in our study ($1\mu\text{M}$) may have contributed to the poor relaxation response with both ACh and BK. It would be important to investigate this using sub maximal doses of U46619 and leaving the vessels for a longer period of time before adding the different vasodilators.

In direct contrast to ACh and BK, the most potent and reproducible relaxation response was seen with the NO donor SNP, which exerts a response by directly targeting SMC. The response to SNP with CPA was matched by SVA across each pO_2 setting and the

most significant relaxation response was seen at 5% pO₂. The NO donor SNP has previously been reported to induce a relaxation response to be in the range of 50-70% relaxation with placental CPA and CPV (Mondon, Doualla-Bell Kotto Maka et al., 1995, Wareing, Crocker et al., 2002, Sweeney, Wareing et al., 2008) to support our findings. Sabry (et al., 1995a) demonstrated an endothelium-dependent relaxation with isolated SVA preparations and stripping the endothelium using human hair reduced the relaxation response to ACh and histamine which are both endothelium-dependent vasodilators. We chose to focus on SNP in our study but it would be interesting to observe the effects of these stimulants in our studies also. The response to SNP highlights the role of the EC layer in mediating vessel tone. Any damage to the EC layer has the potential to impair the production and release of PGI₂, which is a potent vasodilator (Walsh, 1985).

5.8.4. Response to RIL

This study was the first to show the direct effects of the neuroprotectant RIL on both CPA and SVA placental vessels. RIL is an important antiglutamate agent with US Food and Drug Administration approval with minimal side effects reported (**Figure 5.8.4-1**). RIL has been shown to oppose inward currents induced by VGCC and voltage dependent Na⁺ channels (Na_v) to decrease the release of ACh and glutamate from pre synaptic neurons (McIntosh, Smith et al., 1996, Stutzmann, Pratt et al., 1996). It was revealed that 1µm produced a potent relaxation that reached upwards of 75% with CPA and 78% with SVA at 20% pO₂. CPA also showed that the relaxation was increased with lowering pO₂ levels and the highest relaxation was produced in 2% pO₂. In direct contrast, SVA showed an enhanced

response to RIL when the pO_2 was lowered from 20% to 5%. However, when the pO_2 was further reduced to 2%, we observed a significant reduction in the response produced by the placental vessels to suggest that pO_2 is crucial for determining the effect of RIL. Low pO_2 can alter the gating of ion channels and at SVA showed a potent contractile response to U46619, a higher dose of RIL was required to produce an equivalent relaxation to that seen with 20% or 5% pO_2 .

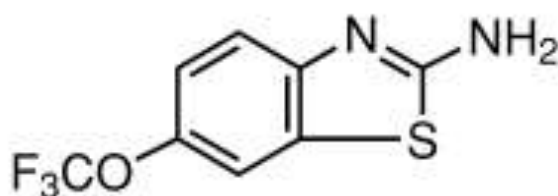


Figure 5.8.4-1 showing the structure of RIL (2-amino-6-trifluoromethoxy benzothiazole). Image obtained from www.sigma.com

RIL slows disease progress of amyotrophic lateral sclerosis which is caused by a defect in axon transport of neurofilament proteins. RIL administration delays the progression of the disease and is currently used in a clinical setting (Stutzmann, Pratt et al., 1996). A recent finding by Stevenson (et al., 2009) helped to understand the protective role provided by RIL treatment as it was shown that RIL did not directly induce glutamate release but instead RIL decreased the phosphorylation of ERK and p38 to slow neurofilament transport.

RIL has also shown an important role in protection against ischaemic brain injury linked with trauma and inflammation. This was demonstrated using a pressure induced model of retinal ischaemia in rats (Ettaiche, Fillacier et al., 1999). A 30min exposure to increased retinal pressure could induce ischaemia and this was significantly reduced with RIL

treatment. RIL can open K₂P channels and inhibit Na_v, and the authors speculated that this would reduce the depolarisation triggered by ischaemia to then prevent the over stimulation of glutamate receptors. This finding may also help to understand why we found that the response to RIL was partially pO₂ dependent.

More significantly, RIL has also been used to study VEGF signalling in human umbilical vein endothelial cells (HUVEC) (Yoo, Hyun et al., 2005). Hypoxia is an important stimulant for VEGF production to promote new blood vessel formation. This study (Yoo, Hyun et al., 2005) showed that the VEGF induced cell proliferation could be successfully inhibited by RIL and provides further support for the anti-ischaemic protection provided by RIL. This could also have significance for developing future anti-ischaemia therapies to treat placental pathologies and warrants further investigation. RIL is emerging as an important therapeutic tool due to its multiple actions on intracellular signalling pathways. At high concentrations RIL displays anaesthetic like properties and can modulate the action of TREK-1 and TRAAK while also showing the potential to finely regulate its action on target tissues (Fink, Lesage et al., 1998, Duprat, Lesage et al., 2000, Reyes, Lauritzen et al., 2000, Cadaveira-Mosquera, Ribeiro et al., 2011). The potent response produced by both CPA and SVA demonstrates that RIL is also an important future candidate for regulating placental vascular function. The dose dependent and O₂ dependent actions of the drug also provide avenues to target specific pathways without causing unwanted side effects. However to achieve this we firstly need to disseminate the precise ion channel targets of RIL and has been investigated in [Chapter 7](#).

5.8.5. Response to stress stimuli

Small vessels need to maintain their vessel diameters to keep a constant level of myogenic tone. This is achieved through the immediate response of vessels to stimuli such as repeated cycles of ischaemia/reperfusion (I/R) will be met with a redirection of blood flow as vessel tone alters (Archer and Michelakis, 2002, Bruce, Taggart et al., 2004). I/R and chronic hypoxia have been shown to be part of disease pathways including PE and are linked with the alterations in proton homeostasis which can also alter vascular tone directly or indirectly (Holzer, 2009).

5.8.5.1. Importance of pO_2

Our investigations revealed that lowering tissue perfusion from 20% to 2% could alter the maximum constriction and vasodilatation responses of placental vessels when the same stimulant was applied. The most contrasting change was seen with SVA which showed an elevation in the vessels contractile ability. The intrauterine environment has an important influence over development of the placental and fetal tissue. Early stage low pO_2 has a protective role to prevent accumulation of ROS (Nicolaidis, Economides et al., 1989, Boura, Leitch et al., 1998, Burton, Jauniaux et al., 2009). The level of pO_2 was also an important factor in determining the response of placental vessels to SNP. SVA produced the most relaxation to SNP at 2% which is also when we observed the greatest response to U46619. In contrast 2% pO_2 had the reverse effect on CPA which showed a loss in relaxation and a potent response to SNP at 5% pO_2 . The dose-response curve also showed a steep response to

SNP at 10^{-8} M with this pO_2 setting which suggests a key threshold limit was reached and the vessels demonstrated their full vasodilatation capacity in response to the agonist. This also suggests that tissue oxygenation is a determining factor for vessel functions and shows how changes in maternal oxygenation are instantly matched by changes in placental blood flow. The response to SNP was also demonstrated with isolated vessels from healthy placental samples (Wareing, Crocker et al., 2002) under different O_2 perfusion settings (21, 7 and 2% O_2). It was shown that the response to SNP was unaltered with CPA with changing pO_2 while our study used 5% perfusion and CPA showed a steep response to SNP and highlights how a narrow change in pO_2 from 7% to 5% can have dramatic changes on the vessels response to the same stimuli. In contrast this study did demonstrate that the level of tissue O_2 was important for controlling the response to SNP with CPV (Wareing, Crocker et al., 2002), which has parallels with our own observations with the SVA response to SNP in 2% pO_2 .

The level of tissue perfusion also has an important influence on vessel function and this was demonstrated in a recent study (Maenhaut and Van de Voorde, 2011). Increases in cell mass will increase the level of tissue hypoxia as sufficient O_2 is not delivered to all the tissue. This is a particular risk for adipose tissue and it was shown that hypoxia (95% N_2) could cause a loss in vessel tone with mouse mesenteric vessels which had the surrounding fat tissue removed. In contrast vessels which still had a layer of adipose tissue intact produced a biphasic response with an initial contraction immediately followed by a relaxation. This finding demonstrates the role of surrounding tissue on controlling vessel function. This also highlights how small alternations in the resistance sized vessels which set the total peripheral resistance could have detrimental effects for the wider tissue (Bayliss, 1902, Bruce, Taggart et al., 2004, Maenhaut and Van de Voorde, 2011). Cipolla (et al., 2009) showed that repeated

treatments with I/R reduced basal NO production in rat parenchymal vessels. The vessels were still responsive to SNP to suggest SMC could still bring about a relaxation. A recent study examined placental tissue from terminated pregnancies at 7-16wks of development (Jauniaux, Watson et al., 2000). It was shown that the antioxidants CAT, GPx and SOD increase with increasing gestational age and the most significant correlation was with GPx which helps to breakdown the ROS H_2O_2 . Our data showed that changing the perfusion of mounted vessels produced significant changes to the contractile and relaxation response of both CPA and SVA and provides an important parallel to the placental conditions found *in vivo*. The pO_2 significantly alters at different stages of development and we have been able to show that this may then be translated with a change in the functional role of the placental vessels.

5.8.5.2. H_2O_2

Prolonged periods of low pO_2 will also lead to an increase in ROS which used *in vitro* have demonstrated the ability to alter vascular function. In light of this evidence the action of H_2O_2 in CPA and SVA was investigated. It was shown that both vessels could relax in response to H_2O_2 but crucially this treatment was toxic. It was also shown that the vessels could also produce a transient contraction in response to H_2O_2 stimulation which was reversible as the vessel returned to baseline. It has been previously demonstrated that H_2O_2 can induce a biphasic contraction and relaxation cycle that is only when pathophysiological concentrations were applied (Yang, Zheng et al., 1998). It was shown that the response was the result of moving Ca^{2+} ions as removing extracellular Ca^{2+} could block the contractions. A

recent study also supported our findings. Mills (et al., 2009) used a single dose of H_2O_2 (10^{-4}M) to stimulate CPA at rest and found the vessels could contract but the contraction was followed with an immediate relaxation as the vessels returned to their baseline tension. This response was completely inhibited in the presence of CAT. Importantly for our studies they failed to report evidence of H_2O_2 induced vasodilatation when applied at 10^{-8} - 10^{-4}M while they did however demonstrate the peroxynitrite ONOO^- could relax CPA. These findings demonstrate a role for ROS in regulating placental basal tone and may facilitate the long term adaptations to placental insufficiency. The lack of relaxation response H_2O_2 seen with this study may be attributed to the preparation of H_2O_2 . H_2O_2 is a very unstable molecule that is rapidly broken down and we used fresh preparations of H_2O_2 during our investigations and found that this had an important influence on our results.

The treatment with H_2O_2 was found to be toxic for both the CPA and SVA. Perfusing the vessels with 20% pO_2 may itself have been elevating the ROS concentrations as this level of perfusion represents the hyperoxia level for placental vessels. Adding further ROS insults may have overwhelmed the antioxidant pool of the isolated vessels and may have caused the loss in vessel function. This observation also highlights the danger of ROS accumulation which could be causing permanent changes to vessel physiology (McQuillan, Leung et al., 1994).

5.8.5.3. pH

Prolonged periods of hypoxia can alter the pH of circulating blood and will have important consequences for the control of vascular tone. Acidic pH will also lead to chronic

metabolic inhibition as ATP levels can further fall to prolong the pH insult (Canzanelli, Greenblatt et al., 1939, Blechner, 1993, Burton, 2008). During our investigations, CPA and SVA were exposed to relative hypoxia (2% pO₂) and we did not find a significant change in the pH of the bathing saline. Directly altering the external pH environment was then investigated and it was found that a potent response was produced across the pH range applied. It was shown that both CPA and SVA could constrict in response to alkaline conditions with increasing levels of NaHCO₃. In contrast, acidic pH conditions (via application of lactic acid) did not alter the baseline tension but caused a biphasic relaxation response in pre-constricted vessels.

Levels of metabolic acids such as lactic acid have been shown to increase at time of low tissue perfusion such as following the immediate delivery of the placenta (van Laar, Peters et al., 2010). Perfusing the tissue helps to remove lactate and reverse the tissue stress. One possible explanation for the transient response we observed is that as the tissue is continually perfused the lactate molecules are quickly removed from the tissue to restore normal vessel function (Weil and Tang, 1997). This could be investigated by reducing or removing perfusion from the vessel baths to see if tissue oxygenation is a determining factor of the response to lactic acid.

Our results are supported by the findings of Shah (2008) who demonstrated that rat pulmonary arteries could firstly contract when the pH was increased from pH 7.3 to 8.3 using 1M Sodium hydroxide (NaOH). In addition it was reported that the baseline tension when vessels were at rest was reduced when the vessels were exposed to acidic pH of 6.3 with 1M HCl. An exposure to low pH would be expected to inhibit K⁺ and increase baseline tension via depolarisation of the cell membrane (Bevan and Yeats, 1991). However this example

highlights the tissue specific differences that exist across different vascular systems. The pulmonary circulation is a good model for predicting the responses of placental vessels which have previously shown to produce similar responses (Hampl, Bibova et al., 2002).

The response to an acidic pH stimulus has parallels with the response to seen with I/R treatments. Lowering the pH by 0.2 units will introduce a massive H^+ challenge to cause an immediate loss of vessel tone which is transient as the vessel can recover its contractile function. This second phase of the response (recovery phase II) is likened to the re-oxygenation phase and may be the consequences of buffering agents within the saline which work to restore basal pH levels (Gaus, Demir-Weusten et al., 2002, Cowley, Sellers et al., 2005). The most likely candidate could be HCO_3^- which can buffer the bathing solution to maintain a constant pH value. It was also interesting to see that an immediate contraction was produced in response to washout as the pH is switched from 6.4 to the normal pH of 7.4. This provides further support for our observations that increasing $NaHCO_3$ concentrations to invoke alkaline conditions can produce a contraction in placental vessels. A recent study also investigated the response of vessels to lactic acid (Maenhaut and Van de Voorde, 2011). This study demonstrated a relaxation response of rat mesenteric vessels to hypoxia (95% N_2). In contrast the same vessels did not produce a response to lactic acid application but crucially this study was with adult vessels and could highlight a response that is limited to the pulmonary (Shah, 2008) and placental circulations.

The link between prolonged hypoxia and low pH environments was demonstrated with metabolic inhibitor 2,4-Dinitrophenol (DNP) in Chinese hamster ovary cells (COS) cells (Duprat, Lesage et al., 2000). This treatment lowered intracellular pH levels as ATP stores were rapidly depleted. A similar study (Byrne, Howard et al., 1997) used perfused whole

placenta with hypoxic conditioned media to mimic the effects of placental insufficiency and showed that a 20mins exposure to hypoxia was sufficient to lower the pH across the placental tissue. They also showed that the basal lactate levels were significantly higher and contributed to the lower pH recordings found within the placenta circulation. They also reported the venous blood samples showed the most rapid reductions in pH levels and provides a better understanding of how low placental perfusion can have wide ranging consequences for the whole placenta (Byrne, Howard et al., 1997, Otter and Austin, 1999).

HFPV has been hypothesised to improve O₂ uptake by redirecting blood flow to better perfused regions (Hampl, Bibova et al., 2002). In a similar light the relaxation/constriction coupled response produced by placental vessels challenged with acidic pH insults may restrict blood flow to limit the spread of H⁺ ions to the wider placental circulation. This could also allow for tissue perfusion to take place in order to remove the excess H⁺ ions in to the maternal circulation. Placental vessels have shown the capacity to respond to pH stress and this provides an insight into how the placenta can maintain its acid-base balance whilst maintaining its vascular tone. Placental vessels need to match the maternal perfusion pressure whilst maintaining a low resistance to blood flow. Applying chronic stress stimuli has demonstrated that the vessels are suitably adapted to perform this role while optimising the tissue perfusion (Howard, 1987, Byrne, Howard et al., 1997, Weil and Tang, 1997). This also provides further evidence that the placenta is an important organ that has yet much to reveal.

5.8.6. CPA from PE samples

Examining the responses of vessels from healthy patients helps to better understand the differences between normal and adverse pregnancies. The functional responses from a small population of CPA from PE placenta were examined. The contractile response with U46619 was significantly altered with this group which agrees with published data (McCarthy, Woolfson et al., 1994, Myatt, 2002, Abad, Estan et al., 2003, Wareing, Greenwood et al., 2006b). The SNP response was similar between NORM and PE and the vessels were capable of responding to RIL which may be an important observation. The main difference was seen with the response to stress as the response to H_2O_2 was exaggerated as the PE CPA were highly sensitive to the effects of H_2O_2 . An important factor to consider with this observation is that the vessels were perfused with 20% pO_2 and this may be contributing to the production of ROS and a further insult with high doses of H_2O_2 may have resulted in overwhelming the antioxidant capacity of the already stressed tissue.

The response to acidic pH stimuli was also seen with PE CPA samples but more significantly, the loss in tone was reduced when compared to the NORM group across the dose range. This also suggests that the placental vessels can adapt to changing conditions depending on the intrauterine environment and may alter the expression of key pH sensing ion channels to result in this altered response. This limited data set provides an insight into the altered vascular function of adverse pregnancy samples. The reduced ability to relax in response to an acidic pH stimulus could potentially be harmful as the excess H^+ cannot be efficiently buffered out of the placental blood. This would carry the risk of spreading the low pH insult to other areas of the placenta and more importantly expose the fetus to the same

stress (Archer and Michelakis, 2002). It was significant that the pH response was blunted with PE samples and suggests the vessels may be less sensitive to low pH which is often the case when cells have been repeatedly exposed to the same stimuli (Bevan and Yeats, 1991, Gitterman, Wilson et al., 2005). However this study needs to be expanded to include more samples in order to better understand the importance of these differences.

5.8.7. Future research

The functional role of the CPA and SVA were compared across different pO₂ settings to investigate different extremities of tissue perfusion. However it would have been more physiologically relevant to alter the pO₂ within the same experimental set up. This would allow us to then observe the changes in vessel activity when a switch is made from normoxia to hypoxia for instance. The same pO₂ settings were used for both CPA and SVA, however the pO₂ varies across placental regions. For example, at term (≥ 37 wks) the pO₂ recorded within umbilical veins is 38mmHg and 16mmg within the arteries (Campbell, Dawes et al., 1966, Kaufmann, 1982). The latter is also the level of pO₂ that we used in our study to observe relative hypoxia for both SVA and CPA. The recorded pO₂ within the IVS is 5% and was appropriate for SVA but 2% may potentially reflect normoxic conditions for CPA due to the close proximity to the umbilical vessels. It would be interesting to see the effects of <1% pO₂ particularly with the CPA to see how this may alter vessel physiology.

The main limitation with studying SVA was the reduced vessel viability which severely reduced our sample numbers. The vessels were sensitive to mechanical stretch, which significantly limited the opportunity to observe the effects of pre-incubating vessels

with various blockers. We should consider alternative methods of both collecting and storage of vessels to improve viability such as cold storage at 4 °C of isolated placental explants (McIntyre, Williams et al., 1998). In this example it was shown that the EC was still viable after 6h. The lower temperature storage has the benefit that this will slow down apoptosis linked enzymes including caspases and proteases. It also has the benefit of reducing the metabolic rate of the tissue and slowing down hormones such as insulin from being released. The resulting reduction in glucose consumption also means that the O₂ requirement will also fall so the tissue can be stored without the need for perfusion.

Another alternative would be to increase the glucose concentration of PSS from the 5.5mM used which reflects adult basal levels of glucose (Hay, 1995). Increasing the concentration may help to improve tissue viability, particularly for SVA, but may introduce oxidative stress and alter the pH. This would however help to improve the inclusion of invaluable samples such as PE or IUGR placentae which currently cannot be stored for long periods of time and as a result we had a limited number of samples in our study.

A permanent change in the vessel activity was observed post H₂O₂ application as the vessels were no longer responsive to further stimulations. To investigate this we could collect examine the vessels and examine thin tissue preparations using IHC and/or confocal imaging of fresh tissue slices. This will let us examine any changes in the expression of ion channels which in the example of BK_{Ca} have been shown to occur following hypoxia. Evidence of oxidative stress could also be investigated to evaluate the vessel viability and this could help to better understand the response to H₂O₂. Another option to consider could be to use pressurised vessels to better investigate the role of H₂O₂. This method would allow for a

better distinction to be made as to the role of the EC and SMC in generating the biphasic response to H₂O₂ (Halpern, Osol et al., 1984, Dunn and Gardiner, 1995).

Finally alternative vasoconstrictors such as Ang II, 5-HT, or the potent stimulant Et-1 could be explored, as they may have a more potent influence on SVA in particular. The poor response by SVA may also be due to the method for tissue collection. Allen (1987) showed that the anaesthetics used during ELLSCS can alter the function of placental SVA and may explain why we encountered difficulties when working with these vessels. This could be investigated using samples following vaginal delivery where no anaesthetics have been administered.

5.8.8. Conclusion

In summary, the vascular responses of CPA and SVA were compared to gain a better insight into how blood flow is regulated across the fetomaternal interface of the placenta. The hypothesis was supported as the vessels could respond to the same stimuli to generate a response but crucially the force of the responses was significantly altered across CPA and SVA. It was also found that the level of tissue oxygenation had a powerful influence over the final response that was produced to each agonist investigated. The data presented from normal healthy pregnancies goes a long way in helping to build an understanding of the differences that exist in compromised pregnancies and secondly what effective treatments can be devised.

6. Expression of ion channels in CPA and SVA

6.1. Introduction

Ion channels have an important role in controlling the resting membrane potential and as a result have a central role in controlling vascular tone due to their influence on SMC. However there is very limited data available on K^+ channels found within the placental vascular tissue. Electrophysiology data has demonstrated the role for hypoxia sensitive ion channels in resistance vessels (Hampl, Bibova et al., 2002) but limited information is available for these ion channels at the protein level. Our specific hypothesis here is that key O_2 and pH sensitive K^+ channels are differentially expressed across CPA and SVA.

6.2. Objectives

- Determine expression of 6 key K2P ion channels (TASK-1, TASK-3, TRAAK, TREK-1, TREK-2, and TWIK-2), along with the $Ca_v1.2$, BK_{Ca} and the K_{ATP} channel in CPA and SVA using the Western blotting technique.
- To quantitate tissue specific differences in the expression of each ion channel across the different placental vessels using Western blotting.
- Determine the cellular distribution of the key ion channels identified within CPA and SVA SMC using confocal microscopy.

6.3. Materials and methods

Fresh CPA and SVA samples from NORM and PE placentae were immediately placed in liquid N₂ (Chapter 3.4) and used for Western blotting analysis with the antibodies listed in Appendix II. The same antibodies were also used to investigate the subcellular location of each ion channel within cultured SMC using confocal microscopy (Chapter 3.6).

6.4. Results

6.4.1. Patient population

In order to compare NORM and PE samples the first objective was to collect additional information contained within each patient's medical records. The patient and obstetric data has been summarised in **Table 6.4.1-1** and all samples were obtained from ELLSCS (described in Chapter 3.2) from singleton pregnancies. The cord blood was sampled routinely for all complicated pregnancies such as PE, while NORM pregnancies were sampled at the discretion of health professionals. As a result, only 30 patients from the NORM pregnant group had complete cord blood pH recordings in their patient notes.

Table 6.4.1-1 summarising the patient demographics of samples prepared for Western blot analysis. Data are presented as mean (\pm SEM) or median [\pm IQR]. ** $p < 0.01$ *** $p < 0.001$.

Parameter		NORM (N=40)	PE (N=6)	p
Maternal age (yrs)		31.25 \pm 0.9	29 \pm 2.3	0.3 ns
Primipara n (%)		11 (27.5%)	4 (66%)	-
Body mass index (kg/m ²)		25 [22-32]	26.5 [23-30]	0.9 ns
Max. systolic blood pressure outside labour (mmHg)		125 \pm 3.2	150 \pm 6.1	0.01 *
Max. diastolic blood pressure outside labour (mmHg)		63 \pm 1.5	96 \pm 4	0.003 **
Proteinuria g/L		-	3.97 \pm 0.7	-
Gestational age at delivery (days)		271 \pm 1.2	236 \pm 8.0	0.0009 ***
Birth weight (g)		3242 \pm 73	2128 \pm 320	0.0003 ***
Birth weight centile		48 [15-73]	30 [18-50]	0.4 ns
Placenta/Birth weight ratio		0.2 \pm 0.02	0.3 \pm 0.09	0.2 ns
Gender n (% male)		14 (35%)	3 (50%)	-
Cord blood pH	Venous (N)	7.28 \pm 0.02 (30)	7.27 \pm 0.03 (6)	0.3 ns
	Arterial (N)	7.34 \pm 0.01 (30)	7.32 \pm 0.01 (6)	0.9 ns

Only one patient out of the six PE samples was delivered post term (37wks) and the data showed that the gestational age at delivery and the birth weights were significantly lower in the PE group. However it was also shown that the normalised birth weight centile was not significantly different ($p > 0.05$) between the two groups. Furthermore none of our samples were complicated with IUGR and that both arterial and venous cord blood samples did not show evidence of acidosis (pH < 7.05 (van Laar, Peters et al., 2010)) across both NORM and PE patient populations. Examining the individual PE cases revealed some interesting information. One patient had a BP which could not be controlled and remained elevated 9 days post-delivery. The patient displayed no other symptoms and was finally discharged. A second PE case had a

previous history of PE as the patient's own mother had been diagnosed with PE during the respective pregnancy while a final patient underwent an emergency LLSCS due to fetal distress. The final analysis was to determine the mean blood pressure for the PE patients. This was 150/96 and therefore meets the clinical parameter used to diagnose PE (>140/90) (detailed in [Chapter 1.8.1](#)). The second clinical marker for PE is proteinuria and this was determined using urinalysis with a simple dipstick test (Medi-Test® Protein 2) which gives a range from 1-5g/L. Recordings of >0.5g/L are considered to be indicators of PE and all 6 patients in this study had recordings above this critical value with a mean average of 4g/L of protein.

6.4.2. Expression of BK_{Ca}

The initial Western blot analysis was carried out using a monoclonal antibody (BD Transduction). However, this only revealed a 60 kDa band along with multiple non-specific bands as the blot was exposed for longer (not shown). We then opted for the polyclonal antibody as an alternative and found the 60 kDa band was seen along with the predicted 120 kDa band which corresponds to the large α subunit of the BK_{Ca} channel. The polyclonal antibody also had the advantage that the blot was cleaner as less non specific binding was observed. **Figure 6.4.2-1A** shows a detectable signal for the 120 kDa protein and the smaller 60 kDa band. The positive control RB produced strong expression for the 120 kDa band while the 60 kDa was not seen. In contrast the MYO and both CPA and SVA samples from normotensive pregnancies produced a strong band at 60 kDa and a fainter band at 120 kDa which was not always observed

with each sample studied. Each sample is shown with its paired sample where the BK_{Ca} antibody has been pre-absorbed using the control peptide. Only the RB produced a small amount of positive stain but the remaining samples failed to produce any bands when both blots were developed alongside each other. The next objective was to analyse our PE sample population and as a result we repeated the Western blot using the 6 PE matched CPA and SVA placental samples along with a NORM and PE MYO biopsy. The normalised signal intensities are shown for BK_{Ca} in **Figure 6.4.2-1** and semi quantitative analysis shows no significant difference in expression of BK_{Ca} when comparing each pair of sample (**Table 6.4.2-1**). **Figure 6.4.2-1C** shows the results for the α subunit detection in PE samples which was equally expressed across each pair of sample Comparing the mean values post normalisation failed to show any significant differences across the NORM and PE patient groups (**Table 6.4.2-1**).

Expression of ion channels in CPA and SVA

Table 6.4.2-1 showing the densitometry data for each band detected in NORM and PE samples. Comparing the average values across each band size showed no significant difference in the expression of BK_{Ca} when comparing matched CPA and SVA samples or MYO samples

BK _{Ca}	N	MW (kDa)	60		p	120		p
			MEDIAN ± IQR	MEAN ± SEM		MEDIAN ± IQR	MEAN ± SEM	
CPA	24		30 (23-58)	38±5	0.7 ns	24 (11-53)	92±28	0.2 ns
PE-CPA	6		44 (39-53)	46±2		50 (37-71)	55±9	
SVA	24		31 (20-58)	38±5	0.4 ns	25 (13-111)	73±22	0.6 ns
PE-SVA	6		43 (31-59)	44±4		65 (56-103)	76±10	
MYO	8		20 (0-28)	17±6	0.1 ns	96 (47-112)	92±15	0.9 ns
PE-MYO	3		36 (26-41)	35±2		70 (60-90)	73±9	
RB	6		4 (0-20)	9±4		186 (107-329)	242±45	

Expression of ion channels in CPA and SVA

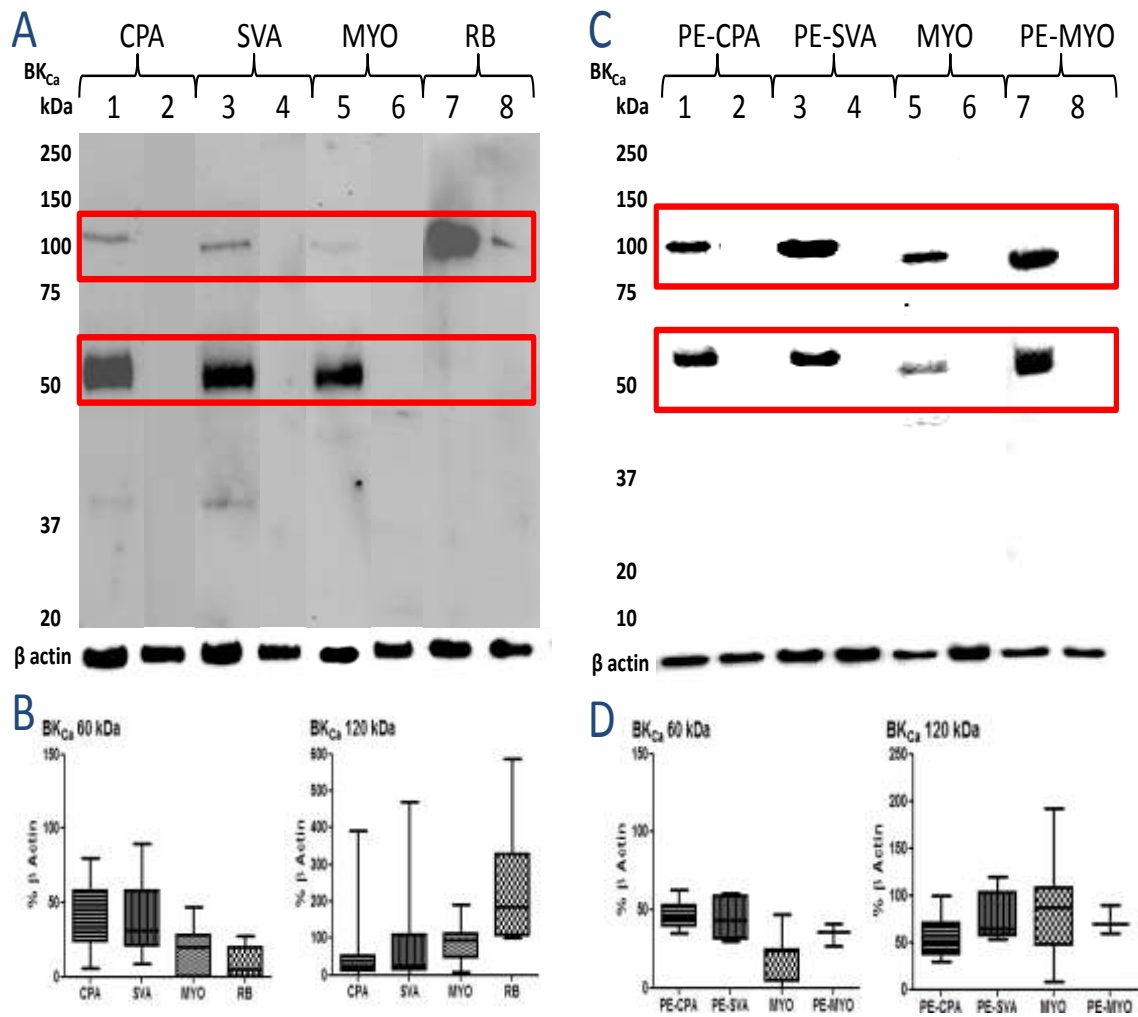


Figure 6.4.2-1 shows BK_{Ca} expression (red box) in CPA (lane 1), SVA (lane 3), and MYO (lane 5) from normal pregnancies and RB samples (lane 7) (A). Matched CPA and SVA samples were immunoblotted for the expression of the BK_{Ca} . Each blot was then stripped and re-blotted with β actin for loading control and is shown below each lane. **B** shows the box and whisker plot for each protein normalised to its individual β actin expression. **C** shows BK_{Ca} expression in CPA and SVA samples from PE samples (red box). Similar expression was observed in both CPA and SVA samples for the 60 kDa band but the 120 kDa was detected in abundance and appears to be higher in the SVA samples. **D** shows the box and whisker plot for each protein normalised to its individual β actin expression. Each sample (A&C) is shown alongside anti BK_{Ca} antibody that has been pre-absorbed with control peptide (lanes 2, 4, 6 & 8). Values shown are expressed as median \pm IQR.

6.4.3. Expression of K_{ATP}

A large 50 kDa protein size was observed which corresponds to the intracellular C domain of K_{ATP} ([Appendix III](#)). CPA, SVA and MYO samples were consistently positive for K_{ATP} expression and has been summarised in **Figure 6.4.3-1A**. Comparing the placental vessels revealed no significant difference in expression across CPA and SVA samples (N=22, p=0.3 **Figure 6.4.3-1B**). The RB samples failed to produce a band in the predicted 50 kDa region so the data was not used for further analysis (discussed in [Chapter 6.4.3.1](#)). Control peptide was also used to validate the specificity of the antibody and developed alongside each sample of interest and revealed no non-specific signal. The following Western blot analysis involved PE samples of both CPA and SVA tissue (N=6) and **Figure 6.4.3-1C&D** shows the results for K_{ATP} expression across the PE placental samples alongside the normal and PE MYO biopsies. A 50 kDa protein was identified in each of the 6 samples and no significant difference in the expression of K_{ATP} across the NORM and PE samples was found (**Table 6.4.3-1**).

Expression of ion channels in CPA and SVA

Table 6.4.3-1 summarising the densitometry data for K_{ATP} expression in NORM and PE samples. CPA and SVA samples show no significant difference in the expression of K_{ATP} across the patient groups.

K_{ATP}	N	MW (kDa)	50		<i>p</i>
			MEDIAN \pm IQR	MEAN \pm SEM	
CPA	22		48 (29-68)	51 \pm 4	0.8 ns
PE-CPA	6		61 (58-68)	63 \pm 2	
SVA	22		45 (32-55)	49 \pm 5	0.5 ns
PE-SVA	6		63 (53-77)	64 \pm 7	
MYO	6		73 (53-94)	77 \pm 11	0.3 ns
PE-MYO	3		107 (104-123)	111 \pm 3	

Expression of ion channels in CPA and SVA

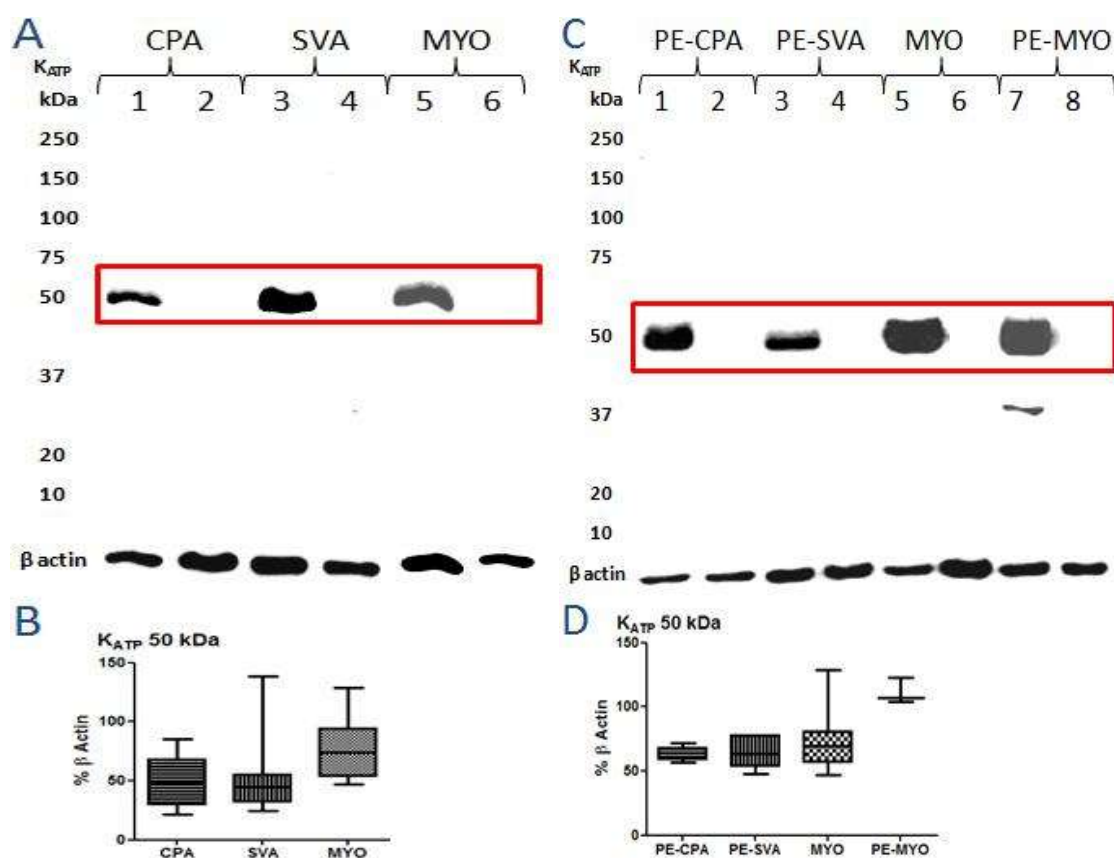


Figure 6.4.3-1 showing a representative image for K_{ATP} expression (red box) in NORM CPA and SVA samples along with the positive controls MYO and RB (A). The 50 kDa target band was seen in CPA, SVA and MYO samples. **B** shows the box and whisker plot for each protein normalised to its individual β actin expression. **C** showing the detection of K_{ATP} in PE tissue samples (red box). **D** summarises the box and whisker plot for each protein normalised to its individual β actin expression and no difference was found across the samples. Each sample (A&C) is shown alongside anti K_{ATP} antibody that has been pre-absorbed with control peptide (lanes 2, 4, 6 & 8). Values shown are expressed as median ± IQR.

6.4.3.1. Antibody validation

The positive control RB was chosen for its reported abundant expression levels for a range of ion channels including the K2P family of ion channels (Patel, Honore et al., 1998). However the Western blotting analysis failed to produce a

positive signal for expression of ion channels with RB, namely K_{ATP}, TASK-1, TASK-3 TRAAK and TWIK-2, although RB is a recommended positive control according to the information contained in the individual datasheets provided by the manufacturers (Alomone). Replacing the blocking agent marvel with BSA could not resolve this issue (not shown). Another possible explanation could be the poor separation of proteins during homogenisation of RB tissue, and was further investigated with the RB cell line SH SY57. SH SY57 cells produced a positive band within in the predicted region for each ion channel (**Figure 6.4.3.1-1**). However the β actin levels were significantly lower than that for the crude tissue samples, and as a result made statistical analysis difficult, so the cells were not used further. The MYO tissue was then used as a positive control for the antibodies in question.

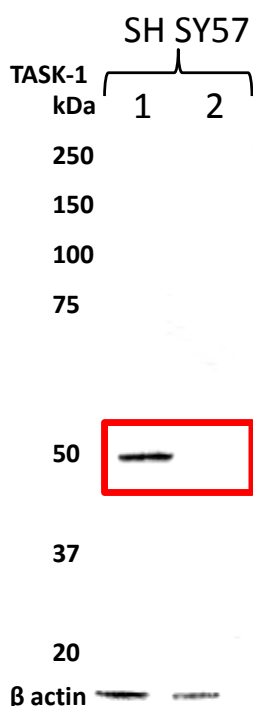


Figure 6.4.3.1-1 showing the expression of TASK-1 in SH SY57 cells (red box) alongside anti TASK-1 antibody that has been pre-absorbed with control peptide (lane 2).

We were also aware of the need for consistency with our Western blot blots, and used crude tissue preparations of tissue, instead of cultured cell lines. The MYO was a better reference control for validating the quality of the antibodies, as it was consistently positive for expression of our ion channels of interest. One MYO patient sample was used to validate each new batch of antibody ordered, to check for any variation in epitope specificity. From all the antibodies used in this study, an inconsistency was identified with the anti TREK-1 antibody, which had previously produced bands at 100-90, 60 and 50 kDa (**Figure 6.4.3.1-2**). However as new batches of the same antibody were ordered again, the 50 kDa band was detected only (see [Chapter 6.4.4.4](#)) with a loss of the larger proteins. During the course of this study,

it was also found that the manufacture's datasheet had also been updated to reflect this change in antibody sensitivity.

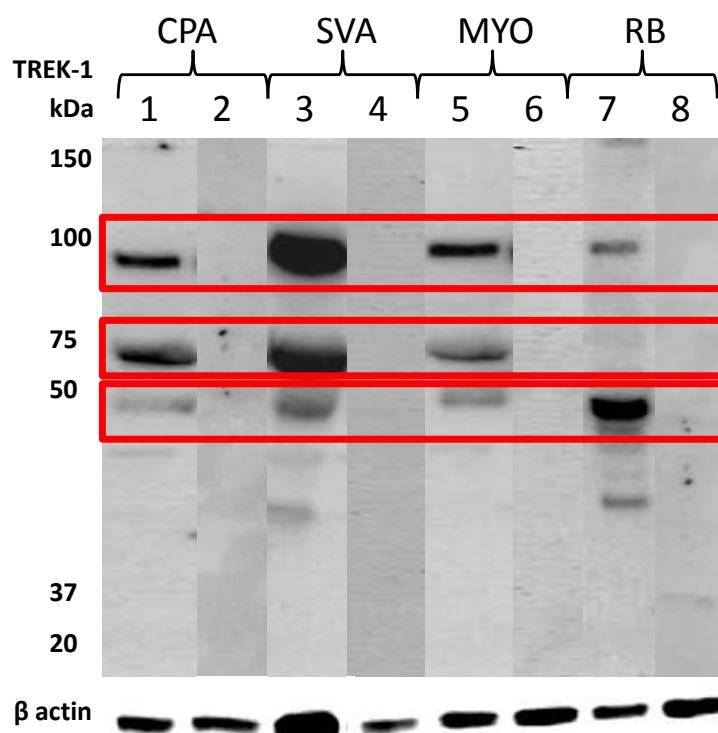


Figure 6.4.3.1-2 showing the preliminary detection of TREK -1 in (red box) alongside anti TREK-1 antibody that has been pre-absorbed with control peptide (lanes 2, 4, 6 &8). The blot shows the early Western blot images that were obtained with TREK-1 which produced three distinct bands (100, 60 and 50 kDa). However these bands were not seen with every patient samples examined and may be attributed to differences in antibody batches.

6.4.4. Expression of K2P channels

6.4.4.1. Expression of TASK-1

Figure 6.4.4.1-1A shows the results with TASK-1 Western blotting. The antibody is raised against the intracellular C terminal which has a predicted molecular weight of 45 kDa ([Appendix III](#)). A clear band with a MW of 50 kDa was observed and was assumed to be the TASK-1 channel in both CPA and SVA tissue samples along with the MYO muscle biopsy while RB was negative for TASK-1 expression. A band at the 71/75 kDa region was observed in some samples which had a lower signal intensity compared with the 50 kDa protein. The percentage intensity of the different TASK-1 bands has been summarised in **Figure 6.4.4.1-1B**. Semi quantitative analysis showed that there was no significant difference in TASK-1 expression across CPA and SVA both for the 50 kDa (N=31, p=0.37) and 71 kDa proteins (N=31, p=0.5). The MYO tissue was also positive for TASK-1 (50 kDa) and revealed an additional band at ~60kDa that was not seen with either CPA or SVA.

PE samples were also analysed for expression of TASK-1 and a representative Western blot image has been shown in **Figure 6.4.4.1-1C**. The image revealed a dense band at 50 kDa across each sample as both the PE CPA and PE SVA tissue are positive along with NORM and PE-MYO tissue samples. However in contrast to the NORM CPA and SVA tissue the 71/75 kDa was not detected in abundance in any of the 6 samples obtained from PE placentae. The MYO was also analysed for expression of TASK-1 and revealed the same 50 kDa band, we also found that the 71

Expression of ion channels in CPA and SVA

kDa was not revealed in either the normal or the PE-MYO. The normalised densitometry data has been summarised in **Table 6.4.4.1-1** and we observed no significant differences in the expression of TASK-1 across the CPA and SVA tissue as well as the NORM MYO and PE-MYO tissue lysate.

Table 6.4.4.1-1 summarising the average expression of TASK-1 in each sample studied. There was no significant difference in expression of TASK-1 (both protein sizes) in SVA and CPA samples.

TASK-1	N	MW (kDa)	50		<i>p</i>	71		<i>p</i>
			MEDIAN ± IQR	MEAN ± SEM		MEDIAN ± IQR	MEAN ± SEM	
CPA	31		37 (27-49)	49 ± 7	0.6 ns	23 (19-48)	19 ± 4	0.9 ns
PE-CPA	6		54 (45-58)	52 ± 3		19 (17-23)	20 ± 3	
SVA	31		42 (32-60)	48 ± 4	0.2 ns	31 (20-58)	29 ± 6	0.7 ns
PE-SVA	6		55 (37-59)	55 ± 5		25 (19-31)	24 ± 3	
MYO	8		36 (26-56)	45 ± 7	0.8 ns	4 (0-56)	9 ± 1	0.5 ns
PE-MYO	3		39 (38-55)	44 ± 5		0 (0-41)	13 ± 10	

Expression of ion channels in CPA and SVA

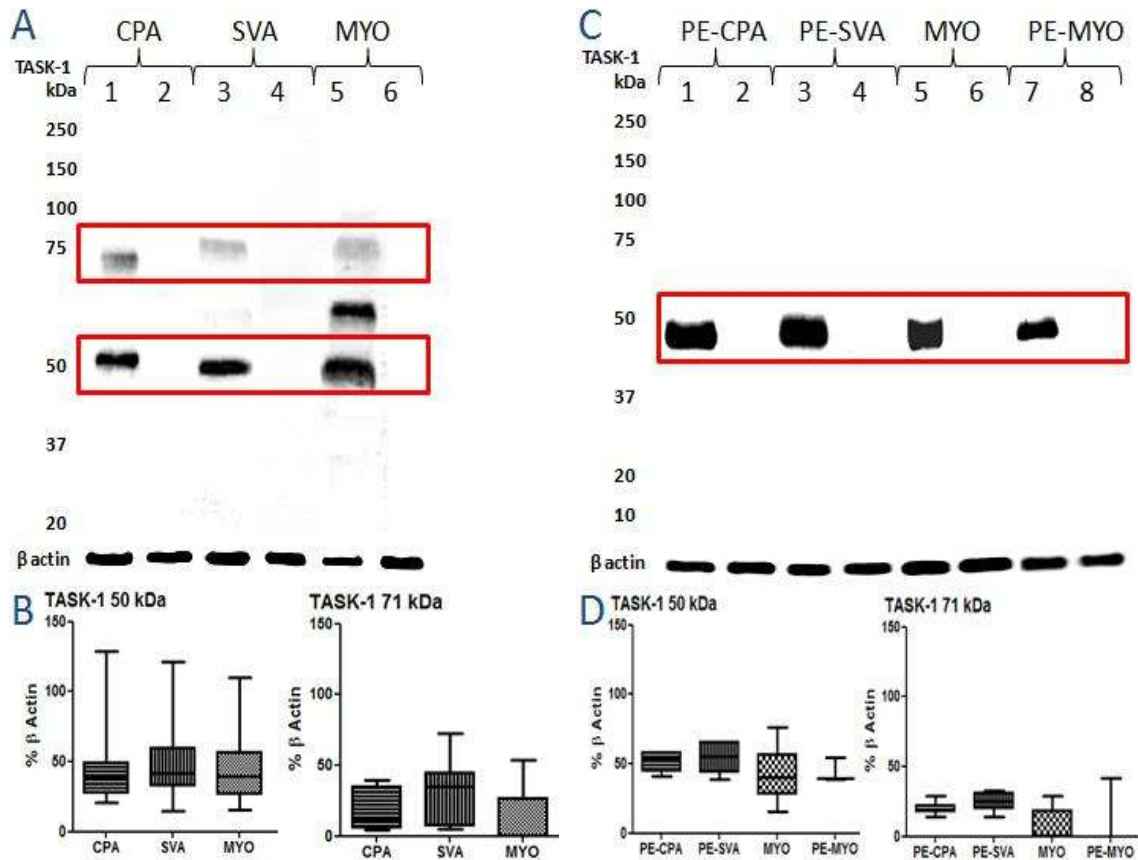


Figure 6.4.4.1-1 showing a representative blot of TASK-1 expression (red box) in matched CPA and SVA samples along with MYO from normotensive controls (A). Two distinct bands were identified in CPA and SVA samples. These bands were also seen with MYO samples along with an additional band around the 65 kDa region. **B** shows the normalised densitometry data for the two main target proteins considered to be TASK-1. **C** shows a representative blot of TASK-1 expression in matched PE-CPA and SVA samples along with MYO from normal and PE pregnancies (red box). The 50 kDa protein was consistently observed while the 71 kDa protein was not detected in abundance. **D** shows the normalised densitometry data for the expression of TASK-1. Each sample (A&C) is shown alongside anti TASK-1 antibody that has been pre-absorbed with control peptide (lane 2, 4, 6 & 8). Values shown are expressed as median \pm IQR.

6.4.4.2. Expression of TASK-3

Figure 6.4.4.2-1A shows a representative Western blot image for the detection of TASK-3. Based on the data sheet provided with the antibody the predicted molecular weight is 47 kDa corresponding to the extracellular P1 loop of TASK-1 (**Appendix III**). Western blot analysis revealed a protein band of approximately 51 kDa which was consistently detected with each sample analysed (N=23) and was assumed to be TASK-3. The band was also observed in MYO tissue at the same MW while RB again did not produce any staining. No significant difference was shown in the expression levels of TASK-3 when comparing CPA and SVA (**Figure 6.4.4.2-1B**). **Figure 6.4.4.2-1C** shows the Western blot analysis with PE derived placental samples. We again observed a band at 50 kDa and there was no significant difference in the expression levels of TASK-3 across each NORM and PE sample (**Table 6.4.4.2-1**).

Expression of ion channels in CPA and SVA

Table 6.4.4.2-1 showing the average densitometry data for TASK-3 expression in each sample. No significant difference was found in the level of TASK-3 when comparing matched samples of CPA, SVA and MYO.

TASK-3	N	MW (kDa)	50		P
			MEDIAN \pm IQR	MEAN \pm SEM	
CPA	23		46 (34-65)	52 \pm 4	0.7 ns
PE-CPA	6		54 (44-58)	52 \pm 6	
SVA	23		46 (29-60)	49 \pm 4	0.5 ns
PE-SVA	6		55 (44-65)	54 \pm 4	
MYO	6		41 (26-74)	44 \pm 9	0.4 ns
PE-MYO	3		39 (38-54)	44 \pm 7	

Expression of ion channels in CPA and SVA

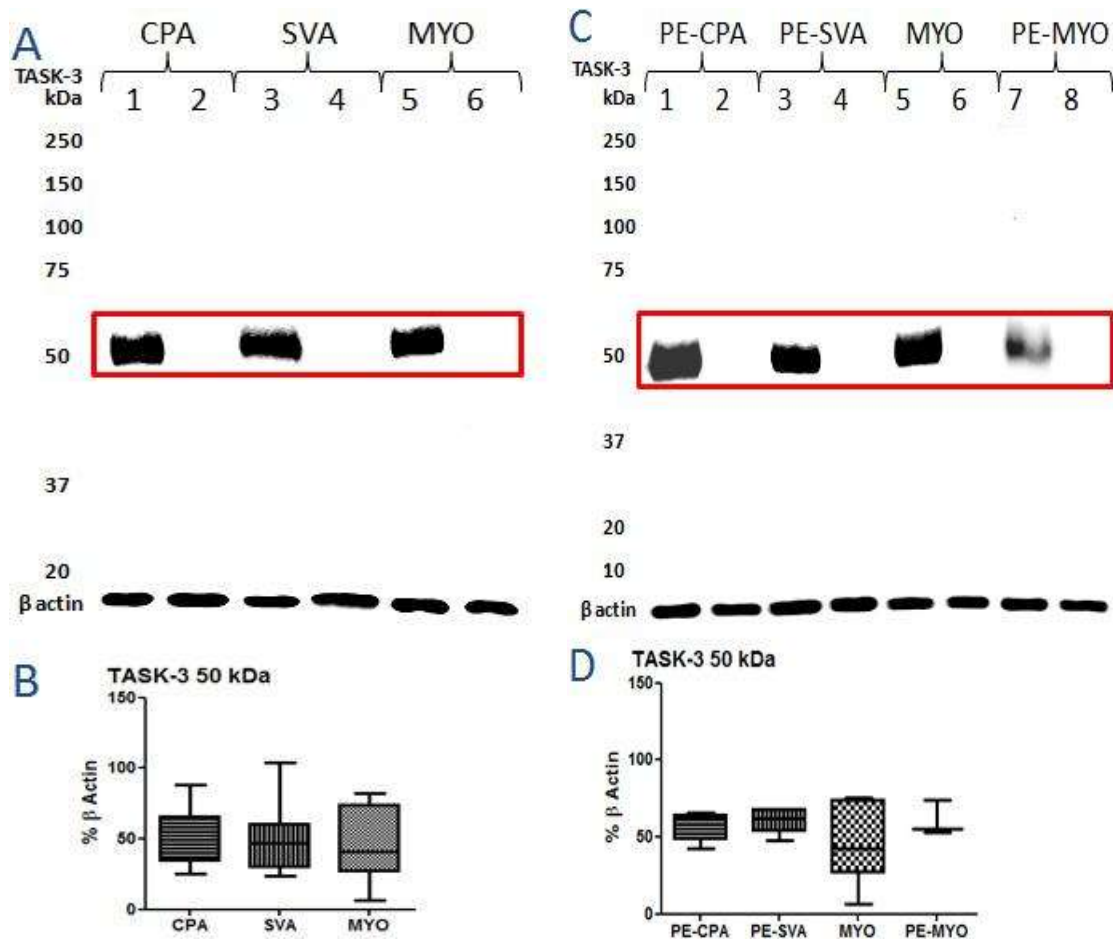


Figure 6.4.4.2-1 showing TASK-3 expression (red box) in placental CPA and SVA from NORM samples (A). The MYO tissue lysate was also positive for TASK-3 expression. **B** shows the box and whisker plot for each protein normalised to its individual β actin expression. **C** summarises the Western blot analysis of PE CPA and SVA and MYO from NORM and PE patient samples. Each sample produced a band at 50 kDa which corresponds to the monomer for TASK-3 (red box). **D** shows the box and whisker plot for TASK-3 expression for each sample analysed. Each sample (**A** & **C**) is also shown alongside anti TASK-3 antibody that has been pre-absorbed with control peptide (lanes 2, 4, 6 & 8). Values are expressed as median \pm IQR.

6.4.4.3. Expression of TRAAK

TRAAK is another key K2P channel that we were interested in studying as this ion channel is closely related to TREK and shares a lot of its pharmacological properties. A small number of samples were analysed for the expression of TRAAK (N=8). **Figure 6.4.4.3-1A** shows the Western blot image for TRAAK revealing a single band at 51 kDa which closely matches the predicted molecular weight for the intracellular C terminus (52 kDa) ([Appendix III](#)). **Figure 6.4.4.3-1B** summarises the average band intensities for each sample analysed and we found no significant difference in the expression for TRAAK when comparing CPA with SVA ($p=0.43$). MYO (N=3) was also positive for the ion channel which appeared to be less abundant when compared to human placental tissue and may require further validation while RB failed to produce positive stain and was not used in further analysis. **Figure 6.4.4.3-1C** shows a representative Western blot image for TRAAK in PE-CPA and SVA samples. A dense band at 50 kDa was observed which was similar to the band that was revealed using the NORM samples. **Table 6.4.4.3-1** shows the normalised densitometry data for each sample and we did not see any significant differences in the expression TRAAK across the different tissue samples analysed.

Expression of ion channels in CPA and SVA

Table 6.4.4.3-1 showing the normalised pixel intensity data for the TRAAK channel in NORM and PE samples. No significant difference was found in the expression of TRAAK across the two placental vascular beds.

TRAAK	N	MW (kDa)	50		<i>p</i>
			MEDIAN ± IQR	MEAN ± SEM	
CPA	8		68 (35-77)	61±8	0.4 ns
PE-CPA	6		37 (31-40)	35±4	
SVA	8		64 (38-78)	55±9	0.5 ns
PE-SVA	6		48 (33-63)	47±7	
MYO	4		46 (35-73)	51±10	0.2 ns
PE-MYO	3		75 (65-90)	76±7	

Expression of ion channels in CPA and SVA

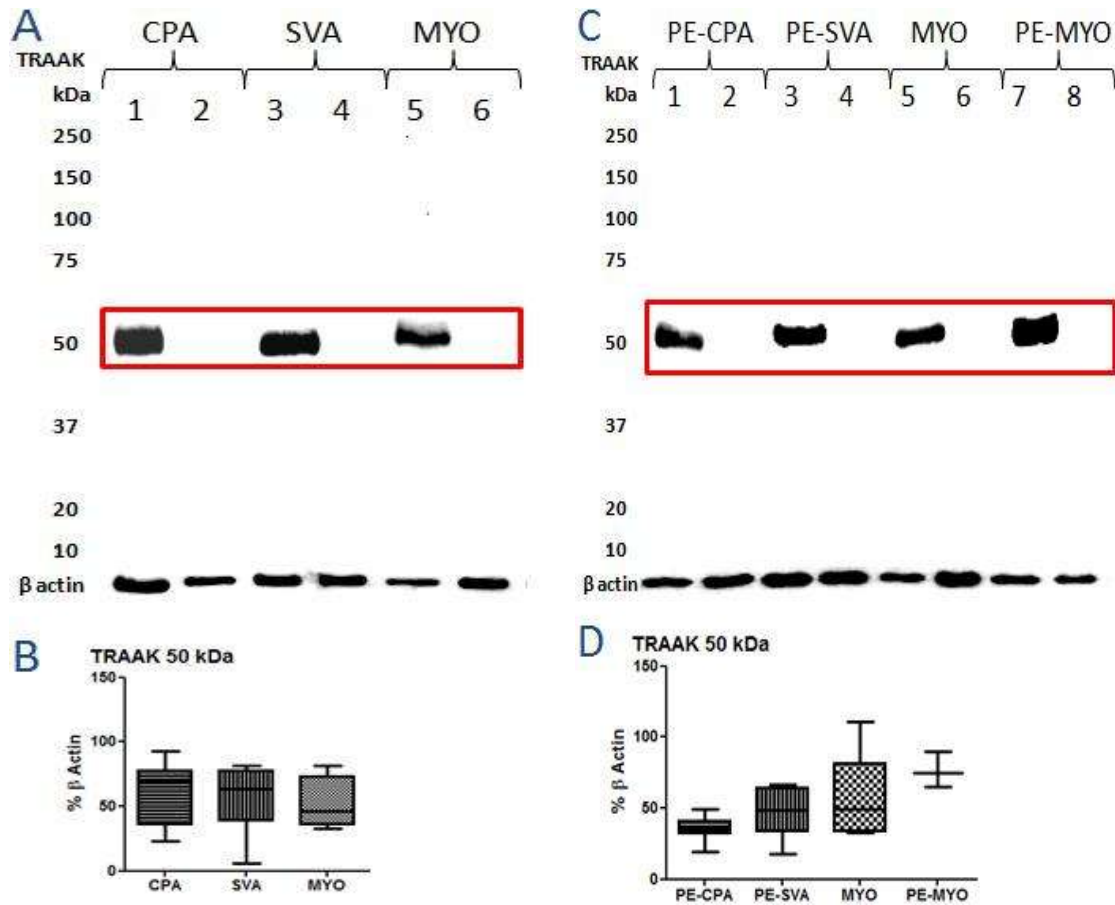


Figure 6.4.4.3-1 showing TRAAK expression (red box) in CPA, SVA and MYO samples from NORM samples (A). B shows the % expression levels in each sample relative to β actin. C shows a representative Western blot for TRAAK expression in PE-CPA and SVA samples (red box). D shows the box and whisker plot which summarises the average pixel intensities once the data has been normalised to β actin. Each sample (A&C) is also shown alongside anti TRAAK antibody that has been pre-absorbed with control peptide (lane 2, 4, 6&8). Values are expressed as median \pm IQR.

6.4.4.4. Expression of TREK-1

Early work with the TREK-1 antibody revealed three distinct bands, one at 100-90 kDa, one dense band at 75 kDa and a smaller band at 50 kDa. As the analysis was expanded to include more samples the 100 kDa was not always revealed each time. The datasheet provided with the antibody has also since been updated to show a single band at 50 kDa which represents the intracellular N terminal of TREK-1 ([Appendix III](#)). **Figure 6.4.4.4-1A** shows a representative Western blot image and RB produced two bands at 100 and 50 kDa so we chose to discount the 75 kDa band from further analysis. The 50 and 100 kDa were closely related as when one band was seen in abundance the second was reduced. This suggests that the two bands may represent the monomer and dimer configuration of TREK-1. No difference was shown in expression between CPA and SVA (**Figure 6.4.4.4-1B**) while the CPA expression of the 50 kDa band was found to be significantly higher ($p<0.05$) when compared to MYO samples. The PE samples were also analysed and a clear band at 50 kDa was found across all the samples with a faint 100 kDa band which was difficult to identify (**Figure 6.4.4.4-1C**) (discussed in [Chapter 6.4.3.1](#)). Comparing matched CPA and SVA samples (**Table 6.4.4.4-1**) showed that there was no significant difference in the expression of TREK-1 (50 kDa) across the placental vascular beds while the 100 kDa was found to be significantly lower ($p<0.05$) in PE samples.

Expression of ion channels in CPA and SVA

Table 6.4.4.4-1 showing the average densitometry data for TREK-1 in NORM and PE CPA, SVA, MYO along with RB tissue. We focused on the 50 and 100 kDa proteins which were also found with the RB positive control. Comparing the average expression levels for TREK-1 at 50 kDa showed no significant difference across the different tissue samples while the 100 kDa was detected in significantly lower levels in the PE vessel samples.

TREK-1	N	MW (kDa)	50		<i>p</i>	100		<i>p</i>
			MEDIAN ± IQR	MEAN ± SEM		MEDIAN ± IQR	MEAN ± SEM	
CPA	40		67 (31-121)	93±10	0.1 ns	23 (9-76)	43±5	<0.05*
PE-CPA	6		44 (36-47)	42±3		2 (1-5)	3±0.6	
SVA	40		50 (33-94)	69±6	0.3 ns	18 (18-142)	41±6	<0.05*
PE-SVA	6		41 (36-49)	41±2		3 (6-4)	3±0.4	
MYO	10		33 (0-40)	30±6	0.8 ns	15 (7-36)	23±6	0.4 ns
PE-MYO	3		32 (17-46)	31±8		15 (13-20)	17±0.8	
RB	6		29 (13-38)	34±6		13 (0-54)	24±6	

Expression of ion channels in CPA and SVA

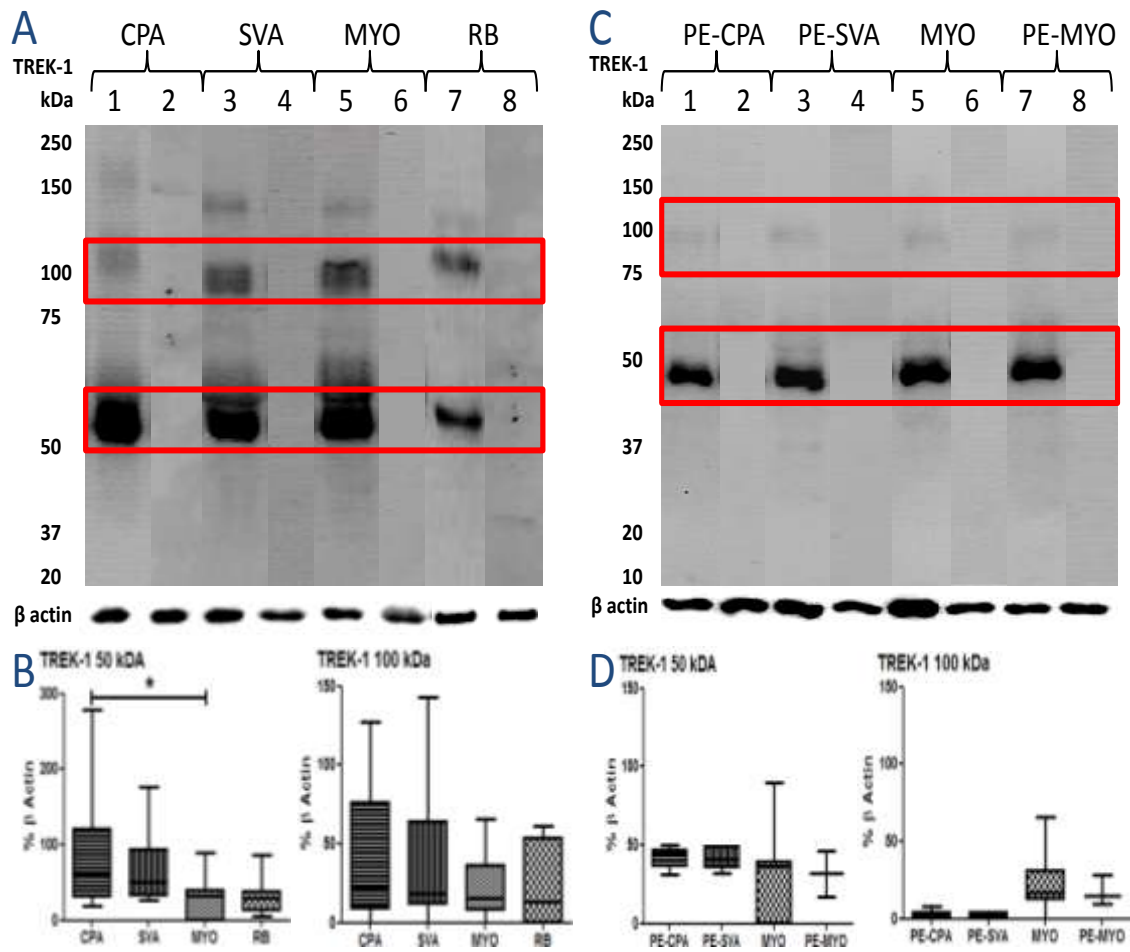


Figure 6.4.4-1 showing TREK-1 expression (red box) in NORM CPA and SVA with MYO tissue (A) RB was also positive showing two bands at 50 and 100 kDa which may represent the monomer and dimer proteins of TREK-1. **B** shows the % expression following normalisation to β actin. **C** shows a representative Western blot image for TREK-1 in PE-CPA and SVA. A clear 50 kDa band is visible but the 100 kDa can only be seen at a low level in the two MYO samples (red box). **D** shows the box and whisker plot which summarises the average pixel intensities once the data has been normalised to β actin. Each sample (A&C) is also shown alongside anti TREK-1 antibody that has been pre-absorbed with control peptide (lane 2, 4, 6&8). Values are expressed as median ± IQR.

6.4.4.5. Expression of TREK-2

The TREK-2 antibody recognises the intracellular C terminus and has a predicted molecular weight of 59 kDa ([Appendix III](#)). **Figure 6.4.4.5-1A** shows a representative Western blot image for the expression of TREK-2 in human placental CPA, SVA and MYO. RB was also included, and produced multiple bands on the Western blot confirming the presence of the ion channel including a dense band that was observed at 100 kDa. However the human tissue samples produced two distinct bands, also seen with RB, at 40 kDa and a doublet at 52-56 kDa which formed the focus of our analysis. The CPA expression for TREK-2 appeared to be lower but analysis of the data set showed that this was not significantly different to SVA (N=8, $p>0.05$) (**Figure 6.4.4.5-1B**). TREK-2 expression was examined in PE-CPA and SVA (**Figure 6.4.4.5-1C**). In contrast to the normal tissue samples the PE tissue produced a dense band at 40 kDa both with CPA and SVA tissue which appears to be expressed in abundance when compared with the higher 52-56 kDa band but failed to show any significance ($p>0.05$). The average densitometry data has been summarised in **Table 6.4.4.5-1** and showed no significant difference in the TREK-2 across the different tissue samples analysed.

*Expression of ion channels in CPA and SVA***Table 6.4.4.5-1** summarising TREK-2 expression data form NORM and PE samples. No significant difference was found in the expression for TREK-2 across each subunit.

TREK-2	N	MW (kDa)	40		P	52-56		p
			MEDIAN ± IQR	MEAN ±SEM		MEDIAN ± IQR	MEAN ±SEM	
CPA	8		36 (24-46)	36±4	0.8 ns	34 (24-39)	34±3	0.3 ns
PE-CPA	6		33 (24-47)	35±5		20 (17-22)	20±1	
SVA	8		43 (37-63)	56±13	0.3 ns	34 (22-37)	29±4	0.2 ns
PE-SVA	6		27 (18-40)	29±6		15 (13-20)	16±2	
MYO	3		45 (38-73)	52±10	0.8 ns	19 (0-38)	19±11	0.8 ns
PE-MYO	3		41 (33-66)	46±9		16 (16-19)	17±1	
RB	4		59 (32-84)	60±8	-	76 (18-142)	79±33	-

Expression of ion channels in CPA and SVA

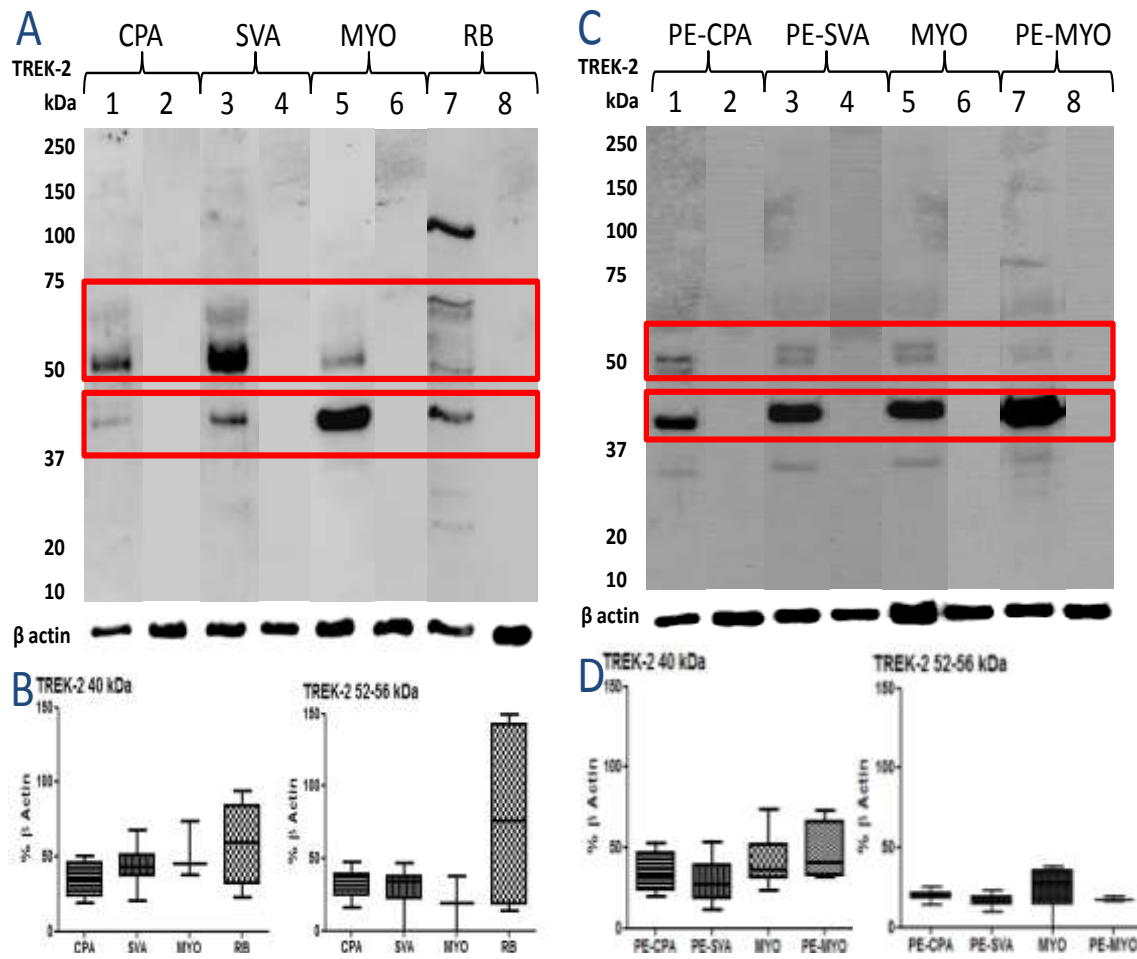


Figure 6.4.5-1 showing TREK-2 expression (red box) in placental samples (A). Multiple bands in the RB sample were found but the human tissue showed two bands one at 40 kDa and secondly a doublet at 52-56 kDa which was analysed. **B** shows the box and whisker plot which summarises the average pixel intensities once the data has been normalised to β actin. **C** shows a representative Western blot image for TREK-2 in PE-CPA and SVA samples along with normal and PE-MYO tissue (red box). All samples showed positive expression for the K2P channel and control lanes confirm that this stain is specific. **D** shows the box and whisker plot which summarises the average pixel intensities once the data has been normalised to β actin. Each sample (**A**&**C**) is also shown alongside anti TREK-2 antibody that has been pre-absorbed with control peptide (lane 2, 4, 6&8). Values are expressed as median \pm IQR.

6.4.4.6. Expression of TWIK-2

The anti TWIK-2 antibody is raised against the intracellular C terminus with a predicted molecular weight of 35 kDa ([Appendix III](#)). Our results showed a 37 kDa band was seen along with the more abundant band at 50 kDa which was visible with CPA and SVA along with the MYO tissue (**Figure 6.4.4.6-1A**), while no staining was evident in RB. Analysis of these two bands revealed no significant difference in the expression of TWIK-2 across the two placental vessels (N=40, $p<0.05$). (**Figure 6.4.4.6-1B**) Western blot analysis with our PE samples revealed that both CPA and SVA were positive for TWIK-2 expression along with the normal and PE MYO (**Figure 6.4.4.6-1C**). Comparing the samples shows that PE CPA expression for the 37 kDa was higher when compared to PE SVA (N=6, $p<0.05$). The 50 kDa band was also significantly higher in PE CPA when compared to NORM CPA ($p<0.001$) (**Table 6.4.4.6-1**).

Expression of ion channels in CPA and SVA

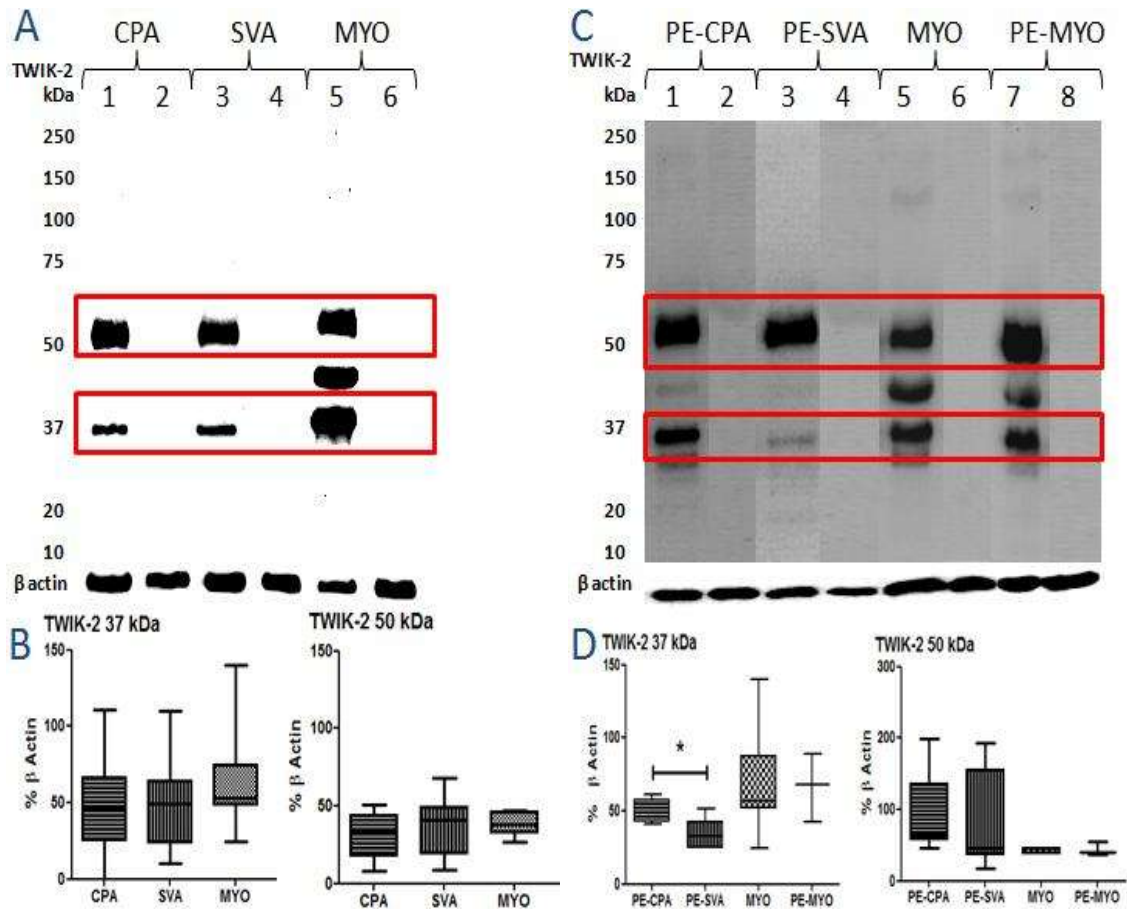


Figure 6.4.4.6-1 showing the difference in TWIK-2 expression (red box) across CPA and SVA (**A**) and revealed a 37 kDa protein along with a more abundant 50 kDa band which is also seen in MYO samples. **B** shows the box and whisker plot for each sample and includes analysis of both bands that were observed. **C** shows a representative Western blot image for TWIK-2 in PE-CPA and SVA samples along with normal and PE-MYO tissue (red box). All samples demonstrated positive expression for the K2P channel. **D** shows the box and whisker plot which summarises the average pixel intensities once the data has been normalised to β-actin. Each sample (**A** & **C**) is also shown alongside anti TWIK-2 antibody that has been pre-absorbed with control peptide (lanes 2, 4, 6 & 8). Values are expressed as median ± IQR.

Expression of ion channels in CPA and SVA

Table 6.4.4.6-1 summarising the calculated densitometry data for TWIK-2. The RB failed to give a positive signal and was not included in our analysis. Comparing matched CPA and SVA tissue samples revealed that only the 50 kDa band was significantly higher in PE CPA.

TWIK-2	N	MW (kDa)	37		P	50		P
			MEDIAN \pm IQR	MEAN \pm SEM		MEDIAN \pm IQR	MEAN \pm SEM	
CPA	40		49 (24-110)	49 \pm 3	0.8 ns	33 (18-43)	30 \pm 4	0.01**
PE-CPA	6		52 (42-58)	51 \pm 3		67 (58-135)	92 \pm 23	
SVA	40		48 (23-108)	46 \pm 4	0.5 ns	41 (19-50)	37 \pm 5	0.2 ns
PE-SVA	6		32 (24-43)	34 \pm 4		45 (37-156)	81 \pm 28	
MYO	10		53 (25-74)	65 \pm 9	0.9 ns	38 (32-46)	39 \pm 4	0.6 ns
PE-MYO	3		68 (42-89)	66 \pm 13		39 (36-55)	43 \pm 6	

6.4.5. Confocal analysis of CPA and SVA SMC

6.4.5.1. Subcellular localisation of Cav1.2

Initial attempts with Western blotting failed to identify the target protein in the range of 210-240 kDa predicted for Cav1.2 (**Appendix III**) and instead a series of smaller bands were isolated (not shown). Due to time constraints this was not investigated further. Instead, the expression of Cav1.2 was investigated using IF staining. **Figure 6.4.5.1-1** shows the cellular distribution of Cav1.2 in CPA and SVA SMC. The positive IF is found throughout the cell body, and higher magnification shows the nucleus is completely clear of IF stain in both cell types. The ion channel is organised in a tight linear mesh that is spread across the cell body to allow the cell to

rapidly respond to external stimuli. No IF was produced when primary antibody (both mouse monoclonal & rabbit polyclonal) was replaced with control IgG (not shown).

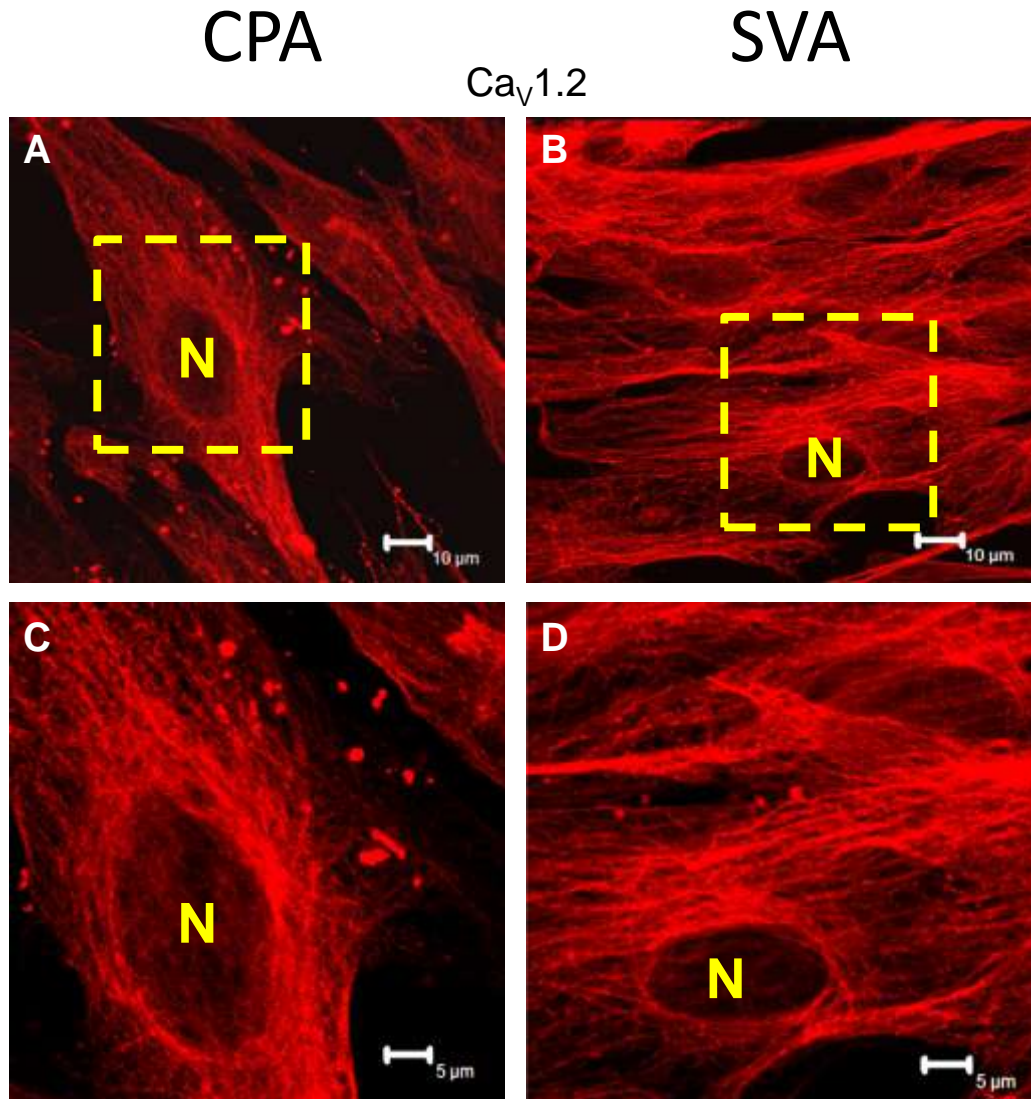


Figure 6.4.5.1-1 showing immunodetection for $\text{Ca}_v1.2$ in SMC cultured from CPA (A) and SVA (B) (N=4). Images were captured using confocal microscopy and each row shows paired CPA and SVA samples at the same magnification. The yellow box (A&B) labels the region of the original images that was used to take images at higher magnification (C&D). The $\text{Ca}_v1.2$ channel shows similar expression pattern in both types of SMC with linear expression across the cell body while the nucleus (N) remains unstained.

6.4.5.2. Subcellular localisation of TASK 1

Figure 6.4.5.2-1 shows the early images that were taken showing positive IF for TASK-1 in placental SMC confirmed by the IF for α actin. The IF staining pattern was observed to be evenly distributed across the cell body with a granular distribution for TASK-1. The SVA SMC also showed evidence of intense staining around the nucleus which is most prominent in showing the peri-nuclear region in detail (white arrow). In contrast, CPA derived cells in **Figure 6.4.5.2-1C** show staining inside the nuclei which has also stained positive with α actin so may be due to an artefact caused by antibody retention. No stain was observed with primary antibody that was pre-absorbed with control peptide added in excess (not shown).

SMC from the MYO also stained positive for TASK-1 expression (**Figure 6.4.5.2-2**) along with the rat brain cell line SH SY57. The TASK-1 staining shows linear distribution in MYO cells across the cell body and the cell membrane with positive co-localisation with α actin expression. The TASK-1 expression is highly organised as all the staining is linear with very little granular distribution. SH SY57 cells instead show only granular distribution which supports our observations made with CPA and SVA cells and suggests that K2P channels may have tissue specific distribution expression patterns.

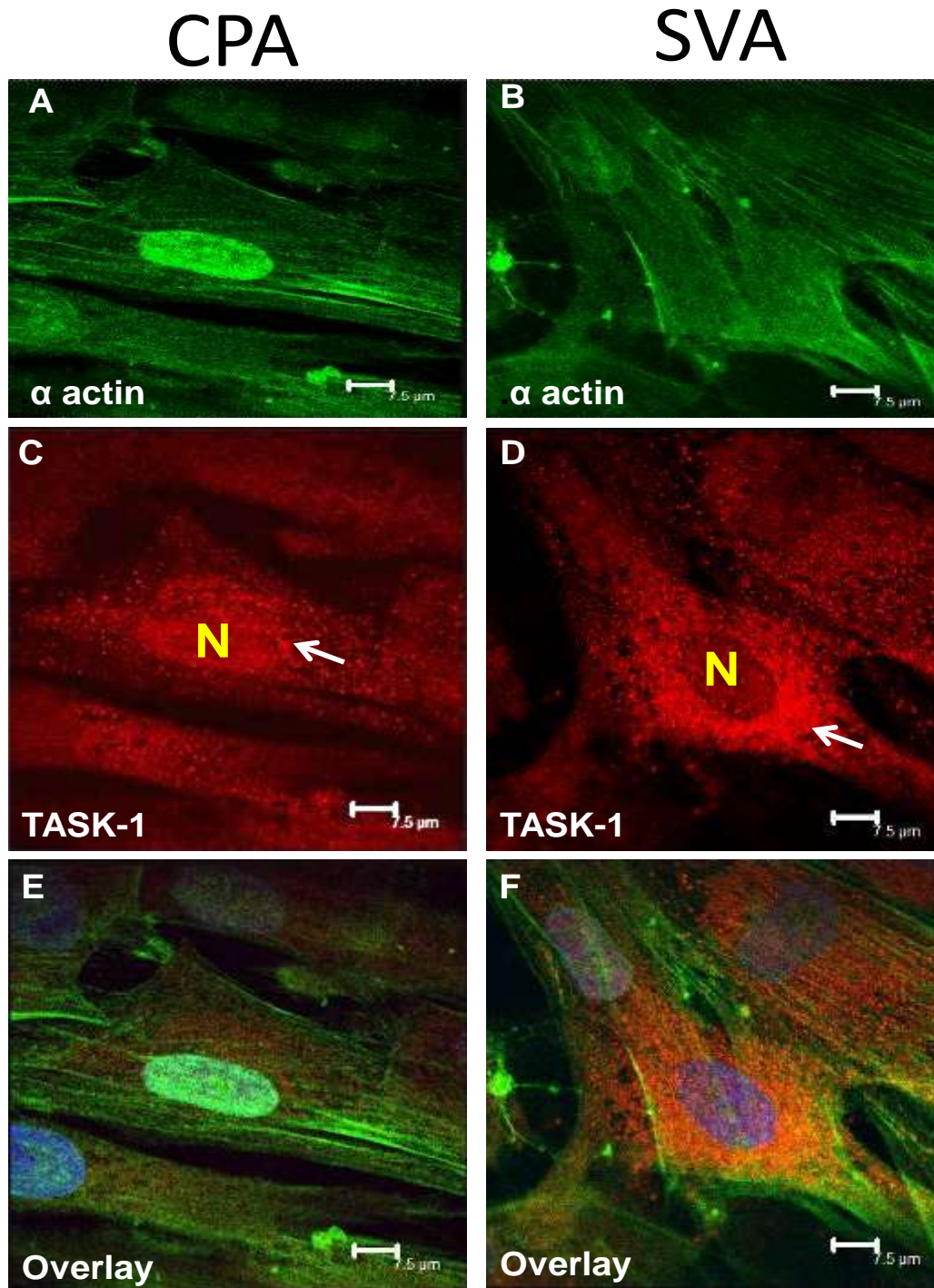


Figure 6.4.5.2-1 showing TASK-1 positive IF in CPA and SVA SMC (N=10). The high magnification photomicrograph shows the distribution of TASK-1 within the cells. **C&D** show TASK-1 stain is diffuse across the cell body but there is an intense stain around the nucleus (white arrow) and is most prominent in SVA cells. In this instance the nucleus was also labelled with DAPI (blue) and the merged images do not show any co-localisation with α actin (**E&F**).

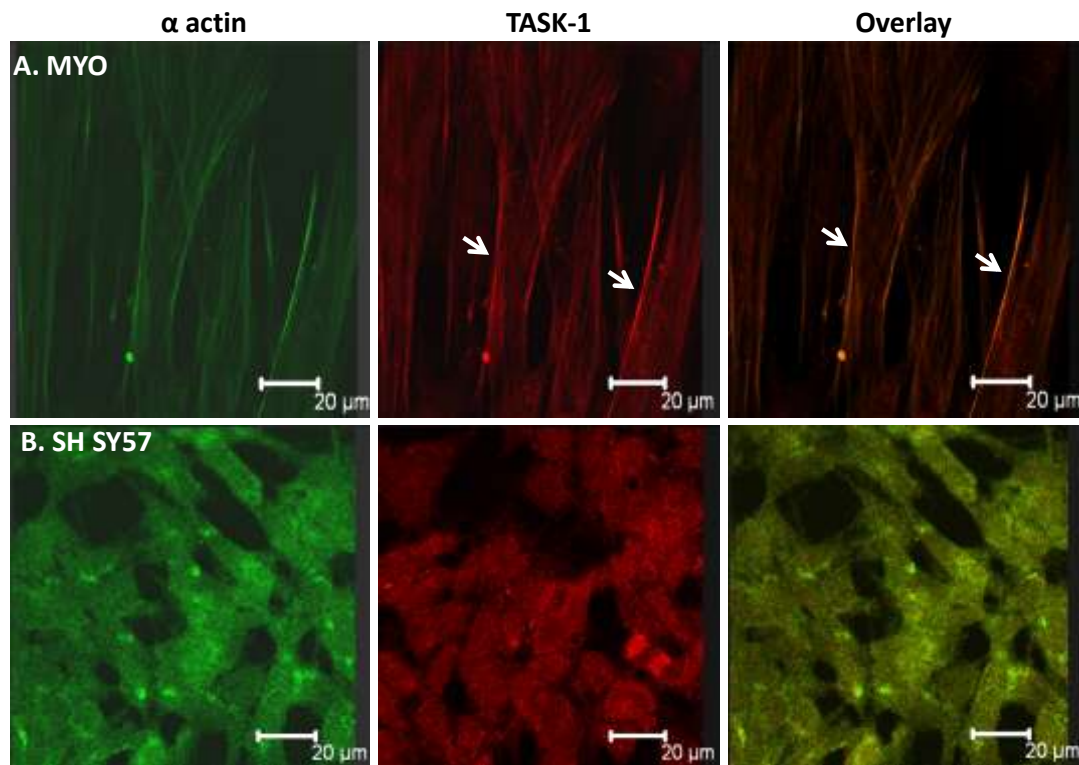


Figure 6.4.5.2-2 showing TASK-1 staining in MYO SMC (A) and SH SY57 cells (B) (N=4). MYO show linear distribution of TASK-1 across the cell body and at the cell membrane (white arrow) which appears to overlap with α actin. In contrast SH SY57 cells demonstrated a granular expression pattern across the cell body.

6.4.5.3. Subcellular localisation of TASK-3

Figure 6.4.5.3.1-1 shows a representative IF image for TASK-3 expression using the polyclonal TASK-3 antibody (Alomone) in cells which are also positive for α actin. The TASK-3 positive stain is produced strongly across the cell body and the SVA image shows one large in the centre of the image where the nucleus has also stained highly positive for TASK-3 which is also seen to a lesser extent with CPA cells. Some overlay with α actin IF was also observed (**Figure 6.4.5.3.1-1E&F** white arrow)

6.4.5.3.1. TASK-3 co-localisation with related K2P channel members

The remaining images show representative IF photomicrographs using the monoclonal TASK-3 antibody (**Appendix II** (Abcam)) to investigate the co-localisation with 3 related K2P channel members. TASK-3 and TASK-1 IF staining was positive in CPA and SVA cells however only the SVA cells showed evidence of co-localisation for the two different ion channels (**Figure 6.4.5.3.1-2**). TASK-1 staining in CPA cells showed no overlap with TASK-3 but we observed an intense staining pattern outside the nuclear membrane (N) with both ion channels. The positive controls MYO and SH SY57 also stained positive for TASK-3 using the monoclonal antibody. It was interesting to see the MYO cells produced an intense stain at the peri-nuclear region (**Figure 6.4.5.3.1-3A**). In contrast the SH SY57 cells

show an expression pattern that is similar to the placental SMC expression for TASK-3 with granular distribution across the cell body as well as staining inside the nucleus (**Figure 6.4.5.3.1-3B**). Merging the two separate images shows some evident co-expression exists between TASK 1 and TASK-3 with SH SY57 cells. The TASK-3 and TREK-1 dual staining has been summarised in **Figure 6.4.5.3.1-4**. The CPA and SVA cells staining pattern was again granular for TASK-3 and found across the cell body with a dense stain around the nuclear membrane. Overlaying the two images revealed pockets of yellow IF stain to suggest some co-expressions, however further analysis failed to show any evidence of co-expression between the two closely related members of the K2P family (not shown). This is also similar to the pattern observed when TASK-3 and TWIK-2 was stained for in the same cells. **Figure 6.4.5.3.1-5** shows a diffuse IF stain was produced across the cell body with TASK-3 again showing staining at the nuclear membrane. However when we merge the images for TWIK-2 and TASK-3 we find that SVA cells show evidence of co-localisation with TASK-3 while CPA cells do not produce any yellow IF stain.

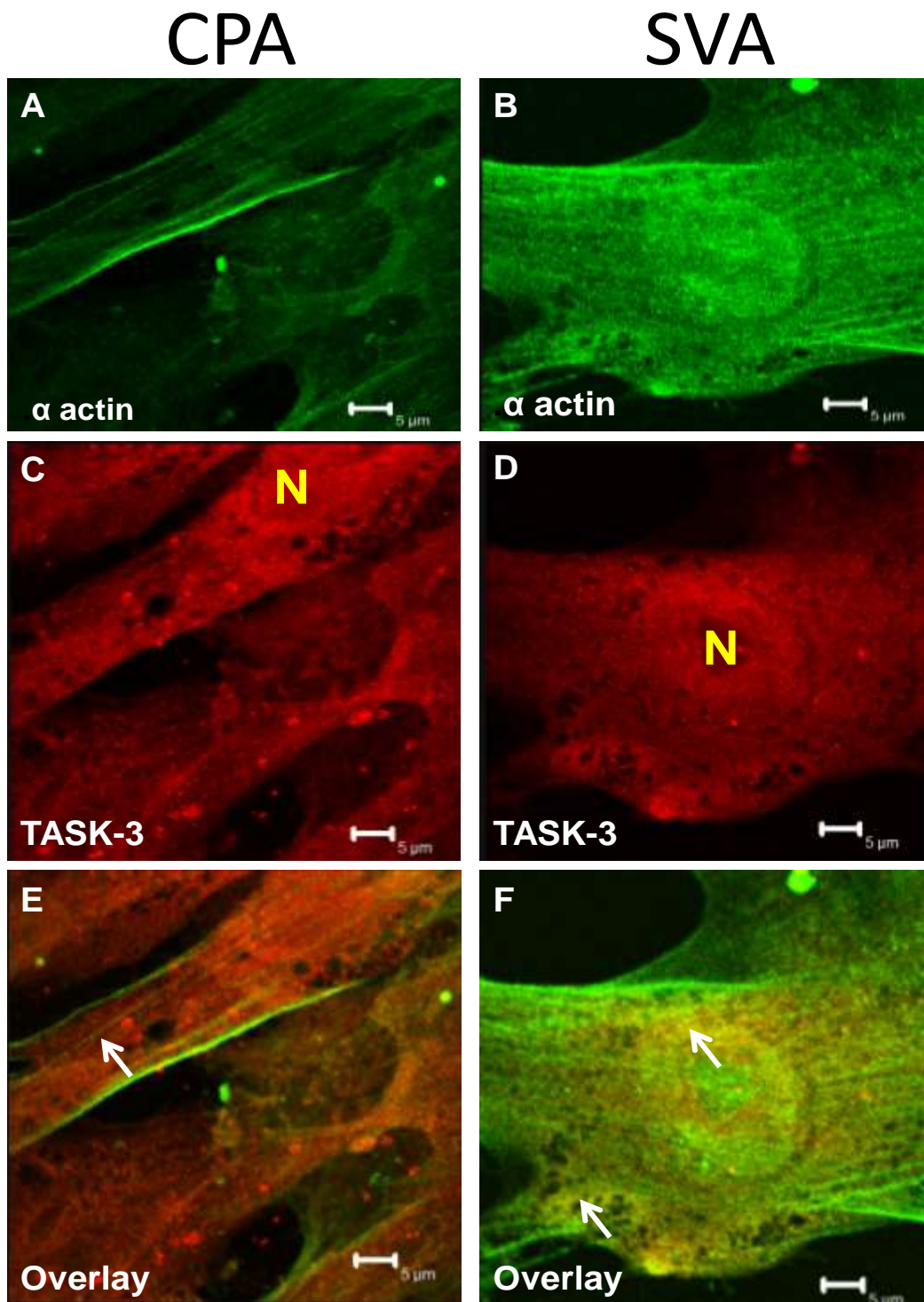


Figure 6.4.5.3.1-1 showing positive stain for TASK-3 using the rabbit polyclonal antibody (N=3). CPA and SVA SMC both demonstrate granular expression which is found across the cell body. Positive IF stain is also seen inside the nucleus (N) with both cells (C&D). E&F show the merged images and the SMC showed some evidence of TASK-3 expression along α actin filaments (white arrow) was observed.

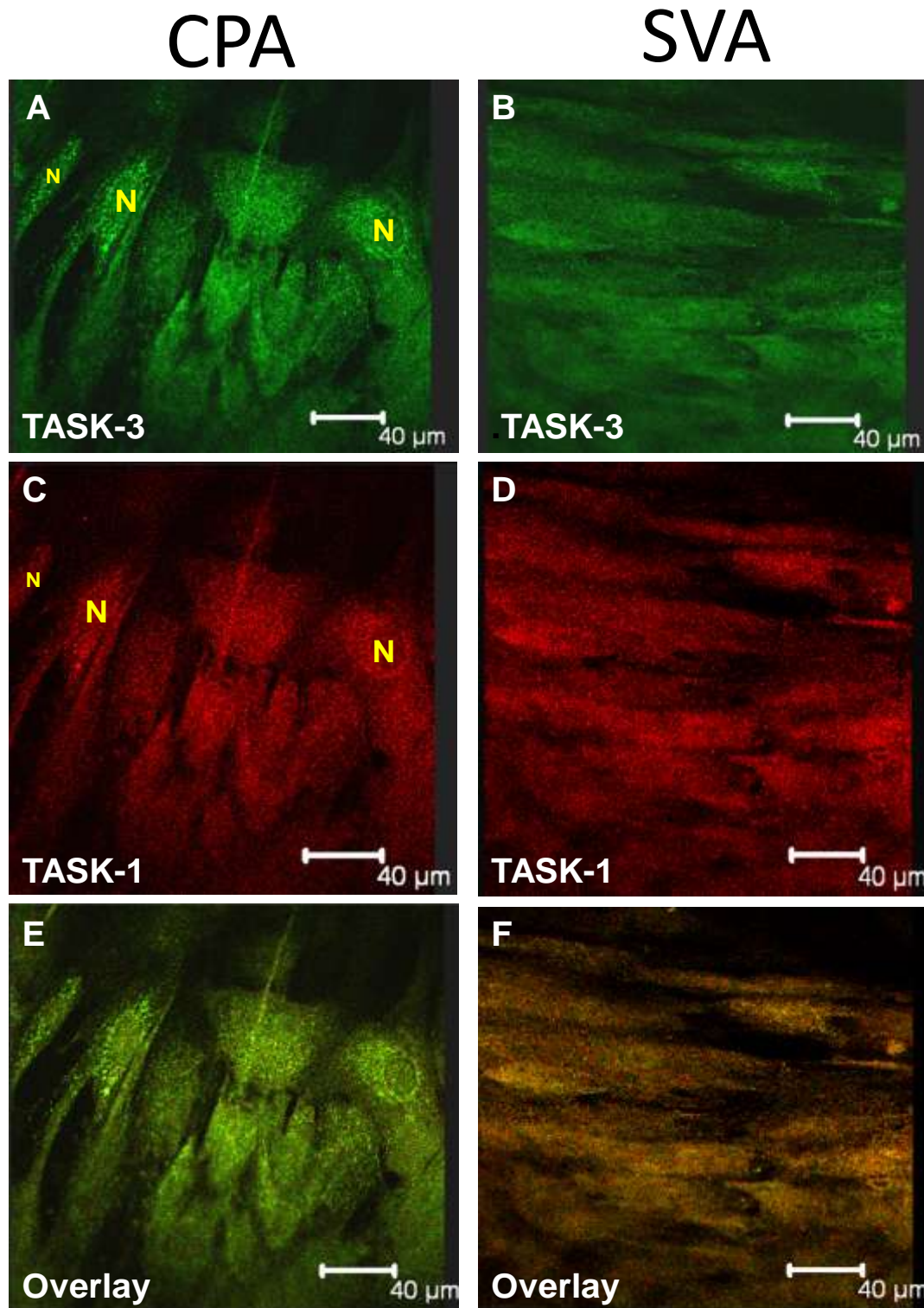


Figure 6.4.5.3.1-2 showing dual staining with TASK-1 and TASK-3 in CPA (A&C) and SVA (B&D) SMC (N=6). The monoclonal TASK-3 antibody was used to investigate the relationship between the two ion channels. The IF staining was seen across the cell body but more intense outside the nucleus (N). Comparing the merged images shows that SVA cells (F) show most evidence of co-expression with TASK-1 as we can see areas of yellow IF.

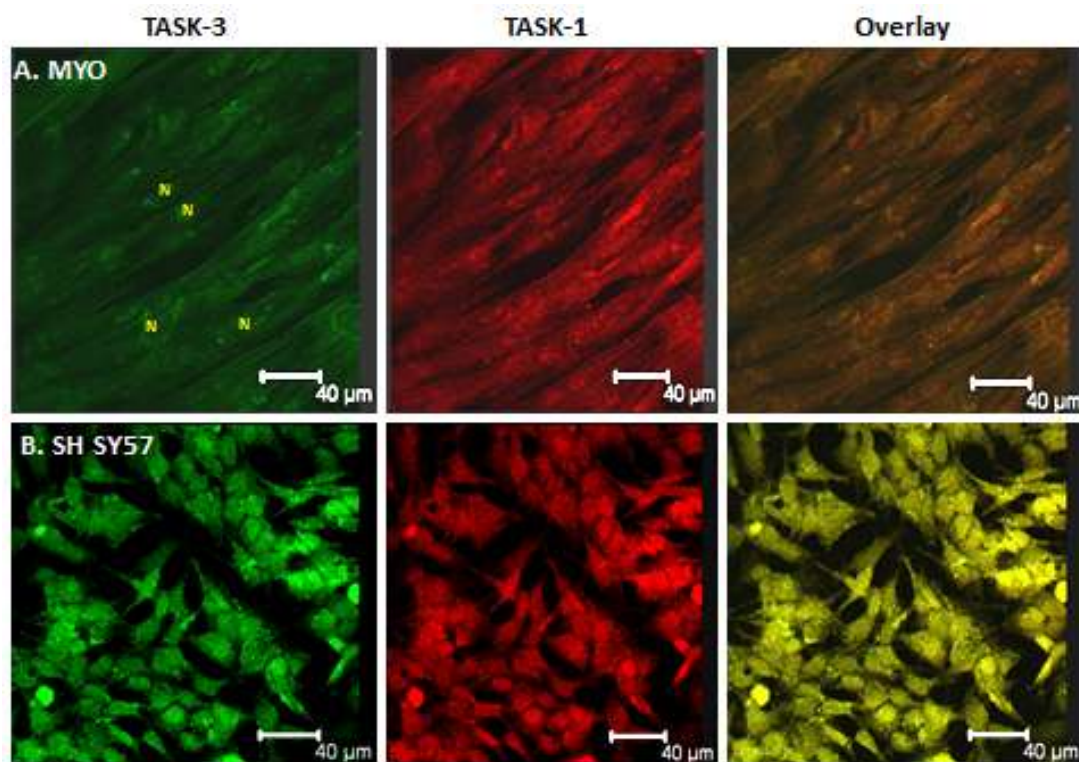


Figure 6.4.5.3.1-3 showing TASK-3 and TASK-1 dual staining in the two positive controls MYO SMC (**A**) and SH SY57 cells (**B**) (N=4). The MYO produced a low signal for both TASK-1 and TASK-3 but we can see some intense stain around the nucleus (N). In contrast the stain intensity was high in SH SY57 cells and shows evidence of co-localisation when the images are merged. The stain pattern is very similar to that observed with TASK-1/3 staining in CPA and SVA SMC.

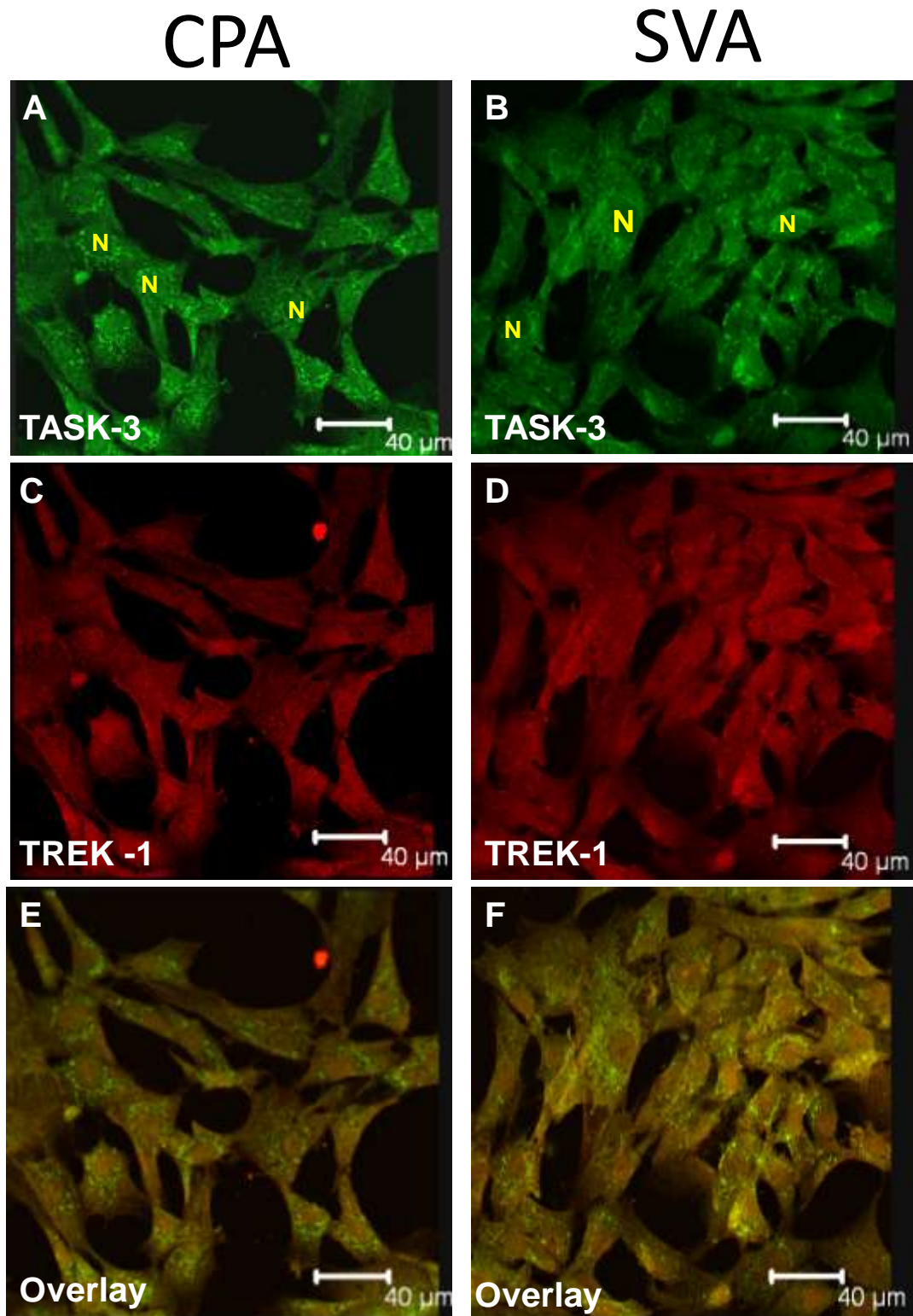


Figure 6.4.5.3.1-4 showing double staining with TASK-3 and TREK-1 (N=6). TASK-3 shows a punctuate staining that is clustered around the nuclear membrane (A&B). Merging the images shows that TREK-1 and TASK-3 may potentially overlap in the cell body of both cells (E&F).

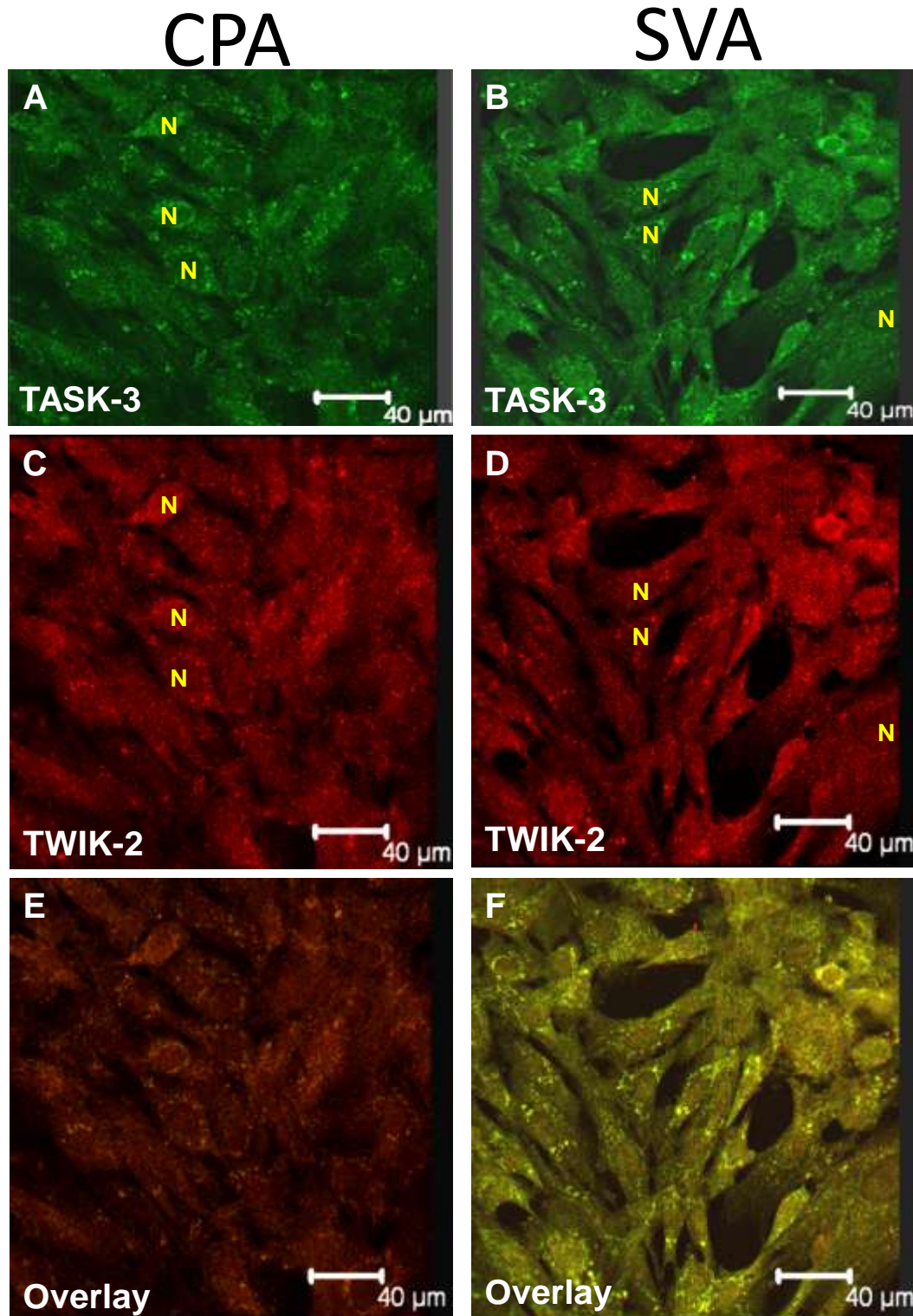


Figure 6.4.5.3.1-5 showing dual IF staining with TASK-3 and TWIK-2 (N=6). TASK-3 stain appears lower in CPA SMC when compared with SVA. Merging TWIK-2 and TASK-3 images shows some overlap as pockets of yellow IF stain are produced and this is most obvious in SVA cells (F). The increase in IF staining around the nuclear (N) membrane was also seen with TASK-3 and TWIK-2 (C&D).

6.4.5.4. Subcellular localisation of TREK-1

Confocal imaging of CPA and SVA SMC showed positive TREK-1 expression summarised in **Figure 6.4.5.4-1**. CPA and SVA SMC imaged at high magnification demonstrate a highly organised staining pattern for TREK-1 which is found in linear filaments that extend across the length of the cell. It was also found that the nucleus remained unclear in both cell types and control samples did not produce any non specific IF stain (not shown). One SVA SMC (**Figure 6.4.5.4-1D**) can be seen growing in isolation and increased TREK-1 expression was observed at the cell protrusions as the cell is extending its surface area (arrow). Merging the images with α actin shows high co-expression between the two proteins as TREK-1 overlaps with α actin and this was observed in both SVA and CPA SMC. The association between two or more proteins can be examined by studying the precise distribution of the pixels in each image. This was performed using the line scans that were taken for both TREK-1 and the matched α actin image of each cell sample. **Figure 6.4.5.4-2** shows the pixel distribution pattern for α actin in green and TREK-1 in red. Any positive overlay will be seen as yellow pixels and the percentage of overlap can be expressed as a value between 0 and 1. **Figure 6.4.5.4-3** also shows the line scans for a ROI that was selected (boxed) in each image. This scan was then converted to a graph to show the intensity of stain at specific μm across the cell. The IF stain pattern shows a linear distribution for both α actin and TREK-1 which overlap in both CPA and more prominently with SVA SMC and supports the findings from the pixel distribution analysis. In further support of our observation with CPA

and SVA SMC, TREK-1 also shows linear distribution in MYO cells with co-expression with α actin (**Figure 6.4.5.4-4A**). In contrast SH SY57 cells have a granular expression pattern of TREK-1 (**Figure 6.4.5.4-4B**) which suggests the linear expression may be a specialised feature of SMC. SH SY57 cells also produces stain for TREK-1 within the nucleus as was seen with TASK 1/3 and suggests that this may be a real observation with this class of K2P channels. This also suggests our early work which also showed this in CPA and SVA SMC may not have been an artefact due to DAPI nuclear staining.

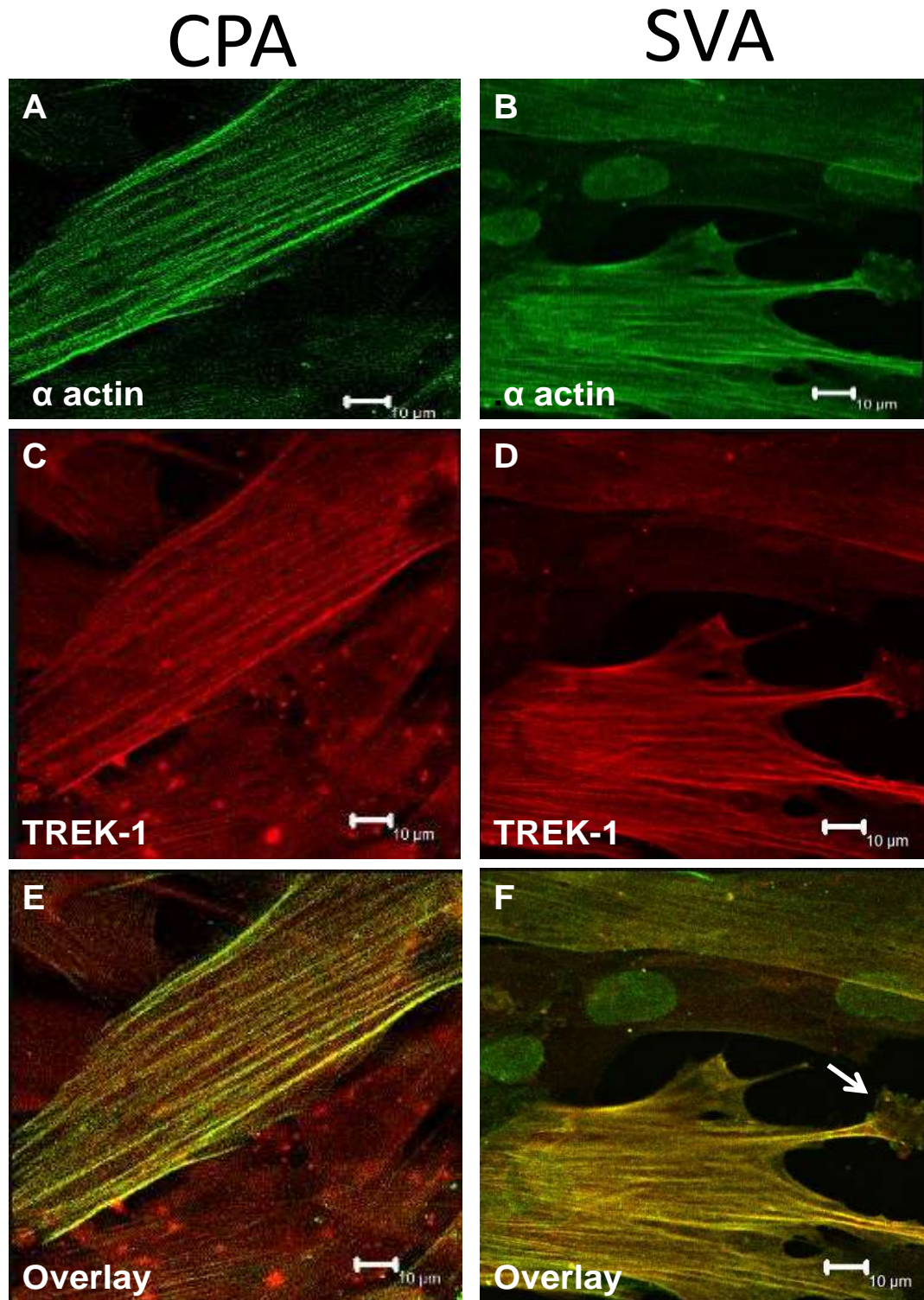


Figure 6.4.5.4-1 showing a close examination of TREK-1 staining in CPA (C) and SVA (D) vascular SMC (N=12). TREK-1 is organised in linear filaments across the cell body and merging with α actin shows clear overlap (yellow IF) (E&F). F shows the cell protrusions that help to increase the cell surface area and are important for cell to cell communication (white arrow).

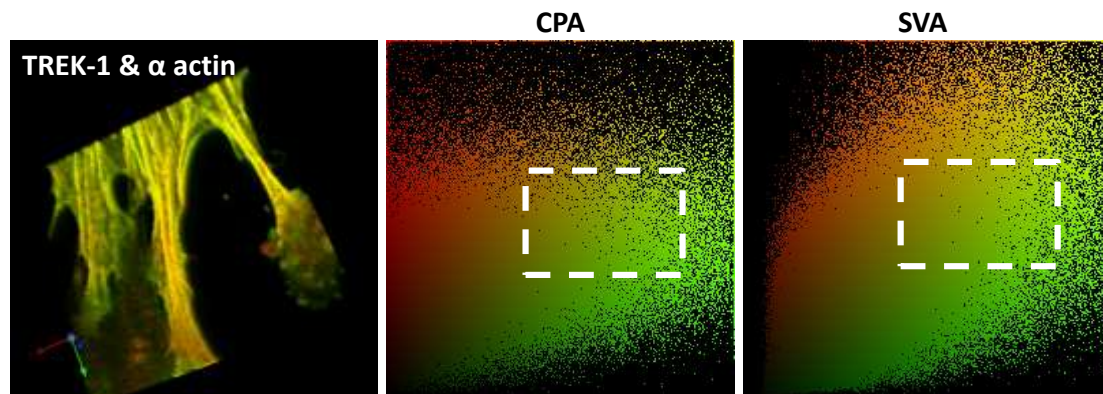


Figure 6.4.5.4-2 showing the analysis that was been performed to determine the co-localisation with α actin and TREK-1 expression (N=12). Each scan taken of the cell is used to create a 3D image (A) and can be explored along the X, Y and Z axis. **B&C** shows the pixel distribution when both images are merged and any yellow stain shows the areas of co-localisation (white box).

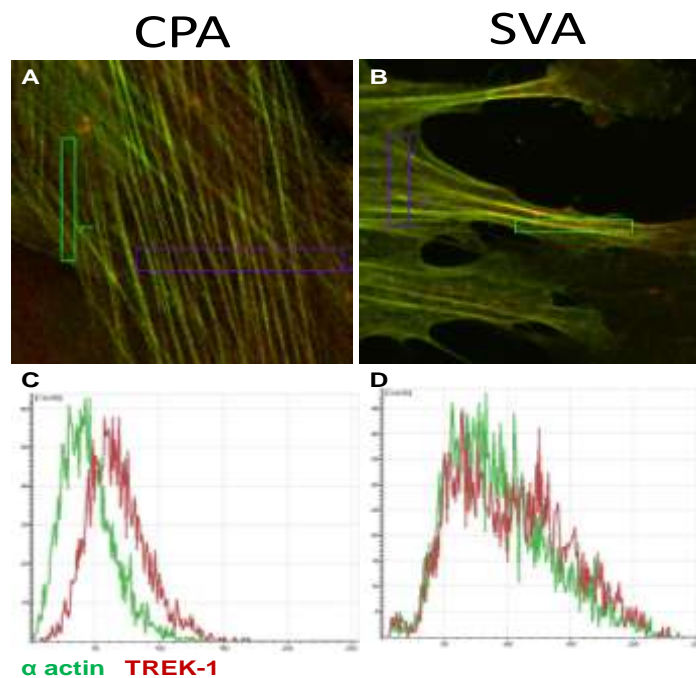


Figure 6.4.5.4-3 showing the line scan analysis that were performed for each image (N=12). The boxed areas show the ROI that was selected for analysis. The graphical representation shows how the expression of α actin closely overlaps the stain for TREK-1 in both SVA and CPA SMC. The X axis represents the distance in μm and the Y axis shows the intensity of IF stain.

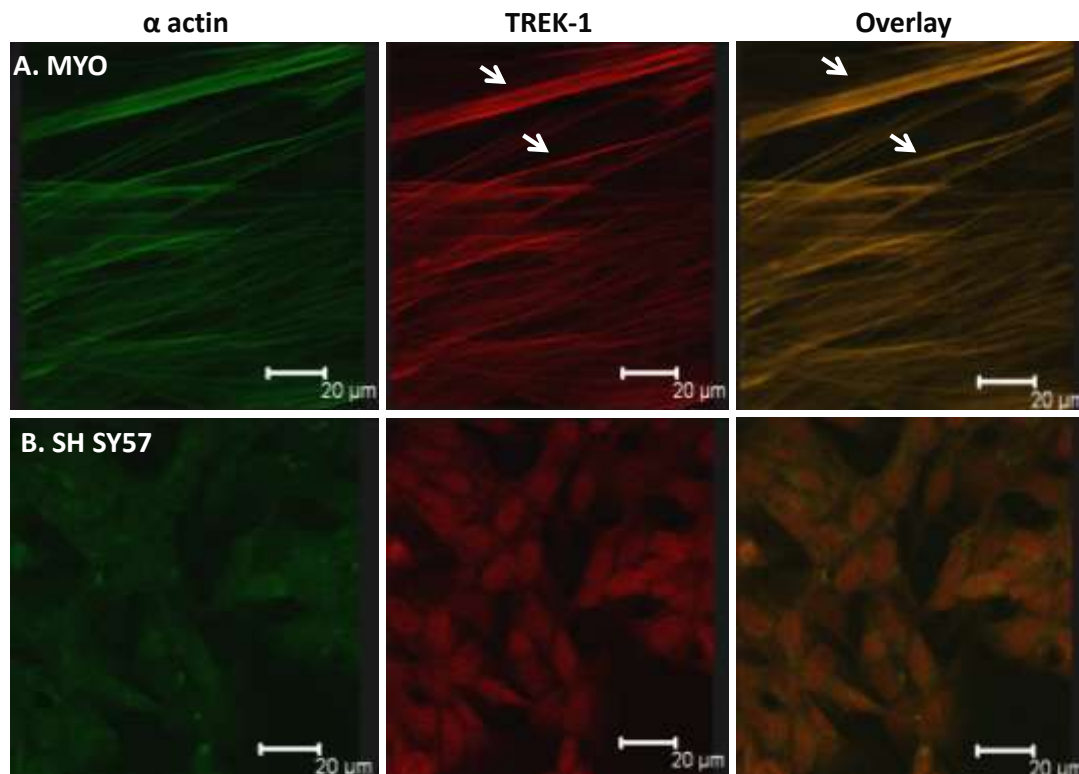


Figure 6.4.5.4-4 showing TREK-1 staining in MYO SMC (A) and the cell line SH SY57 (B) (N=4). MYO show a similar expression pattern which like CPA and SVA vascular SMC shows positive co-localisation with α actin. In contrast the TREK-1 shows granular distribution in the cell and nucleus of SH SY57 cells and there is no co-localisation with α actin.

6.4.5.5. Subcellular localisation of TWIK-2

TWIK-2 IF staining was positive in both CPA and SVA SMC and has been shown in **Figure 6.4.5.5-1**. The images show SVA cells in particular produce a dense staining around the nuclear membrane (**Figure 6.4.5.5-1C**). Merging the images with α actin shows that isolated regions of TWIK-2 expression do overlap with α actin (white arrows) and this is most clear at the cell membrane region. No stain was observed with primary antibody that was pre-absorbed with control peptide added in

excess (not shown). We then examined this staining pattern further by using line scan images to create a 3D image of the cells (**Figure 6.4.5.5-2**). The pixel distribution shows that there is no significant overlap with actin as very few yellow sections are seen. The graphical representation of the Z stacks shows that TWIK-2 stain does overlap with DAPI stain in the CPA example shown (**Figure 6.4.5.5-3**). But there is also a peak in TWIK-2 stain which coincides with the region immediately outside the nucleus and supports our observation that TWIK-2 is found in a high concentration around the nuclear membrane. TWIK-2 was also positive in SMC cultured from the MYO (**Figure 6.4.5.5-4A**) and also displays granular distribution across the cell body. However we also find that the nucleus has also been stained. This was also seen with SH SY57 cells (**Figure 6.4.5.5-4B**) which could be an important functional feature of K2P channels.

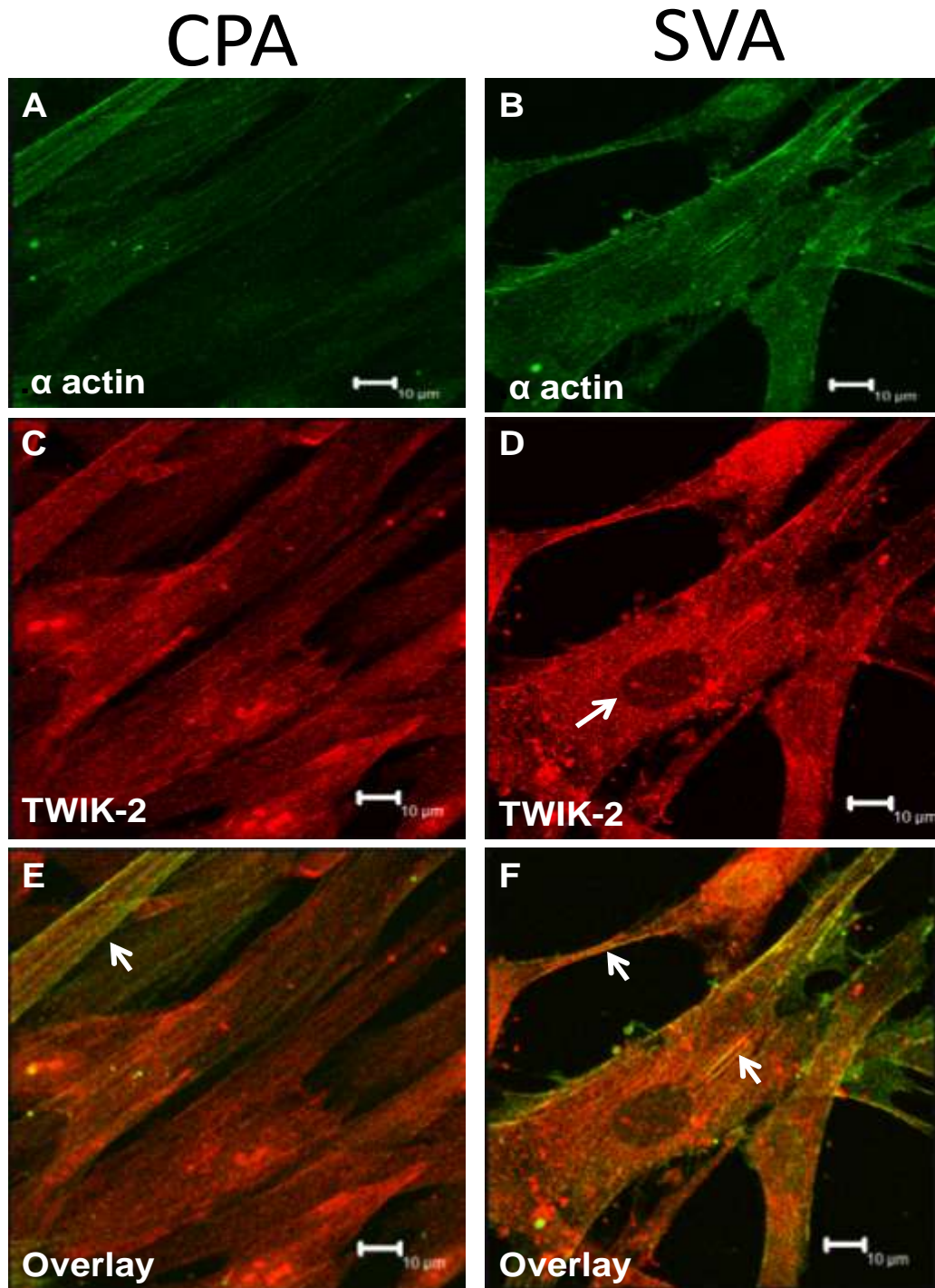


Figure 6.4.5.5-1 showing TWIK-2 positive immunoreactions in SMC cultured from CPA and SVA SMC (N=12). TWIK-2 shows granular distribution within the SMC and the SVA origin cells (**D**) shows an intense stain around the nuclear membrane (white arrow). **E&F** also show no significant overlap with TWIK-2 and α actin while the white arrows show the regions that occasionally show TWIK-2 co-localising with α actin

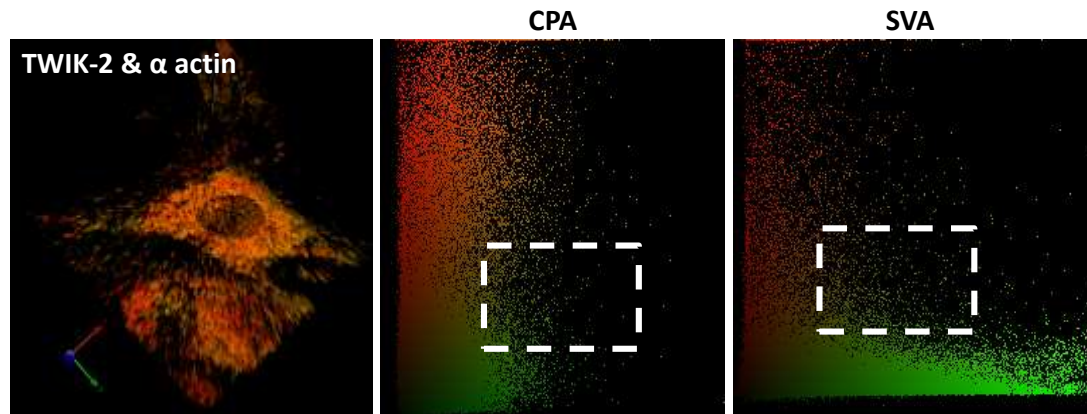


Figure 6.4.5.5-2 showing the distribution of actin and TWIK-2 stain (N=12). A 3D image was generated using the Z stack profile of each cell that is captured. The white box in shows the region where the stain overlaps and we failed to observe and significant overlap with the two proteins.

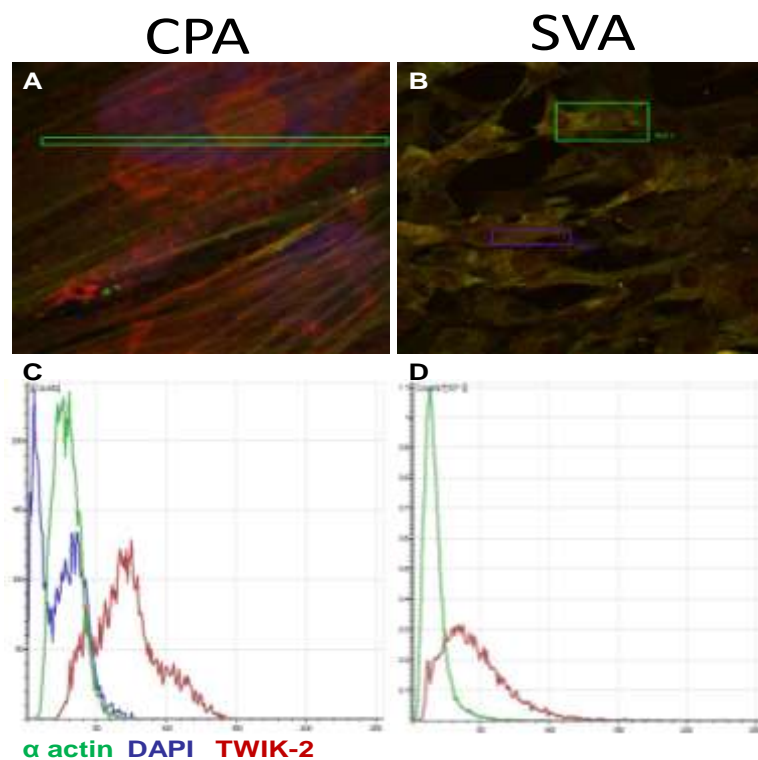


Figure 6.4.5.5-3 line scans for TWIK-2 (red) and α actin (green) (N=12). A&B show the ROI (boxed) that were randomly selected for analysis. C shows TWIK-2 does overlap with DAPI stain (blue) suggesting some nuclear expression but more interestingly the TWIK-2 stain also peaks immediately outside the nucleus which suggests expression at the nuclear membrane. The stain distribution shows that the peak of α actin expression does not match TWIK-2 so there is no significant overlap between the two proteins (C&D).

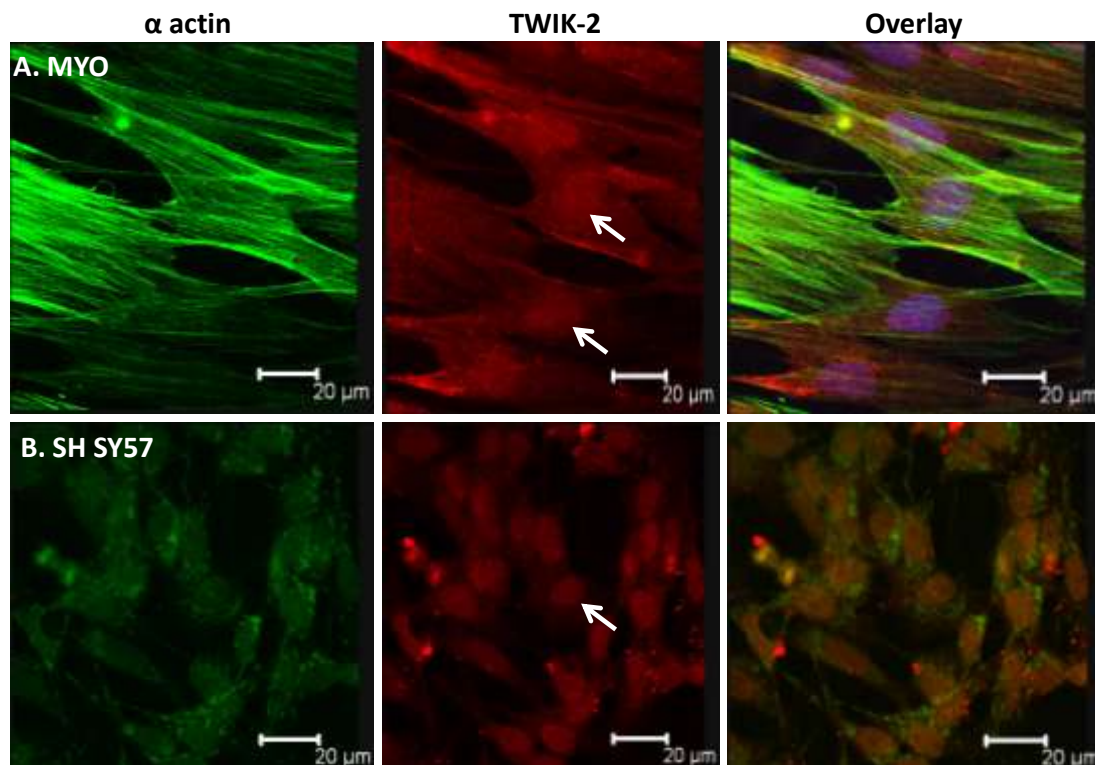


Figure 6.4.5.5-4 showing TWIK-2 expression in MYO SMC (A) and the SH SY57 cells (B) (N=4). A granular distribution is seen and there is positive staining with TWIK-2 in the nucleus which is seen with both cell types (white arrow). The MYO cells also show linear staining that is noticeable at the cell membrane with some evidence of overlap with α actin expression (E&F).

6.5. Discussion

The aim of this chapter was to investigate the expression of a range of ion channels that have been linked with the response to stress due to its importance in the placenta. The first objective was to confirm the presence of each ion channel using Western blotting. This information was then used to investigate any potential inter tissue variations that may exist between CPA and SVA. The main ion channel candidates examined consisted of members that have been shown to be present in the placental vasculature along with the K2P members TWIK-2, TREK-2, TRAAK and

TASK-3 which were of particular interest to us due to their sensitivity to pH. To undertake this analysis matched samples of CPA and SVA from NORM and PE patients were collected for comparisons using Western blotting. In addition SMC from NORM samples were also used to examine the cellular localisation of each ion channel of interest.

6.5.1. **Ca_v1.2 channels**

Depolarisation of the cell membrane will open VGCC to allow $[Ca^{2+}]_i$ to increase and this is crucial for driving an increase in the contraction of SMC. Most Ca^{2+} entry across the cell membrane is via the Ca_v1.2 channel which makes the ion channel an important target for controlling cell excitation. The protein structure for Ca_v1.2 reveals a large protein with a predicted molecular weight of 210-240 kDa ([Appendix III](#)) which was not identified by this study when using Western blotting analysis. Instead IF showed Ca_v1.2 expression in cultured SMC from both NORM CPA and SVA and shows an organised expression across the cell body. Ca_v1.2 are postulated to be important in the response mechanisms that detect changes in O₂ levels in the cell and in support of this, the placental response to hypoxia has shown to be inhibited with NIFED (Jakoubek, Bibova et al., 2006), implying a role for Ca_v1.2 in the HFPV response (Robertson, Hague et al., 2000, Hampl, Bibova et al., 2002, Jakoubek, Bibova et al., 2006). This study identified expression of the ion channel across the SMC while the nucleus was devoid of positive IF as expected for a

membrane associated protein thus enabling the ion channel to respond to changes in depolarisation across the cell membrane to initiate a cell wide response.

6.5.2. BK_{Ca} channels

The BK_{Ca} channel is widely distributed in vascular tissue and is an important regulator of blood flow (Khan, Smith et al., 1997, Meera, Wallner et al., 1997). Our analysis showed that the BK_{Ca} was equally present across NORM and PE samples as no significant change in the level of expression between CPA and SVA samples was detected. Two bands were identified at 120 and 60 kDa which represents the α subunit of BK_{Ca}. The smaller 60 kDa band has been identified as a breakdown product of the larger BK_{Ca} protein and has also been described in bovine tracheal smooth muscle (Garcia-Calvo, Knaus et al., 1994). The MYO samples were also positive for BK_{Ca} while the highest expression was seen with the RB sample. The α protein is the pore forming part of the ion channel and is needed for the channel to open while the regulatory β subunit confers the channel's activation threshold and is responsible for sensing Ca²⁺ levels (Meera, Wallner et al., 1997). The BK_{Ca} has previously been identified in the myometrium and proteins in the range of 110-120 kDa have been reported (Benkusky, Fergus et al., 2000, Matharoo-Ball, Ashford et al., 2003). In addition, the presence of BK_{Ca} in the CPA and CPV has previously been reported using the Alomone polyclonal antibody (Wareing, Bai et al., 2006) and agrees with our observations. This study (Wareing, Bai et al., 2006) reported a high density band in the region of 125 kDa in CPA with higher expression in CPV. They also showed

the presence of smaller bands at 70 and 40 kDa. In addition mRNA for BK_{Ca} has been identified within the placental vasculature (Hampl, Bibova et al., 2002) however a low quantity signal for BK_{Ca} protein was identified to be in the region of 116 kDa in this study.

A role for BK_{Ca} as an important O₂ sensing ion channel has been demonstrated with fetal lung tissue (Resnik, Herron et al., 2006). The combined role of an increased pO₂, post-delivery increase in ventilation, and increase in shear stress brings about widespread pulmonary vasodilatation to cope with the influx of pulmonary blood with the newly delivered baby. The lungs switch from being fluid filled to air filled and the pO₂ increases 4-fold. This study examined the role of BK_{Ca} in modulating this adaptation to different pO₂ environments using ovine pulmonary arterial SMC cultured under hypoxic (90% N₂) or normoxic conditions (95% air). It was reported that specifically expression of the α and β_1 but not β_2 subunits of BK_{Ca} were up regulated under hypoxic culture conditions. This provides an insight into how low pO₂ prepares the tissue for a rise in pO₂ by maintaining high levels of K⁺ channel expression perhaps as a mechanism to redirect blood flow (Resnik, Herron et al., 2006). This finding also illustrates how different tissues can adapt to changing pO₂ conditions by altering ion channel expression and may have parallels to when pO₂ changes upon entry of maternal blood in the IVS.

6.5.3. K_{ATP} channels

K_{ATP} are important candidates as potential early markers of metabolic disease due to their dependence on low ATP within the cell to activate the ion channel. K_{ATP} is important for both long and severe exposure to pO_2 stress and has been implicated in ischaemic preconditioning (Murry, Jennings et al., 1986). The K^+ channel is widely expressed and has been shown to have a role in providing cardio-protection (Chen and Simard, 2001), inhibiting neural cell activity and is central in the mediating insulin release as part of glucose homeostasis (Hussain and Cosgrove, 2005). The pancreas is vulnerable to acidic environments making the K_{ATP} channel a suitable candidate as a pH sensing ion channel and K_{ATP} provides an important link between glucose metabolism and insulin secretion (Ashcroft, 2007). The activity of the ion channel is coupled to the cells metabolic status and ATP levels will therefore determine the gating of the ion channel (Tammaro and Ashcroft, 2009)

The functional importance of K_{ATP} has been indirectly demonstrated with CGRP which induced a relaxation response across a range of placental vessels and this was inhibited in the presence of GLB (Dong, Vegiraju et al., 2004). In further support of this, a number of K_{ATP} channel openers such as KRN2391 have shown to induce a potent relaxation in placental vessels implicating K_{ATP} channels in contributing to the control of vessel tone in the placenta (Wareing, Bai et al., 2006, Jewsbury, Baker et al., 2007). Western blot analysis revealed a band, thought to be K_{ATP} , at 55 kDa which has also been previously reported with CPA and CPV tissue (Wareing, Bai et al., 2006). The level of K_{ATP} was similar across both NORM and PE

paired CPA and SVA samples, which could be an important observation. The glucose demand of the placenta is particularly high during the second and third trimester when the fetus is growing at its fastest rate (DiGiacomo and Hay, 1989, Hay, 1995) and levels of CGRP are also high during this period (Dong, Vegiraju et al., 2004). The level of K_{ATP} expression identified in our study maybe a reflection of the altered placental function at term gestation and it would be interesting to see how the K_{ATP} protein levels vary with gestational age. This could also be important for understanding how glucose metabolism varies and how high maternal blood glucose seen with IDDM can alter the metabolic status of the placenta as glucose is readily transported across the placental membranes (Hay, 1995).

6.5.4. K2P channels

K2P channels are a newly identified family of K^+ channels and very little is known as to their expression within the placental vasculature. The ion channels are important for maintaining the resting membrane potential and due to their properties of being leak channels, may have a role in maintaining the low resistance seen in the placenta.

6.5.4.1. TASK 1/3 channels

TASK channels open at rest maintain the resting membrane potential and are a target for anaesthetics and acidic pH. TASK-3 shares 55% homology with TASK-1 (Czirjak, Fischer et al., 2000) which makes both isoforms important candidates for responding to pH stress within the placenta. In addition to pH, TASK channels have also demonstrated O₂ sensing properties and have been linked to cell death making them important oncogenic candidates (Duprat, Guillemare et al., 1995, Bayliss, Sirois et al., 2003, Voloshyna, Besana et al., 2008). TASK-1 mRNA has also been shown to be high within the placenta (Duprat, Lesage et al., 1997) and expression for the ion channel appears to increase with gestational age (Bai, Greenwood et al., 2005) implicating the ion channel in regulating cellular excitability within the placenta. The presence of both sub types of ion channels may be required to ensure the cell can respond to pH changes over a wide range and we found expression of both TASK 1/3 at the whole tissue level and more importantly within SMC from CPA and SVA.

Acidic environments will inhibit both TASK 1/3 but studies have shown that the exact pH value has contrasting effects on each ion channel. TASK-1 will be inhibited at pH 7.1-7.4 while TASK-3 is inactive at pH <6.7 (Duprat, Lesage et al., 1997, Kim, Bang et al., 1999). The same stimuli can differently modulate channel activity such that the ion channels can respond to varying degrees of cell stress to bring about a rapid cell response. (Bayliss, Sirois et al., 2003). A role for TASK-3 but not TASK-1 was demonstrated to provide a link between the detection of low pH and the wake reflex which increases ventilation when pCO₂ and therefore the pH of the

ECM in the brain falls (Holzer, 2009, Pang, Robledo et al., 2009). TASK channel gene expression has also been investigated in the human cytotrophoblast cells of the placenta. Bai (et al 2005) reported the presence of mRNA for TASK-1, 2, 4 and 5 but not TASK-3. Western blotting analysis revealed bands of 78 and 150 kDa and IHC analysis showed TASK-1 was positive in the cytotrophoblast region and more importantly showed co-expression with cytokeratin-7. We also observed a band at 71 kDa which could be the same as the band reported with TASK-1 (Bai, Greenwood et al., 2005) or it could represent an additional breakdown product for TASK-1. TASK-1 has been shown to produce a low intensity band at 122 kDa in CPA and CPV with no evidence of any inter-tissue differences. The same Western blot analysis showed an abundant band at 54-60 kDa with only RB and was absent with the placental tissue (Wareing, Bai et al., 2006). mRNA for TASK-3 was not detected in the cytotrophoblast cells (Bai, Greenwood et al., 2005) which indicates that TASK-3 may be restricted to the placental vasculature. We can investigate this by examining gene expression across the different placental membranes. Western blot analysis of MYO has also shown expression for TASK-1 with reported band sizes of 44 and 65 kDa (Bai, Bugg et al., 2005), the latter of which may also be the same band that we also identified. The Western blotting analysis for TASK-1 in particular highlights the variation in reporting of TASK-1 within the literature with studies that also used the same Alomone antibody.

The localisation and tissue distribution of K^+ channels such as K2P channels can give an insight into the how cellular functions are regulated. The two K2P channels TASK-1 and TASK-3 were shown to be expressed in SMC cultured from

placental vascular tissue. The IF staining pattern revealed a granular distribution for both TASK 1/3 and there was an intense stain around the peri-nuclear membrane and evidence of nuclear staining. The two ion channels do also appear to co-localise and this could enable the cells to amplify the response to external pH. Co-expression could suggest a common mechanism exists to ensure a rapid response is produced to the cell stimuli through the involvement of related ion channels to help bring about activation of a signalling cascade (Duprat, Lesage et al., 1997, Gonzalez, Jensen et al., 2009). In vascular SMC this could modulate contractility to control vascular tone which is important for the placenta and has previously been shown to occur with TASK-1 and TREK-1 in cardiacmyocytes (**Figure 6.5.4.1-1**).

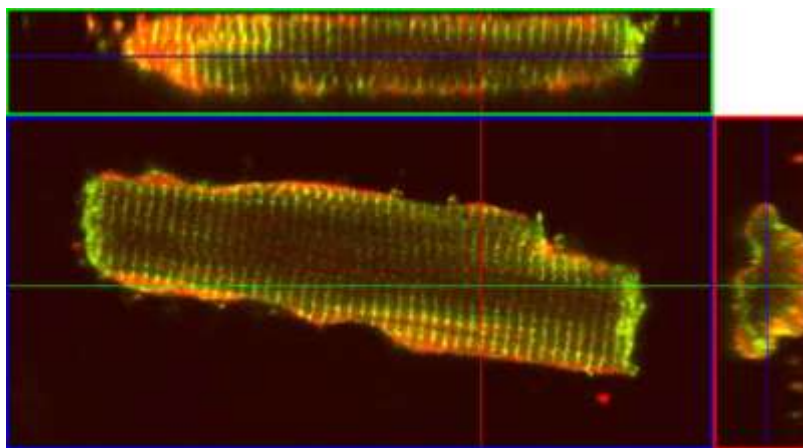


Figure 6.5.4.1-1 shows TREK-1 (red) and TASK-1 (green) subcellular localisation in rat cardiac myocytes. TREK-1 is expressed along longitudinal strips and is concentrated at the cell membrane. TASK-1 is also visualised and shows co-expression at the cell membrane (Image obtained from Xian Tao, Dyachenko et al., 2006).

Cross talk has previously been shown to occur with the use of selective knock downs of specific sequences for both ion channels (Kang, Han et al., 2004, Gonzalez, Jensen et al., 2009). We also observed evidence of co-localisation between TASK-3

and the closely related TWIK-2 and TREK-1, the latter of which supports the observations of Xian Tao (et al., 2006). The close association between K2P channels members may explain why the same stimuli can activate a response from more than one K2P member and why blockers such as halothane can block both TREK and TASK channel currents (Hartness, Lewis et al., 2001, Kang, Han et al., 2004). The presence of TASK-1/3 channels in CPA and SVA may help the placenta to respond to changes in the rate of flow from maternal blood and gives an insight into how the transport capacity of the placenta can be regulated by ion channels. The pH sensing property makes TASK channels important candidates for generating the vascular response to pH stimulus observed with CPA and SVA.

6.5.4.2. TRAAK channels

A small selection of CPA and SVA samples were used to demonstrate TRAAK expression within the placental vasculature with a single band at 50 kDa which was comparable across the two vessel samples. TRAAK channels have very similar properties to TASK and TREK channels and are potently activated by AA and stretch. mRNA for the ion channel has shown to be exclusively expressed in neuronal tissue (brain, spinal cord and retina) while the placenta is the only example of the peripheral localisation for TRAAK (Fink, Lesage et al., 1998, Reyes, Lauritzen et al., 2000). The predicted molecular weight for TRAAK is in the region of 48 kDa ([Appendix III](#)) and we were able to isolate a protein band within this region.

TRAAK has been postulated to have a role in the placenta due to the abundance of AA which is a strong activator of TRAAK (Fink, Lesage et al., 1998). In neurons, AA is released at the pre-synaptic neuron to decrease neurotransmitter release and TRAAK activation would return the baseline potential (Fink, Lesage et al., 1998, Maingret, Patel et al., 2000). In the vascular tissue, placental TRAAK channels could function in a similar way and maintain the low vascular resistance. AA is also released under stress particularly ischaemia and inflammation and TRAAK activation can reduce cellular activity through hyperpolarisation of the membrane to prevent further action potentials and limit the damage possibly by preventing cell death (Maingret, Patel et al., 2000). TRAAK can also be distinguished from TREK as its currents are increased with intracellular alkalosis while acidification does not produce the same response (Fink, Lesage et al., 1998). This implicates TRAAK with the response that we observed to rising pH (alkalosis) that resulted in contraction of the placental vessels. In addition, TRAAK is also a target for RIL activation (Duprat, Lesage et al., 2000) and has similar activation affinities as TREK due to a similar motif that is shared (Maingret, Patel et al., 2000) but crucially application of 500 μ M of RIL activates TRAAK while it has a dual effect on TREK (discussed in [Chapter 6.5.4.3](#)). TRAAK expression is high within the neuronal tissue and may explain the neuroprotective effects seen with RIL treatment (Duprat, Lesage et al., 2000). This may also explain the potent response we observed with RIL which may open TRAAK channels to bring about a potent relaxation of the placental vessels and provides an avenue for further work.

6.5.4.3. TREK 1/2 channels

TREK-1 currents were first reported in rat brain slices where the ion channel has the highest expression levels (Fink, Duprat et al., 1996). Subsequent studies have shown that TREK is widely expressed in most tissue types with conserved regions between mammals. Many diverse stimuli trigger TREK channel activity which in turn has an incredible capacity to control cell function as most stimuli such as temperature, pH_i and stretch are transmitted to the cell via TREK-1. It is an important mechanosensor as cell stretch and/or swelling will activate the ion channel and altered expression will directly reflect the ion channel's importance in that specific tissue/organ (Duprat, Guillemare et al., 1995, Maingret, Lauritzen et al., 2000, Maingret, Patel et al., 2000).

The Western blotting analysis revealed a band for TREK-1 at 50 and 100 kDa and the two bands closely match the information provided by the datasheet (Alomone) as well as bioinformatics which predicts a 47 kDa protein size for the TREK-1 channel subunit. However there is a discrepancy within the literature as to the size of the TREK-1 protein. TREK-1 expression in rat arteries revealed three bands at 100, 45 and 25 kDa (Gardener, Johnson et al., 2004) while examination of airway epithelial cells has shown TREK-1 protein at 130 and 50 kDa (Davis and Cowley, 2006) both of which used the same Alomone antibody. Within the uterus, MYO samples have been shown to express two bands at 56 and 90 kDa (Bai, Bugg et al., 2005) while a 90 kDa and a larger 130 kDa band size has been reported within the cytotrophoblast cells of the human placenta (Bai, Greenwood et al., 2005). This small

selection of studies highlights the differences that can be reported when using the same antibody. During our investigations, we found that the 100 kDa was not readily detected with the same samples and may be due to changes in the antibody batches used. This can lead to false differences being identified when comparing tissue expression for TREK1 and as a result we cannot draw firm conclusions in the difference in expression for TREK-1 across the NORM and PE sample group. A recent study revealed that different splice variants of TREK-1 had dramatically altered the channel sensitivity to ions (Thomas, Plant et al., 2008). The two closely related isoforms of TREK-1 identified in the rat brain were shown to have opposing actions in allowing Na^+ to enter the cell and this may be important for the pH sensitivity of TREK-1 which can activate NHE to restore the pH gradient across the cell membrane. The difference in TREK-1 expression can also alter the cellular response produced. RIL has the ability to both activate and inhibit TREK channel currents (Duprat, Lesage et al., 2000) which can help to distinguish the role of TREK from TRAAK in different tissues. This was shown with the response of mouse taste bud cells in response to acidic pH (Richter, Dvoryanchikov et al., 2004). Application of a low dose of RIL (500 μM) could increase the response to citric acid as blocking TREK-1 enhanced the acid induced cell depolarisation. The identification of different TREK-1 isoforms requires further investigation to fully understand the importance of each different subtype. A recent study demonstrated a more accurate and reproducible method for detecting TREK-1 expression (Sandoz, Bell et al., 2011). This study utilised fluorescent tagging of the C-terminal to show expression of the ion channel was located at the cell membrane and the intensity of the fluorescent stain correlated

with TREK-1 activation. The same approach could be used in our studies to examine the functional subunits of TREK-1 within the placenta.

pH sensitivity can change depending on which ion channel is expressed. The closely related TREK-1 and TREK-2 share 78% homology and can be distinguished by their pH sensitivity (Ketchum, Joiner et al., 1995, Fink, Duprat et al., 1996). TREK-1 is closed at pH 7.32 within the cell while the same pH level outside the cell membrane will open TREK-2. TREK-2 is also activated by mechanical pressure in the cell although mRNA for TREK-2 has previously been shown to be absent in the MYO (Medhurst, Rennie et al., 2001, Bai, Bugg et al., 2005). However we did show positive expression for the ion channel using Western blot analysis in CPA, SVA, MYO and RB. Two main protein bands at 40 kDa and a 52-56 kDa were observed and the presence of a doublet has similarities to the doublet reported for TASK-1 expression in cultured cytotrophoblast cells (Bai, Greenwood et al., 2005). The close association with TREK-1 and TREK-2 was investigated using site specific mutations (Sandoz, Douguet et al., 2009). It was shown that a conserved histidine sequence with TREK-1 and TREK-2 formed the pH sensor but a crucial difference in the short extracellular domain immediately after the proton sensor sequence P2Ct was responsible for producing the varied sensitivity to pH across TREK-1 and TREK-2 (Sandoz, Douguet et al., 2009) and may underlie the capacity of the placental vessels are able to produce a response across the pH range.

Examining the cellular distribution of TREK-1 revealed two staining patterns. Firstly TREK-1 expression was organised in linear filaments with some granular expression in both CPA and SVA cell types. The mechanosensitivity of TREK-1 may

be closely linked with α actin expression and in support of this it was shown that TREK-1 and α actin did significantly overlap which also supports the observations of Lauritzen (et al. , 2005). They showed that TREK-1 activity could be altered when the α actin network was disrupted and the embryonic striatal neurons had a reduced surface area and reduced growth cones which are vital for neuronal cell migration. Xian Tao (et al., 2006) also reported a linear expression pattern for TREK in ventricular cardiac muscle cells (**Figure 6.5.4.1-1**) and shows how the mechanosensitive nature of TREK-1 may be conferred by its close proximity with α actin filaments. Linear organisation of an ion channel across the length of the cell can be important for the detecting and responding to changes in the cell volume which would occur under cell stretch or contraction. TREK-1 and other K2P channels work to oppose contraction and restore the cell membrane potential (Fink, Lesage et al., 1998). Co-localisation is important for giving the cell a rapid response mechanism and protein crosstalk facilitates the activation of signalling cascades. Co-localisation also allows local regulation of channel activity to govern cell excitation. TREK-1 expression at the membrane shows the ion channel can hyperpolarise the cell membrane upon stimulation and modulate Ca^{2+} entry into cell (Davis and Cowley, 2006, Beckett, Han et al., 2008). This could be vital for controlling cell processes such as growth, migration, volume and cell shape and could also help it detect small changes in flow to increase stress on the blood vessel. The importance of the TREK-1 response to stretch was shown in a recent study (Baker, Hennig et al., 2008) using bladder SMC. The bladder wall is stretched during the process of bladder filling however stretch sensitive ion channels have been implicated in maintaining SMC

quiescence to prevent unregulated contraction of the bladder wall. This study showed that the membrane potential remained stable under stretch which could be inhibited in the presence of the TREK-1 blocker L-METH. This finding implicates a role for TREK-1 in detecting and responding to stretch to modulate cellular activity (Baker, Hennig et al., 2008, Beckett, Han et al., 2008). TREK-1 may also respond in a similar manner to increases in stretch in the form of physical stress on the vessel to alter vascular SMC function and bring about a change in the vessel diameter and secondly provides an important target for pharmacological interventions to improve placental perfusion.

TREK-1 expression was predominantly linear across the cell body but we did also observe some positive stain within the nucleus of SMC. Nuclear expression has previously been reported for TASK-1 within the cytotrophoblasts (Bai, Greenwood et al., 2005). TREK-1 expression was also found in SMC cultured from MYO and supports the findings of Bai (et al., 2005). This study reported TREK-1 expression to be localised to the membrane but interestingly also in the nucleus (Bai, Bugg et al., 2005, Bai, Greenwood et al., 2005). In our study SH SY57 cells showed TREK-1 positive staining inside the nucleus which has also been reported with neurons (**Figure 6.5.4.3-1**) (Maingret, Lauritzen et al., 2000, Nicolas, Lesage et al., 2004, Xian Tao, Dyachenko et al., 2006). This is an interesting observation which we initially did observe with placental SMC and attributed it to a processing artefact and chose to reduce the TREK-1 antibody concentration from 1:50 to 1:100 which resolved this issue along with removing the DAPI staining. However examining the

literature along with and our positive control (SH SY57 cells) and requires further validations to support this finding.

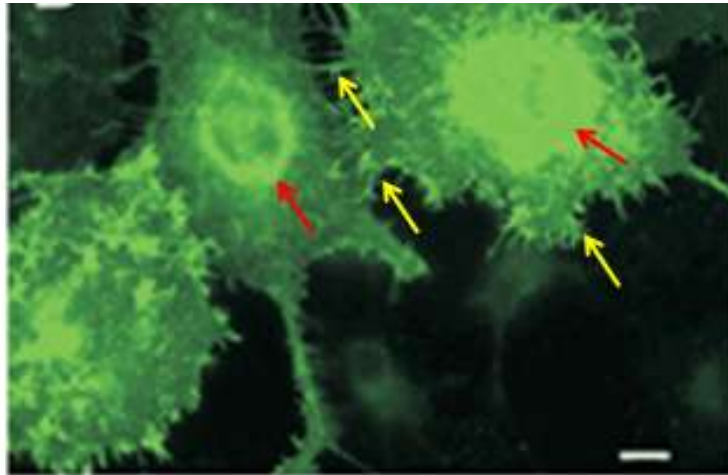


Figure 6.5.4.3-1 immunofluorescence staining of TREK-1 in COS-7 cells transfected with human TREK-1. There is evidence of nuclear staining (red arrow) and the cells show an increase in cellular protrusions (yellow arrow). Scale bar 1 μ m. (Image adapted from Xian Tao, Dyachenko et al., 2006)).

The localisation of TREK-1 in the nucleus suggests a role for TREK-1 in cell division as it may respond to an increase in the size of the nucleus to initiate cell division. TREK-1 has been shown to be selectively expressed in prostate cancer cells while healthy tissue remains clear. TREK-1 is an important oncogene for the detection of prostate cancer and inhibitors of TREK-1 have shown to reduce the population of cancerous cells (Voloshyna, Besana et al., 2008). Curcumin is an example of an antiproliferative agent that can block TREK-1 currents and maybe targeting TREK-1 channels on the nuclear membrane to alter cellular function. TREK-1 in the nucleus of placental vascular SMC may also form a similar function to trigger cell division and new vessel formation and maybe important in the placenta.

6.5.4.4. TWIK-2 channels

TWIK channels are of particular interest to our study as the ion channel has been identified in tissues such as the stomach, pancreas, and small intestine, all of which maintain low $[pH]_o$ (Chavez, Gray et al., 1999, Patel, Maingret et al., 2000, Medhurst, Rennie et al., 2001). Expression for the ion channel was detected in CPA and SVA and two dominant bands at 37 and 50 kDa were identified. The 50 kDa band has also been shown (Davis and Cowley, 2006) along with a band at 83 kDa in airway epithelial cells. The study showed that cells which line the airway may have a role in gas exchange and the same pathway may function inside the placenta.

The presence of TWIK-2 channels can provide an insight into how the pH gradient of the placenta maybe maintained. We observed an importance difference in the expression of TWIK-2 in PE samples and it was shown that TWIK-2 was specifically higher in PE CPA when compared to SVA and the 50 kDa band in PE CPA was higher when compared to the respective CPA expression levels in NORM samples. This apparent ion channel up regulation in PE suggests TWIK-2 expression may vary with diseased states and may provide a potential early indicator of altered vascular function. This could also help us to understand the reduced ability of PE CPA to relaxation in response to acidic pH environments ([Chapter 5.7](#)) and the ion channel up-regulation may be the result of an increased sensitivity of the PE vessels to pH. The increased presence of TWIK-2 may help to regulate vascular tone and furthermore suggests the TWIK-2 expression can be up regulated to increase the sensitivity of the tissue to changes in pH and prevent a loss in tone. Differences in

TWIK regulation give more information about cellular regulation. Liu (et al., 2003) showed that the expression profile of K^+ channels in the human decidua altered with a change in the labour state and shows that the placenta can actively alter its ion channel profile to adapt to changing environments. Reduced TWIK-2 expression in SVA would favour cell membrane depolarisation and may contribute to the increase resistance seen with PE. This would hamper the ability of the placenta to regulate flow. Loss of TWIK-2 activity may reduce the vessels ability to detect and respond to low pH conditions. K2P channels may have a stabilising role to keep the membrane potential constant and loss of ion channel activity will promote cell depolarisation in response to $[H^+]_i$ and allow Ca^{2+} to increase inside the cell.

SMC from CPA and SVA showed granular distribution of TWIK-2 in CPA and SVA cells with a dense staining pattern around the nuclear membrane. SVA cells also show some linear filaments of TWIK-2 which show positive overlap with α actin filaments and has been reported previously in rat cerebral vascular SMC (Bryan, You et al., 2006). Davis (et al., 2006) also showed granular punctuate expression in airway epithelial cells but most TWIK-2 expression was membrane bound. More importantly it was shown that the TWIK-2 co-localisation with TASK-3 was most prominent in the SVA which may be an important difference to allow the two ion channels to regulate pH gradients across the placental interface. TWIK-2 has previously been shown to co-localise with TREK-1 in the rat hippocampal astrocyte cells (Zhou, Xu et al., 2009) and the functional association is responsible for the rapid response to ischaemia in this tissue. The presence of both TWIK-2 and TASK-3 at the SVA region of the placenta could help to amplify the response to changes in pH.

SVA at the fetal side of the placenta will be exposed to acidic pH as a result of reduced perfusion. Excess protons are harmful to the cell as they can cross the cell membrane with ease and alter the optimal working conditions for many important cellular pathways. pH sensitive sensors are important for reacting to this by triggering a Ca^{2+} influx to depolarise the membrane and in neurons this will trigger neurotransmitter release (Lesage, Mattei et al., 1996, Patel, Maingret et al., 2000). The taste bud cells found in the tongue have been used to demonstrate this reflex response. However to better understand the link between pH changes and Ca^{2+} movements Richter (et al., 2004) investigated the expression of key acid sensing channels and showed that the mRNA for the K2P members TWIK 1/2, TREK 1/2, and TASK-1/2 were found on mouse taste bud cells with TWIK 1/2 levels being the highest. TWIK and TREK are sensitive to intracellular pH while TASK responds to extracellular changes in pH. This study also demonstrated that K2P channels may work to stabilise the cell membrane instead of directly initiating depolarisation (Cooper, Johnson et al., 2004, Lin, Burks et al., 2004, Duprat, Lauritzen et al., 2007) and similarly TWIK-2 may be important for restoring vessel function in the placental vasculature.

6.5.5. Future research

The results in this chapter presented Western blot analysis for whole placental vessel tissue and confocal IF was used to characterise the cellular location of our ion channels of interest within the SMC. This data analysis can be supported further by examining the mRNA expression levels across CPA and SVA in order to identify any

variations that may exist with channel regulation across CPA and SVA at the transcriptional level.

In our investigations RB failed to give a positive signal with anti K_{ATP}, TASK-1, TASK-3, TRAAK and TWIK-2 with Western blotting analysis although the epitopes used are highly conserved between mouse, rat and human species. This could reflect a problem with the method of homogenisation of the neuronal tissue which is less compact when compared to the tougher MYO tissue. We could consider using an alternative control tissue such as mouse brain or human brain, or alternatively pancreatic tissue could be used as it is also a rich source for K_{2P} channels. In contrast, the neuroblastoma cell line SH-SY57 gave more reproducible results when the same antibodies were applied (**Figure 6.4.3.1-1**) and could be used as an alternative control sample with Western blotting analysis.

The data presented here shows NORM and PE samples from separate Western analysis. This can introduce bias and it is more relevant to include a mixture of both NORM and PE blood vessels which have been randomised within the same blot. This would allow for a more representative comparison to be made across the two patient groups and reduce any bias in the analysis.

The method used to quantify each Western blot image could also be improved. Semi quantification involves converting the captured image into a TIFF file to then measure the optical density of each band. The background intensity was then removed using the rolling disc option and the average density was normalised to β actin and expressed as a percentage. However the converted images gave limited information about the size of the band for example TASK-1 was 2 fold larger in size on the blot

but following normalisation, the data showed that the expression was <50% of the β actin. A better option may have been to measure total pixels for the entire band or the integral intensity, or peak height and then normalise this value to β actin (Gassmann, Grenacher et al., 2009). Another limitation of applying the rolling disc is that vital pixel information can also be removed as overlapping lanes can distort this process. This may lead to the loss of smaller bands that could represent smaller sub units of our protein of interest. The molecular weights for our proteins of interest were deduced by comparing the separation of the pre-stained kaleidoscope molecular weight markers that were loaded with each western blot. However protein bands that were predicted to be 45 kDa in size were often detected at 50 kDa. This may be due to a poor separation of the pre-stained markers, particularly with proteins that are closely overlapping. A better alternative could be to use biotinylated molecular weight markers which have a greater accuracy and have the additional advantage that they can be developed using chemiluminescence detection.

All of our data was normalised to the housekeeping protein β actin but it would have been better to perhaps normalise to MYO which proved to be a good control sample to use for each Western blot. This has the further advantage that the blot does not need to be stripped in order to be re-probed for β actin as some protein could be lost with this extra process. In addition more than one housekeeper-protein should be used to quantify protein levels as diseased states, as well as gestational age can alter the expression of such proteins to distort the analysis (Ferguson, Carroll et al., 2005). β tubulin or glyceraldehyde-3-phosphate are additional alternatives that have been used with RT-PCR analysis (Gassmann, Grenacher et al., 2009). Another

modification could be to include a wider range of SMC marker proteins such as β -tropomyosin, and h-caldesmon which are SMC specific proteins in addition to α actin. This could resolve ambiguity regarding the nuclear stain which was seen sporadically with the α actin antibody.

To extend the confocal staining it would be useful to firstly include TREK-2 along with TRAAK to investigate the full spectra of K2P channel expression in placental vessels. Each ion channel shares homology with different members of the K2P family and it would be interesting to see if there is a degree co-localisation. The development of monoclonal antibodies will help with this. The main limitation with studying K2P channels was with the limited choice of antibodies available that recognise various epitopes. The only commercially available ones are supplied by Alomone or Santa Cruz while the recent anti-TREK-1 antibody supplied by Abcam is not yet widely cited in the literature. Some peri-nuclear staining was observed particularly with TASK-3 may be organelles that are found at the nuclear membrane that express the ion channel. To investigate this we added monoclonal antibodies that stain the endoplasmic reticulum (ER) and Golgi but our pilot data did not show significant overlap with TASK 1, TWIK-2 and TREK-1 (not shown). One improvement to this method would be to use organelle markers in live cells which take up the fluorescent tags in normal cellular process and may be a more accurate way to label the cell organelles. Live cell imaging would also allow us to add pH sensitive fluorophores such as carboxyl SNARF (Swietach, Camelliti et al., 2010) to see the precise SMC response to acidic pH stimuli. Co-localisation was important to our study but despite the accurate nature of dual confocal imaging some staining can

be due to the poor signal separation of the different fluorescent tags which can emit fluorescence in the wrong focal plane. An alternative technique to explore could be co-immunoprecipitation which is another method for investigating protein-protein cross links. This method involves separating functional structures of protein combinations according to the precise molecular weight of the protein dimer as well as probing these interactions through co-immunoprecipitation.

6.5.6. Conclusion

This study has reported for the first time the expression of key members of the K2P channel family, TWIK-2, TASK-3, TREK-2 and TRAAK both in whole tissue and within the SMC. Crucially there was no significant difference at the protein levels between the CPA and SVA while it was shown that expression of TWIK-2 significantly varied between NORM and PE samples and may have important implications for the ability of the placenta to respond to pH stress. The examination of SMC expression for each ion channel revealed important differences in the sub cellular localization of each ion channel and we observed an important interaction between α actin and K2P channels and this was particularly evident with TREK-1. The data also shows evidence for co-localisation of TASK-3 with other closely related K2P channels and requires further investigations.

7. Functional investigations of ion channels in CPA

7.1. Introduction

The Western blotting and confocal staining of CPA and SVA SMC findings described in [Chapter 6](#) demonstrated the presence of the key O₂ and pH sensing ion channels. The results also suggest the K2P member TREK-1 may have a role in controlling vasoconstriction and vasodilatation of the resistance vessels due to its close association with SMC α actin. The hypothesis that the response by CPA to external stress is mediated by O₂ sensitive ion channels was tested.

7.2. Objectives

- Investigate the functional role of K⁺ channels in mediating CPA contractile and relaxation responses.
- Determine the precise role of K⁺ channels in mediating the response to H₂O₂ and pH.

7.3. Materials and methods

CPA from the NORM patient group were studied using wire myography ([Chapter 3.7](#)) using the K⁺ activators and blockers listed in **Table 3.7.8-1** and **Table 3.7.11-1**.

7.4. Results

7.4.1. Effect of ion channel blockers on the U46619 contraction

The effect of pre-incubation with a range of blockers on the U46619 vasoconstrictions was investigated. The first series of blockers were specific for the Ca^{2+} activated and voltage gated K^+ channels. The effect on basal tone was assessed pre and post application of the different drugs and it was found that 4-AP caused an increase in the basal tone upon application (**Figure 7.4.1-1**).

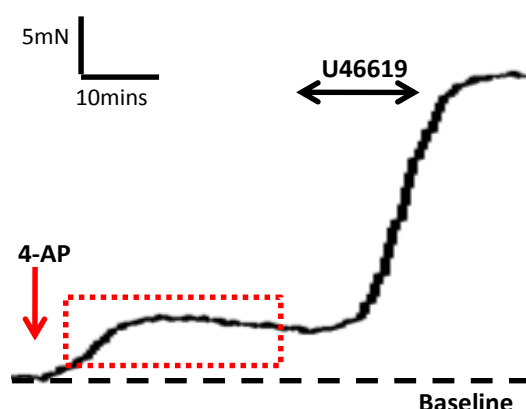


Figure 7.4.1-1 shows the effect of 4-AP pre-incubation. CPA were treated with the blocker 20mins prior to the U46619 dose-response to stimulate the vessels. The red arrow shows the point at which the blocker is added and causes an immediate increase in the baseline tension.

The blockers that produced a significant shift in the dose-response to U46619 have been summarised **Figure 7.4.1-2**. APA inhibited the contractile response at low doses which was reversed at the higher concentrations of U46619 ($p < 0.001$ at $10^{-7.5}\text{M}$) and reached

plateau at 10^{-7} M. The $\text{CaV}_{1.2}$ blocker NIFED caused a significant reduction in the maximum response ranging from 10^{-8} - 10^{-6} M as the vessels failed to achieve the maximum constriction. **Figure 7.4.1-2B** shows the response to U46619 is enhanced in the presence of 4-AP which causes a leftward shift in the dose-response curve and achieves significance at 10^{-8} M ($p < 0.05$). GLB produced a decreased response that was significant at 10^{-7} M ($p < 0.05$). **Table 7.4.1-1** summarises the resulting $\log\text{EC}_{50}$ values based on the best fit curve in the presence of each channel blocker and it was found that 4-AP along with APA had a significantly different EC_{50} value.

*Functional investigation of ion channels in CPA***Table 7.4.1-1** summarising the EC₅₀ values which have been obtained with U46619 in the presence of specific blockers.

Treatment (n)	LogEC₅₀(M) ± SEM	p
U46619 (12)	-7.5 ± 0.1	<0.01
U46619 + 4-AP (9)	-7.8 ± 0.1	
U46619 + AMIL (9)	-7.3 ± 0.1	ns
U46619 + APA (9)	-7.8 ± 0.1	<0.01
U46619 + BaCl ₂ (9)	-7.6 ± 0.2	ns
U46619 + Choline Cl (9)	-7.6 ± 0.2	ns
U46619 + CuCl ₂ (9)	-7.6 ± 0.1	ns
U46619 + GLB (9)	-7.2 ± 0.2	ns
U46619 + IBTX (9)	-7.1 ± 0.1	ns
U46619 + L-NAME (9)	-7.2 ± 0.2	ns
U46619 + NaCl (9)	-7.4 ± 0.1	ns
U46619 + NIFED (9)	-7.3 ± 0.1	ns
U46619 + TEA (9)	-7.1 ± 0.1	ns
U46619 + ZnCl ₂ (9)	-7.6 ± 0.1	ns

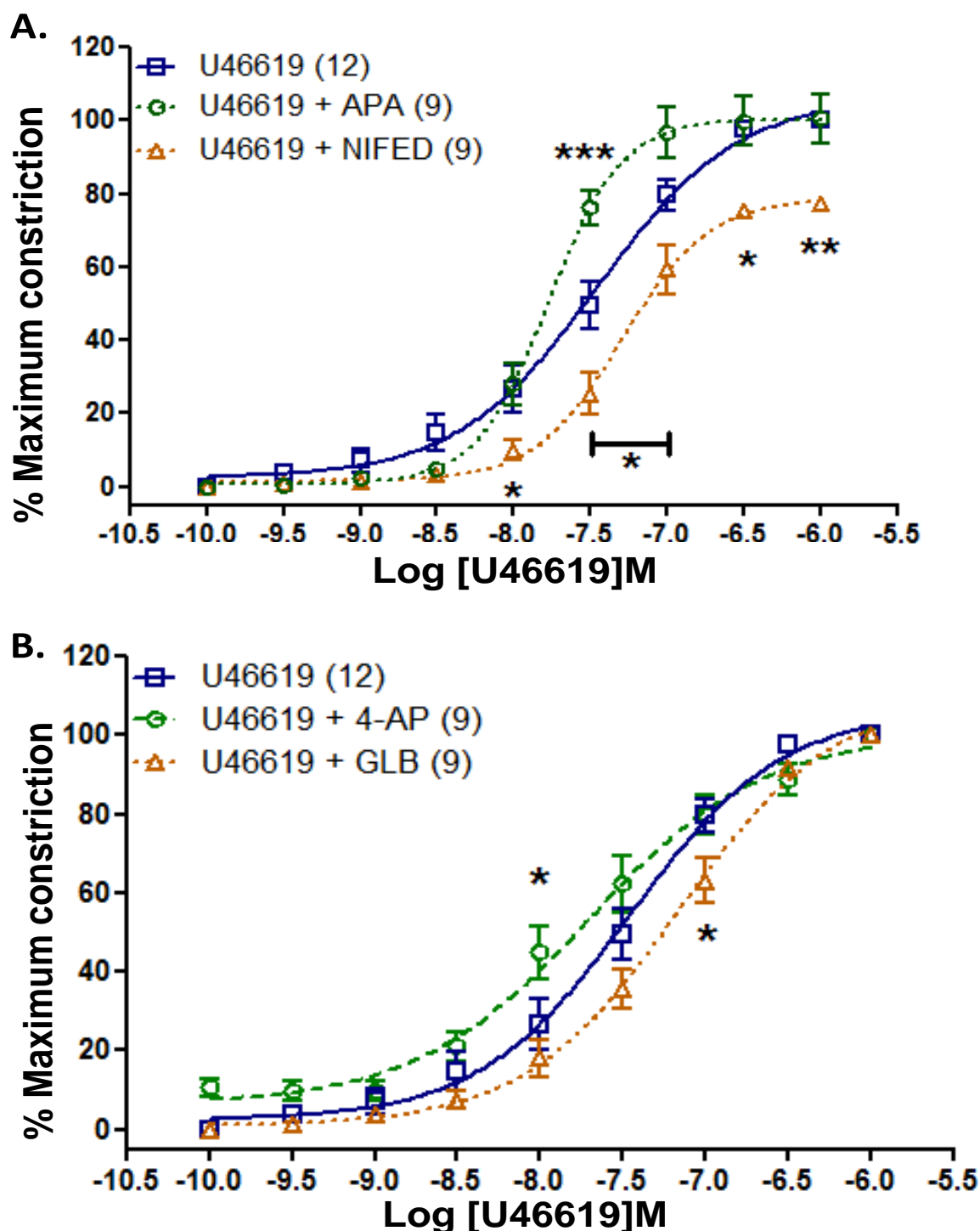


Figure 7.4.1-2 summarising the U46619 (N=12) constriction when CPA have been pre-treated with ion channel blockers. A shows the effect of APA (N=9) incubation which causes an initial inhibition to the U46619 response but this is reversed with the higher dose concentrations to elevate the U46619 response. NIFED (N=9) significantly reduces the maximum constriction. **B** shows how 4-AP (N=9) caused a significant left ward shift while GLB (N=9) pre-treatment produced a significant rightward shift as the maximum response was reduced. Data are presented as mean \pm SEM along with vessels treated (n) from placentae (N). * p <0.05, ** p <0.01, *** p <0.001.

Replacing NaCl with Choline Cl ($C_5H_{14}ClNO$) in the PSS buffer markedly enhanced the constriction produced by U46619 and achieved significance at the highest concentrations (10^{-8} - $10^{-7}M$) (**Figure 7.4.1-3**). BUP markedly reduced the maximal response to U46619 and achieved significance at the highest concentrations ($10^{-6.5}$ - $10^{-6}M$, $p<0.01$). The $logEC_{50}$ values extrapolated from the best fit curve in the presence of each channel blocker have been summarised **Table 7.4.1-2**. The next group of blockers to be analysed included the TWIK-2 blocker QUIN and the Na^+/H^+ pump blocker OUAB. **Figure 7.4.1-3B** shows that OUAB caused a leftward shift in the dose-response curve which achieved significance at 10^{-8} - $10^{-7.5}M$ ($p<0.01$). In contrast QUIN restricted the maximum constriction to 45% of the original U46619 response and was significantly different ($p<0.05$) at 10^{-8} - $10^{-6}M$. The $logEC_{50}$ values extrapolated from the best fit curve in the presence of each channel blocker have been summarised in **Table 7.4.1-2** and the EC_{50} values were significantly different with QUIN and OUAB pre-incubation when compared to the vehicle controls.

*Functional investigation of ion channels in CPA***Table 7.4.1-2** summarising the EC₅₀ values which have been obtained with U46619 in the presence of specific blockers.

Treatment (n)	LogEC₅₀(M) ± SEM	p
U46619 (12)	-7.5 ± 0.1	ns
U46619 + BUP (9)	-7.3 ± 0.1	ns
U46619 + CURC (9)	-7.3 ± 0.2	ns
U46619 + LIDO (9)	-7.1 ± 0.2	ns
U46619 + L-METH (9)	-7.2 ± 0.2	ns
U46619 + M.ANAN (9)	-7.0 ± 0.1	ns
U46619 + OMP (6)	-7.6 ± 0.1	ns
U46619 + OUAB (6)	-8.0 ± 0.2	<0.001
U46619 + QUIN (4)	-7.0 ± 0.1	<0.01
U46619 + R.RED (6)	-7.4 ± 0.1	ns

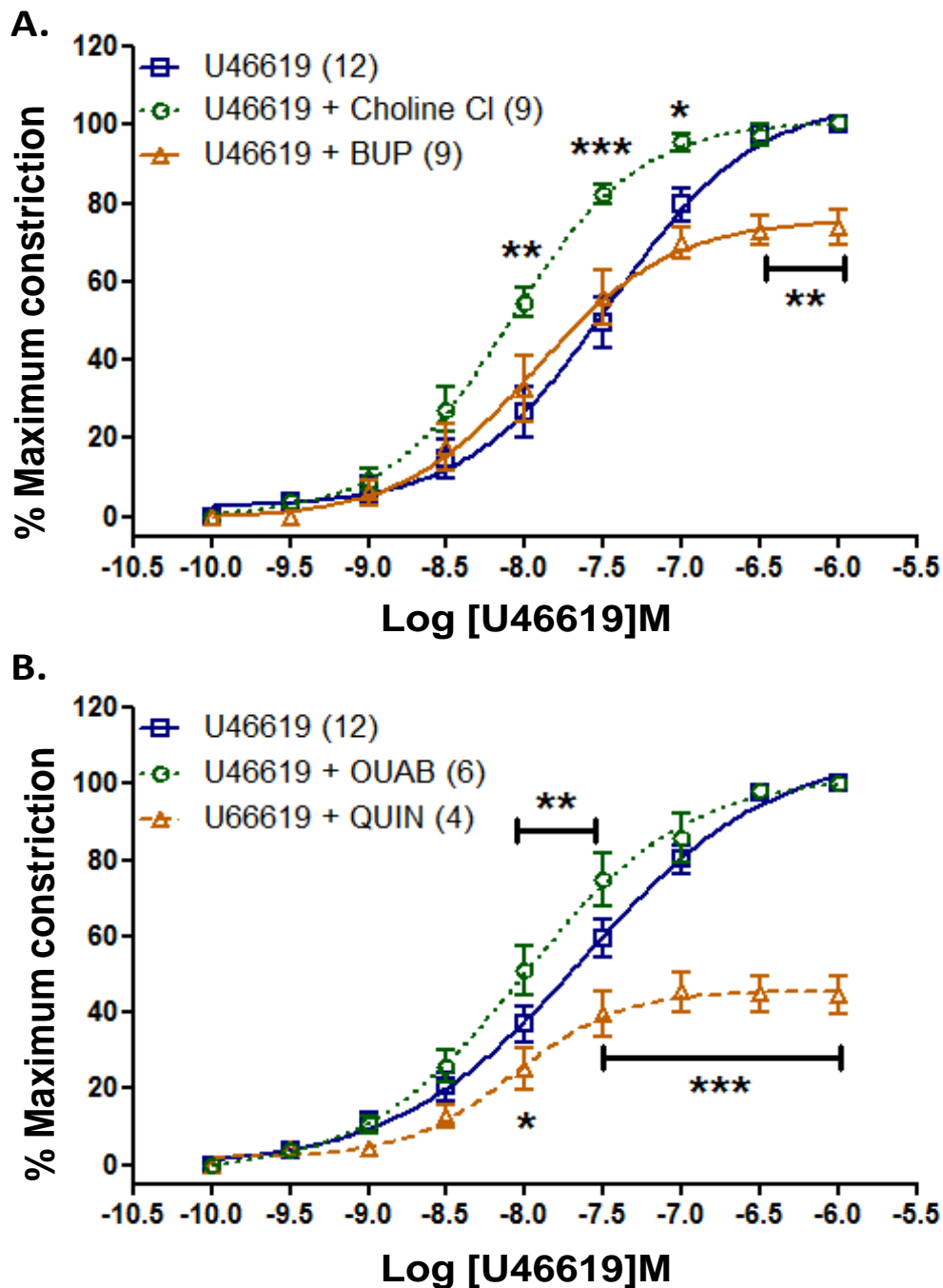


Figure 7.4.1-3 summarising the U46619 (N=12) constriction when CPA have been pre-treated with different blockers. A shows the response with Choline Cl (N=9) which causes a significant increase in the response while BUP (N=9) showed a blunted contractile response. **B.** OUAB (N=6) caused a rightward shift to the response curve and this was only significant at 10^{-8} - $10^{-7.5}$ M. QUIN (N=4) restricted the maximum constriction to 45% and achieved significance with the highest doses. Data are presented as mean \pm SEM along with vessels treated (n) from placentae (N). * $p < 0.05$, ** $p < 0.01$, *** $p < 0.001$.

7.4.2. Response of ion channel activators

7.4.2.1. NS1619

The response to the BK_{Ca} agonist NS1619 was investigated with CPA. An original trace recording is shown in **Figure 7.4.2.1-1** with CPA at 20% pO_2 . The vessels produced a dose dependent relaxation with a maximum relaxation of 92% (**Table 7.4.2.1-1**). The dose-response in the presence and absence of the K^+ channel blockers TEA and IBTX been summarised in **Figure 7.4.2.1-2**. IBTX also produced the highest degree of inhibition to the NS1619 response and this was significant at 10^{-6} - $10^{-5}M$ ($p<0.05$).

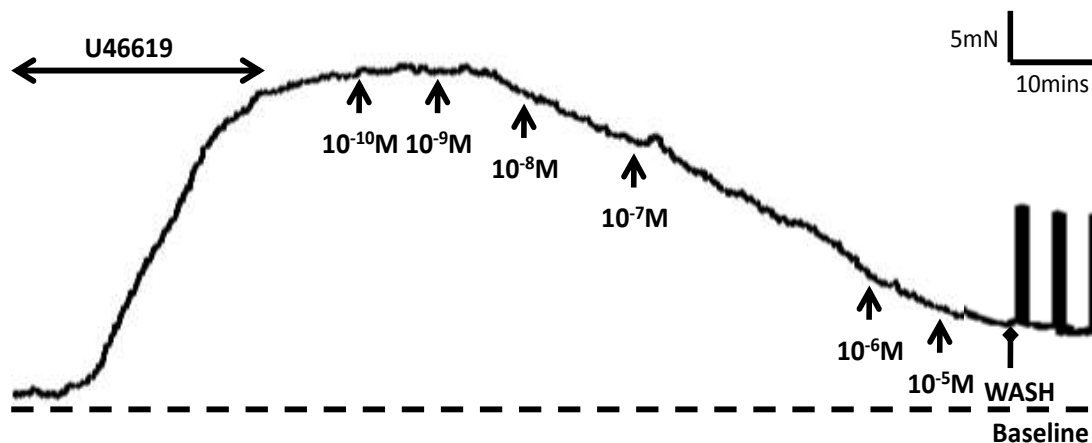


Figure 7.4.2.1-1 showing an original trace with application of NS1619 (10^{-10} - $10^{-5}M$) in pre-constricted CPA. The vessels could produce a marked relaxation with increasing doses of the BK_{Ca} opener which almost reaches 100%. The vessel was then washed with fresh PSS to allow for recovery.

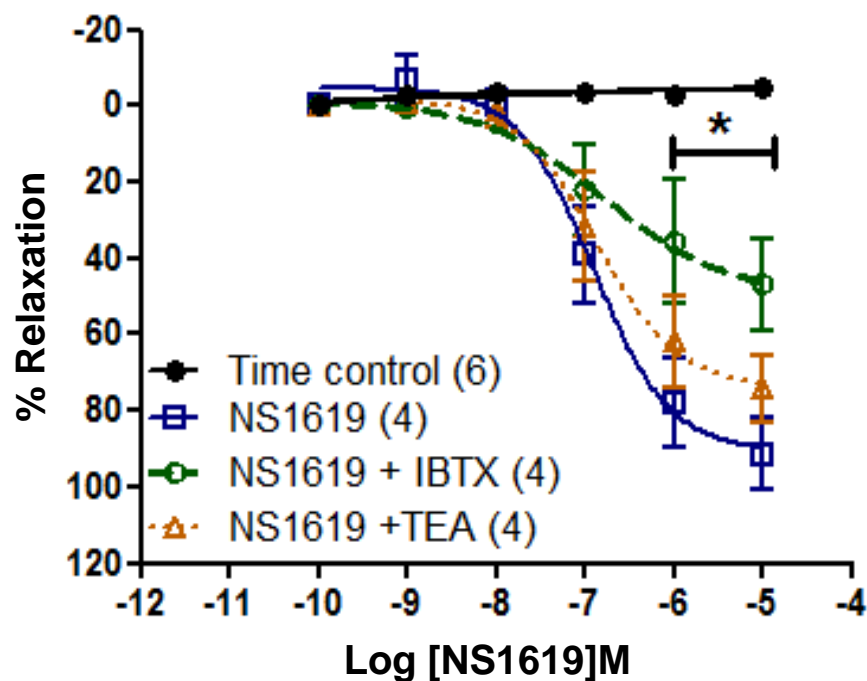


Figure 7.4.2.1-2 showing the dose-response curve with NS1619 (N=4) in CPA. Only IBTX (N=4) gave a significant inhibition with the highest doses (10^{-6} - 10^{-5} M) used and time control responses were unchanged throughout. Data are presented as mean \pm SEM along with vessels treated (n) from placentae (N). * $p < 0.05$.

Table 7.4.2.1-1 summarising the EC_{50} values for NS1619 in the presence and absence of BK_{Ca} inhibitors.

Treatment (n)	$LogEC_{50}(NS1619)M \pm SEM$	p	Maximum Relaxation (%) $\pm SEM$
NS1619 (4)	-6.9 ± 0.2		92 ± 9
NS1619 + IBTX (4)	-6.8 ± 0.7	ns	53 ± 18
NS1619 + TEA (4)	-6.9 ± 0.3	ns	75 ± 8

7.4.2.2. Response to RIL in the presence of ion channel blockers at 20% pO₂

A potent and reproducible RIL induced vasodilatation in CPA and SVA has been demonstrated (see [Chapter 5.6.4](#)). The next objective was to investigate the potential ion channels that maybe targeted by the stimulant to bring about the relaxation response using CPA, and the response in the presence of TEA has been shown in **Figure 7.4.2.2-1**.

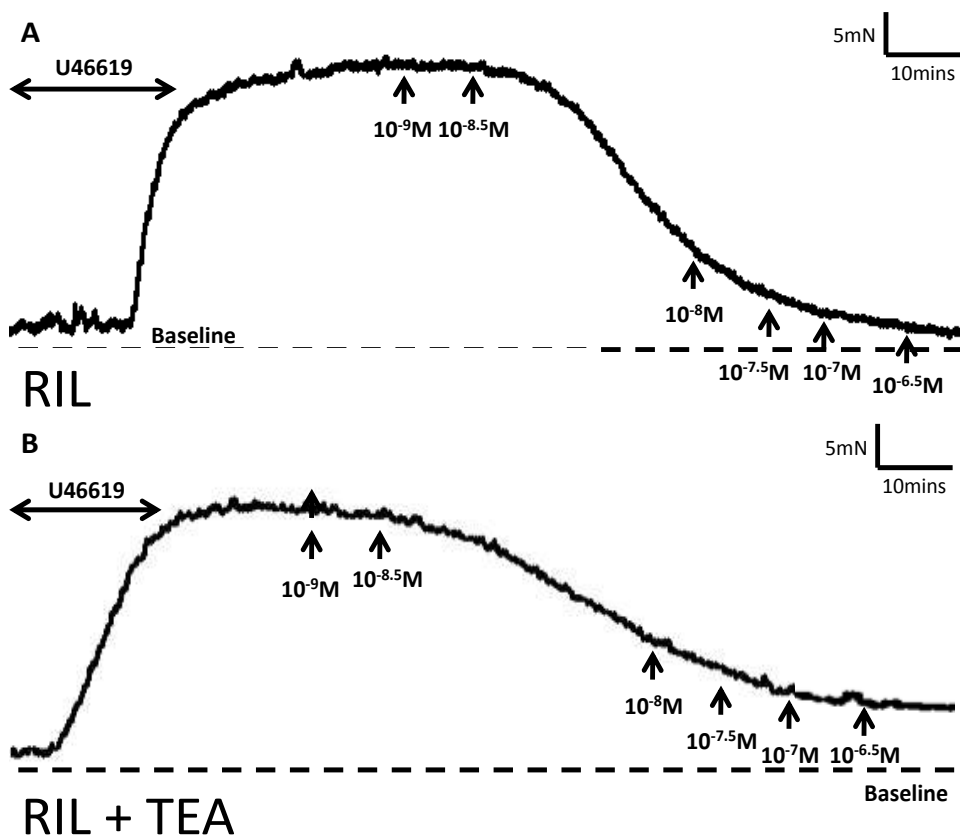


Figure 7.4.2.2-1 showing a representative trace of RIL induced concentration dependent relaxation of pre-contracted CPA. A shows the response to RIL which can induce a potent vasodilatation which appears to reach 100%. B shows the response in the presence of TEA which appears to inhibit the maximum relaxation and prevents the vessel from reaching its baseline tension.

The same experiment was repeated in the presence of a range of specific ion channel blockers. From the range of inhibitors applied only TEA caused a significant inhibition to the relaxation observed at 10^{-7} - $10^{-6.5}$ M ($p<0.001$) (**Figure 7.4.2.2-2**). 4-AP caused a significant inhibition to the RIL response but only with the highest dose used $10^{-6.5}$ M ($p<0.05$). The extrapolated EC_{50} values for RIL have summarised in **Table 7.4.2.2-1** along with the maximum % relaxation values in the presence of specific channel antagonists.

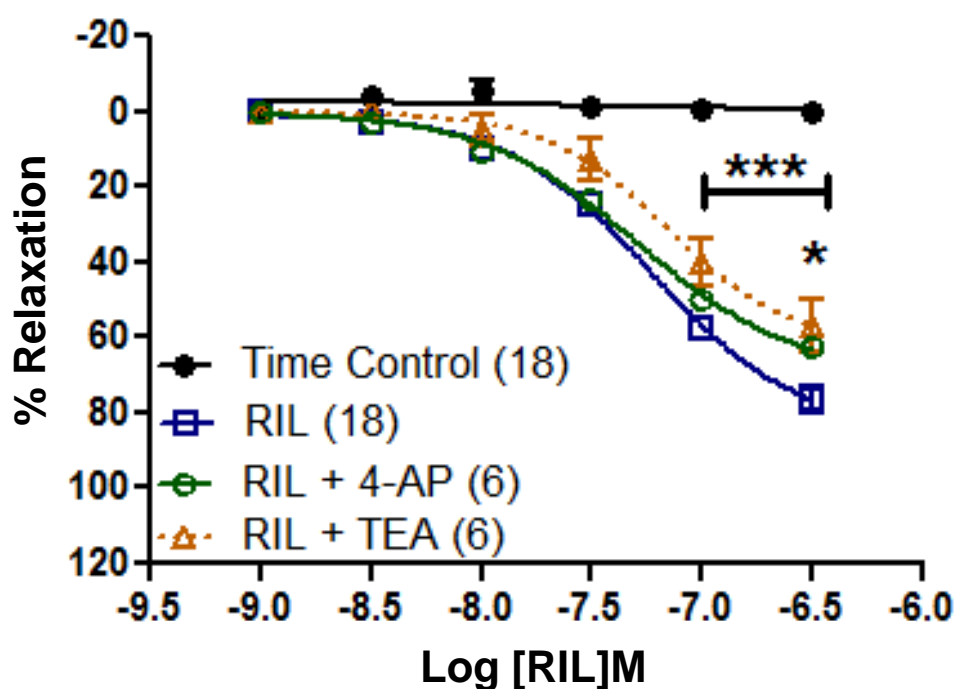


Figure 7.4.2.2-2 showing the dose-response with RIL (N=18) in the presence of specific ion channel blockers. The dose-response curve shows TEA (N=6) caused a reduction in relaxation which was significant at 10^{-7} - $10^{-6.5}$ M. 4-AP (N=6) cause an upward shift to the curve as the response was partially inhibited but only achieved significance at $10^{-6.5}$ M. Data are presented as mean \pm SEM along with vessels treated (n) from placentae (N).. * $p<0.05$, *** $p<0.001$.

*Functional investigation of ion channels in CPA***Table 7.4.2.2-1** summarising the EC₅₀ values which have been obtained with RIL in the presence of different blockers.

Treatment (n)	LogEC₅₀(M) ± SEM	p	Maximum Relaxation (%) ± SEM
RIL (18)	-7.2 ± 0.1		76 ± 4
RIL + 4-AP (6)	-7.3 ± 0.2	ns	62 ± 4
RIL + AMIL (6)	-7.3 ± 0.1	ns	75 ± 6
RIL + BaCl ₂ (6)	-7.2 ± 0.1	ns	83 ± 7
RIL + BUP (6)	-7.2 ± 0.1	ns	79 ± 6
RIL + CuCl ₂ (6)	-7.5 ± 0.3	ns	89 ± 6
RIL + CURC (13)	-7.3 ± 0.1	ns	74 ± 7
RIL + GLB (6)	-7.2 ± 0.2	ns	67 ± 7
RIL + IBTX (6)	-7.1 ± 0.1	ns	67 ± 6
RIL + LIDO (6)	-7.1 ± 0.1	ns	80 ± 4
RIL + L-METH (6)	-7.3 ± 0.1	ns	75 ± 6
RIL + L-NAME (12)	-7.2 ± 0.2	ns	68 ± 5
RIL + M.ANAN (6)	-7.4 ± 0.1	ns	83 ± 7
RIL + NIFED (6)	-7.3 ± 0.1	ns	63 ± 4
RIL + R.RED (6)	-7.3 ± 0.1	ns	83 ± 6
RIL + TEA (6)	-7.1 ± 0.1	ns	58 ± 7
RIL + ZnCl ₂ (6)	-7.5 ± 0.2	ns	83 ± 9

7.4.3. Response to H₂O₂ in the presence of ion channel blockers at 20% pO₂

The relaxation response of CPA to H₂O₂ was investigated in the presence of a range of specific blockers at 20% pO₂ perfusion. The first H₂O₂ antagonist to be used was CAT which metabolises H₂O₂ into H₂O. The response to H₂O₂ was significantly attenuated with CAT pre-incubation at 10⁻⁷M and 10⁻⁵M (**Figure 7.4.3-1**). CURC is known for its antioxidant properties, as well as being a TREK-1 blocker, could not demonstrate a significant shift in the response of CPA to H₂O₂. **Figure 7.4.3-1B** also shows the response to H₂O₂ in the presence of IBTX which appears not to be involved in the vasodilatation brought about through the application of H₂O₂. In contrast, a very interesting response was seen in the presence of L-NAME which caused an increased relaxation at the low concentrations and achieved significance at 10⁻⁸M (p<0.05, n=3). Only TEA demonstrated an inhibition of the H₂O₂ response at the lower doses of 10⁻⁸-10⁻⁷M and also at 10⁻⁵M (p<0.05, n=4). **Table 7.4.3-1** summarises the EC₅₀ values for each treatment and blocker used.

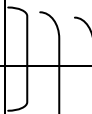

The role of H₂O₂ as a vasoconstrictor has also been demonstrated in **Figure 7.4.3-2A** which shows the original response of CPA stimulated with H₂O₂ at rest with 20% pO₂. The response was not reproducible with each subsequent stimulation with the agonist and we again found that this experiment proved to be toxic as vessels failed to produce a response to a stimulant following washout of H₂O₂. **Figure 7.4.3-2A** also shows the response when a CPA from the same placenta was pre-treated with CAT. The response was inhibited with the exception of only one

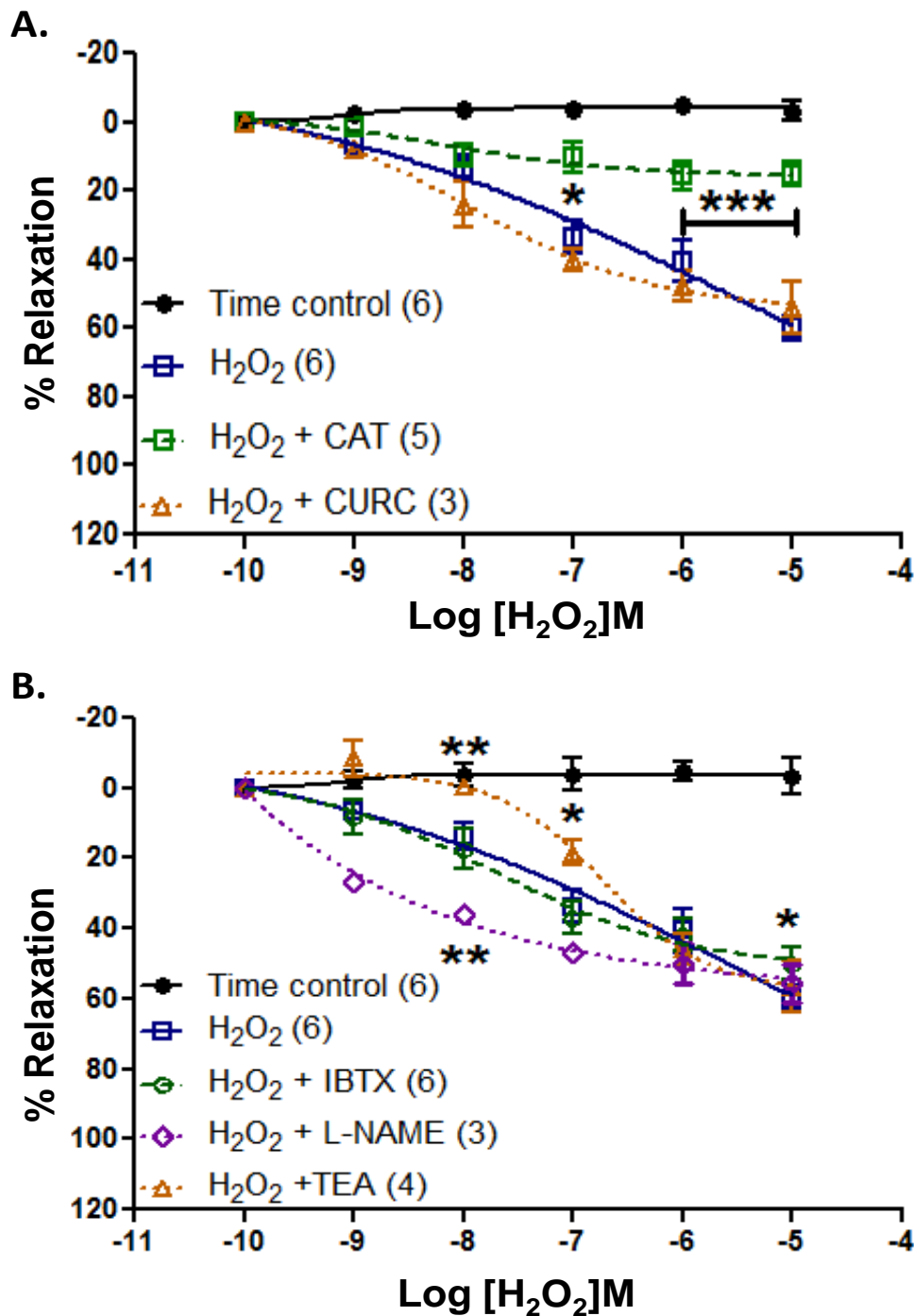
Functional investigation of ion channels in CPA

substantial contraction that was produced with the higher dose of H_2O_2 (10^{-6}M). The varied nature of the response produced by the vessels made it difficult to produce a dose-response curve as all the points did not follow a classic sigmoid dose-response.

Figure 7.4.3-2B shows the smooth curve with H_2O_2 stimulation of CPA in the presence of CAT and the BK_{Ca} inhibitor IBTX both of which did not exert a statistically significant effect on the vascular response.

Table 7.4.3-1 summarising the EC_{50} values which have been obtained with H_2O_2 in the presence of specific blockers.

Treatment (n)	$\text{LogEC}_{50}(\text{H}_2\text{O}_2)\text{M} \pm \text{SEM}$	P	Maximum Relaxation (%) $\pm \text{SEM}$
H_2O_2 (6)	-5.5 ± 0.1		54 ± 2
$\text{H}_2\text{O}_2 + \text{CAT}$ (5)	-3.8 ± 0.1		69 ± 2
$\text{H}_2\text{O}_2 + \text{CURC}$ (3)	-6.1 ± 0.1	ns	54 ± 7
$\text{H}_2\text{O}_2 + \text{IBTX}$ (6)	-5.7 ± 0.1	ns	50 ± 4
$\text{H}_2\text{O}_2 + \text{L-NAME}$ (3)	-7.2 ± 0.2		54 ± 2
$\text{H}_2\text{O}_2 + \text{TEA}$ (4)	-6.0 ± 0.1		57 ± 7



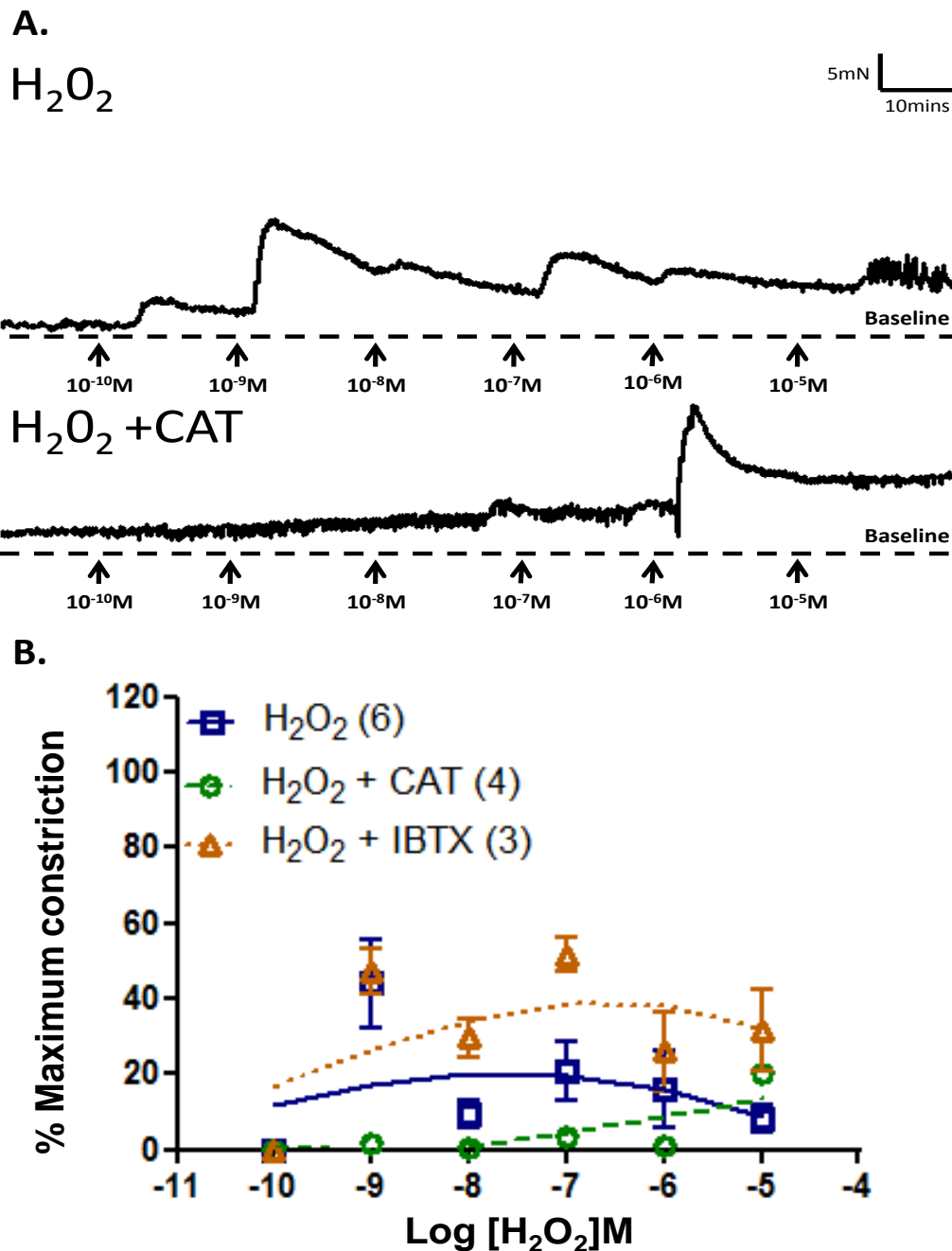


Figure 7.4.3-2 showing the results of H_2O_2 application (10^{-10} - 10^{-5}M) to CPA in 20% pO_2 . **A** shows an original trace recording which produces a contraction that was short lived as the vessel begins to return to its resting tension. The lower panel shows the response in the presence of CAT which could abolish the response to the agonist. Only a single contraction was produced at 10^{-6}M . **B** shows the smooth curve for the response to H_2O_2 (N=6). CAT (N=4) blunts the response to the agonist while IBTX (N=3) causes an upward shift as the contraction appears to be enhanced. Data are presented as mean \pm SEM along with vessels treated (n) from placentae (N).

7.4.4. Response to acidic pH in the presence of ion channel blockers at 20% pO₂

The effect of pre-incubation with a range of ion channel blockers on the acidic pH relaxation was also investigated using CPA. **Figure 7.4.4-1** shows an original trace recording showing the effect when vessels have been pre-incubated with CuCl₂ which inhibited the recovery phase (red box) that was seen in response to the pH stress. Instead it was shown that the relaxation to pH stimuli stabilised in the presence of the ion channel blocker and interestingly the same effect was also observed with ZnCl₂ (**Figure 7.4.4-2**). **Figure 7.4.4-4B** summarises the concentration response curves with lowering pH treatments. CuCl₂ and ZnCl₂ evoked a downward shift in the response curve as the relaxation was enhanced which achieved significance at pH <7.0. **Table 7.4.4-1** summarises the resulting EC₅₀ values based on the best fit curve in the presence of each channel blocker. The U46619 response in the presence of NIFED (**Figure 7.4.4-3**) was greatly reduced and the response to pH was altered as the vessel recovery following a pH insult was blunted. This had the effect of producing a steep relaxation curve to acidic pH in the presence of NIFED which was significant at pH 6.8-6.4 (**Figure 7.4.4-4**). From all the blockers that were investigated, only L-NAME was able to show an inhibition to the relaxation to pH stimulation which achieved significance at the highest doses used (pH 6.6-6.4) (**Figure 7.4.4-4A**).

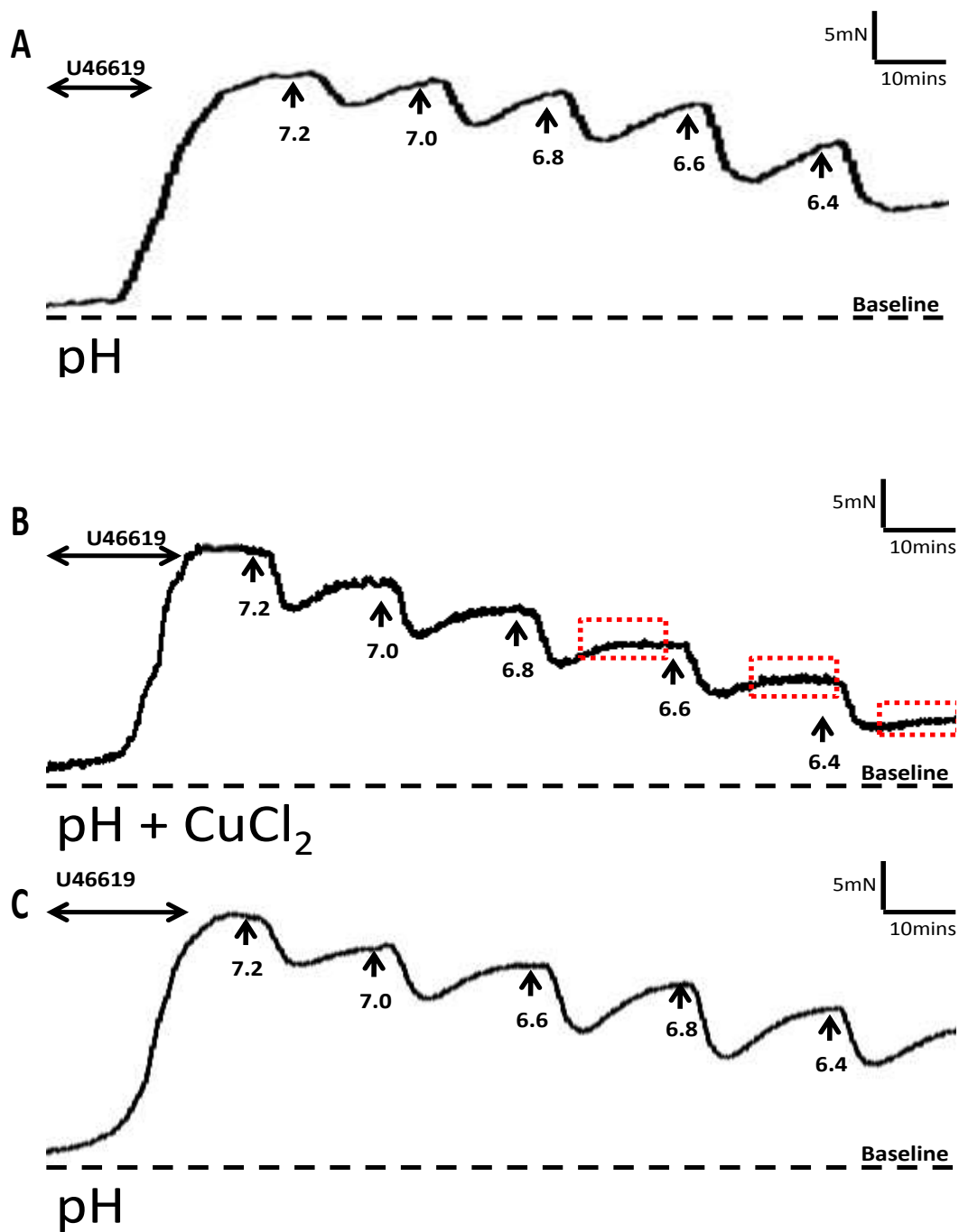


Figure 7.4.4-1 shows a representative trace of the pH response in the presence (B) and absence (A&C) of CuCl_2 . The vessel was firstly treated with increasing doses of lactic acid (A) to record the maximal response to acidic pH stimulation. The vessel was then pre-treated with CuCl_2 (B) and the pH response was again repeated. The biphasic response with lactic acid stimulation was altered (red box) as the phase II response is almost completely absent. The final panel shows recovery of the original pH response following successful washout of the blocker (C).

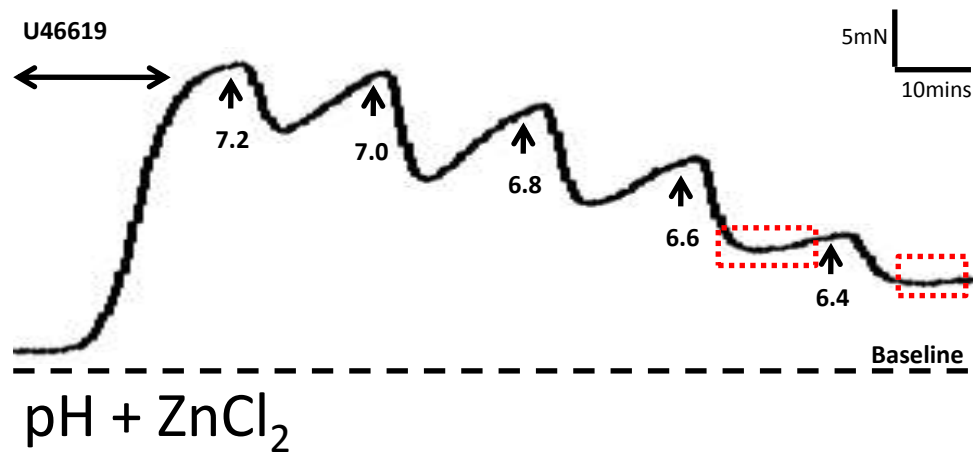


Figure 7.4.4-2 illustrating the experimental protocol used to assess the effect of ZnCl₂ on the lactic acid response. The vessel was then pre-treated with ZnCl₂, and the pH response was again repeated. The red box shows the absence of the phase II response which is blunted in the presence of the ion channel modulator.

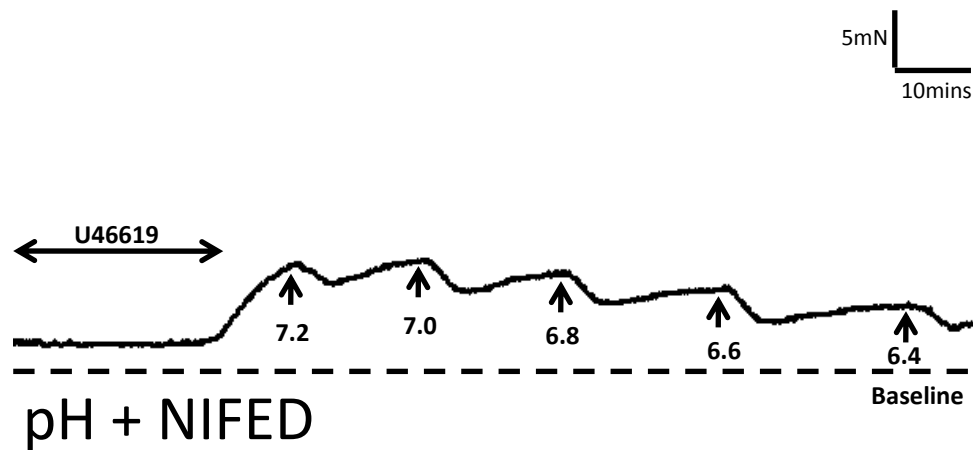


Figure 7.4.4-3 shows a representative trace of the pH response in the presence of the Ca_v1.2 blocker NIFED. The contraction to U46619 was blunted but the pre-treated vessel could still demonstrate a biphasic response with lactic acid stimulation.

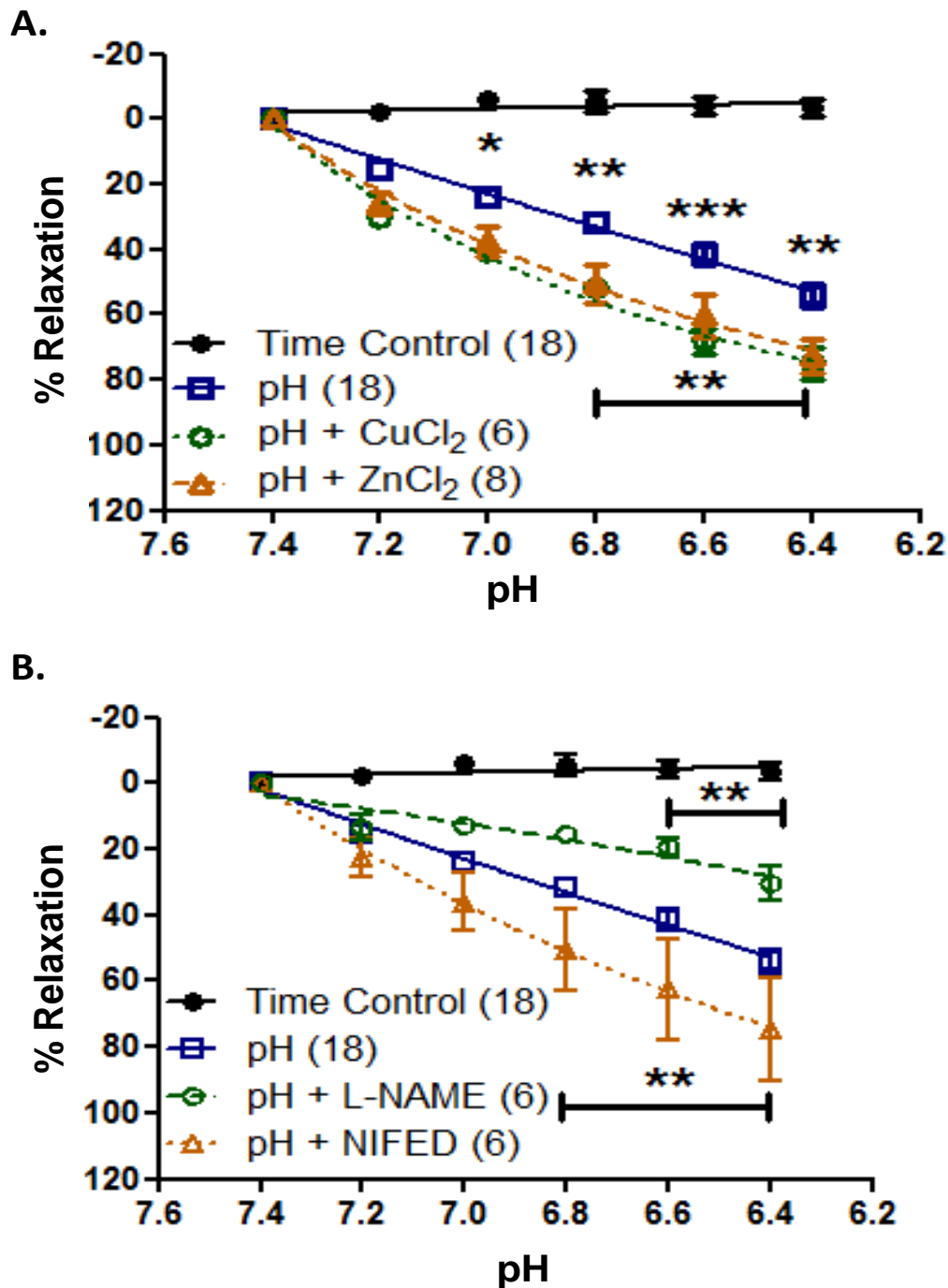


Figure 7.4.4-4 summarising the lactic acid induced relaxation when CPA (N=18) have been pre-treated with various blockers. **A** shows the responses to lactic acid in the presence of the TASK channel blockers. Both CuCl_2 (N=6) and ZnCl_2 (N=8) evoked a downward shift as the relaxation was enhanced and ZnCl_2 achieved significance at $\text{pH} < 7.0$. **B** shows the responses to lactic acid in the presence of the L-NAME (N=6) which produced an attenuation to the pH response at the highest doses. NIFED (N=6) causes a downward shift to the response curve as the relaxation was significantly elevated in the presence of the ion channel inhibitor ($\text{pH} < 6.8$). Data are presented as mean \pm SEM along with vessels treated (n) from placenta (N). * $p < 0.05$, ** $p < 0.01$, *** $p < 0.001$.

*Functional investigation of ion channels in CPA***Table 7.4.4-1** summarising the EC₅₀ values for the lactic acid concentration response curves in the presence of specific ion channel blockers.

Treatment (n)	EC₅₀(M) ± SEM	p	Maximum Relaxation (%) ± SEM
pH (18)	6.9 ± 0.1		54 ± 3
pH + 4-AP (9)	6.9 ± 0.2	ns	55 ± 7
pH + GLB (6)	7.0 ± 0.2	ns	45 ± 4
pH + IBTX (6)	7.0 ± 0.1	ns	58 ± 6
pH + L-NAME (6)	6.8 ± 0.1	ns	30 ± 7
pH + NIFED (6)	7.0 ± 0.1	ns	74 ± 5
pH + TEA (6)	7.0 ± 0.2	ns	44 ± 5

The effect of using TREK-1 blockers on the response to lactic acid was also examined. **Figure 7.4.4-5** shows an original trace recording to show the effect of CURC on the pH response. The vessel displays an increase in spontaneous tone oscillations (boxed) with CURC pre-incubation and when the pH was lowered, the relaxation was partially inhibited (**Figure 7.4.4-5** red box) as the vessels can quickly recover the original contraction. In contrast, the second TREK-1 inhibitor L-METH (**Figure 7.4.4-6**) increased the amplitude of the original pH stimulus as the vessel tone is dramatically reduced with each repeated lactic acid dose. **Figure 7.4.4-7** shows the response to lactic acid in the presence of the CURC which produced a significant inhibition to the response. L-METH evoked a downward shift as the relaxation was enhanced and achieved significance ($p < 0.001$) at pH 7.2. **Table 7.4.4-3** summarises the resulting EC₅₀ values based on the best fit curve in the presence of each channel blocker.

*Functional investigation of ion channels in CPA***Table 7.4.4-2** summarising the EC₅₀ values for the lactic acid concentration response curves in the presence of specific ion channel blockers.

Treatment (n)	EC₅₀(M) ± SEM	p	Maximum Relaxation (%) ± SEM
pH (18)	6.9 ± 0.1		54 ± 3
pH + AMIL (9)	6.9 ± 0.2	ns	45 ± 8
pH + BaCl ₂ (6)	6.8 ± 0.1	ns	62 ± 5
pH + CuCl ₂ (6)	7.0 ± 0.1	ns	75 ± 5
pH + NaCl (6)	6.9 ± 0.2	ns	35 ± 4
pH + OMP (6)	6.9 ± 0.1	ns	54 ± 3
pH + OUAB (6)	6.8 ± 0.2	ns	39 ± 7
pH + ZnCl ₂ (8)	7.0 ± 0.1	ns	72 ± 5

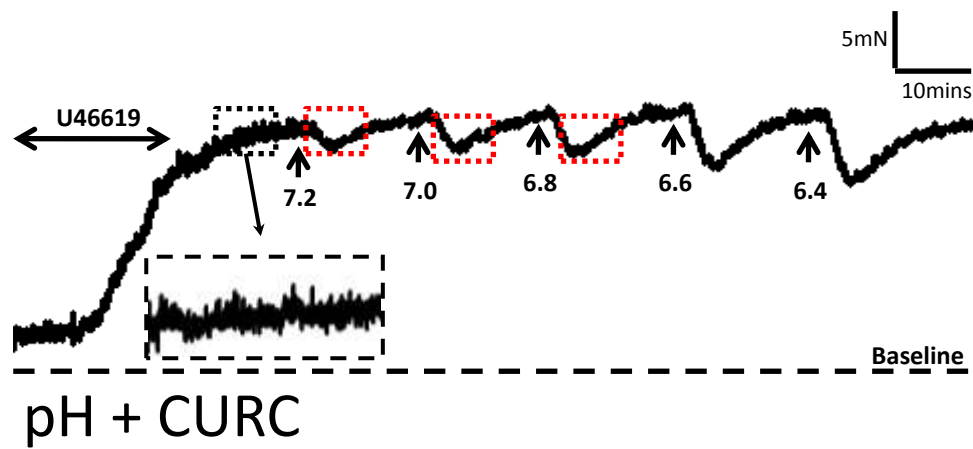


Figure 7.4.4-5 shows a representative trace of the pH response in the presence of CURC. The vessel displays an increase in spontaneous tone oscillations (boxed). The biphasic response to lactic acid stimulation was altered (red boxes) and a reduced relaxation was produced in response to lactic acid.

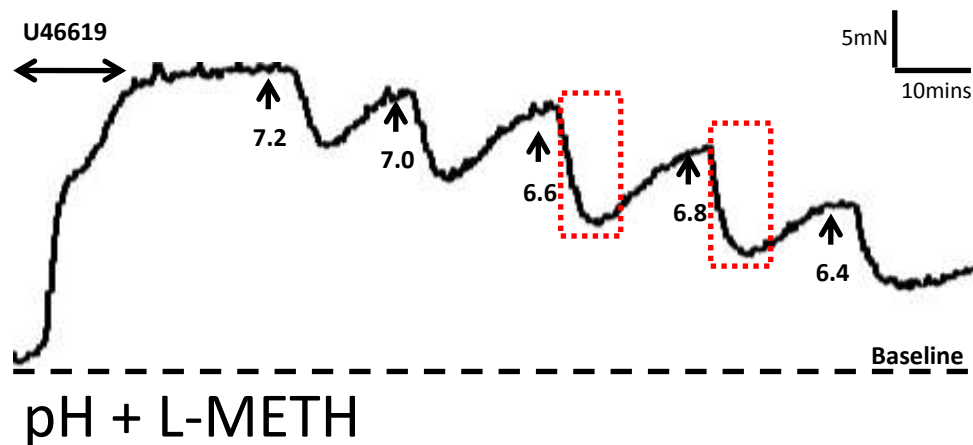


Figure 7.4.4-6 shows a representative trace of the pH response in the presence of L-METH. The main difference in the presence of L-METH was that the loss in contraction in response to acidic pH was greatly increased (red box) with each pH stimulus.

Functional investigation of ion channels in CPA

Table 7.4.4-3 summarising the EC₅₀ values for the lactic acid concentration response curves in the presence of different ion channel blockers.

Treatment (n)	EC ₅₀ (M) ± SEM	p	Maximum Relaxation (%) ± SEM
pH (18)	6.9 ± 0.1		54 ± 3
pH + CURC (6)	6.7 ± 0.1	ns	34 ± 5
pH + LIDO (8)	6.9 ± 0.2	ns	55 ± 7
pH + L-METH (6)	7.2 ± 0.1	ns	67 ± 7
pH + M.ANAN (6)	7.1 ± 0.2	ns	57 ± 6
pH + R.RED (6)	6.9 ± 0.1	ns	62 ± 4

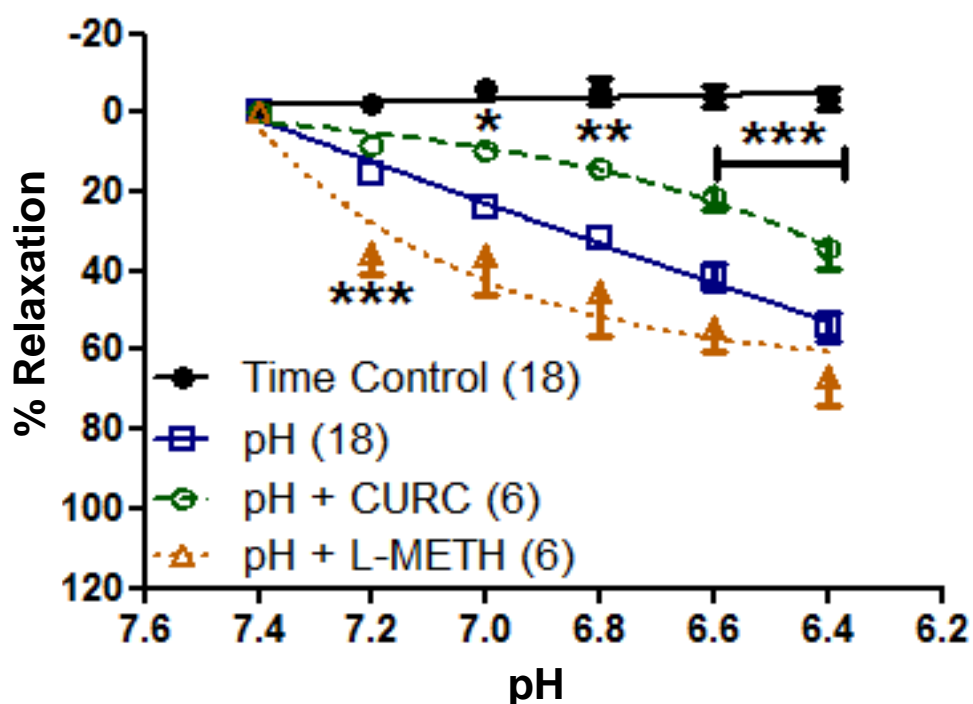


Figure 7.4.4-7 summarising the lactic acid induced relaxation when CPA (N=18) have been pre-treated with different blockers. CURC (N=6) produced a significant inhibition to the response. In contrast L-METH (n=6) evoked a downward shift as the relaxation was enhanced and achieved significance at pH 7.2. Data are presented as mean ± SEM along with vessels treated (n) from placentae (N). *p<0.05, **p<0.01, ***p<0.001.

7.4.4.1. Response to acidic pH response in the presence of ion channel blockers at 5% pO₂

Figure 7.4.4-1 summarises the dose-response curve for the acidic pH treatment with vessels perfused at 5% pO₂. Directly replacing NaCl with Choline Cl could reduce the relaxation response and this was significant at the highest concentrations used (pH 6.6-6.4). The SK_{CA} channel inhibitor APA caused a downward shift to the curve as a steep response was produced with the lowest doses of lactic acid which was most prominent at pH 7.0 (p<0.001). **Table 7.4.4.1-1** summarises the EC₅₀ values which have been obtained with lactic acid in the presence of different blockers as well as the % maximum relaxation produced.

Table 7.4.4.1-1 summarising the EC₅₀ values for the lactic acid concentration response curves in the presence of specific ion channel blockers.

Treatment (n)	EC ₅₀ (M) ± SEM	p	Maximum Relaxation (%) ± SEM
pH (14)	6.9 ± 0.1] *<0.05	37 ± 3
pH + APA (6)	7.2 ± 0.2		48 ± 1
pH + Choline Cl (8)	6.8 ± 0.2	ns	24 ± 4
pH + QUIN (4)	6.7 ± 0.1	ns	46 ± 5

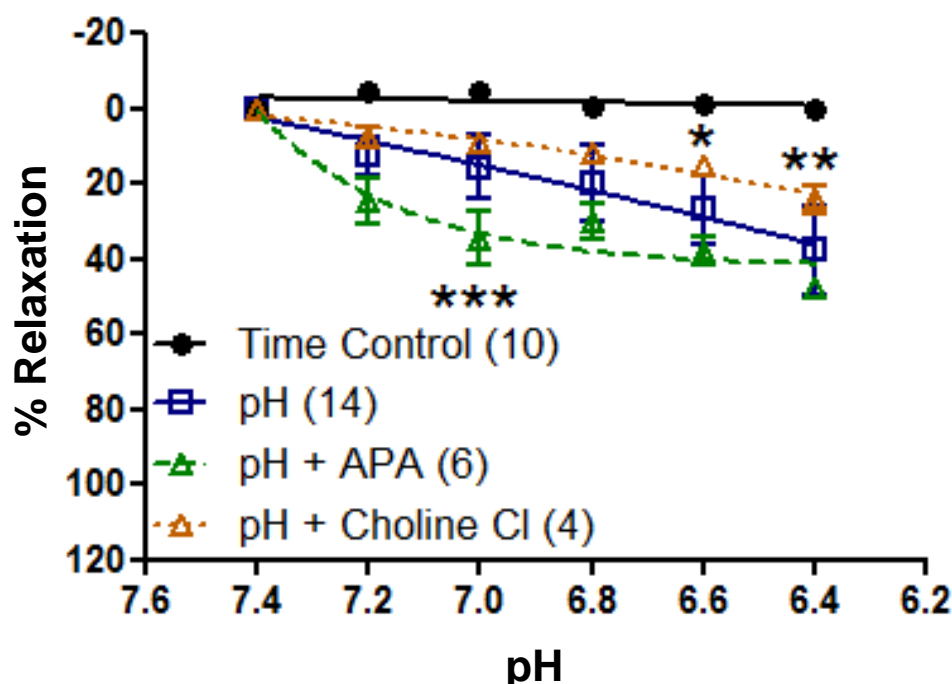


Figure 7.4.4.1-1 showing the dose-response to acidic pH with CPA (N=14) perfused in 5% pO₂. Choline Cl (N=4) could inhibit the relaxation response which was significant at the highest doses (pH 6.6-6.4). In contrast APA (N=6) caused a downward shift in the dose-response curve and achieved significance at pH 7.0. Data are presented as mean \pm SEM along with vessels treated (n) from placentae (N). *p<0.05, **p<0.01, ***p<0.001.

The response to lactic acid in the presence of CuCl₂ and ZnCl₂ with 5% pO₂ to examine the effects of TASK and TREK ion channel blockers which had demonstrated significant changes to the pH response at 20% pO₂. A strikingly similar effect on the vessel response was seen with both CuCl₂, ZnCl₂, along with the anaesthetic BUP (**Figure 7.4.4.1-2A**). L-METH also increased the magnitude to the pH response as was the case at 20% pO₂. The most interesting response was evoked by CURC which did not demonstrate a significant inhibition to the pH response. The maximal relaxation produced at 5% pO₂ ($37 \pm 3\%$) was similar to the relaxation produced in the presence of CURC at 20% pO₂ ($34 \pm 5\%$ p>0.05). **Table 7.4.4.1-2**

Functional investigation of ion channels in CPA

summarises the resulting EC_{50} values based on the best fit curve in the presence of each channel blocker.

Table 7.4.4.1-2 summarising the EC_{50} values for the lactic acid concentration response curves in the presence of specific ion channel blockers.

Treatment (n)	$EC_{50}(M) \pm SEM$	p	Maximum Relaxation (%) $\pm SEM$
pH (14)	6.9 ± 0.1		37 ± 3
pH + BUP (4)	6.9 ± 0.2	ns	69 ± 4
pH + $CuCl_2$ (3)	6.9 ± 0.1	ns	79 ± 3
pH + CURC (6)	6.7 ± 0.2	ns	34 ± 5
pH + L-METH (6)	6.9 ± 0.1	ns	61 ± 5
pH + $ZnCl_2$ (4)	7.0 ± 0.2	ns	87 ± 4

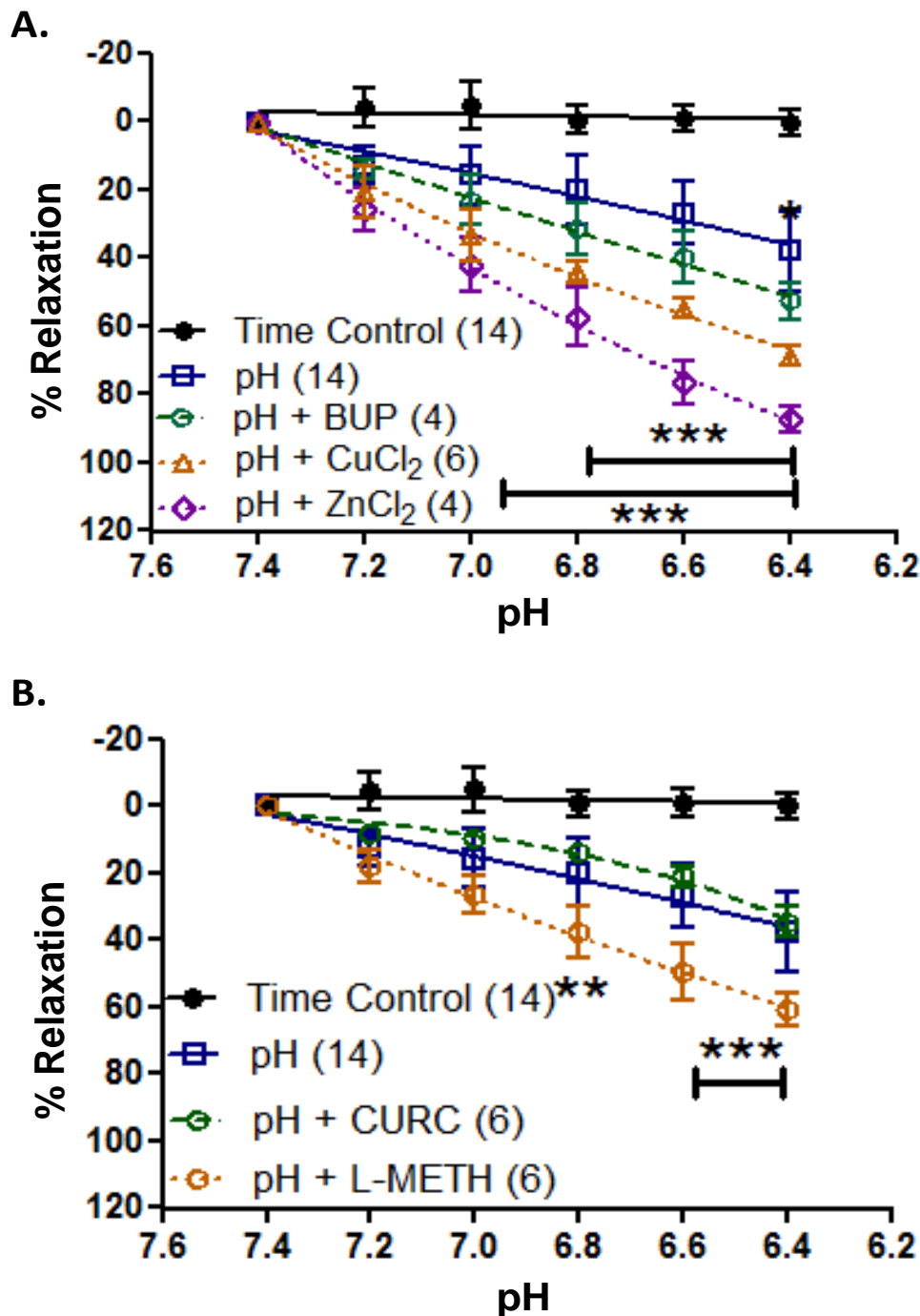


Figure 7.4.4.1-2 summarising the lactic acid induced relaxation when CPA (N=14) have been pre-treated with blockers. A shows the response to TASK channel blockers. A significant increase in the relaxation response was seen with all inhibitors (BUP: N=4, CuCl₂: N=6) and was most prominent with ZnCl₂ (N=4) which achieved significance at \geq pH 7.0. **B** shows the responses to lactic acid in the presence of the TREK-1 blockers CURC (N=6) and L-METH (N=6). Only L-METH produced a significantly greater relaxation response to acidic pH at \geq pH 6.8. Data are presented as mean \pm SEM along with vessels treated (n) from placentae (N). *p<0.05, **p<0.01, ***p<0.001.

7.5. Discussion

Ion channels play a major role in the control of vascular function and have a powerful influence over the cell membrane potential. The expression of a number of key ion channels has been described in [Chapter 6](#). The aim of the studies described in this chapter was to investigate the functional significance of candidate ion channels in the responses to modulators described in [Chapter 5](#). Initially the responses of CPA in 20% pO₂ were examined for comparison to data already presented in the literature. A limited selection of experiments were again then performed in 5% pO₂ to obtain data that would be more reflective of the responses *in vivo*.

7.5.1. Alterations to the baseline resting tension

The vessels of the placenta need to maintain a low resistance to flow and a change in the activity of CPA was seen in the presence of 4-AP. The peptide based inhibitor is similar to TEA in that it can inhibit a broad number of K_v (shaker) channels (Kaczorowski and Garcia, 1999). Application of the blocker altered the basal tone to suggest that K⁺ channels are open at rest are voltage gated ion channels and likely contribute to maintaining the basal tone of CPA. The contractile response to U46619 was elevated and may itself be the result of altered baseline activity. The most important role for K_v channels in the placental vasculature was shown by Hampl (et al., 2002). They demonstrated that the HFPV response seen could also be mimicked by application of 4-AP as K_v channel currents were also shown to inhibited

by hypoxia. They also demonstrated that the $K_v1.5$ and $K_v 2.1$ subunits were the most likely candidates for modulating the vasoconstriction in response to hypoxia and are targets for 4-AP. However for our studies it would be essential to determine the expression profile of the K_v channel expression in the placental vessels to fully understand the significance of this observation. The increase in baseline tension may have also contributed to the enhanced response to U46619 and is supported within the literature (Wareing, Bai et al., 2006).

7.5.2. Modulation of the U46619 response

K_v channels represent the largest family of K^+ channels are also a target for TEA inhibition. From the present study it was noted that 4-AP and TEA along with the SK_{Ca} blocker APA increased the contractile activity of CPA in response to U46619 which suggests these K^+ channels have a stabilising role and counteract vasoconstriction. A recent study demonstrated regional differences in the response to K_v channel openers across CPA and CPV to suggest a differential tissue distribution of the ion channels (Wareing, Bai et al., 2006, Kiernan, Barrie et al., 2010). This observation may hold the key to understanding the differences in response to changing pO_2 between CPA and SVA and needs further explorations by examining the expression of K_v channels across both vessels.

A twofold response was observed in the presence of APA with an initial inhibition to the contraction followed by an elevated contractile response as the concentration of U46619 was gradually increased. The dose-response curve suggests

a key threshold was reached to evoke a response from the CPA and provides evidence for the contribution of SK_{Ca} channel activity to vasoactivity within CPA. The role of SK_{Ca} channels has been investigated with uterine arteries and it was shown that the response to AVP was increased with APA pre-treatment (Kostrzewska, Modzelewska et al., 2008). Furthermore it was shown that the response to SNP was inhibited by APA implicating the ion channel as a target for NO mediated relaxation of blood vessels. SK_{Ca} together with IK_{Ca} channels are important for small resistance sized vessels and the blocker APA in combination with Triarylmethane-34 (TRAM-34) to block IK_{Ca} was shown to inhibit NO synthesis and promote hyperpolarisation in isolated HUVECs (Sheng and Braun, 2007). An increase in cytosolic $[Ca^{2+}]_i$ stimulated the release of NO to oppose cell hyperpolarisation which could be successfully blocked in the presence of NOS inhibitors and crucially APA together with TRAM-34. This shows how ion channel activity is needed for NO synthesis to detect the changes in $[Ca^{2+}]_i$. SK_{Ca} in EC may help to maintain vessel quiescence and promote relaxation while in SMC blocking these channels may prolong that contraction and may explain the two stage response observed to U46619 in the presence of APA. The action of ion channels can vary across the EC and SMC and this would be better investigated with electrophysiological recordings of EC and SMC cultures in isolation to help dissect out the dual action of APA inhibition, as well as performing wire myography experiments with EC stripped vessels.

In addition to the responses seen with K⁺ channel modulators, it was shown that replacing NaCl with Choline Cl increased the response to U46619 and OUAB pre-incubation also increased the vessel contraction in response to U46619 which has

parallels to the increased contractile response seen in the presence of Choline Cl. This implicates voltage gated Na^+ (Na_v) channels as being involved with controlling basal tone of CPA which may have a role in the removal of the excess H^+ load to rapidly recover vessel function (discussed in [Chapter 7.5.6](#)).

The inhibition in the response of CPA to U46619 was most obvious with NIFED which suggests the contraction to the agonist is dependent on Ca^{2+} movements, specifically extracellular Ca^{2+} (Striessnig, 1999). NIFED is an L-type Ca^{2+} channel antagonist and is widely used in an obstetric setting to treat pregnancy related hypertension as well as pre-term labour due to its potent anti-contractile properties. The drug is safe to use and has been shown not to alter blood flow to the placenta or uterine arteries (Allen, Andersson et al., 1991). However, paradoxically, our data suggests that the ion channel antagonist has a profound effect on CPA function and requires further investigations. The effect of the NIFED on placental vessels was also investigated using isolated vessels pre-contracted with 5-HT (Marin, Reviriego et al., 1990). This study showed that NIFED was effective in blocking the 5-HT induced contractions while no effect was reported on the response to 40mM KPSS. It was also shown that removing extracellular Ca^{2+} from the bathing saline could mimic NIFED evoked responses and reduce the 5-HT induced contractions. This suggests that NIFED can exert a response by disrupting the movement of Ca^{2+} across the cell membrane while KPSS maybe dependent on VGCC (Marin, Reviriego et al., 1990, Cooper, Wareing et al., 2006). This also shows that gating mechanisms that control Ca^{2+} influxes operate differently in response to different vasoconstrictors and highlights the importance of using endogenous contractile agents to observe a

response that closely represents the physiological condition. Tanko (et al., 2000) demonstrated that the effect of NIFED action was dependent upon the contractile agent used. It was shown that NIFED could induce a dose dependant relaxation in porcine coronary arteries pre-contracted with prostaglandin F2 α (PGF2 α) (Tanko, Simonsen et al., 2000). It was also shown that that isobaric preparations of vessels were more sensitive to the addition of extracellular Ca²⁺ when compared with wire myography based vessel preparations. This illustrates how the experimental method used to study vessel in isolation can influence the response of isolated vessels, and the amount of pressure and stretch applied may potentially alter the activation of voltage sensitive Ca²⁺ channels.

The functional role for K_{ATP} channels was investigated using the non-specific inhibitor GLB which reduced the contraction to U46619 while the basal tone was unaffected. K_{ATP} is an ion channel of interest for treating pregnancy related complications as its activity is dependent upon the cells' metabolic status and tissue oxygenation can modulate the function of K_{ATP} (Chen and Simard, 2001, Seino and Miki, 2003, Dong, Vegiraju et al., 2004). K_{ATP} ion channel openers such as pinacidil produce potent relaxations and may have a future role in IUGR/PE treatment (Wareing, Greenwood et al., 2006b, Jewsbury, Baker et al., 2007). In support of this it has been demonstrated that the CGRP produced relaxation is K_{ATP} dependent (Dong, Vegiraju et al., 2004). It was surprising that application of GLB opposed the response to U46619 and we can consider our observation in light of a related study. Wareing (et al., 2006) showed that the response pinacidil was not oxygen dependent as a pO₂ of 2% did not alter the relaxation response of CPA. The lower pO₂ setting would be

expected to decrease ATP levels to open the ion channels and enhance the response to pinacidil but this was not seen. K_{ATP} is a key O_2 sensing ion channel and ATP levels are closely linked to the oxidative state of the cell. High metabolism will increase the oxidative stress which has been shown to reduce K_{ATP} activity (Duprat, Guillemare et al., 1995, Seino and Miki, 2003, Tammaro and Ashcroft, 2009). We showed that in 20% pO_2 , the contraction to U46619 was reduced which was surprising as blocking the ion channel should allow Ca^{2+} to increase inside the cell and reflects multiple effects of ion channels on controlling placental vascular function. K_{ATP} channels are important sensors of tissue ischaemia and the importance of this has been demonstrated in the brain. The cerebral tissue, like the placenta maintains a low pO_2 to limit ROS production. The main tissue damage linked with ischaemia is the resulting oedema due to cell swelling and understanding the molecular mechanisms that curtail to the development of tissue oedema have been crucial for reducing tissue damage in the brain (Chen and Simard, 2001, Sato, Costa et al., 2006). A recent study (Zhou, Fathali et al., 2009) compared neonatal rats treated with both severe and acute episodes of I/R with and without pre-treatment with GLB. It was shown that GLB could promote ischaemic protection treated but only with mild conditions of hypoxia. In severe I/R GLB was instead causing hypoglycaemia as blood glucose levels fell rapidly and this observation helps to understand why the CPA with GLB pre-incubation gave a reduced response to U46619 stimulation (Chen and Simard, 2001, Zhou, Fathali et al., 2009).

It was also shown that inhibition of TASK (BUP) and TWIK (QUIN) did not alter the resting tension of CPA but gave a significant attenuation to the U46619

response. A related study showed that application of BUP with rat pulmonary arteries could increase the baseline tension (Shah, 2008) and may reflect tissue specific differences with the action of the anaesthetic. The TWIK channel has highest expression in the placenta when compared to other related K2P members (Lesage, Guillemare et al., 1996). Modulation of the ion channel is complex and each blocker can exert different effects depending upon the tissue and cell type that is targeted (Goldstein, Bayliss et al., 2005). The blockers BaCl₂ and QUIN were used and only QUIN reduced contraction to U46619 which can act on TWIK channel currents. The inhibition seen with both BUP and QUIN suggest a similar mechanism is involved in targeting the TASK and TWIK channels and implicates a role for K2P channels in determining the contractile function of placental CPA. A potential role for TWIK-2 function was investigated in a recent publication examining the response of mouse taste buds. These cells, like the placenta have a high density of TWIK-2 channels implicating them in the activation of the cell in response to acidic pH. However this study failed to show a role for QUIN in mediating the action of TWIK-2 and suggested the ion channels have a stabilising role in controlling the cell membrane potential (Richter, Dvoryanchikov et al., 2004). Inhibiting the ion channel currents would result in an increase in the depolarisation of the cells to increase the response to U46619 but we found the opposite which suggests that Ca²⁺ entry into the cell is instead opposed when TWIK channel is blocked. We could investigate this with alternative TWIK blockers such as quinine or halothane (Goldstein, Bayliss et al., 2005) to determine a more definitive role for TWIK in the placenta.

7.5.3. Modulation of the response to NS1619

The BK_{Ca} channel can be activated by a rise in $[Ca^{2+}]_i$, or membrane depolarisation and responds by promoting a K⁺ efflux to hyperpolarise the membrane. In blood vessels this results in a reduced contractility and BK_{Ca} channels have been shown to have a central role in controlling vessel myogenic control (Meera, Wallner et al., 1997). TEA can inhibit the ion channel but a more potent and selective antagonist is the scorpion toxin, IBTX (Kaczorowski and Garcia, 1999). Although we failed to demonstrate a role for BK_{Ca} in the U46619 response with IBTX, the channel opener NS1619 demonstrated a potent relaxation. Our previous data has shown expression of the BK_{Ca} channel using Western blot analysis (Chapter 6) and NS1619 demonstrated a significant relaxation response in CPA (92%) compared to that seen with SNP (50%). In further support of this, the response to NS1619 was inhibited in the presence of TEA and more significantly with IBTX to suggest that the relaxation response is mediated by BK_{Ca} currents.

The BK_{Ca} is largely activated by an influx of Ca^{2+} into the cell or changes in the membrane potential. However the ion channel activation can be optimised by second messenger signalling pathways and NO can also activate BK_{Ca} particularly in EC as part of a positive feedback mechanism to drive the synthesis and release of key vasodilators. (Khan, Smith et al., 1993, Meera, Wallner et al., 1997, Barlow, El-Mowafy et al., 2000, Hampl, Bibova et al., 2002). CGRP can open the channel along with NO to initiate vessel dilatation (Saqueton, Miller et al., 1999). BK_{Ca} is widely expressed in a range of tissues and is an important therapeutic target for the treatment

of cardiovascular diseases such as stroke and hypertension. Moreover mitochondrial BK_{Ca} has also been implicated in providing cardioprotection (Liu, Hudetz et al., 1998, Sato, Saito et al., 2005, Liu, Sun et al., 2010). Ion channels, particularly K^+ channel openers and inhibitors are important targets for diseases where the altered vessel function is the main contributing factor. Our finding that the BK_{Ca} channel opener NS1619 can induce a significant relaxation response in CPA suggests that BK_{Ca} could be a future drug target in the treatment of placental insufficiency and is an important avenue for future studies.

7.5.4. Modulation of the response to RIL

The response to RIL was investigated in the presence of a number of K2P channel inhibitors which have produced varied results. Similar to NS1619, we wanted to identify a suitable K2P channel opener to validate the potency of each ion channel blocker used. Our initial attempts with the TREK-1 agonist AA, which is found in abundance within the placental circulation, along with LA failed to produce a significant relaxation response. This could be attributed to the poor uptake of the lipid based agonists which may not have crossed the cell membrane to evoke a cellular response (Krischer, Eisenmann et al., 1998). We could explore alternative transport mechanisms that may improve the uptake of the lipids into cell.

RIL has also been reported to open K2P channels with a high affinity for TRAAK and TREK-1 and we were able to show for the first time that the drug can induce a potent relaxation of both CPA and SVA ([Chapter 6](#)). The mechanism of RIL

action was investigated by Duprat (et al., 2000) who demonstrated with COS transfected with human TREK-1 and TRAAK, that RIL could stimulate whole cell currents. They crucially showed that the agonist had a transient effect on TREK-1 activity as high doses (100 μ M) of RIL could open the channel which was followed by an inhibition of the TREK-1 currents (Fink, Lesage et al., 1998, Duprat, Lesage et al., 2000). It is also worth noting that this study used 3-100 μ M of RIL to observe TREK-1 and TRAAK currents. In our study 1nM-1 μ M application of RIL produced a relaxation response of $\leq 70\%$ which suggests an additional mechanism may be responsible for the vasodilatation produced. We also examined the response to RIL in the presence of L-NAME which did not alter the relaxation response with CPA suggesting the response is endothelium-independent but requires further validation with alternatives NO inhibitors or eNOS knockout animal models. In contrast, the only inhibition to RIL induced relaxation was seen in the presence of the broad acting K⁺ channel blocker, TEA.

The blocker 4-AP inhibited the relaxation response but only with the highest doses of RIL application. In a similar light, there is also evidence to show that along with altering glutamate release, RIL has a non-specific action on ion channels. The most recent evidence has shown RIL can alter the channel conductance of O₂ sensitive voltage gated K_v channels (Xu, Enyeart et al., 2001, Xing, Zhang et al., 2003). K_v are important O₂ sensors for the cells and their role in the placenta was investigated with placental CPV and CPA (Kiernan, Barrie et al., 2010). This study demonstrated a role for K_v channels using K_v channels openers and showed the most significant response was seen in response to openers of the K_v1.2 subunit. Crucially

we did not observe the same effect with both TEA and 4-AP at 5% pO₂ which suggests the level of tissue oxygenation may be more important for modulating the action of RIL which may target K_v channels (Howard, Hosokawa et al., 1984, Byrne, Howard et al., 1997, Cole, Plane et al., 2005, Plane, Johnson et al., 2005). The inhibition in the presence of 4-AP was only observed at the highest dose of RIL (1µM) and suggests that other candidate K⁺ channels may also be a target for RIL. Alternatively, RIL can bind to imidazoline receptors and such receptors have been shown to increase in the placenta with gestational age (Bagamery, Kovacs et al., 1999). This receptor may be an alternative target for RIL and may help to explain the immediate response that is seen with both CPA and SVA and should be explored further.

7.5.5. Modulation of the response to H₂O₂

H₂O₂ has shown to produce both contractile and relaxation responses in various tissues and the biphasic action appears to involve separate mechanisms (Liu, Sun et al., 2010).

7.5.5.1. Modulation of the H₂O₂ mediated contraction

A small contraction was produced upon H₂O₂ application however the response by CPA was much smaller than the response seen with U46619 suggesting that all the SMC were not activated. The effects of H₂O₂ were abolished by CAT to

suggest the contractile activity produced is a direct response to H_2O_2 . Our data showing that IBTX could enhance the response to H_2O_2 has also been reported within the literature (Liu, Sun et al., 2010). ROS can alter the movement of Ca^{2+} from internal stores to increase $[\text{Ca}^{2+}]_i$ (Burton, 2008, Steinert, Wyatt et al., 2009). Ca^{2+} is important for controlling vessel tone and the finding that IBTX can increase the response suggests H_2O_2 can alter Ca^{2+} movements to evoke a response. However we could not investigate the significance of this as the response was too unstable to allow for a firm conclusion to be made.

7.5.5.2. Modulation of the H_2O_2 mediated relaxation

It was also shown that H_2O_2 could induce a relaxation response in pre-constricted placental vessels. The mechanism of this action was investigated and the response to H_2O_2 was also inhibited by CAT pre-incubation but crucially this did not produce 100% inhibition to suggest that H_2O_2 may also be having an indirect effect on placental vessels to induce a relaxation response and requires further investigation. K^+ channels represent a diverse ion channel family that have a high selectivity for the permeation of K^+ ions. The non-specific K^+ channel blocker TEA can inhibit a wide spectrum of K^+ channels (Kaczorowski and Garcia, 1999) and we demonstrated that the H_2O_2 induced vasodilatation was significantly inhibited in the presence of the ion channel blocker. An earlier study used patch clamping to observe changes in BK_{Ca} activity (see Barlow and White, 1998) where porcine coronary artery SMC were treated with increasing doses of H_2O_2 and recordings showed an increase in BK_{Ca}

opening. This study was followed up by a more recent publication by the same group who investigated how this change in ion channel activity was produced (Barlow, El-Mowafy et al., 2000). They showed that H_2O_2 could not directly act on the ion channel and instead the effect was dependent on phospholipase A(2) activity as specific inhibitors of this molecule could abolish the activity seen with BK_{Ca} . More interestingly the addition of AA could reproduce the changes in BK_{Ca} that were seen when H_2O_2 was added to suggest a similar mechanism is triggered. This study suggested H_2O_2 was producing an effect via opening of BK_{Ca} channels however we were only able to show a significant inhibition to the response in the presence of TEA and not IBTX (Barlow and White, 1998, Yang, Zheng et al., 1998).

The relaxation response to H_2O_2 was significantly increased in the presence of L-NAME. Although this was shown in a small sample group, the result was surprising and appears to show that blocking NO will leave the placental vessels more vulnerable to the toxic effects of ROS to bring about a significant disruption to the control of vessel tone (Gardiner, Compton et al., 1991, Garland, Plane et al., 1995, Byrne, Howard et al., 1997). This also suggests that non-NO mediated relaxation pathways could be compensating for the loss of NO production. The observation that NO inhibition increases the relaxation response could have detrimental effects for the widespread control of vessel tone within the placenta and warrants further investigations. This also helps to understand why we found that PE-CPA also showed an increased sensitivity to H_2O_2 application (see [Chapter 5](#)). The response was investigated at 20% pO_2 which would already lead to the production of ROS and further challenges with a ROS could be overwhelming the limited supply of

antioxidants available (Steinert, Wyatt et al., 2009) and it would be interesting to investigate the response at lower pO₂ settings.

7.5.6. Modulation of the response to acidic pH

The main findings from studies reported in this thesis is that placental vessels can respond to acidic pH but only when the vessels had been pre-contracted with U46619. The most likely candidates implicated in this response are the acid sensing family of ion channels (ASIC). This was then investigated with modulators of Na⁺ transport. H⁺ ions are removed from the cell via ATP dependent Na⁺ transporters (Canzanelli, Greenblatt et al., 1939, Bishop and Weisfeldt, 1976, Aalkjaer, 1990). However OUAB (a Na⁺/K⁺ ATPase inhibitor) and the NHE inhibitor OMP along with the Na⁺ channel blocker AMIL failed to demonstrate a significant role for mediating the response to an acidic pH stimulus. AMIL is a diuretic that can block a number of Na⁺ channels with little subtype selectivity and the alternatives benzamil which is a lipophilic analogue of AMIL or the toxin psalmotoxin-1 (PcTx-1) should also be explored (Gitterman, Wilson et al., 2005). Instead, a reduction in the acidic pH response when NaCl was replaced with Choline Cl was seen. Removing extracellular Na⁺ by replacing it with Choline Cl should reduce the action of NHE. We found the response was indeed significantly attenuated which suggests Na⁺ ions are potentially involved in the recovery from acidic pH insults and could involve the exchange of HCO₃⁻ ion and requires further investigations.

The NO inhibitor L-NAME reduced the response to acidic pH application. One explanation for this observation may be due to the fact that NO may promote the loss in vessel tone in response to lactic acid application and inhibiting this pathway resulted in reduced relaxation response which may have implications for understanding the placental control of blood flow (Byrne, Howard et al., 1997, Aaronson, Sarwar et al., 2006, Holzer, 2009). The pH response at 20% pO₂ was significantly inhibited and this was seen as a reduction in the recovery response (phase II) following a pH insult. This suggests that NO may have a role in recovery of vessel function (Myatt, Brewer et al., 1992, Jovanovic, Grbovic et al., 1994a, Kostrzevska, Modzelewska et al., 2008). L-NAME inhibits endothelial production of NO, yet the response to acidic pH was not completely abolished, which suggests that NO can still be produced from cell layers other than the EC such as SMC within the placental vessels. It also suggests that non NO mediated vasodilators such as EDHF and/or PGI₂ could have a role to play (Jovanovic, Grbovic et al., 1994b, Byrne, Howard et al., 1997, Kublickiene, Kublickas et al., 1997).

Pre-treatment with NIFED enhanced the response pH in 20% pO₂. One explanation for this may be linked to the reduced contraction response to U46619 produced in the presence of NIFED to limit the activation of the SMC. This makes it difficult to interpret the responses as the relaxation capacity is severely reduced. The use of an alternative contractile agent such as PGF₂ α should be investigated as it has been shown that vessels pre-treated with NIFED can still respond to the agonist (Allen, Andersson et al., 1991). CPA could still produce a transient response upon stimulation with lactic acid in the presence of NIFED to suggest that NIFED

insensitive Ca^{2+} channels may still have an influence on placental arteries and Ca^{2+} channels maybe a target for metabolic stress.

The lack of response to acidic pH in the presence of GLB was unexpected as K_{ATP} channels are important metabolic sensors. This can be explained by a recent communication that demonstrated that GLB was ineffective under acidic conditions (Lu, Gao et al., 2007). Sodium cyanide (NaCN) was used to induce metabolic stress in adult male guinea pig ventricular cells and the $[\text{pH}]_i$ was reported to rapidly declined. The authors showed that GLB could not alter the currents induced by NaCN. However activating NO production with L-arginine could enhance the currents seen in the presence of NaCN to implicate a role for NO in this response.

A role for SK_{Ca} channels was demonstrated as the inhibitor APA enhanced the relaxation response with acidic pH at 5% pO_2 . At low pO_2 K^+ channels would be expected to be closed favouring an increase in vessel tone opposing relaxation. The SK_{Ca} and IK_{Ca} channels have been implicated to have a role in EDHF which is a compensatory mechanism that can replace NO function to help vessels recover tone. The ion channels are central to perceiving the stimulus such as shear stress to alter the EC membrane potential. The change in membrane potential will alter Ca^{2+} homeostasis and release Ca^{2+} from intracellular stores. The increase in Ca^{2+} is necessary for the release of diffusible vasodilator substances from the EC which evoke effects on the SMC to bring about relaxation. The spike in Ca^{2+} is essential for the release of NO and/or EDHF and therefore the inhibition of K^+ channels is needed to maintain the $[\text{Ca}^{2+}]_i$. (Lopez-Barneo, Pardal et al., 1999, Cipolla, Smith et al., 2009)

The TREK-1 inhibitor CURC produced a significant inhibition to the response with an increase in tone oscillations. CURC is an anti-proliferative agent that can block actions of TREK-1 and also has important anti-oxidant properties. The inhibition by CURC was not seen at 5% pO₂ and instead matched the response for CPA that were untreated. This suggests that CURC can provide antioxidant protection and may be a potential treatment for protecting placental vessels from oxidative stress. CURC increased tone oscillations to suggest vessel activity is being altered with loss of TREK-1 channel activity, so that hyperpolarisation and excitability are altered. L-METH is an amino acid based molecule that has been shown to inhibit TREK-1 currents (Baker, Hennig et al., 2008). Application of the inhibitor of TREK produced an increase in the relaxation response both in 20% and 5% pO₂. TREK-1 is inhibited by [pH]_i and the enhanced response to acidic pH in the presence of L-METH suggests the cell has lost the ability to detect the fall in pH to allow the loss in tone (phase I) to go unchecked (Buckler and Honore, 2005, Baker, Hennig et al., 2008, Beckett, Han et al., 2008). In this instance L-METH was shown to block the response by bladder SMC to stretch. D-Methionine, which is the inactive form of the molecule, could not produce the effects seen and suggests the stretch sensitive TREK-1 is modulated by L-METH. In a similar way, TREK-1 may also function to detect stretch in the vessel and trigger a relaxation response. However low pH conditions can also alter the ion channel conformation which makes investigating the role of inhibitors difficult to interpret. L-METH may be facilitating this action, or altering the ion channels sensitivity to pH and requires more evidence to support this prediction.

The response seen with acidic pH implicates a role for TASK channels which are inhibited by low $[pH]_o$. Inhibition would prevent a K^+ efflux and result in cell depolarisation and under acidic conditions to lead to constriction in vascular tissue. The depolarisation would also allow Ca^{2+} to enter (possibly via $Ca_v1.2$) the cell unopposed. However we observed that the relaxation response was produced by both CPA and SVA with low pH environments.

We further observed that pre-treatment with both $CuCl_2$ and $ZnCl_2$ could not inhibit the relaxation response triggered by low pH as the vessel could still relax but crucially we demonstrated that the increase in vessel tone (Phase II) seen immediately after the pH stimulus was blunted by both $CuCl_2$ and to a greater extent with $ZnCl_2$. This was seen at both 20% and the physiologically significant pO_2 of 5%. The effectiveness of TASK channel inhibitors was demonstrated with adult rat pulmonary artery preparations. Shah (2008) examined the response of rat pulmonary arteries in response to the main TASK inhibitors BUP and $ZnCl_2$. It was demonstrated that the baseline tension of the ring preparations increased upon inhibition of TASK channels by BUP and M.ANAN while application of 100 μ M of $ZnCl_2$ did not alter vessel tension. Furthermore this increase in tension was most likely via Ca^{2+} entry as pre-treatment with NIFED could abolish this small contraction. Electrophysiological recordings of such channels has shown that application of 100-200 μ M of $ZnCl_2$ can reduce TASK currents by 50% (Gruss, Mathie et al., 2004). We used this concentration as a starting point and also found no change in the baseline response of CPA and opted to use the higher dose of 1mM in order to inhibit a significant number of TASK channels so to observe any effect on isolated arteries. Consistent with our

findings, Shah (2008) also showed the vessels constricted in response to alkaline pH conditions and relaxed in response to acidic pH. This finding suggests that acidic pH may in turn open TASK channels or alternatively activate another pH sensitive ion channel to cause the hyperpolarisation seen (Gurney, Osipenko et al., 2003, Gardener, Johnson et al., 2004). However in the study by Shah (2008), the vessels could no longer respond to both BUP and M.ANAN which does suggest that low pH does inhibit TASK channels to prevent a further K^+ efflux. M.ANAN has multiple actions and can also inhibit the endocannabinoid receptors CB1 and CB2, thus the significance of this observation is also limited. The observation that low pH can induce a loss in vessel tone and secondly oppose the contraction in response to BUP appears to show that low pH could be altering the gating properties of TASK channel currents.

The response to $ZnCl_2$ can also be considered by the effects the trace element has on Ca^{2+} channel currents. $ZnCl_2$ can inhibit the entry of Ca^{2+} into the cell (Busselberg, Michael et al., 1992) and may explain why we observed a blunting of the contraction that proceeds the initial relaxation. $CuCl_2$ and $ZnCl_2$ enhanced the response to pH at both 20% and 5% pO_2 while $NaCl_2$ did not alter the response so we can be confident that the response observed was due to actions of Zn^{2+} and Cu^{2+} ions. Zn^{2+} is present in low concentration within the ECM at $15\mu M$ and most is bound with proteins. In diseased states this can rise to $600\mu M$. Ischaemia is an important modulator of Zn^{2+} levels and an increase in free unbound Zn^{2+} can alter neuronal excitability (Mathie, Sutton et al., 2006). Zn^{2+} can inhibit Ca^{2+} and Na^+ channel currents along with TASK-1 to alter neurotransmitter release. The potency for TASK-

1 makes Zn^{2+} a useful pharmacological tool for distinguishing TASK-1 from TASK-3 currents (Goldstein, Bayliss et al., 2005). Cu^{2+} binds K2P channels with a high affinity and can bind to cysteine, histidine, or glutamate residues which can lead to dissociation between disulphide bridges which in the K2P example hold the pore forming domains in place. It can also cause indirect effects by altering the cells redox state and generate free radicals. Gruss (et al., 2004) examined the role of both trace elements in modulating HEK-293 cells stably transfected with human TREK-1 and TASK-3. It was shown that Cu^{2+} activated TREK-1 while an inhibition was seen with TASK-3. In addition Zn^{2+} can inhibit TASK-3 at a lower doses when compared to the inhibition seen with TREK-1. This provides a method for differentially blocking specific K2P channels and more importantly we used 1mM to observe an effect that may have been inhibiting both TREK and TASK channel currents.

7.5.7. Future research

This study can be extended by examining the response of SVA in the presence of each ion channel blocker to observe any potential variations that may exist. However to do this we need to address some issues with the methodology used in this study. The improvements to the wire myography method used have been highlighted in [Chapter 5.8.7](#). However we can also identify key avenues for future research related to this chapter. The main limitation with our study is that the dose range for both pH and H_2O_2 go beyond physiological concentrations that would be found *in vivo*. Although this has the advantage of demonstrating the responses to chronic stress

the concentration used may be too severe and may have masked the true role of each ion channel in mediating this response.

The work presented in this thesis was greatly hampered by the lack of specific ion channel antagonists particularly for the K2P channels. The trace elements used such as Zn^+ and Cu^+ have high affinities for TASK and TREK channel currents along with a range of voltage dependent ion channels (Gruss, Mathie et al., 2004, Mathie, Sutton et al., 2006). As a result we may have been observing the effects of blocking more than one ion channel. This can give unpredictable results and we may instead be observing some indirect effects of the blockers used. An alternative method could be the use of antibodies that can bind to the pore forming region of each ion channel. This approach has been demonstrated with the anti Kv1.5 antibody which binds to the C terminal domain (amino acid 542-602) close to the pore forming region of the ion channel. Another alternative is to use small interfering RNA (siRNA) knockdowns or antisense oligodeoxynucleotides in cultured EC and SMC preparations, which have successfully been used to inhibit significant levels of TASK currents (Hartness, Lewis et al., 2001). There is also a need to investigate the role of combining ion channel inhibitors to investigate any cross talk. This is particularly important for TASK and TREK channels which have been shown to co-localise in SMC (Xian Tao, Dyachenko et al., 2006) and inhibition of one ion channel may be compensated by the second accessory ion channel. This would also allow us to use lower concentrations of different inhibitors and observe responses that may be more physiologically relevant.

A wide range of ion channel inhibitors were applied often at high doses in order to block sufficient ion channel proteins, and observe an effect in CPA. An alternative could be to partially depolarise the cell membrane with a small dose of KPSS (10mM) to alter the electrochemical gradient of the cell and alter K^+ movements. This would allow us to apply lower doses of the drug although this may introduce unwanted secondary effects on the vessel responses as the K^+ balance of the cells at rest has been altered but is worth exploring. Some interesting responses were observed in the presence of L-NAME, which is an inhibitor of NO release. However we could not demonstrate a significant inhibition to the vasodilatation with ACh ([Chapter 5.5.2.1](#)) which suggests that L-NAME may be exerting other indirect effects on the vessels. As an alternative, methylene blue (MB), which inhibits guanylate cyclase to prevent the formation of NO, should be investigated, along with endothelium-denuded vessel preparations. MB has shown to be better at giving long term inhibition of endothelium-dependent relaxation responses and could be a better alternative to L-NAME (Griffith and Kilbourn, 1996). Another alternative is L-NNA or the cyclooxygenase (COX) inhibitor indomethacin which blocks PGI_2 mediated responses which could be used in combination with NO blockers. Finally, we should also investigate the response of stripped placental vessels, where the EC is mechanically removed, to better dissect the roles of EC and SMC in isolation. An eNOS gene knockout animal models could be utilised to reveal invaluable information as to the role the EC plays in the physiological responses observed in this study. We also found evidence to suggest NO may act on the SMC directly to trigger a response and this could be further investigated with the NO activator-L-arginine

(Gardiner, Compton et al., 1991, King, Gude et al., 1995, Sabry, Mondon et al., 1995b).

7.5.8. Conclusion

Ion channel modulators (both openers and inhibitors) are useful diagnostic tools for determining the role and function each ion channel plays in controlling vessel function. We have provided evidence for the involvement of K2P channels in the response to stress in placental vessels which supports our hypothesis. Response to acidic pH will activate a number of proton sensing ion channels and we have detected the presence of a number of K2P channel members in the placental blood vessels which may have a role in generating a response across the pH range. A difference in the ability of separate blockers to alter the different stages of the response helped to dissect out the two phase response and our findings implicate a role for other potential pH sensing ion channels. The study hypothesis is partly supported and evidence is provided to suggest that compensatory mechanisms may exist in the placental vasculature to facilitate the response to acidic pH stress and such candidate ion channels will be discussed in **Chapter 8**. The development of better pharmacological tools to allow the study of ion channel inhibition would help us to understand the true significance of our findings.

8. Discussion

The placenta forms the main barrier between the maternal and fetal circulations where it serves to ensure the fetal nutrient and O₂ supply. When the normal function of the placenta is perturbed, placental insufficiency may result and is an underlying factor for many pregnancy related disorders. The absence of an effective therapy to improve reduced placental blood flow is due to the poor understanding of the underlying mechanisms that regulate placental vascular function. The vasoactive responses of resistance arteries from the fetal and maternal interface of the placenta were investigated by this study. The work from this thesis has identified the presence of a number of important ion channels, and using wire myography, have determined the potential role of these ion channels in mediating the response to stress encountered *in vivo*, particularly pH.

The arteries used in this study represent the main sites of resistance within the placental tissue. Previous studies have shown that these vessels do not readily respond to a number of agonists (McCarthy, Woolfson et al., 1994, Poston, McCarthy et al., 1995) which presents a unique challenge in the study of the placental circulation which is devoid of neuronal connection. Knowledge of the physiological responses from normal healthy samples is an essential prerequisite for understanding PE and fetal growth restriction which are linked with impaired vascular perfusion. The key observations, that firstly the BK_{Ca} opener NS1619 and secondly the TREK-1 modulator RIL could both produce a potent relaxation response that was greater than SNP induced relaxation may have far reaching implications. This implicates a role for

K⁺ channels in particular, in regulating the vascular function of the placenta. This study also provided the first evidence to show that RIL can relax both CPA and SVA which produced the highest level of relaxation when compared with other vasodilators. This important finding implicates a role for RIL in treating hypertensive related conditions in pregnancy that can alter the vasodilatation of the placenta. In further support of this we were also able to demonstrate that PE CPA could also respond to RIL stimulation with a similar efficacy. RIL could be an important future pharmacological target for treating increased contractile activity of placental vessels associated with conditions such as PE and IUGR. Further work is needed to better understand the precise mechanism of RIL action.

The key findings presented in this thesis include:

- The examination of key structural differences in the vessel cross sectional areas between the SVA and CPA, which represent the maternal and fetal portions of the placenta.
- The demonstration that the pO₂ of the perfusate was the most influential factor governing the contraction and relaxation responses of CPA and SVA.
- The matched expression profiles of key O₂ sensing and pH sensitive ion channels across CPA and SVA as demonstrated by confocal IF and Western blotting analysis.
- Pharmacological investigations with CPA revealed a potential role for key proton sensing ion channels in mediating the response to stress which requires further exploration.

- Analysis of responses from PE samples highlighted some significant differences in ion channel expression, specifically TWIK-2, and response to H₂O₂ and acidic pH stress, and provides a basis for future work.

8.1.Comparing placental vessels

The main limitation in detecting adverse placental effects is that the fetomaternal circulation within the placenta cannot be assessed *in situ*. The study of isolated placental tissue has advanced our understanding of the placental autonomic control of blood flow. Blood vessels obtained at term were compared, namely the CPA and the SVA. The main technique used in this study was wire myography which allowed for a detailed characterisation of the vessel properties ranging from the ideal resting diameter to optimal contractile agent. The structural arrangement of the vessels revealed that the placental vasculature is highly differentiated and the differences that we observed with the contractile ability of CPA and SVA may be reflective of the temporal and spatial differences that exist in the flow of blood throughout the placenta. The most influential factor was shown to be the pO₂ that was used to perfuse the isolated vessel segments. The results presented in this study reveal more about the normal working of the placenta in response to relative hyperoxia (20%), normoxia (5%) and hypoxia (2%). The main difference was seen with the contractile responses. SVA generated a lower constriction than the CPA in 20% pO₂, but this contractile ability could be increased when the pO₂ was lowered. One explanation for this reduced contractility may be that the lower population of SMC

within the thin walled SVA however the responses could almost match the CPA at low pO_2 which suggests that alternative contractile agents should also be investigated. We also observed how a small change in the SNP concentration produced a very steep relaxation response. This latter observation is physiologically relevant, and suggests a key threshold was reached to activate all the relaxation capacity of the vessels. Each vessel also showed the ability to respond to changes in the extracellular environment and it was shown that the ROS, H_2O_2 , could induce a permanent inhibition of the contractile activity of the blood vessels. We have provided further evidence to support the view that placental vessels should be studied at physiological pO_2 , stretch and flow conditions to better reflect the responses that would occur *in vivo*.

The CPA are a continuum of the SVA and we found that the expression profile of key K^+ channels showed comparable expression across the two vascular beds. This further helps to understand how both the CPA and SVA could generate similar responses to the same stimuli which was most evident when vessels were treated with H_2O_2 and changing pH conditions. It may also be possible to predict the effects certain blockers would have when used with SVA based on our CPA observations and is the important future step for advancing this study. The placenta is a rich source of a range of proteins and most ion channels will be expressed within the tissue. However there is a need to develop a more detailed expression profile at the SMC and EC level. The SMC IF staining has revealed some important information about how blood flow may be regulated across the placenta. Expression of the K_2P channels within the placental vessels provides evidence for a potential role in the efficient exchange of nutrients across the placental transport system. This information can reveal new

insights into how the placenta can control and respond to changes within its microenvironment. Positive expression was shown for a number of key K₂P channels along with the BK_{Ca} and K_{ATP} channel within healthy placental vessels. We were then also able to compare this data with that of mild PE cases and compile a detailed breakdown of each ion channel and its expression levels. The precise nature of the different K⁺ channel expressed within a tissue reveals details on how the tissue can bring about a response. More importantly this provides researchers information on how to modulate the tissue activity when targeting disease pathways such as PE.

By comparing the responses of CPA and SVA we have been able to gain an important insight with regards to the control of blood flow within the placental vasculature. The placenta can divert blood flow to well perfused areas similar to that observed in the pulmonary circulations. Hampl (et al., 2002) has demonstrated the existence of HFPV that was significant in small resistance sized placental vessels. The redirection may help to improve tissue perfusion and is specific to resistance sized vessels (Hampl, Bibova et al., 2002, Hampl and Jakoubek, 2009). This also has similarities to the response seen with acidic pH and a change in vessel diameter would help to buffer the blood and remove excess H⁺ ions. Relaxation to pH response will reduce blood flow to allow to exchange and exchange the excess H⁺ ions. This will limit the damage of H⁺ exposure to spread to better ventilated areas. The resulting contraction that follows may help to regain normal blood flow, so that the disruption is not prolonged for longer than necessary. The excess in H⁺ concentration could alter the function of maternal SA which are in close contact with placental vessels at the

SVA junction. A crucial next step to take this study further would be to examine the response to such stress by the maternal SA.

8.2.Importance of pH in other systems

The placental vessels examined in our study demonstrated the presence of a fine control mechanism that can alter the vessel tone to induce a contraction in alkaline conditions and a relaxation with acidic pH. Important parallels can also be made with the regulation of pH within other tissues. A recent publication demonstrated the spatial removal of H^+ from rat neonate cardiac myocytes involved cellular gap junctions which are highly permeable to H^+ and was dependent on the CO_2/HCO_3^- buffering capacity of the cell (Swietach, Camelliti et al., 2010). In addition cells also have Cl^-/HCO_3^- and Cl^-/OH^- exchangers which determine the overall acid load of the cell and are responsible for responding to high concentrations of H^+ . The influx and efflux of H^+ ions is rapid and under normal conditions the H^+ content is maintained low.

Acidosis within a tissue may be caused by inflammation, ischaemia or defective pH homeostasis, microbial acidity, or malignant tumours. Many pH sensors have been identified and are continuing to help understand disease processes (Holzer, 2009, Vaughan-Jones, Spitzer et al., 2009). The most important role for pH sensors has been shown in the perception of pain and inflammation which can trigger a reflex response. Acidic pH will trigger mechanosensitive afferent neurons to cause sensitisation to the noxious stimulus (Holzer, 2004). Maintaining the pH within a

narrow range is of paramount importance for normal cellular functions including the control of vascular tone. Sensory neurons have a spectrum of acid sensing ion channels that respond to a range of noxious stimuli including pH to trigger an autonomic reflex, sensation, pain and inflammation. The autonomic response is mainly initiated by ion channels which have been implicated in the range of physiological and pathophysiological conditions (Bevan and Yeats, 1991, Gardener, Johnson et al., 2004, Holzer, 2009).

The ion channels implicated in the pH response have shown to be tissue specific and reflect the different processes of the body ([Chapter 8.4](#)). The closest parallel with the placenta is the pulmonary system which also carries deoxygenated blood in the arteries. H^+ accumulation has been identified as the main stimulus for coughing reflex. The pulmonary circulations shows evidence of both rapid and slow inactivation currents of afferent neurons that supply the lung tissues. Pulmonary SMC responses to acidic pH load have shown the ability to induce a relaxation response similar to what we observed in the placenta (Gurney, Osipenko et al., 2003, Gardener, Johnson et al., 2004, Shah, 2008). The stomach has a pH of 1 mainly due to the presence of HCl. The acid load is kept separate from other cells due to tightly regulated compartmentalisation and a strong mucosal barrier. The leak of fluids is a major risk factor in the onset of peptic ulcers. The H^+/K^+ ATPase actively increase the H^+ concentration within the stomach. The cells of the gastrointestinal tract are highly specialised to cope with HCl, a factor that is often overlooked by other research groups who expose a range of tissue to HCl to lower the pH content of cell (Bevan and Yeats, 1991). The urogenital tract can also cope with acidic pH environments in

the form of uric acid. The pathology of irritable bowel syndrome has been linked with a dysfunction in the uroepithelial barrier and bladder hyperactivity. The mechanism involved leads to a heightened sensitivity to acidic pH stimulus and treatment with capsaicin can reverse this (Bevan and Yeats, 1991, Holzer, 2009).

The high energy demanding cardiac muscle has provided an important insight into how pH regulation can alter under stress conditions. The most important determinant of pH homeostasis is the cells metabolic status and the cardiac myocytes can maintain an internal pH of 7.2 under normal conditions and small reductions in this can cause a reduction in contraction that is normalised within seconds and this has been attributed to the rapid movement of H^+ across the membrane boundaries and the role of H^+ transporters (Bevan and Yeats, 1991, Vaughan-Jones, Spitzer et al., 2009, Swietach, Camelliti et al., 2010). All of these separate examples highlight the range of strategies that are employed to deal with pH changes which the placenta is also a part of.

8.3. The biphasic response to acidic pH

The most important observation from our study was the transient, short lived response to acidic pH that was seen with CPA and SVA. Low pH has been reported to induce depolarisation while increasing pH will favour hyperpolarisation of the cell membrane (Bevan and Yeats, 1991). However we showed that low pH induced a two stage relaxation response as the contractile response could be recovered. One possible explanation for the biphasic response can be explained by the modulation of Na^+/Ca^{2+}

homeostasis by extracellular and intracellular pH. The close association with pH balance and Ca^{2+} helps to explain how a change in the vascular tone can be produced in response to pH changes. The H^+ load in pre-constricted vessels may trigger the entry of Na^+ via the NHE to restore the normal cellular pH balance. Once this equilibrium has been restored, the excess Na^+ are then pumped out of the cell via the $\text{Na}^+/\text{Ca}^{2+}$ exchanger to cause the phase II contraction (**Figure 8.3-1**). This also implicates a role for TREK-1 which is inhibited by acidic pH environments inside the cell while TASK is an extracellular pH specialist. Inhibiting each of these ion channels enhanced the relaxation response and suggests that a compensatory mechanism may exist that activates an alternative proton sensing ion channel in the absence of TASK currents. The initial loss in tone seen may be due Na^+ moving down its electrochemical gradient to remove the H^+ ions from the cell. As the $[\text{H}^+]_i$ is restored to basal levels, the TREK-1 which may detect a change in cell stretch, may in turn initiate the recovery in vessel tone and to trigger an efflux of Na^+ out of the cell, which may allow Ca^{2+} to enter and cause the slower contraction as part of the phase II response. This may also involve other candidate proton sensing ion channels.

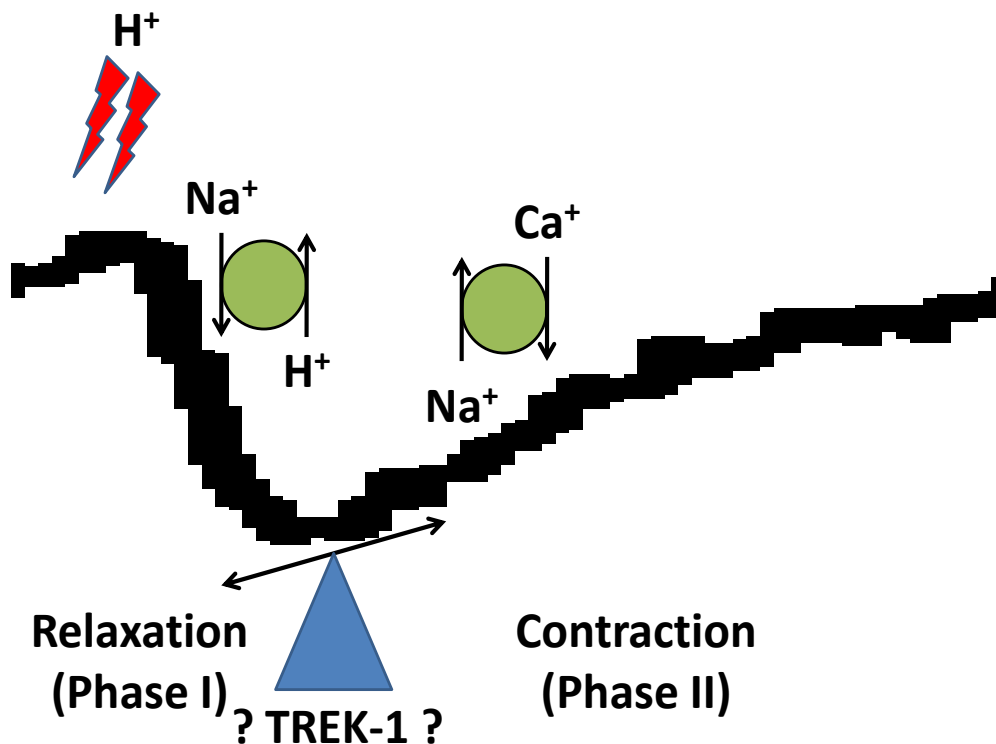


Figure 8.3-1 shows the proposed mechanism that may bring about the biphasic response to acidic pH in placental vessels. The H^+ load causes an immediate relaxation and excess H^+ is removed from the cells via the NHE. Once the H^+ has been buffered we see a net efflux Na $^+$ via the Na $^+$ /Ca $^{2+}$ transporter. This would cause membrane depolarisation and as a result trigger the switch over to the contraction phase (phase II). TREK-1 may have a role in detecting the pH change to shift the balance from phase I to the contractile phase II. This may also explain why the relaxation was prolonged with TREK-1 currents were blocked with L-METH.

8.4. Proton sensing ion channels

The pH balance of a tissue needs to be maintained within a narrow range. The fast acting nature of the response to acidic pH stimuli implicates the involvement of acid sensitive ion channels. Our studies showed that inhibition of the acid sensitive K2P channels TREK-1 and TASK-1/3 could modulate the response to acidic pH. However we failed to show a complete inhibition of the CPA response to low pH

which suggests other pH sensitive ion channels may also have a role in controlling the placental vessel response to extracellular pH changes. The four main types are the ASICs, K2P, TRP and the P2X family of ion channels which have been widely studied while the K_{ir} , K_v and $Ca_v1.2$ have also been implicated in responding to mild changes with pH (see **Table 8.4-1**).

Evidence from skeletal muscle has shown that the ion channels can evoke a biphasic response. It was reported that the human skeletal muscle cell line SJ-RH30 were rapidly depolarised when the pH was reduced to pH 6.5 with immediate fast acting ASICs currents (Gitterman, Wilson et al., 2005). The authors reported a desensitisation and re-sensitisation cycle with further stimulation. This response was both dose and time-dependent as increasing the time interval between pH challenges reduced the amplitude of the rapid inward current observed with a change from pH 7.4 to pH 6.5. Furthermore this was inhibited by AMIL (84%) and the more potent blocker PcTx-1 (91%) implicating a role for ASICs. The biphasic response seen could also have similar parallels with our observations with placental vessel which produced a repeated relaxation-contraction cycle when stimulated directly with lactic acid. It would be interesting to observe the responses in the presence of PcTx-1 which appears to produce a more potent inhibition to the ion channel activations.

Table 8.4-1 listing the main ion channels that have been implicated with pH evoked currents.

Ion channel family	Subunits	Key references
Acid sensitive ion channels (ASICs)	ASIC1a, ASIC2a, ASIC1b, and ASIC3.	(Stephan and Agnew, 1991, Gitterman, Wilson et al., 2005)
Transient receptor potential (TRP)	TRPV1, TRPV4, TRPC4, TRPC5, and TRPP2.	(Waldmann, 2001, Dhaka, Uzzell et al., 2009)
K2P	TALK, TASK-1, TASK-2, TASK-3, TWIK-1, TALK-2, and TRESK.	(Lesage, 2003, Richter, Dvoryanchikov et al., 2004, Bai, Greenwood et al., 2005, Wareing, Bai et al., 2006)
Proton sensing G protein coupled receptors	OGR1, GPR4, G2A, and TDAG8.	(Holzer, 2009, Swietach, Camelliti et al., 2010)
Voltage dependent ion channels	K _v 1.3, K _v 1.4, K _v 11.1, Ca _v 1.2, and TTX sensitive Na ⁺ channels	(Perney and Kaczmarek, 1991, Stephan and Agnew, 1991, Williams, Fyfe et al., 2008, Vaughan-Jones, Spitzer et al., 2009, Kiernan, Barrie et al., 2010)
Ligand gated ion channels	P2x1-5, P2x7, and GABA _A .	(Valera, Hussy et al., 1994, Burnstock, 2000, Lee, Bardini et al., 2000, Dixon, Yu et al., 2004, Roberts, Greenwood et al., 2006, Warren, Harvey et al., 2008)
Other ion channels	Cl ⁻ channels, gap junction ion channels (connexins), hyperpolarisation activated cyclic nucleotide gated channels and epithelial Na ⁺ channels (ENaC)	(Kulanthaivel, Furesz et al., 1992, Drummond, Welsh et al., 2001, Bhalla and Hallows, 2008, Holzer, 2009)

8.5. The placenta as a diagnostic tool

The finding that tissue oxygenation and pH can alter vascular function of the placenta may have far reaching consequences for the fetus. The fetus is at risk of exposure to reduced perfusion occurring in the placenta. Early stress and a failure of maternal SA to adapt to pregnancy will place more demand on the placental perfusion system to prolong the stress exerted on the vulnerable vessels (van Laar, Peters et al., 2010). This can alter the fetal programming in the long term as gene expression may change and emphasises the need for an adequately performing placenta in pregnancy (Jansson and Powell, 2007, Goldenberg, Culhane et al., 2008, van Laar, Peters et al., 2010). In support of this, changes to maternal nutrition during pregnancy can alter the glucose metabolism of the placenta to alter the expression of key glucose transporters within the placental membranes (Settle, Sibley et al., 2006, Jansson and Powell, 2007). Importantly, the fetus is receptive to changes in the intrauterine environment to adapt to the post natal environments. The development plasticity of the hypothalamic pituitary adrenal axis requires vital signals at key points of development to determine the structure and function of cells within each organ system.

This also makes the placenta an important diagnostic tool for detecting fetal stress early on (Pardi, Cetin et al., 1993). The careful monitoring of blood pH during labour is crucial for limiting the spread of fetal stress and is used as a basis for determining the intervention strategies that commonly result in an emergency LLSCS (Jansson and Powell, 2007, van Laar, Peters et al., 2010). In a similar way, the maternal blood pH could be monitored in future to help evaluate the severity and

duration of any potential risk to the fetus across the duration of pregnancy. This study has demonstrated that blood vessels from healthy pregnancies could respond to altered pH environments and crucially this response appears to be altered in PE vessels. This response may be a reflection of the intrauterine environment whereby the placenta can alter its ion channel expression profile to increase its sensitivity to pH stress and may be an important observation.

8.6.Future research

The individual methods used in this study have been validated in **Chapters 4-7**. However we can also identify some important new directions to further advance this body of work.

1. This study focused on resistance arteries within the placenta and the next priority should be the placental veins which carry the oxygenated blood. In addition the placenta cannot be studied in isolation and information gained from vessels within the maternal MYO will provide an insight into the adaptations of the maternal circulation in response to hypoxia and pH insults. The placental needs to modify its own perfusion rate in order to match the blood flow of the maternal circulation and it would be interesting to observe the response of MYO vessels to changing conditions.
2. The level of pO_2 was varied by altering the gas mixture that was used to continually perfuse the myograph chambers. However we should also monitor the dissolved content of O_2 within the saline with an O_2 probe (such as mini Clarke

style electrode). This could allow us to quantify the O_2 consumption by recorded the O_2 input and output. We should also consider altering the level of tissue oxygenation within the same experiment to observe the response when pO_2 is lowered from 20% to 5% and 2%.

3. The pO_2 was an important factor in determining the vessel responses to various stimuli while pCO_2 was constant at 5% in each experiment. Under reduced perfusion conditions when pO_2 is low pCO_2 will rise and this can contribute to low pH environments. We should also explore this by altering the pCO_2 levels when perfusing CPA and SVA in wire myography preparations and for use in SMC cell culture.
4. The level of tissue damage following stress insults (H_2O_2 and low pH) should also be assessed by utilising IHC to identify markers for lipid peroxidation. This method has the further benefit that transverse sectioned vessels can be used to identify precisely which cells are targeted by ROS. This will also gives idea of the tissue redox state as the response to oxidative stress is dependent on the availability of antioxidants within the tissue. We could also measure mitochondrial activity which is more reflective of tissue viability (MTT assay for fixed tissue or Rhodamine 123 for viable tissue) to investigate the mechanism for the apparent H_2O_2 induced toxicity in CPA and SVA. In relation to this, Western blot analysis should be performed on vessels used for wire myography based studies. We could examine the expression of O_2 sensitive ion channels when vessels have been exposed to low pO_2 and H_2O_2 stress.

5. The role of other metabolic inhibitors should be explored, such as NaCN or DNP which can inhibit metabolic activity and rapidly deplete ATP stores to cause the intracellular pH to fall. Similarly the effects of other ROS agents should be examined, including Xanthine oxidase and its inhibitor Xanthine dehydrogenase which are released following hypoxic injury and found in high levels in the placental circulation (Mills, Wareing et al., 2009).
6. Ca^{2+} is important for mediating the cell excitability and we can investigate the role of Ca^{2+} movements in response to different stimuli. We also need to separate the role of extracellular and intracellular stores of Ca^{2+} which can be addressed by removing Ca^{2+} from the PSS while internal Ca^{2+} stores can be depleted with thapsigargin. Another method that allows for the monitoring of Ca^{2+} movements is confocal myography. Wire myography provides information about the force generated by the vessel while confocal myography allows for the incorporation of fluorescent markers to monitor the movement of ions such as Ca^{2+} (with inositol trisphosphate (IP_3) or Fura PE-3) (see Drummond and Tuft, 1999) as well as H^+ ions using pH dyes (carboxyl SNARF) along with ROS molecules. The monitoring of Ca^{2+} can also help us to determine if the tone oscillations that we observed were caused by movements of Ca^{2+} . We can also assess the effectiveness of various blockers applied by comparing the Ca^{2+} spikes to gain temporal and spatial data pre and post incubation with the applied drugs.
7. The functional studies were severely hampered by the 20mins window for tissue collection and as a result a large number of samples were excluded from our studies. This is due to the fact that placental ATP levels have been reported to

reduce by 75% beyond this time point. One way to address this issue may be with the overnight storage of the whole placenta at 37°C to help recover ATP stores and improve tissue survival. Wareing (et al., 2011) have shown evidence to suggest that isolated placental CPA and CPV can remain viable for 48h (*personal communication*) This may help to improve the isolation and longevity of SVA which had the most variable tissue survival rate, however a previous study provided evidence to show the vessel contractility to KCl was diminished in vessels stored at 4°C overnight while fresh vessels gave the most reproducible contractions (Abad, Estan et al., 2003). During this study, we limited our investigations to ≤ 8 hrs as mitochondrial activity can only be maintained for 10-12hrs. To improve this we could also consider increasing the glucose concentration of PSS. However raising glucose levels can alter the pH of PSS and more importantly could alter the metabolic rate of the tissue to introduce oxidative stress. A further modification we could make is to alter the method used to dissect the vessels. In our study we dissected the vessels in an ambient environment and this may have introduced oxidative stress as the tissue was not continually perfused. Furthermore once the vessel is mounted it was then perfused with constant O₂ and this reperfusion will also add to the oxidative stress insult. One solution would be to conduct the dissection in biological safety cabinet perfused with 5% O₂ to match normoxic conditions found within the placenta.

8. The most significant change we can make is to move on to studying single cells from the placental vasculature to dissect the roles of the EC from SMC using

cultured cells and single cell microfluorimetry. We should consider altering the cell culture conditions with respect to the pO_2/pCO_2 levels that are used to grow the freshly isolated SMC, as growing cultures under relative hyperoxia (95% air/5% CO_2 mixture) could indirectly alter O_2 sensitive ion channels. The wire myography data has shown that 5% pO_2 is a good reflection of the physiological growth conditions for the placental vessels, and the same settings should be applied to minimise the risk of altering ion channel expression under different pO_2 environments.

9. We can also use electrophysiology to study single cell responses with the patch clamp technique of the whole cell to gain information about the conductance of a single ion channel (Khan, Smith et al., 1993). This allows for the monitoring of action potentials in more detail and crucially to observe the intracellular and extracellular movements of ions across the cell membrane. Patch clamping also enables the internal cellular environment to be controlled and would allow us to alter the $[pH]_i$ and may also improve delivery of lipid based agonists such as AA across the cell membrane. To do this we ideally require freshly dispersed cells and our preliminary attempts have been shown in **Figure 8.6-1**. The enzyme papain (1.5mg/ml) was used according to the method described by Drummond (et al., 1999, Albarwani, Heinert et al., 1995) who successfully isolated SMC from rat pulmonary arteries. This method achieved some success however I was unable to demonstrate a whole patched SMC in order to record ion channel activities across the cell. As a result the cell dispersal method used requires further

optimisation to obtain a substantial yield of fresh cells and explore this avenue of research.

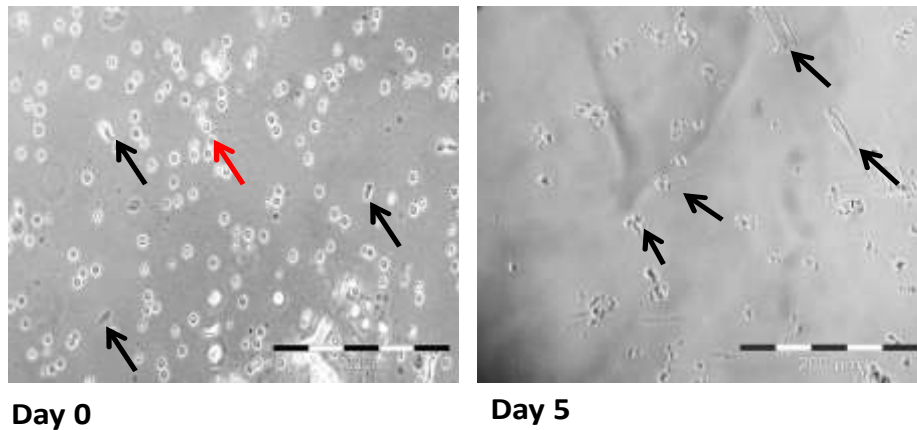


Figure 8.6-1 illustrating the results of fresh cell dispersal using CPA. At day 0 individual SMC (black arrows) were successfully isolated from the vessel explants along with a large population of RBC (red arrow). At day 5 we observed most cells were no longer viable and showed evidence of cell necrosis. Cells which were viable proved to be difficult to patch to record whole cell currents. *Scale bar 200 μ m.*

9. Conclusion

The placenta is an important biological barrier and is the first site of exposure for toxins including H^+ from the maternal and fetal circulations as well as the amniotic fluid. Despite this important role very little research is being undertaken to characterise the response of vessels to chronic stress stimuli and secondly very little information is available to show the contributions of specific ion channels in mediating these responses. The possible reasons for a fall in pH could be due to prolonged hypoxia, impaired removal of fetal metabolites or maternal influences. We have demonstrated how small changes in the extracellular environment can have dramatic consequences for the placental resistance arteries. The CPA and SVA from healthy samples have demonstrated the existence of efficient mechanisms to generate a response to cope with external stress. This information may help to better devise early interventions aimed at improving placental and therefore fetal perfusion. Our observations also implicate a range of key ion channels expressed across the placenta which may have future therapeutic implications in the control of vascular tone in the placenta and forms the basis for further research. However the true importance of these observations will be revealed with the development of highly selective pharmacological tools and single channel electrophysiological recordings. This future research will help to identify the underlying mechanisms of the proton mediated responses and understand its physiological importance in the placental circulation.

10. Bibliography

- AALKJAER, C. (1990) Regulation of intracellular pH and its role in vascular smooth muscle function. *J Hypertens*, 8, 197-206.
- AARONSON, P. I., SARWAR, U., GIN, S., ROCKENBAUCH, U., CONNOLLY, M., TILLET, A., WATSON, S., LIU, B. & TRIBE, R. M. (2006) A role for voltage-gated, but not Ca²⁺-activated, K⁺ channels in regulating spontaneous contractile activity in myometrium from virgin and pregnant rats. *Br J Pharmacol*, 147, 815-24.
- ABAD, A., ESTAN, L., MORALES-OLIVAS, F. J. & SERRA, V. (2003) Reactivity of isolated human chorionic vessels: analysis of some influencing variables. *Can J Physiol Pharmacol*, 81, 1147-51.
- ALBARWANI, S., HEINERT, G., TURNER, J. L. & KOZLOWSKI, R. Z. (1995) Differential K⁺ channel distribution in smooth muscle cells isolated from the pulmonary arterial tree of the rat. *Biochem Biophys Res Commun*, 208, 183-9.
- ALLEN, J., ANDERSSON, E., FORMAN, A., GUDMUNDSSON, S., LINGMAN, G., SVANE, D., MARSAL, K. & ULMSTEN, U. (1991) Effects of nifedipine on isolated arteries and placental perfusion in the human uteroplacental unit. *Hypertens Pregnancy*, 10, 353-369.
- ALLEN, J., MAIGAARD, S., CHRISTENSEN, J. H., ANDREASEN, F. & FORMAN, A. (1987) Effects of thiopentone or chlormethiazole on human placental stem villous arteries. *Br J Anaesth*, 59, 1273-1277.
- ALLEN, J., SKAJAA, K., MAIGAARD, S. & FORMAN, A. (1991) Effects of vasodilators on isolated human uteroplacental arteries. *Obstet Gynecol*, 77, 765-71.
- ANDRESEN, J., LLOYD, E. & BRYAN, R. (2007) The K_{2P} channel, TRAAK; expression and function in cerebral arteries. *The FASEB Journal*.
- ARCHER, S. & MICHELAKIS, E. (2002) The mechanism(s) of hypoxic pulmonary vasoconstriction: potassium channels, redox O(2) sensors, and controversies. *News Physiol Sci*, 17, 131-7.
- ARRIBAS, S. M., HILLIER, C., GONZALEZ, C., MCGRORY, S., DOMINICZAK, A. F. & MCGRATH, J. C. (1997) Cellular aspects of vascular remodelling in hypertension revealed by confocal microscopy. *Hypertension*, 30, 1455-64.
- ASHCROFT, F. M. (2007) The Walter B. Cannon Physiology in Perspective Lecture, 2007. ATP-sensitive K⁺ channels and disease: from molecule to malady. *Am J Physiol Endocrinol Metab*, 293, E880-9.
- ASHWORTH, J. (1997) The role of the vascular endothelium in pregnancy, pre-eclampsia and intrauterine growth restriction. University of Nottingham.
- BABAWALE, M. O., MOBBERLEY, M. A., RYDER, T. A., ELDER, M. G. & SULLIVAN, M. H. (2002) Ultrastructure of the early human fetomaternal interface co-cultured in vitro. *Hum Reprod*, 17, 1351-7.
- BAGAMERY, K., KOVACS, L., VISKI, S., NYARI, T. & FALKAY, G. (1999) Ontogeny of imidazoline binding sites in the human placenta. *Acta Obstet Gynecol Scand*, 78, 89-92.

- BAI, X., BUGG, G. J., GREENWOOD, S. L., GLAZIER, J. D., SIBLEY, C. P., BAKER, P. N., TAGGART, M. J. & FYFE, G. K. (2005) Expression of TASK and TREK, two-pore domain K⁺ channels, in human myometrium. *Reproduction*, 129, 525-30.
- BAI, X., GREENWOOD, S. L., GLAZIER, J. D., BAKER, P. N., SIBLEY, C. P., TAGGART, M. J. & FYFE, G. K. (2005) Localization of TASK and TREK, two-pore domain K⁺ channels, in human cytotrophoblast cells. *J Soc Gynecol Investig*, 12, 77-83.
- BAINBRIDGE, S. A., ROBERTS, J. M., VON VERSEN-HOYNCK, F., KOCH, J., EDMUNDS, L. & HUBEL, C. A. (2009) Uric acid attenuates trophoblast invasion and integration into endothelial cell monolayers. *Am J Physiol Cell Physiol*, 297, C440-50.
- BAKER, P. N. & KINGDOM, J. (2004) *Pre-eclampsia current perspectives on management*, The Parthenon Publishing Group, London.
- BAKER, S. A., HENNIG, G. W., HAN, J., BRITTON, F. C., SMITH, T. K. & KOH, S. D. (2008) Methionine and its derivatives increase bladder excitability by inhibiting stretch-dependent K(+) channels. *Br J Pharmacol*, 153, 1259-71.
- BARKER, D. J., GLUCKMAN, P. D., GODFREY, K. M., HARDING, J. E., OWENS, J. A. & ROBINSON, J. S. (1993) Fetal nutrition and cardiovascular disease in adult life. *Lancet*, 341, 938-41.
- BARLOW, R. S., EL-MOWAFY, A. M. & WHITE, R. E. (2000) H₂O₂ opens BK(Ca) channels via the PLA₂-arachidonic acid signaling cascade in coronary artery smooth muscle. *Am J Physiol Heart Circ Physiol*, 279, H475-83.
- BARLOW, R. S. & WHITE, R. E. (1998) Hydrogen peroxide relaxes porcine coronary arteries by stimulating BKCa channel activity. *Am J Physiol*, 275, H1283-9.
- BAYLISS, D. A., SIROIS, J. E. & TALLEY, E. M. (2003) The TASK family: two-pore domain background K⁺ channels. *Mol Interv*, 3, 205-19.
- BAYLISS, W. M. (1902) On the local reactions of the arterial wall to changes of internal pressure. *J Physiol*, 28, 220-31.
- BECKETT, E. A., HAN, I., BAKER, S. A., HAN, J., BRITTON, F. C. & KOH, S. D. (2008) Functional and molecular identification of pH-sensitive K⁺ channels in murine urinary bladder smooth muscle. *BJU Int*, 102, 113-24.
- BENIRSCHKE, K. (1998) Remarkable placenta. *Clin Anat*, 11, 194-205.
- BENIRSCHKE, K. & KAUFMANN, P. (1995) *Pathology of the human placenta* Springer Verlag, New York
- BENIRSCHKE, K., KAUFMANN, P. & BAERGEN, R. (Eds.) (2006) *Pathology of the human placenta*.
- BENKUSKY, N. A., FERGUS, D. J., ZUCCHERO, T. M. & ENGLAND, S. K. (2000) Regulation of the Ca²⁺-sensitive domains of the maxi-K channel in the mouse myometrium during gestation. *J Biol Chem*, 275, 27712-9.
- BEVAN, J. A. & OSHER, J. V. (1972) A direct method for recording tension changes in the wall of small blood vessels in vitro. *Agents Actions*, 2, 257-60.
- BEVAN, S. & YEATS, J. (1991) Protons activate a cation conductance in a sub-population of rat dorsal root ganglion neurones. *J Physiol*, 433, 145-61.

- BHALLA, V. & HALLOWS, K. R. (2008) Mechanisms of ENaC regulation and clinical implications. *J Am Soc Nephrol*, 19, 1845-54.
- BISHOP, R. L. & WEISFELDT, M. L. (1976) Sodium bicarbonate administration during cardiac arrest. Effect on arterial pH PCO₂, and osmolality. *Jama*, 235, 506-9.
- BLACKBURN, S. (2007) *Maternal and Neonatal Physiology: A Clinical Perspective* Saunders Elsevier.
- BLAUSTEIN, M. P., KAO, J. P. Y. & MATTESON, D. R. (2004) *Cellular Physiology*, Elsevier
- BLAUSTEIN, M. P., KAO, J.P.Y., MATTESON, D.R. (2004) *Cellular Physiology*, Elsevier Mosby.
- BLECHNER, J. N. (1970) Fetal acid-base homeostasis. *Clin Obstet Gynecol*, 13, 621-37.
- BLECHNER, J. N. (1993) Maternal-fetal acid-base physiology. *Clin Obstet Gynecol*, 36, 3-12.
- BOLTE, A. C., VAN GEIJN, H. P. & DEKKER, G. A. (2001) Pathophysiology of preeclampsia and the role of serotonin. *Eur J Obstet Gynecol Reprod Biol*, 95, 12-21.
- BOURA, A., LEITCH, I., READ, M. & WALTERS, W. (1998) The control of fetal vascular resistance in the human placenta. *Trophoblast Research* 11, 299-313.
- BRAINARD, A. M., KOROVKINA, V. P. & ENGLAND, S. K. (2007) Potassium channels and uterine function. *Semin Cell Dev Biol*, 18, 332-9.
- BRAKEMEIER, S., EICHLER, I., KNORR, A., FASSHEBER, T., KOHLER, R. & HOYER, J. (2003) Modulation of Ca²⁺-activated K⁺ channel in renal artery endothelium in situ by nitric oxide and reactive oxygen species. *Kidney Int*, 64, 199-207.
- BRENNER, R., PEREZ, G. J., BONEV, A. D., ECKMAN, D. M., KOSEK, J. C., WILER, S. W., PATTERSON, A. J., NELSON, M. T. & ALDRICH, R. W. (2000) Vasoregulation by the beta1 subunit of the calcium-activated potassium channel. *Nature*, 407, 870-6.
- BROSENS, I. A., ROBERTSON, W. B. & DIXON, H. G. (1972) The role of the spiral arteries in the pathogenesis of preeclampsia. *Obstet Gynecol Annu*, 1, 177-91.
- BROUGHTON PIPKIN, F., CRAVEN, D. J. & SYMONDS, E. M. (1981) The uteroplacental renin-angiotensin system in normal and hypertensive pregnancy. *Contrib Nephrol*, 25, 49-52.
- BRUCE, J., TAGGART, M. & AUSTIN, C. (2004) Contractile responses of isolated rat mesenteric arteries to acute episodes of severe hypoxia and subsequent reoxygenation. *Microvasc Res*, 68, 303-12.
- BRYAN, R. M., JR., YOU, J., PHILLIPS, S. C., ANDRESEN, J. J., LLOYD, E. E., ROGERS, P. A., DRYER, S. E. & MARRELLI, S. P. (2006) Evidence for two-pore domain potassium channels in rat cerebral arteries. *Am J Physiol Heart Circ Physiol*, 291, H770-80.
- BUCKLER, K. J. & HONORE, E. (2005) The lipid-activated two-pore domain K⁺ channel TREK-1 is resistant to hypoxia: implication for ischaemic neuroprotection. *J Physiol*, 562, 213-22.

- BURNSTOCK, G. (2000) P2X receptors in sensory neurones. *Br J Anaesth*, 84, 476-88.
- BURTON, G. J. (2008) Oxygen, the Janus gas; its effects on human placental development and function. *J Anat.*
- BURTON, G. J., JAUNIAUX, E. & CHARNOCK-JONES, D. S. (2009) The influence of the intrauterine environment on human placental development. *Int J Dev Biol.*
- BURTON, G. J., YUNG, H. W., CINDROVA-DAVIES, T. & CHARNOCK-JONES, D. S. (2008) Placental Endoplasmic Reticulum Stress and Oxidative Stress in the Pathophysiology of Unexplained Intrauterine Growth Restriction and Early Onset Preeclampsia. *Placenta*.
- BUSSELBERG, D., MICHAEL, D., EVANS, M. L., CARPENTER, D. O. & HAAS, H. L. (1992) Zinc (Zn²⁺) blocks voltage gated calcium channels in cultured rat dorsal root ganglion cells. *Brain Res*, 593, 77-81.
- BYRNE, B. M., HOWARD, R. B., MORROW, R. J., WHITELEY, K. J. & ADAMSON, S. L. (1997) Role of the L-arginine nitric oxide pathway in hypoxic fetoplacental vasoconstriction. *Placenta*, 18, 627-34.
- CADAVEIRA-MOSQUERA, A., RIBEIRO, S. J., REBOREDA, A., PEREZ, M. & LAMAS, J. A. (2011) Activation of TREK currents by the neuroprotective agent riluzole in mouse sympathetic neurons. *J Neurosci*, 31, 1375-85.
- CAMPBELL, A. G., DAWES, G. S., FISHMAN, A. P., HYMAN, A. I. & JAMES, G. B. (1966) The oxygen consumption of the placenta and foetal membranes in the sheep. *J Physiol*, 182, 439-64.
- CANZANELLI, A., GREENBLATT, M., ROGERS, G. & RAPPORT, D. (1939) The effect of pH changes on the in vitro oxygen consumption of tissues. *Amer J Physiol* 127, 290-300.
- CATELLA, F., LAWSON, J. A., FITZGERALD, D. J. & FITZGERALD, G. A. (1987) Analysis of multiple thromboxane metabolites in plasma and urine. *Adv Prostaglandin Thromboxane Leukot Res*, 17B, 611-4.
- CHADDHA, V., VIERO, S., HUPPERTZ, B. & KINGDOM, J. (2004) Developmental biology of the placenta and the origins of placental insufficiency. *Semin Fetal Neonatal Med*, 9, 357-69.
- CHAMBERLAIN, G. & BROUGHTON PIPKIN, F. (1998) *Clinical Physiology in Obstetrics*, Blackwell science Ltd.
- CHAUDHURI, G. & FURUYA, K. (1991) Endothelium-derived vasoactive substances in fetal placental vessels. *Semin Perinatol*, 15, 63-7.
- CHAVEZ, R. A., GRAY, A. T., ZHAO, B. B., KINDLER, C. H., MAZUREK, M. J., MEHTA, Y., FORSAYETH, J. R. & YOST, C. S. (1999) TWIK-2, a new weak inward rectifying member of the tandem pore domain potassium channel family. *J Biol Chem*, 274, 7887-92.
- CHEMIN, J., PATEL, A. J., DUPRAT, F., SACHS, F., LAZDUNSKI, M. & HONORE, E. (2007) Up- and down-regulation of the mechano-gated K(2P) channel TREK-1 by PIP (2) and other membrane phospholipids. *Pflugers Arch*, 455, 97-103.

- CHEN, M. & SIMARD, J. M. (2001) Cell swelling and a nonselective cation channel regulated by internal Ca^{2+} and ATP in native reactive astrocytes from adult rat brain. *J Neurosci*, 21, 6512-21.
- CINDROVA-DAVIES, T., YUNG, H. W., JOHNS, J., SPASIC-BOSKOVIC, O., KOROLCHUK, S., JAUNIAUX, E., BURTON, G. J. & CHARNOCK-JONES, D. S. (2007) Oxidative stress, gene expression, and protein changes induced in the human placenta during labor. *Am J Pathol*, 171, 1168-79.
- CIPOLLA, M. J., SMITH, J., KOHLMAYER, M. M. & GODFREY, J. A. (2009) SKCa and IKCa Channels, myogenic tone, and vasodilator responses in middle cerebral arteries and parenchymal arterioles: effect of ischemia and reperfusion. *Stroke*, 40, 1451-7.
- CLUZEAUD, F., REYES, R., ESCOUBET, B., FAY, M., LAZDUNSKI, M., BONVALET, J. P., LESAGE, F. & FARMAN, N. (1998) Expression of TWIK-1, a novel weakly inward rectifying potassium channel in rat kidney. *Am J Physiol*, 275, C1602-9.
- COLE, W. C., PLANE, F. & JOHNSON, R. (2005) Role of Kv1 channels in control of arterial myogenic reactivity to intraluminal pressure. *Circ Res*, 97, e1.
- COLEMAN, H. A., TARE, M. & PARKINGTON, H. C. (2004) Endothelial potassium channels, endothelium-dependent hyperpolarization and the regulation of vascular tone in health and disease. *Clin Exp Pharmacol Physiol*, 31, 641-9.
- CONCLIN, K. (Ed.) (1994) *Physiologic changes of pregnancy*, Chestnut DH ed.
- COOPER, B. Y., JOHNSON, R. D. & RAU, K. K. (2004) Characterization and function of TWIK-related acid sensing K^{+} channels in a rat nociceptive cell. *Neuroscience*, 129, 209-24.
- COOPER, E. J., WAREING, M., GREENWOOD, S. L. & BAKER, P. N. (2006) Oxygen tension and normalisation pressure modulate nifedipine-sensitive relaxation of human placental chorionic plate arteries. *Placenta*, 27, 402-10.
- CORCORAN, J., LACEY, H., BAKER, P. N. & WAREING, M. (2008) Altered potassium channel expression in the human placental vasculature of pregnancies complicated by fetal growth restriction. *Hypertens Pregnancy*, 27, 75-86.
- COWLEY, E. A., SELLERS, M. C. & ILLSLEY, N. P. (2005) Intracellular pH homeostasis in cultured human placental syncytiotrophoblast cells: recovery from acidification. *Am J Physiol Cell Physiol*, 288, C891-8.
- CZIRJAK, G., FISCHER, T., SPAT, A., LESAGE, F. & ENYEDI, P. (2000) TASK (TWIK-related acid-sensitive K^{+} channel) is expressed in glomerulosa cells of rat adrenal cortex and inhibited by angiotensin II. *Mol Endocrinol*, 14, 863-74.
- DAVIS, K. A. & COWLEY, E. A. (2006) Two-pore-domain potassium channels support anion secretion from human airway Calu-3 epithelial cells. *Pflugers Arch*, 451, 631-41.
- DAVIS, M. J. & GORE, R. W. (1989) Length-tension relationship of vascular smooth muscle in single arterioles. *Am J Physiol*, 256, H630-40.
- DE LUCA BRUNORI, I., BATTINI, L., BRUNORI, E., LENZI, P., PAPARELLI, A., SIMONELLI, M., VALENTINO, V. & GENAZZANI, A. R. (2005)

- Placental barrier breakage in preeclampsia: ultrastructural evidence. *Eur J Obstet Gynecol Reprod Biol*, 118, 182-9.
- DEMIR, R., KAYISLI, U. A., SEVAL, Y., CELIK-OZENCI, C., KORGUN, E. T., DEMIR-WEUSTEN, A. Y. & HUPPERTZ, B. (2004) Sequential expression of VEGF and its receptors in human placental villi during very early pregnancy: differences between placental vasculogenesis and angiogenesis. *Placenta*, 25, 560-72.
- DEURLOO, K. L., SPREEUWENBERG, M. D., BOLTE, A. C. & VAN VUGT, J. M. (2007) Color Doppler ultrasound of spiral artery blood flow for prediction of hypertensive disorders and intra uterine growth restriction: a longitudinal study. *Prenat Diagn*, 27, 1011-6.
- DHAKA, A., UZZELL, V., DUBIN, A. E., MATHUR, J., PETRUS, M., BANDELL, M. & PATAPOUTIAN, A. (2009) TRPV1 is activated by both acidic and basic pH. *J Neurosci*, 29, 153-8.
- DIGIACOMO, J. E. & HAY, W. W., JR. (1989) Regulation of placental glucose transfer and consumption by fetal glucose production. *Pediatr Res*, 25, 429-34.
- DIXON, S. J., YU, R., PANUPINTHU, N. & WILSON, J. X. (2004) Activation of P2 nucleotide receptors stimulates acid efflux from astrocytes. *Glia*, 47, 367-76.
- DONG, Y. L., GREEN, K. E., VEGIRAGU, S., HANKINS, G. D., MARTIN, E., CHAUHAN, M., THOTA, C. & YALLAMPALLI, C. (2005) Evidence for decreased calcitonin gene-related peptide (CGRP) receptors and compromised responsiveness to CGRP of fetoplacental vessels in preeclamptic pregnancies. *J Clin Endocrinol Metab*, 90, 2336-43.
- DONG, Y. L., VEGIRAJU, S., CHAUHAN, M., GANGULA, P. R., HANKINS, G. D., GOODRUM, L. & YALLAMPALLI, C. (2004) Involvement of calcitonin gene-related peptide in control of human fetoplacental vascular tone. *Am J Physiol Heart Circ Physiol*, 286, H230-9.
- DRUMMOND, H. A., WELSH, M. J. & ABBOUD, F. M. (2001) ENaC subunits are molecular components of the arterial baroreceptor complex. *Ann N Y Acad Sci*, 940, 42-7.
- DRUMMOND, R. M. & TUFT, R. A. (1999) Release of Ca²⁺ from the sarcoplasmic reticulum increases mitochondrial [Ca²⁺] in rat pulmonary artery smooth muscle cells. *J Physiol*, 516 (Pt 1), 139-47.
- DUNN, W. R. & GARDINER, S. M. (1995) Structural and functional properties of isolated, pressurized, mesenteric resistance arteries from a vasopressin-deficient rat model of genetic hypertension. *Hypertension*, 26, 390-6.
- DUNN, W. R., WELLMAN, G. C. & BEVAN, J. A. (1994) Enhanced resistance artery sensitivity to agonists under isobaric compared with isometric conditions. *Am J Physiol*, 266, H147-55.
- DUPRAT, F., GUILLEMARE, E., ROMÉY, G., FINK, M., LESAGE, F., LAZDUNSKI, M. & HONORE, E. (1995) Susceptibility of cloned K⁺ channels to reactive oxygen species. *Proc Natl Acad Sci U S A*, 92, 11796-800.
- DUPRAT, F., LAURITZEN, I., PATEL, A. & HONORE, E. (2007) The TASK background K₂P channels: chemo- and nutrient sensors. *Trends Neurosci*, 30, 573-80.

- DUPRAT, F., LESAGE, F., FINK, M., REYES, R., HEURTEAUX, C. & LAZDUNSKI, M. (1997) TASK, a human background K⁺ channel to sense external pH variations near physiological pH. *Embo J*, 16, 5464-71.
- DUPRAT, F., LESAGE, F., PATEL, A. J., FINK, M., ROMEY, G. & LAZDUNSKI, M. (2000) The neuroprotective agent riluzole activates the two P domain K(+) channels TREK-1 and TRAAK. *Mol Pharmacol*, 57, 906-12.
- ECONOMIDES, D. L. & NICOLAIDES, K. H. (1989) Blood glucose and oxygen tension levels in small-for-gestational-age fetuses. *Am J Obstet Gynecol*, 160, 385-9.
- EICHHORN, B. & DOBREV, D. (2007) Vascular large conductance calcium-activated potassium channels: Functional role and therapeutic potential. *Naunyn Schmiedebergs Arch Pharmacol*, 376, 145-55.
- ETTAICHE, M., FILLACIER, K., WIDMANN, C., HEURTEAUX, C. & LAZDUNSKI, M. (1999) Riluzole improves functional recovery after ischemia in the rat retina. *Invest Ophthalmol Vis Sci*, 40, 729-36.
- FAIRLIE, F. M., MORETTI, M., WALKER, J. J. & SIBAI, B. M. (1991) Determinants of perinatal outcome in pregnancy-induced hypertension with absence of umbilical artery end-diastolic frequencies. *Am J Obstet Gynecol*, 164, 1084-9.
- FELETOU, M. (2009) Calcium-activated potassium channels and endothelial dysfunction: therapeutic options? *Br J Pharmacol*, 156, 545-62.
- FERGUSON, R. E., CARROLL, H. P., HARRIS, A., MAHER, E. R., SELBY, P. J. & BANKS, R. E. (2005) Housekeeping proteins: a preliminary study illustrating some limitations as useful references in protein expression studies. *Proteomics*, 5, 566-71.
- FINK, M., DUPRAT, F., LESAGE, F., REYES, R., ROMEY, G., HEURTEAUX, C. & LAZDUNSKI, M. (1996) Cloning, functional expression and brain localization of a novel unconventional outward rectifier K⁺ channel. *Embo J*, 15, 6854-62.
- FINK, M., LESAGE, F., DUPRAT, F., HEURTEAUX, C., REYES, R., FOSSET, M. & LAZDUNSKI, M. (1998) A neuronal two P domain K⁺ channel stimulated by arachidonic acid and polyunsaturated fatty acids. *Embo J*, 17, 3297-308.
- FIRTH, K. F. & BROUGHTON PIPKIN, F. (1989) Human alpha- and beta-calcitonin gene-related peptides are vasodilators in human chorionic plate vasculature. *Am J Obstet Gynecol*, 161, 1318-9.
- FITZGERALD, D. J., MAYO, G., CATELLA, F., ENTMAN, S. S. & FITZGERALD, G. A. (1987) Increased thromboxane biosynthesis in normal pregnancy is mainly derived from platelets. *Am J Obstet Gynecol*, 157, 325-30.
- FITZGERALD, G. A., FITZGERALD, D. J., LAWSON, J. A. & MURRAY, R. (1987) Thromboxane biosynthesis and antagonism in humans. *Adv Prostaglandin Thromboxane Leukot Res*, 17A, 199-203.
- FOX, H. (1997) *Pathology of the placenta*, London, W. B. Saunders.
- FUJIKURA, T. & CARLETON, J. H. (1968) Unilateral thickening of fetal arteries on the placenta resembling arteriosclerosis. *Am J Obstet Gynecol*, 100, 843-5.

- FUJIKURA, T. & HOSODA, Y. (1990) Unilateral thickening of placental fetal veins. *Placenta*, 11, 241-5.
- GARCIA-CALVO, M., KNAUS, H. G., MCMANUS, O. B., GIANGIACOMO, K. M., KACZOROWSKI, G. J. & GARCIA, M. L. (1994) Purification and reconstitution of the high-conductance, calcium-activated potassium channel from tracheal smooth muscle. *J Biol Chem*, 269, 676-82.
- GARDENER, M. J., JOHNSON, I. T., BURNHAM, M. P., EDWARDS, G., HEAGERTY, A. M. & WESTON, A. H. (2004) Functional evidence of a role for two-pore domain potassium channels in rat mesenteric and pulmonary arteries. *Br J Pharmacol*, 142, 192-202.
- GARDINER, S. M., COMPTON, A. M., KEMP, P. A. & BENNETT, T. (1991) Effects of NG-nitro-L-arginine methyl ester or indomethacin on differential regional and cardiac haemodynamic actions of arginine vasopressin and lysine vasopressin in conscious rats. *Br J Pharmacol*, 102, 65-72.
- GARDOSI, J., CHANG, A., KALYAN, B., SAHOTA, D. & SYMONDS, E. M. (1992) Customised antenatal growth charts. *Lancet*, 339, 283-7.
- GARDOSI, J., MONGELLI, M., WILCOX, M. & CHANG, A. (1995) An adjustable fetal weight standard. *Ultrasound Obstet Gynecol*, 6, 168-74.
- GARLAND, C. J., PLANE, F., KEMP, B. K. & COCKS, T. M. (1995) Endothelium-dependent hyperpolarization: a role in the control of vascular tone. *Trends Pharmacol Sci*, 16, 23-30.
- GAROVIC, V. D. & HAYMAN, S. R. (2007) Hypertension in pregnancy: an emerging risk factor for cardiovascular disease. *Nat Clin Pract Nephrol*, 3, 613-22.
- GASSMANN, M., GRENACHER, B., ROHDE, B. & VOGEL, J. (2009) Quantifying Western blots: pitfalls of densitometry. *Electrophoresis*, 30, 1845-55.
- GAUS, G., DEMIR-WEUSTEN, A. Y., SCHMITZ, U., BOSE, P., KAUFMANN, P., HUPPERTZ, B. & FRANK, H. G. (2002) Extracellular pH modulates the secretion of fibronectin isoforms by human trophoblast. *Acta Histochem*, 104, 51-63.
- GEBREMEDHIN, D., LANGE, A. R., LOWRY, T. F., TAHERI, M. R., BIRKS, E. K., HUDETZ, A. G., NARAYANAN, J., FALCK, J. R., OKAMOTO, H., ROMAN, R. J., NITHIPATIKOM, K., CAMPBELL, W. B. & HARDER, D. R. (2000) Production of 20-HETE and its role in autoregulation of cerebral blood flow. *Circ Res*, 87, 60-5.
- GITTERMAN, D. P., WILSON, J. & RANDALL, A. D. (2005) Functional properties and pharmacological inhibition of ASIC channels in the human SJ-RH30 skeletal muscle cell line. *J Physiol*, 562, 759-69.
- GOLDENBERG, R. L., CULHANE, J. F., IAMS, J. D. & ROMERO, R. (2008) Epidemiology and causes of preterm birth. *Lancet*, 371, 75-84.
- GOLDENBERG, R. L., IAMS, J. D., MIODOVNIK, M., VAN DORSTEN, J. P., THURNAU, G., BOTTOMS, S., MERCER, B. M., MEIS, P. J., MOAWAD, A. H., DAS, A., CARITIS, S. N. & MCNELLIS, D. (1996) The preterm prediction study: risk factors in twin gestations. National Institute of Child Health and Human Development Maternal-Fetal Medicine Units Network. *Am J Obstet Gynecol*, 175, 1047-53.

- GOLDSTEIN, S. A., BAYLISS, D. A., KIM, D., LESAGE, F., PLANT, L. D. & RAJAN, S. (2005) International Union of Pharmacology. LV. Nomenclature and molecular relationships of two-P potassium channels. *Pharmacol Rev*, 57, 527-40.
- GONZALEZ, J. A., JENSEN, L. T., DOYLE, S. E., MIRANDA-ANAYA, M., MENAKER, M., FUGGER, L., BAYLISS, D. A. & BURDAKOV, D. (2009) Deletion of TASK1 and TASK3 channels disrupts intrinsic excitability but does not abolish glucose or pH responses of orexin/hypocretin neurons. *Eur J Neurosci*, 30, 57-64.
- GRANGER, J. P., ALEXANDER, B. T., LLINAS, M. T., BENNETT, W. A. & KHALIL, R. A. (2002) Pathophysiology of preeclampsia: linking placental ischemia/hypoxia with microvascular dysfunction. *Microcirculation*, 9, 147-60.
- GRIFFITH, O. W. & KILBOURN, R. G. (1996) Nitric oxide synthase inhibitors: amino acids. *Methods Enzymol*, 268, 375-92.
- GRUSS, M., MATHIE, A., LIEB, W. R. & FRANKS, N. P. (2004) The two-pore-domain K(+) channels TREK-1 and TASK-3 are differentially modulated by copper and zinc. *Mol Pharmacol*, 66, 530-7.
- GUIET-BARA, A., IBRAHIM, B., LEVETEAU, J. & BARA, M. (1999) Calcium channels, potassium channels and membrane potential of smooth muscle cells of human allantochoial placental vessels. *Bioelectrochem Bioenerg*, 48, 407-13.
- GURNEY, A. M., OSIPENKO, O. N. & MACMILLAN, D. (2003) Two-pore domain potassium channel, TASK-1, in pulmonary artery smooth muscle cells. *Circ Res*, 14, 957-964.
- GUTTERMAN, D. D., MIURA, H. & LIU, Y. (2005) Redox modulation of vascular tone: focus of potassium channel mechanisms of dilation. *Arterioscler Thromb Vasc Biol*, 25, 671-8.
- HALL, S. E., HAN, W. C., HARRIS, D. N., HEDBERG, A. & OGLETREE, M. L. (1989) 9,11-Epoxy-9-homo-14-thiaprost-5-enoic acid derivatives: potent thromboxane A2 antagonists. *J Med Chem*, 32, 974-84.
- HALPERN, W., MULVANY, M. J. & WARSHAW, D. M. (1978) Mechanical properties of smooth muscle cells in the walls of arterial resistance vessels. *J Physiol*, 275, 85-101.
- HALPERN, W., OSOL, G. & COY, G. S. (1984) Mechanical behavior of pressurized in vitro prearteriolar vessels determined with a video system. *Ann Biomed Eng*, 12, 463-79.
- HAMPL, V., BIBOVA, J., STRANAK, Z., WU, X., MICHELAKIS, E. D., HASHIMOTO, K. & ARCHER, S. L. (2002) Hypoxic fetoplacental vasoconstriction in humans is mediated by potassium channel inhibition. *Am J Physiol Heart Circ Physiol*, 283, H2440-9.
- HAMPL, V. & JAKOUBEK, V. (2009) Regulation of fetoplacental vascular bed by hypoxia. *Physiol Res*, 58 Suppl 2, S87-93.
- HARTNESS, M. E., LEWIS, A., SEARLE, G. J., O'KELLY, I., PEERS, C. & KEMP, P. J. (2001) Combined antisense and pharmacological approaches implicate

- hTASK as an airway O(2) sensing K(+) channel. *J Biol Chem*, 276, 26499-508.
- HAY, W. W., JR. (1995) Regulation of placental metabolism by glucose supply. *Reprod Fertil Dev*, 7, 365-75.
- HEDBERG, A., MENTO, P. F., LIU, E. C., HOLLANDER, A. M. & WILKES, B. M. (1989) Evidence for functional thromboxane A₂-prostaglandin H₂ receptors in human placenta. *Am J Physiol*, 256, E256-63.
- HODGKIN, A. L. & HUXLEY, A. F. (1952) Currents carried by sodium and potassium ions through the membrane of the giant axon of *Loligo*. *J Physiol*, 116, 449-72.
- HOFFMAN, G. E., LE, W. W. & SITA, L. V. (2008) The importance of titrating antibodies for immunocytochemical methods. *Curr Protoc Neurosci*, Chapter 2, Unit 2 12.
- HOLZER, P. (2004) Vanilloid receptor TRPV1: hot on the tongue and inflaming the colon. *Neurogastroenterol Motil*, 16, 697-9.
- HOLZER, P. (2009) Acid-sensitive ion channels and receptors. *Handb Exp Pharmacol*, 283-332.
- HONORE, E. (2007) The neuronal background K₂P channels: focus on TREK1. *Nat Rev Neurosci*, 8, 251-61.
- HOWARD, R., HOSOKAWA, T. & MAGUIRE, M. (1984) Hypoxia-induced fetoplacental vasoconstriction in cotyledons of human term placentas: antagonism by selected drugs. *Pharmacologist*, 26, 144.
- HOWARD, R. B. (1987) Control of human placental blood flow. *Med Hypotheses*, 23, 51-8.
- HUPPERTZ, B. (2007) The feto-maternal interface: setting the stage for potential immune interactions. *Semin Immunopathol*, 29, 83-94.
- HUPPERTZ, B., ABE, E., MURTHI, P., NAGAMATSU, T., SZUKIEWICZ, D. & SALAFIA, C. (2007) Placental angiogenesis, maternal and fetal vessels--a workshop report. *Placenta*, 28 Suppl A, S94-6.
- HUPPERTZ, B., KINGDOM, J., CANIGGIA, I., DESOYE, G., BLACK, S., KORR, H. & KAUFMANN, P. (2003) Hypoxia favours necrotic versus apoptotic shedding of placental syncytiotrophoblast into the maternal circulation. *Placenta*, 24, 181-90.
- HUSSAIN, K. & COSGROVE, K. E. (2005) From congenital hyperinsulinism to diabetes mellitus: the role of pancreatic beta-cell KATP channels. *Pediatr Diabetes*, 6, 103-13.
- JAKOUBEK, V., BIBOVA, J. & HAMPL, V. (2006) Voltage-gated calcium channels mediate hypoxic vasoconstriction in the human placenta. *Placenta*, 27, 1030-3.
- JANSSON, T. & POWELL, T. L. (2007) Role of the placenta in fetal programming: underlying mechanisms and potential interventional approaches. *Clin Sci (Lond)*, 113, 1-13.
- JAUNIAUX, E., WATSON, A. L., HEMPSTOCK, J., BAO, Y. P., SKEPPER, J. N. & BURTON, G. J. (2000) Onset of maternal arterial blood flow and placental oxidative stress. A possible factor in human early pregnancy failure. *Am J Pathol*, 157, 2111-22.

- JEWSBURY, S., BAKER, P. N. & WAREING, M. (2007) Relaxation of human placental arteries and veins by ATP-sensitive potassium channel openers. *Eur J Clin Invest*, 37, 65-72.
- JOVANOVIĆ, A., GRBOVIĆ, L. & TULIĆ, I. (1994a) Endothelium-dependent relaxation in response to acetylcholine in the human uterine artery. *Eur J Pharmacol*, 256, 131-9.
- JOVANOVIĆ, A., GRBOVIĆ, L. & TULIĆ, I. (1994b) L-arginine induces relaxation of human uterine artery with both intact and denuded endothelium. *Eur J Pharmacol*, 256, 103-7.
- JOVANOVIĆ, A., GRBOVIĆ, L. & TULIĆ, I. (1994c) Predominant role for nitric oxide in the relaxation induced by acetylcholine in human uterine artery. *Hum Reprod*, 9, 387-93.
- KACZOROWSKI, G. J. & GARCIA, M. L. (1999) Pharmacology of voltage-gated and calcium-activated potassium channels. *Curr Opin Chem Biol*, 3, 448-58.
- KANG, D., HAN, J., TALLEY, E. M., BAYLISS, D. A. & KIM, D. (2004) Functional expression of TASK-1/TASK-3 heteromers in cerebellar granule cells. *J Physiol*, 554, 64-77.
- KAUFMANN, P. (1982) Development and differentiation of the human placental villous tree. *Bibl Anat*, 29-39.
- KAUFMANN, P., MAYHEW, T. M. & CHARNOCK-JONES, D. S. (2004) Aspects of human fetoplacental vasculogenesis and angiogenesis. II. Changes during normal pregnancy. *Placenta*, 25, 114-26.
- KAUFMANN, P., SEN, D. K. & SCHWEIKHART, G. (1979) Classification of human placental villi. I. Histology. *Cell Tissue Res*, 200, 409-23.
- KELLY, B., STONE, S. & POSTON, L. (2000) Cardiovascular adaptation to pregnancy: the role of altered vascular structure. *Fetal and Maternal Medicine Review* 11, 105-116.
- KETCHUM, K. A., JOINER, W. J., SELLERS, A. J., KACZMAREK, L. K. & GOLDSTEIN, S. A. (1995) A new family of outwardly rectifying potassium channel proteins with two pore domains in tandem. *Nature*, 376, 690-5.
- KHALIL, R. A. & GRANGER, J. P. (2002) Vascular mechanisms of increased arterial pressure in preeclampsia: lessons from animal models. *Am J Physiol Regul Integr Comp Physiol*, 283, R29-45.
- KHAN, R. N., SMITH, S. K., MORRISON, J. J. & ASHFORD, M. L. (1993) Properties of large-conductance K⁺ channels in human myometrium during pregnancy and labour. *Proc Biol Sci*, 251, 9-15.
- KHAN, R. N., SMITH, S. K., MORRISON, J. J. & ASHFORD, M. L. (1997) Ca²⁺ dependence and pharmacology of large-conductance K⁺ channels in nonlabor and labor human uterine myocytes. *Am J Physiol*, 273, C1721-31.
- KIERNAN, M. F., BARRIE, A., SZKOLAR, J., MILLS, T. A. & WAREING, M. (2010) Functional evidence for oxygen-sensitive voltage-gated potassium channels in human placental vasculature. *Placenta*, 31, 553-5.
- KIM, Y., BANG, H. & KIM, D. (1999) TBAK-1 and TASK-1, two-pore K(+) channel subunits: kinetic properties and expression in rat heart. *Am J Physiol*, 277, H1669-78.

- KING, R. G., GUDE, N. M., DI IULIO, J. L. & BRENNECKE, S. P. (1995) Regulation of human placental fetal vessel tone: role of nitric oxide. *Reprod Fertil Dev*, 7, 1407-11.
- KINGDOM, J., HUPPERTZ, B., SEAWARD, G. & KAUFMANN, P. (2000) Development of the placental villous tree and its consequences for fetal growth. *Eur J Obstet Gynecol Reprod Biol*, 92, 35-43.
- KINGDOM, J. C. & KAUFMANN, P. (1999) Oxygen and placental vascular development. *Adv Exp Med Biol*, 474, 259-75.
- KINGDOM, J. C., MACARA, L. M. & WHITTLE, M. J. (1994) Fetoplacental circulation in health and disease. *Arch Dis Child Fetal Neonatal Ed*, 70, F161-3.
- KLEINER-ASSAF, A., JAFFA, A. J. & ELAD, D. (1999) Hemodynamic model for analysis of Doppler ultrasound indexes of umbilical blood flow. *Am J Physiol*, 276, H2204-14.
- KO, E. A., HAN, J., JUNG, I. D. & PARK, W. S. (2008) Physiological roles of K⁺ channels in vascular smooth muscle cells. *J Smooth Muscle Res*, 44, 65-81.
- KOROVKINA, V. P. & ENGLAND, S. K. (2002) Molecular diversity of vascular potassium channel isoforms. *Clin Exp Pharmacol Physiol*, 29, 317-23.
- KOSTRZEWSKA, A., MODZELEWSKA, B., KLESZCZEWSKI, T. & BATRA, S. (2008) Effect of nitric oxide on responses of the human uterine arteries to vasopressin. *Vascul Pharmacol*, 48, 9-13.
- KRISCHER, S. M., EISENMANN, M. & MUELLER, M. J. (1998) Transport of arachidonic acid across the neutrophil plasma membrane via a protein-facilitated mechanism. *Biochemistry*, 37, 12884-91.
- KUBLICKIENE, K. R., KUBLICKAS, M., LINDBLOM, B., LUNELL, N. O. & NISELL, H. (1997) A comparison of myogenic and endothelial properties of myometrial and omental resistance vessels in late pregnancy. *Am J Obstet Gynecol*, 176, 560-6.
- KULANTHAIVEL, P., FURESZ, T. C., MOE, A. J., SMITH, C. H., MAHESH, V. B., LEIBACH, F. H. & GANAPATHY, V. (1992) Human placental syncytiotrophoblast expresses two pharmacologically distinguishable types of Na⁽⁺⁾-H⁺ exchangers, NHE-1 in the maternal-facing (brush border) membrane and NHE-2 in the fetal-facing (basal) membrane. *Biochem J*, 284 (Pt 1), 33-8.
- LAEMMLI, U. K. (1970) Cleavage of structural proteins during the assembly of the head of bacteriophage T4. *Nature*, 227, 680-5.
- LAURITZEN, I., CHEMIN, J., HONORE, E., JODAR, M., GUY, N., LAZDUNSKI, M. & JANE PATEL, A. (2005) Cross-talk between the mechano-gated K2P channel TREK-1 and the actin cytoskeleton. *EMBO Rep*, 6, 642-8.
- LAWSON, K. (1996) Potassium channel activation: a potential therapeutic approach? *Pharmacol Ther*, 70, 39-63.
- LEE, H. Y., BARDINI, M. & BURNSTOCK, G. (2000) Distribution of P2X receptors in the urinary bladder and the ureter of the rat. *J Urol*, 163, 2002-7.
- LEIK, C. E., WILLEY, A., GRAHAM, M. F. & WALSH, S. W. (2004) Isolation and culture of arterial smooth muscle cells from human placenta. *Hypertension*, 43, 837-40.

- LESAGE, F. (2003) Pharmacology of neuronal background potassium channels. *Neuropharmacology*, 44, 1-7.
- LESAGE, F., GUILLEMARE, E., FINK, M., DUPRAT, F., LAZDUNSKI, M., ROMEY, G. & BARHANIN, J. (1996) TWIK-1, a ubiquitous human weakly inward rectifying K⁺ channel with a novel structure. *Embo J*, 15, 1004-11.
- LESAGE, F., LAURITZEN, I., DUPRAT, F., REYES, R., FINK, M., HEURTEAUX, C. & LAZDUNSKI, M. (1997) The structure, function and distribution of the mouse TWIK-1 K⁺ channel. *FEBS Lett*, 402, 28-32.
- LESAGE, F. & LAZDUNSKI, M. (2000) Molecular and functional properties of two-pore-domain potassium channels. *Am J Physiol Renal Physiol*, 279, F793-801.
- LESAGE, F., MATTEI, M., FINK, M., BARHANIN, J. & LAZDUNSKI, M. (1996) Assignment of the human weak inward rectifier K⁺ channel TWIK-1 gene to chromosome 1q42-q43. *Genomics*, 34, 153-5.
- LESAGE, F., TERRENOIRE, C., ROMEY, G. & LAZDUNSKI, M. (2000) Human TREK2, a 2P domain mechano-sensitive K⁺ channel with multiple regulations by polyunsaturated fatty acids, lysophospholipids, and Gs, Gi, and Gq protein-coupled receptors. *J Biol Chem*, 275, 28398-405.
- LIN, W., BURKS, C. A., HANSEN, D. R., KINNAMON, S. C. & GILBERTSON, T. A. (2004) Taste receptor cells express pH-sensitive leak K⁺ channels. *J Neurophysiol*, 92, 2909-19.
- LIU, B., ARULKUMARAN, S., HILL, S. J. & KHAN, R. N. (2003) Comparison of potassium currents in human decidua before and after the onset of labor. *Biol Reprod*, 68, 2281-8.
- LIU, B., SUN, X., ZHU, Y., GAN, L., XU, H. & YANG, X. (2010) Biphasic effects of H₂O₂ on BK(Ca) channels. *Free Radic Res*.
- LIU, Y., HUDETZ, A. G., KNAUS, H. G. & RUSCH, N. J. (1998) Increased expression of Ca²⁺-sensitive K⁺ channels in the cerebral microcirculation of genetically hypertensive rats: evidence for their protection against cerebral vasospasm. *Circ Res*, 82, 729-37.
- LODISH, H., BERK, A. & ZIPURSKY, S. (Eds.) (2000) *Molecular Cell Biology*, New York, WH Freeman.
- LOH, S. F., WOODWORTH, A. & YEO, G. S. (1998) Umbilical cord blood gas analysis at delivery. *Singapore Med J*, 39, 151-5.
- LOPEZ-BARNEO, J., PARDAL, R., MONTORO, R. J., SMANI, T., GARCIA-HIRSCHFELD, J. & URENA, J. (1999) K⁺ and Ca²⁺ channel activity and cytosolic [Ca²⁺] in oxygen-sensing tissues. *Respir Physiol*, 115, 215-27.
- LU, Z., GAO, J., ZUCKERMAN, J., MATHIAS, R. T., GAUDETTE, G., KRUKENKAMP, I. & COHEN, I. S. (2007) Two-pore K⁺ channels, NO and metabolic inhibition. *Biochem Biophys Res Commun*, 363, 194-6.
- LYALL, F. (2005) Priming and remodelling of human placental bed spiral arteries during pregnancy--a review. *Placenta*, 26 Suppl A, S31-6.
- LYALL, F. (2006) Mechanisms regulating cytotrophoblast invasion in normal pregnancy and pre-eclampsia. *Aust N Z J Obstet Gynaecol*, 46, 266-73.
- MAENHAUT, N. & VAN DE VOORDE, J. (2011) Effect of hypoxia in mice mesenteric arteries surrounded by adipose tissue. *Acta Physiol (Oxf)*.

- MAIGAARD, S., FORMAN, A. & ANDERSSON, K. E. (1986) Relaxant and contractile effects of some amines and prostanoids in myometrial and vascular smooth muscle within the human uteroplacental unit. *Acta Physiol Scand*, 128, 33-40.
- MAINGRET, F., FOSSET, M., LESAGE, F., LAZDUNSKI, M. & HONORE, E. (1999) TRAAK is a mammalian neuronal mechano-gated K⁺ channel. *J Biol Chem*, 274, 1381-7.
- MAINGRET, F., LAURITZEN, I., PATEL, A. J., HEURTEAUX, C., REYES, R., LESAGE, F., LAZDUNSKI, M. & HONORE, E. (2000) TREK-1 is a heat-activated background K(+) channel. *Embo J*, 19, 2483-91.
- MAINGRET, F., PATEL, A. J., LESAGE, F., LAZDUNSKI, M. & HONORE, E. (1999) Mechano- or acid stimulation, two interactive modes of activation of the TREK-1 potassium channel. *J Biol Chem*, 274, 26691-6.
- MAINGRET, F., PATEL, A. J., LESAGE, F., LAZDUNSKI, M. & HONORE, E. (2000) Lysophospholipids open the two-pore domain mechano-gated K(+) channels TREK-1 and TRAAK. *J Biol Chem*, 275, 10128-33.
- MARIN, J., REVIRIEGO, J., FERNANDEZ-ALFONSO, M. S. & GUERRA, P. (1990) Effect of nifedipine in arterial vasculature of human placenta. *Gen Pharmacol*, 21, 629-33.
- MARTIN, A., GAILLARD, M., MIOT, S., RIETHMULLER, D. & SCHAAAL, J. P. (2003) [Lactate measurements and acid-base balance in cord blood]. *J Gynecol Obstet Biol Reprod (Paris)*, 32, 713-9.
- MATHAROO-BALL, B., ASHFORD, M. L., ARULKUMARAN, S. & KHAN, R. N. (2003) Down-regulation of the alpha- and beta-subunits of the calcium-activated potassium channel in human myometrium with parturition. *Biol Reprod*, 68, 2135-41.
- MATHIE, A., SUTTON, G. L., CLARKE, C. E. & VEALE, E. L. (2006) Zinc and copper: pharmacological probes and endogenous modulators of neuronal excitability. *Pharmacol Ther*, 111, 567-83.
- MAWISSA, D., JAUNIAUX, E. & RODESCH, F. (1993) [Evaluation of umbilical Doppler parameters in relation to placental morphology in the third trimester of normal pregnancy]. *J Gynecol Obstet Biol Reprod (Paris)*, 22, 179-83.
- MAYNARD, S., EPSTEIN, F. H. & KARUMANCHI, S. A. (2007) Preeclampsia and Angiogenic Imbalance. *Annu Rev Med*.
- MAYNARD, S. E., MIN, J. Y., MERCHAN, J., LIM, K. H., LI, J., MONDAL, S., LIBERMANN, T. A., MORGAN, J. P., SELLKE, F. W., STILLMAN, I. E., EPSTEIN, F. H., SUKHATME, V. P. & KARUMANCHI, S. A. (2003) Excess placental soluble fms-like tyrosine kinase 1 (sFlt1) may contribute to endothelial dysfunction, hypertension, and proteinuria in preeclampsia. *J Clin Invest*, 111, 649-58.
- MCCARTHY, A. L., TAYLOR, P., GRAVES, J., RAJU, S. K. & POSTON, L. (1994) Endothelium-dependent relaxation of human resistance arteries in pregnancy. *Am J Obstet Gynecol*, 171, 1309-15.
- MCCARTHY, A. L., WOOLFSON, R. G., EVANS, B. J., DAVIES, D. R., RAJU, S. K. & POSTON, L. (1994) Functional characteristics of small placental arteries. *Am J Obstet Gynecol*, 170, 945-51.

- MCINTOSH, T. K., SMITH, D. H., VODDI, M., PERRI, B. R. & STUTZMANN, J. M. (1996) Riluzole, a novel neuroprotective agent, attenuates both neurologic motor and cognitive dysfunction following experimental brain injury in the rat. *J Neurotrauma*, 13, 767-80.
- MCINTYRE, C. A., WILLIAMS, B. C., LINDSAY, R. M., MCKNIGHT, J. A. & HADOKE, P. W. (1998) Preservation of vascular function in rat mesenteric resistance arteries following cold storage, studied by small vessel myography. *Br J Pharmacol*, 123, 1555-60.
- MCPHERSON, G. A. (1992) Assessing vascular reactivity of arteries in the small vessel myograph. *Clin Exp Pharmacol Physiol*, 19, 815-25.
- MCQUILLAN, L. P., LEUNG, G. K., MARSDEN, P. A., KOSTYK, S. K. & KOUREMBANAS, S. (1994) Hypoxia inhibits expression of eNOS via transcriptional and posttranscriptional mechanisms. *Am J Physiol*, 267, H1921-7.
- MEDHURST, A. D., RENNIE, G., CHAPMAN, C. G., MEADOWS, H., DUCKWORTH, M. D., KELSELL, R. E., GLOGER, II & PANGALOS, M. N. (2001) Distribution analysis of human two pore domain potassium channels in tissues of the central nervous system and periphery. *Brain Res Mol Brain Res*, 86, 101-14.
- MEERA, P., WALLNER, M., SONG, M. & TORO, L. (1997) Large conductance voltage- and calcium-dependent K⁺ channel, a distinct member of voltage-dependent ion channels with seven N-terminal transmembrane segments (S0-S6), an extracellular N terminus, and an intracellular (S9-S10) C terminus. *Proc Natl Acad Sci U S A*, 94, 14066-71.
- MEUTH, S. G., BITTNER, S., MEUTH, P., SIMON, O. J., BUDDE, T. & WIENDL, H. (2008) TWIK-related acid-sensitive K⁺ channel 1 (TASK1) and TASK3 critically influence T lymphocyte effector functions. *J Biol Chem*, 283, 14559-70.
- MILLS, T. A., WAREING, M., SHENNAN, A. H., POSTON, L., BAKER, P. N. & GREENWOOD, S. L. (2009) Acute and chronic modulation of placental chorionic plate artery reactivity by reactive oxygen species. *Free Radic Biol Med*, 47, 159-66.
- MOLL, W. (2001) [Physiological cardiovascular adaptation in pregnancy--its significance for cardiac diseases]. *Z Kardiol*, 90 Suppl 4, 2-9.
- MONDON, F., DOUALLA-BELL KOTTO MAKAKA, F., SABRY, S. & FERRE, F. (1995) Endothelin-induced phosphoinositide hydrolysis in the muscular layer of stem villi vessels of human term placenta. *Eur J Endocrinol*, 133, 606-12.
- MOORE, R. J., ONG, S. S., TYLER, D. J., DUCKETT, R., BAKER, P. N., DUNN, W. R., JOHNSON, I. R. & GOWLAND, P. A. (2007) Spiral artery blood volume in normal pregnancies and those compromised by pre-eclampsia. *NMR Biomed*.
- MOUTQUIN, J. M. (2003) Classification and heterogeneity of preterm birth. *Bjog*, 110 Suppl 20, 30-3.
- MULVANY, M. J. (2007) Small artery structure: time to take note? *Am J Hypertens*, 20, 853-4.

- MULVANY, M. J. & AALKJAER, C. (1990) Structure and function of small arteries. *Physiol Rev*, 70, 921-61.
- MULVANY, M. J. & HALPERN, W. (1977) Contractile properties of small arterial resistance vessels in spontaneously hypertensive and normotensive rats. *Circ Res*, 41, 19-26.
- MULVANY, M. J. & WARSHAW, D. M. (1979) The active tension-length curve of vascular smooth muscle related to its cellular components. *J Gen Physiol*, 74, 85-104.
- MURRY, C. E., JENNINGS, R. B. & REIMER, K. A. (1986) Preconditioning with ischemia: a delay of lethal cell injury in ischemic myocardium. *Circulation*, 74, 1124-36.
- MYATT, L. (1992) Control of vascular resistance in the human placenta. *Placenta*, 13, 329-41.
- MYATT, L. (2002) Role of placenta in preeclampsia. *Endocrine*, 19, 103-11.
- MYATT, L., BREWER, A. S., LANGDON, G. & BROCKMAN, D. E. (1992) Attenuation of the vasoconstrictor effects of thromboxane and endothelin by nitric oxide in the human fetal-placental circulation. *Am J Obstet Gynecol*, 166, 224-30.
- MYATT, L. & WEBSTER, R. P. (2009) Vascular biology of preeclampsia. *J Thromb Haemost*, 7, 375-84.
- NICOLAIDES, K. H., ECONOMIDES, D. L. & SOOTHILL, P. W. (1989) Blood gases, pH, and lactate in appropriate- and small-for-gestational-age fetuses. *Am J Obstet Gynecol*, 161, 996-1001.
- NICOLAS, M. T., LESAGE, F., REYES, R., BARHANIN, J. & DEMEMES, D. (2004) Localization of TREK-1, a two-pore-domain K⁺ channel in the peripheral vestibular system of mouse and rat. *Brain Res*, 1017, 46-52.
- NIKKELS, P. (2007) Placenta pathology associated with maturation abnormalities and late intra uterine fetal death *Forum of pathology* Brussels, .
- OTTER, D. & AUSTIN, C. (1999) Mechanisms of hypoxic vasodilatation of isolated rat mesenteric arteries: a comparison with metabolic inhibition. *J Physiol*, 516 (Pt 1), 249-59.
- PADDOCK, S. W. (2000) Principles and practices of laser scanning confocal microscopy. *Mol Biotechnol*, 16, 127-49.
- PANG, D. S., ROBLEDO, C. J., CARR, D. R., GENT, T. C., VYSSOTSKI, A. L., CALEY, A., ZECHARIA, A. Y., WIDEN, W., BRICKLEY, S. G. & FRANKS, N. P. (2009) An unexpected role for TASK-3 potassium channels in network oscillations with implications for sleep mechanisms and anesthetic action. *Proc Natl Acad Sci U S A*, 106, 17546-51.
- PARDI, G., CETIN, I., MARCONI, A. M., LANFRANCHI, A., BOZZETTI, P., FERRAZZI, E., BUSCAGLIA, M. & BATTAGLIA, F. C. (1993) Diagnostic value of blood sampling in fetuses with growth retardation. *N Engl J Med*, 328, 692-6.
- PARKINGTON, H. C., TONTA, M. A., BRENNECKE, S. P. & COLEMAN, H. A. (1999) Contractile activity, membrane potential, and cytoplasmic calcium in human uterine smooth muscle in the third trimester of pregnancy and during labor. *Am J Obstet Gynecol*, 181, 1445-51.

- PATEL, A. J. & HONORE, E. (2001) Properties and modulation of mammalian 2P domain K⁺ channels. *Trends Neurosci*, 24, 339-46.
- PATEL, A. J., HONORE, E., LESAGE, F., FINK, M., ROMÉY, G. & LAZDUNSKI, M. (1999) Inhalational anesthetics activate two-pore-domain background K⁺ channels. *Nat Neurosci*, 2, 422-6.
- PATEL, A. J., HONORE, E., MAINGRET, F., LESAGE, F., FINK, M., DUPRAT, F. & LAZDUNSKI, M. (1998) A mammalian two pore domain mechano-gated S-like K⁺ channel. *Embo J*, 17, 4283-90.
- PATEL, A. J., MAINGRET, F., MAGNONE, V., FOSSET, M., LAZDUNSKI, M. & HONORE, E. (2000) TWIK-2, an inactivating 2P domain K⁺ channel. *J Biol Chem*, 275, 28722-30.
- PERNEY, T. M. & KACZMAREK, L. K. (1991) The molecular biology of K⁺ channels. *Curr Opin Cell Biol*, 3, 663-70.
- PIJNENBORG, R., ANTHONY, J., DAVEY, D. A., REES, A., TILTMAN, A., VERCRUYSE, L. & VAN ASSCHE, A. (1991) Placental bed spiral arteries in the hypertensive disorders of pregnancy. *Br J Obstet Gynaecol*, 98, 648-55.
- PIJNENBORG, R., DIXON, G., ROBERTSON, W. B. & BROSENS, I. (1980) Trophoblastic invasion of human decidua from 8 to 18 weeks of pregnancy. *Placenta*, 1, 3-19.
- PIJNENBORG, R., ROBERTSON, W. B., BROSENS, I. & DIXON, G. (1981) Review article: trophoblast invasion and the establishment of haemochorial placentation in man and laboratory animals. *Placenta*, 2, 71-91.
- PIJNENBORG, R., VERCRUYSE, L. & HANSSENS, M. (2006) The uterine spiral arteries in human pregnancy: facts and controversies. *Placenta*, 27, 939-58.
- PLANE, F., JOHNSON, R., KERR, P., WIEHLER, W., THORNELOE, K., ISHII, K., CHEN, T. & COLE, W. (2005) Heteromultimeric Kv1 channels contribute to myogenic control of arterial diameter. *Circ Res*, 96, 216-24.
- POLIN, R., FOX, W. & ABMAN, S. (2004) *Fetal and neonatal physiology* Philadelphia, Saunders.
- POSTON, L., MCCARTHY, A. L. & RITTER, J. M. (1995) Control of vascular resistance in the maternal and feto-placental arterial beds. *Pharmacol Ther*, 65, 215-39.
- POUNTNEY, D. J., GULKAROV, I., VEGA-SAEENZ DE MIERA, E., HOLMES, D., SAGANICH, M., RUDY, B., ARTMAN, M. & COETZEE, W. A. (1999) Identification and cloning of TWIK-originated similarity sequence (TOSS): a novel human 2-pore K⁺ channel principal subunit. *FEBS Lett*, 450, 191-6.
- PRYSTOWSKY, H. (1961) Physiology of the placenta. *Annu Rev Med*, 12, 281-8.
- RAMSEY, E. M. (1962) Circulation in the intervillous space of the primate placenta. *Am J Obstet Gynecol*, 84, 1649-63.
- RESNIK, E., HERRON, J., FU, R., IVY, D. D. & CORNFIELD, D. N. (2006) Oxygen tension modulates the expression of pulmonary vascular BKCa channel alpha- and beta-subunits. *Am J Physiol Lung Cell Mol Physiol*, 290, L761-L768.
- REYES, R., DUPRAT, F., LESAGE, F., FINK, M., SALINAS, M., FARMAN, N. & LAZDUNSKI, M. (1998) Cloning and expression of a novel pH-sensitive two pore domain K⁺ channel from human kidney. *J Biol Chem*, 273, 30863-9.

- REYES, R., LAURITZEN, I., LESAGE, F., ETTAICHE, M., FOSSET, M. & LAZDUNSKI, M. (2000) Immunolocalization of the arachidonic acid and mechanosensitive baseline traak potassium channel in the nervous system. *Neuroscience*, 95, 893-901.
- RICHTER, T. A., DVORYANCHIKOV, G. A., CHAUDHARI, N. & ROPER, S. D. (2004) Acid-sensitive two-pore domain potassium (K2P) channels in mouse taste buds. *J Neurophysiol*, 92, 1928-36.
- ROBERTS, J. M. & LAIN, K. Y. (2002) Recent Insights into the pathogenesis of pre-eclampsia. *Placenta*, 23, 359-72.
- ROBERTS, J. M., TAYLOR, R. N., MUSCI, T. J., RODGERS, G. M., HUBEL, C. A. & MCLAUGHLIN, M. K. (1989) Preeclampsia: an endothelial cell disorder. *Am J Obstet Gynecol*, 161, 1200-4.
- ROBERTS, V. H., GREENWOOD, S. L., ELLIOTT, A. C., SIBLEY, C. P. & WATERS, L. H. (2006) Purinergic receptors in human placenta: evidence for functionally active P2X4, P2X7, P2Y2, and P2Y6. *Am J Physiol Regul Integr Comp Physiol*, 290, R1374-86.
- ROBERTSON, B. E., SCHUBERT, R., HESCHELER, J. & NELSON, M. T. (1993) cGMP-dependent protein kinase activates Ca-activated K channels in cerebral artery smooth muscle cells. *Am J Physiol*, 265, C299-303.
- ROBERTSON, T. P., HAGUE, D., AARONSON, P. I. & WARD, J. P. (2000) Voltage-independent calcium entry in hypoxic pulmonary vasoconstriction of intrapulmonary arteries of the rat. *J Physiol*, 525 Pt 3, 669-80.
- ROBERTSON, W. B., BROSENS, I. A. & DIXON, H. G. (1973) Placental bed vessels. *Am J Obstet Gynecol*, 117, 294-5.
- RODESCH, F., SIMON, P., DONNER, C. & JAUNIAUX, E. (1992) Oxygen measurements in endometrial and trophoblastic tissues during early pregnancy. *Obstet Gynecol*, 80, 283-5.
- ROMO, A., CARCELLER, R. & TOBAJAS, J. (2009) Intrauterine growth retardation (IUGR): epidemiology and etiology. *Pediatr Endocrinol Rev*, 6 Suppl 3, 332-6.
- RYTER, A. (1988) Contribution of new cryomethods to a better knowledge of bacterial anatomy. *Ann Inst Pasteur Microbiol*, 139, 33-44.
- SABRY, S., MONDON, F., FERRE, F. & DINH-XUAN, A. T. (1995a) In vitro contractile and relaxant responses of human resistance placental stem villi arteries of healthy parturients: role of endothelium. *Fundam Clin Pharmacol*, 9, 46-51.
- SABRY, S., MONDON, F., LEVY, M., FERRE, F. & DINH-XUAN, A. T. (1995b) Endothelial modulation of vasoconstrictor responses to endothelin-1 in human placental stem villi small arteries. *Br J Pharmacol*, 115, 1038-42.
- SAND, A., ANDERSSON, E. & FRIED, G. (2006) Nitric oxide donors mediate vasodilation in human placental arteries partly through a direct effect on potassium channels. *Placenta*, 27, 181-90.
- SANDOZ, G., BELL, S. C. & ISACOFF, E. Y. (2011) Optical probing of a dynamic membrane interaction that regulates the TREK1 channel. *Proc Natl Acad Sci U S A*, 108, 2605-10.

- SANDOZ, G., DOUGUET, D., CHATELAIN, F., LAZDUNSKI, M. & LESAGE, F. (2009) Extracellular acidification exerts opposite actions on TREK1 and TREK2 potassium channels via a single conserved histidine residue. *Proc Natl Acad Sci U S A*, 106, 14628-33.
- SAQUETON, C. B., MILLER, R. B., PORTER, V. A., MILLA, C. E. & CORNFIELD, D. N. (1999) NO causes perinatal pulmonary vasodilation through K⁺-channel activation and intracellular Ca²⁺ release. *Am J Physiol*, 276, L925-32.
- SATO, T., COSTA, A. D., SAITO, T., OGURA, T., ISHIDA, H., GARLID, K. D. & NAKAYA, H. (2006) Bepridil, an antiarrhythmic drug, opens mitochondrial KATP channels, blocks sarcolemmal KATP channels, and confers cardioprotection. *J Pharmacol Exp Ther*, 316, 182-8.
- SATO, T., SAITO, T., SAEGUSA, N. & NAKAYA, H. (2005) Mitochondrial Ca²⁺-activated K⁺ channels in cardiac myocytes: a mechanism of the cardioprotective effect and modulation by protein kinase A. *Circulation*, 111, 198-203.
- SAUNDERS, M. (2009) Transplacental transport of nanomaterials. *Wiley Interdiscip Rev Nanomed Nanobiotechnol*, 1, 671-84.
- SCHNEIDER, H., DANKO, J., HUCH, R. & HUCH, A. (1984) Homeostasis of fetal lactate metabolism in late pregnancy and the changes during labor and delivery. *Eur J Obstet Gynecol Reprod Biol*, 17, 183-92.
- SCHWARTZMAN, M. L., FALCK, J. R., YADAGIRI, P. & ESCALANTE, B. (1989) Metabolism of 20-hydroxyecosatetraenoic acid by cyclooxygenase. Formation and identification of novel endothelium-dependent vasoconstrictor metabolites. *J Biol Chem*, 264, 11658-62.
- SCIFRES, C. M. & NELSON, D. M. (2009) Intrauterine growth restriction, human placental development and trophoblast cell death. *J Physiol*, 587, 3453-8.
- SCIFRES, C. M., STAMILIO, D., MACONES, G. A. & ODIBO, A. O. (2009) Predicting perinatal mortality in preterm intrauterine growth restriction. *Am J Perinatol*, 26, 723-8.
- SCOTLAND, R. S., CHAUHAN, S., VALLANCE, P. J. & AHLUWALIA, A. (2001) An endothelium-derived hyperpolarizing factor-like factor moderates myogenic constriction of mesenteric resistance arteries in the absence of endothelial nitric oxide synthase-derived nitric oxide. *Hypertension*, 38, 833-9.
- SEINO, S. & MIKI, T. (2003) Physiological and pathophysiological roles of ATP-sensitive K⁺ channels. *Prog Biophys Mol Biol*, 81, 133-76.
- SEN, C. K. & SEMENZA, G. L. (Eds.) (2004) *Methods in enzymology: Oxygen sensing*
- SERR, D. M., CZACZKES, J. W. & ZUCKERMAN, H. (1963) Comparative studies on uric-acid levels in amniotic fluid, fetal blood, and maternal blood. *Obstet Gynecol*, 21, 551-3.
- SETTLE, P., SIBLEY, C. P., DOUGHTY, I. M., JOHNSTON, T., GLAZIER, J. D., POWELL, T. L., JANSSON, T. & D'SOUZA, S. W. (2006) Placental lactate transporter activity and expression in intrauterine growth restriction. *J Soc Gynecol Investig*, 13, 357-63.
- SHAH, D. S. (2008) Effects of modulators of TASK potassium channels

- on rat pulmonary artery tone. *Bioscience Horizons*, 1, 8.
- SHENG, J. Z. & BRAUN, A. P. (2007) Small- and intermediate-conductance Ca^{2+} -activated K^{+} channels directly control agonist-evoked nitric oxide synthesis in human vascular endothelial cells. *Am J Physiol Cell Physiol*, 293, C458-67.
- SHEPPARD, C. J. & WILSON, T. (1981) The theory of the direct-view confocal microscope. *J Microsc*, 124, 107-17.
- SHI, S. R., KEY, M. E. & KALRA, K. L. (1991) Antigen retrieval in formalin-fixed, paraffin-embedded tissues: an enhancement method for immunohistochemical staining based on microwave oven heating of tissue sections. *J Histochem Cytochem*, 39, 741-8.
- SHIREY, T., ST PIERRE, J. & WINKELMAN, J. (1996) Cord lactate, pH, and blood gases from healthy neonates. *Gynecol Obstet Invest*, 41, 15-9.
- SMIT, M. J. & IYENGAR, R. (1998) Mammalian adenylyl cyclases. *Adv Second Messenger Phosphoprotein Res*, 32, 1-21.
- SMITH, G. L., AUSTIN, C., CRICHTON, C. & WRAY, S. (1998) A review of the actions and control of intracellular pH in vascular smooth muscle. *Cardiovasc Res*, 38, 316-31.
- SOARES, M. J. & HUNT, J. S. (2006) *Placenta and Trophoblast: Methods and protocols*, Totowa, New Jersey, Humana Press.
- SPIERS, A. & PADMANABHAN, N. (2005) A guide to wire myography. *Methods Mol Med*, 108, 91-104.
- STANEK, J. (2009) Acute and chronic placental membrane hypoxic lesions. *Virchows Arch*, 455, 315-22.
- STEINERT, J. R., WYATT, A. W., JACOB, R. & MANN, G. E. (2009) Redox modulation of Ca^{2+} signaling in human endothelial and smooth muscle cells in pre-eclampsia. *Antioxid Redox Signal*.
- STEPHAN, M. & AGNEW, W. S. (1991) Voltage-sensitive Na^{+} channels: motifs, modes and modulation. *Curr Opin Cell Biol*, 3, 676-84.
- STEVENSON, A., YATES, D. M., MANSER, C., DE VOS, K. J., VAGNONI, A., LEIGH, P. N., MCLOUGHLIN, D. M. & MILLER, C. C. (2009) Riluzole protects against glutamate-induced slowing of neurofilament axonal transport. *Neurosci Lett*, 454, 161-4.
- STRIESSNIG, J. (1999) Pharmacology, structure and function of cardiac L-type Ca^{2+} channels. *Cell Physiol Biochem*, 9, 242-69.
- STUTZMANN, J. M., PRATT, J., BORAUD, T. & GROSS, C. (1996) The effect of riluzole on post-traumatic spinal cord injury in the rat. *Neuroreport*, 7, 387-92.
- SWEENEY, M., JONES, C. J., GREENWOOD, S. L., BAKER, P. N. & TAGGART, M. J. (2006) Ultrastructural features of smooth muscle and endothelial cells of isolated isobaric human placental and maternal arteries. *Placenta*, 27, 635-47.
- SWEENEY, M., WAREING, M., MILLS, T. A., BAKER, P. N. & TAGGART, M. J. (2008) Characterisation of tone oscillations in placental and myometrial arteries from normal pregnancies and those complicated by pre-eclampsia and growth restriction. *Placenta*, 29, 356-65.
- SWIETACH, P., CAMELLITI, P., HULIKOVA, A., KOHL, P. & VAUGHAN-JONES, R. D. (2010) Spatial regulation of intracellular pH in multicellular strands of neonatal rat cardiomyocytes. *Cardiovasc Res*, 85, 729-38.

- SYMONDS, E. M. (1981) The renin-angiotensin system in pregnancy. *Obstet Gynecol Annu*, 10, 45-67.
- TAMMARO, P. & ASHCROFT, F. M. (2009) A cytosolic factor that inhibits KATP channels expressed in *Xenopus* oocytes by impairing Mg-nucleotide activation by SUR1. *J Physiol*, 587, 1649-56.
- TANAKA, C., KUWABARA, Y. & SAKAI, T. (1999) Structural identification and characterization of arteries and veins in the placental stem villi. *Anat Embryol (Berl)*, 199, 407-18.
- TANKO, L. B., SIMONSEN, U., FROBERT, O., GREGERSEN, H., BAGGER, J. P. & MIKKELSEN, E. O. (2000) Vascular reactivity to nifedipine and Ca(2+) in vitro: the role of preactivation, wall tension and geometry. *Eur J Pharmacol*, 387, 303-12.
- THOMAS, D., PLANT, L. D., WILKENS, C. M., MCCROSSAN, Z. A. & GOLDSTEIN, S. A. (2008) Alternative translation initiation in rat brain yields K2P2.1 potassium channels permeable to sodium. *Neuron*, 58, 859-70.
- TISELIUS, A. (1937) Electrophoresis of Purified Antibody Preparations. *J Exp Med*, 65, 641-6.
- TOWBIN, H., STAEBELIN, T. & GORDON, J. (1979) Electrophoretic transfer of proteins from polyacrylamide gels to nitrocellulose sheets: procedure and some applications. *Proc Natl Acad Sci U S A*, 76, 4350-4.
- TUFFNELL, D. J., JANKOWICZ, D., LINDOW, S. W., LYONS, G., MASON, G. C., RUSSELL, I. F. & WALKER, J. J. (2005) Outcomes of severe pre-eclampsia/eclampsia in Yorkshire 1999/2003. *Bjog*, 112, 875-80.
- VALERA, S., HUSSY, N., EVANS, R. J., ADAMI, N., NORTH, R. A., SURPRENANT, A. & BUELL, G. (1994) A new class of ligand-gated ion channel defined by P2x receptor for extracellular ATP. *Nature*, 371, 516-9.
- VAN LAAR, J. O., PETERS, C. H., VULLINGS, R., HOUTERMAN, S., BERGMANS, J. W. & OEI, S. G. (2010) Fetal autonomic response to severe acidaemia during labour. *Bjog*, 117, 429-37.
- VAUGHAN-JONES, R. D., SPITZER, K. W. & SWIETACH, P. (2009) Intracellular pH regulation in heart. *J Mol Cell Cardiol*, 46, 318-31.
- VOLOSHYNA, I., BESANA, A., CASTILLO, M., MATOS, T., WEINSTEIN, I. B., MANSUKHANI, M., ROBINSON, R. B., CORDON-CARDO, C. & FEINMARK, S. J. (2008) TREK-1 is a novel molecular target in prostate cancer. *Cancer Res*, 68, 1197-203.
- WALDMANN, R. (2001) Proton-gated cation channels--neuronal acid sensors in the central and peripheral nervous system. *Adv Exp Med Biol*, 502, 293-304.
- WALSH, S. W. (1985) Preeclampsia: an imbalance in placental prostacyclin and thromboxane production. *Am J Obstet Gynecol*, 152, 335-40.
- WANG, Y. & ZHAO, S. (2010) *Vascular Biology of the Placenta*, San Rafael (CA).
- WAREING, M., BAI, X., SEGHER, F., TURNER, C. M., GREENWOOD, S. L., BAKER, P. N., TAGGART, M. J. & FYFE, G. K. (2006) Expression and function of potassium channels in the human placental vasculature. *Am J Physiol Regul Integr Comp Physiol*, 291, R437-46.

- WAREING, M., CROCKER, I. P., WARREN, A. Y., TAGGART, M. J. & BAKER, P. N. (2002) Characterization of small arteries isolated from the human placental chorionic plate. *Placenta*, 23, 400-9.
- WAREING, M., GREENWOOD, S. L. & BAKER, P. N. (2006a) Reactivity of human placental chorionic plate vessels is modified by level of oxygenation: differences between arteries and veins. *Placenta*, 27, 42-8.
- WAREING, M., GREENWOOD, S. L., FYFE, G. K. & BAKER, P. N. (2006b) Reactivity of human placental chorionic plate vessels from pregnancies complicated by intrauterine growth restriction (IUGR). *Biol Reprod*, 75, 518-23.
- WAREING, M., GREENWOOD, S. L., TAGGART, M. J. & BAKER, P. N. (2003) Vasoactive responses of veins isolated from the human placental chorionic plate. *Placenta*, 24, 790-6.
- WARREN, A. Y., HARVEY, L., SHAW, R. W. & KHAN, R. N. (2008) Interleukin-1 beta secretion from cord blood mononuclear cells in vitro involves P2X 7 receptor activation. *Reprod Sci*, 15, 189-94.
- WEIL, M. H. & TANG, W. (1997) Management of acidosis: the role of buffer agents. *Crit Care*, 1, 51-52.
- WESER, H. & KAUFMANN, P. (1978) [Lightmicroscopical and histochemical studies on the chorionic plate of the mature human placenta (author's transl)]. *Arch Gynakol*, 225, 15-30.
- WESTGREN, M., DIVON, M., HORAL, M., INGEMARSSON, I., KUBLICKAS, M., SHIMOJO, N. & NORDSTROM, L. (1995) Routine measurements of umbilical artery lactate levels in the prediction of perinatal outcome. *Am J Obstet Gynecol*, 173, 1416-22.
- WHITLEY, E. & BALL, J. (2002) Statistics review 3: hypothesis testing and P values. *Crit Care*, 6, 222-5.
- WILDMAN, D. E., CHEN, C., EREZ, O., GROSSMAN, L. I., GOODMAN, M. & ROMERO, R. (2006) Evolution of the mammalian placenta revealed by phylogenetic analysis. *Proc Natl Acad Sci U S A*, 103, 3203-8.
- WILLIAMS, J. L., FYFE, G. K., SIBLEY, C. P., BAKER, P. N. & GREENWOOD, S. L. (2008) K⁺ channel inhibition modulates the biochemical and morphological differentiation of human placental cytotrophoblast cells in vitro. *Am J Physiol Regul Integr Comp Physiol*, 295, R1204-13.
- WILSON, G. D., HUNTER, J. T., DERRICK, G. H., AITKEN, W. M. & KRONFELD, D. S. (1977) Fetal and maternal plasma electrolytes, blood gases, and pH in dairy cows during late gestation. *J Dairy Sci*, 60, 1110-6.
- XIAN TAO, L., DYACHENKO, V., ZUZARTE, M., PUTZKE, C., PREISIG-MULLER, R., ISENBERG, G. & DAUT, J. (2006) The stretch-activated potassium channel TREK-1 in rat cardiac ventricular muscle. *Cardiovasc Res*, 69, 86-97.
- XING, Y., ZHANG, Y., STABERNACK, C. R., EGER, E. I., 2ND & GRAY, A. T. (2003) The use of the potassium channel activator riluzole to test whether potassium channels mediate the capacity of isoflurane to produce immobility. *Anesth Analg*, 97, 1020-4, table of contents.

- XU, L., ENYEART, J. A. & ENYEART, J. J. (2001) Neuroprotective agent riluzole dramatically slows inactivation of Kv1.4 potassium channels by a voltage-dependent oxidative mechanism. *J Pharmacol Exp Ther*, 299, 227-37.
- YAMANAKA, A., ISHIKAWA, T. & GOTO, K. (1998) Characterization of endothelium-dependent relaxation independent of NO and prostaglandins in guinea pig coronary artery. *J Pharmacol Exp Ther*, 285, 480-9.
- YANG, Z. W., ZHENG, T., ZHANG, A., ALTURA, B. T. & ALTURA, B. M. (1998) Mechanisms of hydrogen peroxide-induced contraction of rat aorta. *Eur J Pharmacol*, 344, 169-81.
- YOO, M. H., HYUN, H. J., KOH, J. Y. & YOON, Y. H. (2005) Riluzole inhibits VEGF-induced endothelial cell proliferation in vitro and hyperoxia-induced abnormal vessel formation in vivo. *Invest Ophthalmol Vis Sci*, 46, 4780-7.
- YUNG, H. W., CALABRESE, S., HYNX, D., HEMMINGS, B. A., CETIN, I., CHARNOCK-JONES, D. S. & BURTON, G. J. (2008) Evidence of placental translation inhibition and endoplasmic reticulum stress in the etiology of human intrauterine growth restriction. *Am J Pathol*, 173, 451-62.
- ZHOU, M., XU, G., XIE, M., ZHANG, X., SCHOOLS, G. P., MA, L., KIMELBERG, H. K. & CHEN, H. (2009) TWIK-1 and TREK-1 are potassium channels contributing significantly to astrocyte passive conductance in rat hippocampal slices. *J Neurosci*, 29, 8551-64.
- ZHOU, Y., FATHALI, N., LEKIC, T., TANG, J. & ZHANG, J. H. (2009) Glibenclamide improves neurological function in neonatal hypoxia-ischemia in rats. *Brain Res*, 1270, 131-9.
- ZHOU, Y., FISHER, S. J., JANATPOUR, M., GENBACEV, O., DEJANA, E., WHEELLOCK, M. & DAMSKY, C. H. (1997) Human cytotrophoblasts adopt a vascular phenotype as they differentiate. A strategy for successful endovascular invasion? *J Clin Invest*, 99, 2139-51.

Appendix

I. Solution compositions

0.1M PBS working dilution

200ml PBS stock, 300ml 5M NaCl, 770ml H₂O.

0.5M PBS stock

5mM Na₂HPO₄, 5mM NaH₂PO₄, pH 7.2-7.4 with 1M NaOH

10% Ammonium persulphate (AP)

0.1g Ammonium persulphate in 1ml H₂O.

3% H₂O₂

280ml PBS stock, 20ml 30% H₂O₂.

4% w/v Paraformaldehyde

4g PFA dissolved in dH₂O at 60°C. pH 7.4 using 1M NaOH. Stored at -80°C for 3 months.

Bouin's solution

75ml Picric acid, 25ml 40% Formaldehyde, 5ml Glacial acetic acid.

DMEM

500ml tissue culture medium supplemented with 10% (v/v) heat inactivated fetal bovine serum (FBS), 100 units/ml penicillin and 100µg/ml streptomycin.

HBSS

5ml of 1mol/l HEPES & 5ml penicillin/streptomycin in 500ml HBSS.

Homogenisation buffer

320mM Sucrose, 10mM Tris base pH 7.8, 50mM KCl, 1mM ethylenediaminetetraacetic acid (EDTA), 0.5% Igepal, protease inhibitor cocktail (Sigma) (1:500) supplemented with fresh phosphatase inhibitor cocktail (Sigma) 1:100.

KPSS (mmol/l)

60 KCl, 25 NaHCO₃, 2.5 MgSO₄, 3.2 CaCl₂, 1.2 KH₂PO₄, 5.5 glucose, 0.034 EDTA pH7.4, stored at 4°C.

Lamelli buffer/sample loading buffer

50µl β-mercaptoethanol, 950 µl sample loading buffer (Biorad).

PBS:Glycerol

Equal v/v of PBS:Glycerol.

PSS (mmol/l)

119 NaCl, 4.7 KCl, 25 NaHCO₃, 2.5 MgSO₄, 1.6 CaCl₂, 1.2 KH₂PO₄, 5.5 glucose, 0.034 EDTA pH7.4, Stored at 4°C.

Resolving gel (12%)

4.1ml dH₂O, 3.3ml Acrylamide, 2.5ml resolving gel buffer (Tris base pH8.8), 100µl 10% SDS, 100µl ammonium persulfate (APS), 4µl N,N,N',N'-Tetramethylethylenediamine (TEMED).

Running buffer

15.1g Tris, 94g Glycine, 50ml 10% SDS in 1L H₂O.

Solubilisation buffer

20mM Tris base pH 7.5, 10mM EDTA, 120mM NaCl, 50mM KCl, 2.5% Igepal supplemented with fresh protease inhibitor cocktail (Sigma) (1:500) and phosphatase inhibitor cocktail (Sigma) 1:100).

Stacking gel (4%)

3.4ml dH₂O, 0.85ml Acrylamide, 0.625ml resolving gel buffer (Tris base pH6.8), 50µl 10% SDS, 50µl APS, 5µl TEMED.

TBS-Tween (TBST) 0.1%

1L TBS, 1ml Tween-20.

Transfer buffer

24mM Tris Base, 80mM glycine, 20% methanol.

Tris buffered saline (TBS)

12.11g Tris, 146.1g NaCl, in 5L H₂O pH to 7.4 with 5M HCl.

II. Working dilutions of antibodies

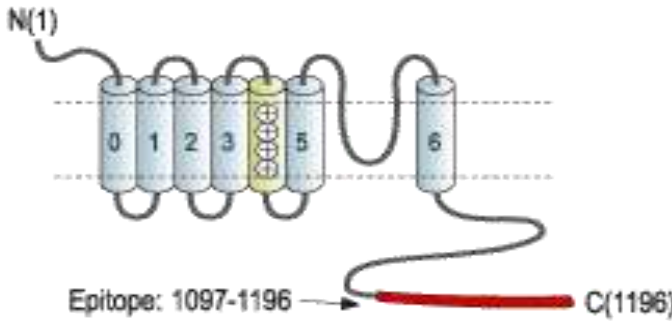
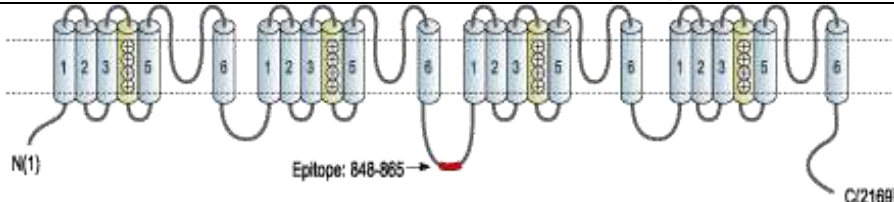
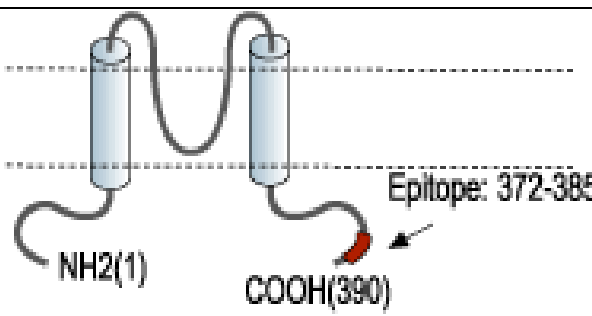
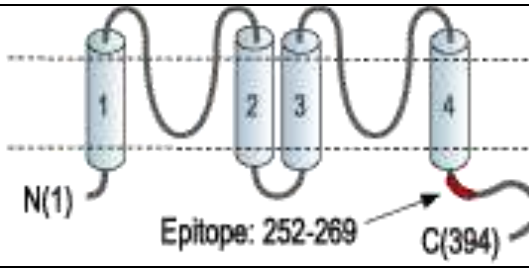
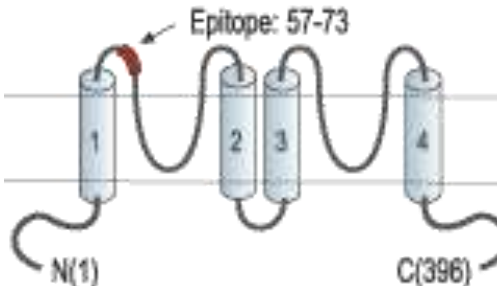
Table II-1 detailing the dilution factor for each antibody included in our studies according to which technique was used.

Antibody	Host	Type	Working Dilution & Technique	Secondary antibody & Conjugate
Alpha actin (DakoCytomation)	Mouse	Monoclonal	1:50 IF 1:50 IHC	1:50 FITC (Sigma) 1:1000 FITC (Molecular Probes) Vectorstain Elite Kit (Universal) (Vector laboratories)
Beta actin (Abcam)	Rabbit	Polyclonal	1:8000 WB	1:30000 AP (Sigma) 1:2000 AP (DakoCytomation)
BK _{Ca} (Alomone)	Rabbit	Polyclonal	1:500 WB 1:40 IF	1:30000 AP (Sigma) 1:2000 AP (DakoCytomation) 1:50 FITC (Sigma) 1:1000 TRITC (Molecular Probes)
BK _{Ca} (BD Transduction laboratories)	Mouse	Monoclonal	1:750 WB 1:40 IF	1:1000 AP (DakoCytomation) 1:50 FITC (Sigma) 1:1000 FITC (Molecular Probes)
CD31 (Abcam)	Mouse	Monoclonal	Ready to use	1:50 FITC (Sigma)
Cytokeratin (DakoCytomation)	Mouse	Monoclonal	1:50 IF 1:50 IHC	1:50 FITC (Sigma) Vectorstain Elite Kit (Universal) (Vector laboratories)
Cytokeratin AE1 (Abcam)	Mouse	Monoclonal	1:50 IF 1:50 IHC	1:50 FITC (Sigma) Vectorstain Elite Kit (Universal) (Vector laboratories)
Fibroblast (DakoCytomation)	Mouse	Monoclonal	1:50 IF 1:50 IHC	1:50 FITC (Sigma) Vectorstain Elite Kit (Universal) (Vector laboratories)
Ca _v 1.2 (Alomone)	Rabbit	Polyclonal	1:200 WB 1:50 IF	1:2000 AP (DakoCytomation) 1:50 FITC (Sigma) 1:1000 TRITC (Molecular Probes)
K _{ATP} (Alomone)	Rabbit	Polyclonal	1:200 WB	1:30000 AP (Sigma)

TASK-1 (Alomone)	Rabbit	Polyclonal	1:200 WB 1:50 IF	1:30000 AP (Sigma) 1:2000 AP (DakoCytomation) 1:50 FITC (Sigma) 1:1000 TRITC (Molecular Probes)
TASK-3 (Abcam)	Mouse	Monoclonal	1:50 IF	1:1000 TRITC (Molecular probes)
TASK-3 (Alomone)	Rabbit	Polyclonal	1:200 WB 1:50 IF	1:30000 AP (Sigma) 1:2000 AP (DakoCytomation) 1:50 FITC (Sigma) 1:1000 TRITC (Molecular Probes)
TRAAK (Alomone)	Rabbit	Polyclonal	1:200 WB	1:30000 AP (Sigma)
TREK-1 (Alomone)	Rabbit	Polyclonal	1:500 WB 1:100 IF	1:30000 AP (Sigma) 1:2000 AP (DakoCytomation) 1:50 FITC (Sigma) 1:1000 TRITC (Molecular probes)
TREK-2 (Abcam.)	Rabbit	Polyclonal	1:300 WB	1:30000 (Sigma)
TWIK-2 (Alomone)	Rabbit	Polyclonal	1:200 WB 1:50 IF	1:30000 AP (Sigma) 1:2000 AP (DakoCytomation) 1:50 FITC (Sigma) 1:1000 TRITC (Molecular Probes)
Vimentin (DakoCytomation)	Mouse	Monoclonal	1:20 IF	1:50 FITC
Von Wilebrand (DakoCytomation)	Rabbit	Polyclonal	1:200 IF 1:200 IHC	1:50 FITC Vectorstain Elite Kit (Universal) (Vector laboratories)

III. Antibody amino acid target sites and predicted molecular weight (mw).

Table III-1 summarising the epitope target sites for each antibody used along with the predicted mw. (Information obtained from www.alomone.com/p_postcards/database)

Antibody	Epitope location	Amino acid residue	Predicted mw (kDa)
BK _{Ca}	Intracellular C-terminal	 <p>Epitope: 1097-1196 C(1196)</p>	132
Cav1.2	Intracellular loop between domains II and III.	 <p>Epitope: 848-865 C(2169)</p>	240
K _{ATP}	Intracellular C-terminal	 <p>Epitope: 372-385 NH2(1) COOH(390)</p>	43
TASK-1	Intracellular C-terminal	 <p>Epitope: 252-269 C(394)</p>	45
TASK-3	Extracellular P1 loop	 <p>Epitope: 57-73 N(1) C(396)</p>	47

TRAAK	Intracellular C-terminal	<p>Diagram of TRAAK protein structure showing four transmembrane helices (1-4). The N-terminus is labeled N(1). The C-terminus is labeled C(393). An epitope is indicated at residues 343-359.</p>	52
TREK-1	Intracellular N-terminal	<p>Diagram of TREK-1 protein structure showing four transmembrane helices (1-4). The N-terminus is labeled N(1). The C-terminus is labeled C(426). An epitope is indicated at residues 8-25.</p>	50
TREK-2	Intracellular C-terminal	<p>Diagram of TREK-2 protein structure showing four transmembrane helices (1-4). The N-terminus is labeled N(1). The C-terminus is labeled C(538). An epitope is indicated at residues 475-494.</p>	59
TWIK-2	Intracellular C-terminal	<p>Diagram of TWIK-2 protein structure showing four transmembrane helices (1-4). The N-terminus is labeled N(1). The C-terminus is labeled C(313). An epitope is indicated at residues 295-313.</p>	35

IV. Suppliers

Abcam	330 Cambridge Science Park Cambridge CB4 0FL UK Web http://www.abcam.com
Abnova	Abnova GmbH c/o EMBLEM Boxberggring 107 69126 Heidelberg Germany Web: http://www.abnova.com E-mail: sales@abnova.com
ADI	ADInstruments Ltd Unit B, Bishops Mews Transport Way Oxford OX4 6HD Tel: +44 (0)1865 332050 Fax: +44 (0)1865 332051 Web: http://www.adinstruments.com
Alomone	Caltag-Medsystems Ltd. Whiteleaf Business Centre 11, Little Balmer Buckingham, Bucks MK18 1TF UK Tel:+44 (0)1280 827466 Web http://www.alomone.com/ E-mail: sales@caltagmedsystems.co.uk
BD Transduction Laboratories	BD Biosciences 21588 Network Place Chicago, IL 60673-1215 Tel: 44.1865.78.16.66 Fax: 44.1865.78.16.27 Web http://www.bdbiosciences.com/home.jsp E-mail admetox@bd.com
Biorad	Bio-Rad Laboratories Ltd. Bio-Rad House Maxted Road Hemel Hempstead Hertfordshire HP2 7DX Tel: +44 (0)208 328 2000 Fax: +44 (0) 208 328 2550 Web: http://www3.bio-rad.com/ E-mail: uk.lsg.marketing@bio-rad.com

British oxygen company (BOC)	<p>BOC Ltd The Priestley centre Guilford Surrey GU2 7XY Tel: 01483579857 Fax: 01483505211 Web: www.boconline.co.uk</p>
DakoCytomation	<p>Dako UK Ltd Cambridge House St Thomas Place, Ely Cambridgeshire CB7 4EX Tel: +44 (0)1 353 66 99 11 Fax: +44 (0)1 353 66 73 09 Web: www.dako.co.uk E-mail: info.uk@dako.com</p>
Danish Myotechnologies (DMT)	<p>Skejby Science Ctr. Skejbyparken 152 DK-8200 Aarhus N Denmark Tel: +45 87 41 11 00 Fax: +45 87 41 11 01 Web: http://www.dmt.dk E-mail: administration@dmtdk</p>
Enzo Life Sciences	<p>Enzo Life Sciences (UK) Ltd (<i>Formerly BIOMOL Int, L.P.</i>) Palatine House Matford Court Exeter EX2 8NL UK Tel: 0845 601 1488 (UK customers) Fax: +44 1392 825910 Web: http://www.enzolifesciences.com/contact-us/ E-mail: info-uk@enzolifesciences.com</p>
Fisher Scientific	<p>Fisher Scientific UK Ltd, Bishop Meadow Road, Leicestershire LE11 5RG Tel: 01509 231166 Fax: 01509 231893 Web: http://www.fisher.co.uk</p>
Lonza	<p>Lonza Biologics Granta Park Great Abington Cambridge CB216GS Tel: +44 1223 895100 Fax: +44 1223 895191 Web: http://www.lonza.com E-mail: contact.slough@lonza.com</p>
Molecular probes	<p>Invitrogen Ltd Inchinnan Business Park Paisley UK PA4 9RF</p>

Santa Cruz	<p> Tel: 0141 814 6100 Fax: 0141 814 6260 Web: http://www.invitrogen.com E-mail: euoinfo@invitrogen.com Santa Cruz Biotechnology, Inc. Bergheimer Str. 89-2 69115 Heidelberg Germany </p>
Sigma Aldrich	<p> Tel: +49 6221 4503 0 Fax: +49 6221 4503 45 Web: http://www.scbt.com E-mail: europa@scbt.com Sigma-Aldrich Company Ltd. The Old Brickyard New Road Dorset SP8 4XT UK Tel: +44 1202 712300 Fax: +44 1202 715460 Web: http://www.sigmaaldrich.com/united-kingdom.html E-mail: ukcustsv@europe.sial.com </p>
Tocris	<p> Tocris Bioscience Tocris House, IO Centre Moorend Farm Avenue Bristol, BS11 0QL United Kingdom Tel: + 44 (0)117 916-3333 Fax: + 44 (0)117 916-3344 Web: http://www.tocris.com/contact.php E-mail: customerservice@tocris.co.uk </p>
Vector Laboratories	<p> 3, Accent Park, Bakewell Road Orton Southgate Peterborough PE2 6XS Tel: (01733) 237999 Fax: (01733) 237119 Web: http://www.vectorlabs.com/uk E-mail: vector@vectorlabs.co.uk </p>
VWR (formerly BDH)	<p> Hunter Boulevard Magna Park Leicestershire LE17 4XN Tel: 0800 22 33 44 Web: http://uk.vwr.com E-mail: uksales@uk.vwr.com </p>
WPI	<p> World Precision Instruments UK Astonbury farm business centre Stevenage Herts SG2 7EG Tel: (01438) 880 025 Fax: (01438) 880 026 Web: http://www.wpiinc.com </p>

V. Patient information sheet & Consent forms

VI. Transmission Electron Microscopy (TEM) imaging of CPA and SVA

CPA and SVA matched samples (N=3) were prepared for TEM work by an AMU technician on our behalf. From the 3 paired samples that were prepared 1 CPA and 1 SVA ultrathin (70nm) slice was selected for TEM imaging. The slides were viewed using a FEI Tecnai 12 BioTWIN microscope and the images were captured with a Megaview III camera using Soft Imaging System software.

Protocol

Briefly the tissue samples were cut into small 1mm³ rings and fixed overnight with 3% Glutaraldehyde. Following this incubation the tissue specimens are washed in 0.1M cacodylate buffer. The tissue was then post fixed in 1% osmium tetroxide in 0.1M cacodylate buffer. Following five 1min washes in distilled water the samples were dehydrated with graded alcohol treatments (50%, 70%, 90% and 100% for 15mins each) before finally being treated with 100% propylene oxide for a final 15mins. The samples were then infiltrated with resin (mixed with propylene oxide at ratio of 3:1) for 4h at RT. Finally the tissue was embedded in a plastic mould which was left to polymerise overnight at which point the sections were ready for cutting. Semi-thin (0.5µm) sections were prepared to correctly orientate the tissue before cutting ultrathin (70nm) sections. This was performed using a diamond knife (Diatome) and collected on a copper mesh grid ready for viewing.

Results

Tissue slices were imaged with TEM which gave a more detailed examination of the cell layers within the CPA and SVA. The advantage of TEM imaging is that cell types can be identified with greater clarity according to their ultrastructural detail. The SMC can be identified by the presence of myofilaments while the single cell layer of EC can be distinguished by the elastic lamina (EL) which separates the EC layer from SMC. The semi-thin sections that were used to orientate the CPA and SVA sections and localise the area of interest for ultra thin sections (white box) for TEM are shown in **Figure VIA**. A single red blood cell (RBC) can be seen inside the vessel lumen (L) of the CPA (**Figure VIA**). SVA were imaged at the same magnification as CPA but many more cell layers can be seen including the EC and SMC along with CT which marks the area outside the vessel (**Figure VIB**). The SMC appeared to be evenly distributed around the thin vessel wall while it was not possible to image all three layers within a single photomicrograph with CPA. The three important portions of a blood vessel; namely the lumen, EC and SMC where are present in both CPA and SVA tissue slices. These images also show that the EC layer does appear to remain intact following vessel isolation. More importantly no cytokeratin or fibroblast cells were observed as the vessels consisted predominantly of SMC. Some fat droplets (not shown) were found sporadically around the SMC layer of CPA. This is an important sign of metabolically active cells as fat droplets are vital long term energy stores (Weser and Kaufmann, 1978).

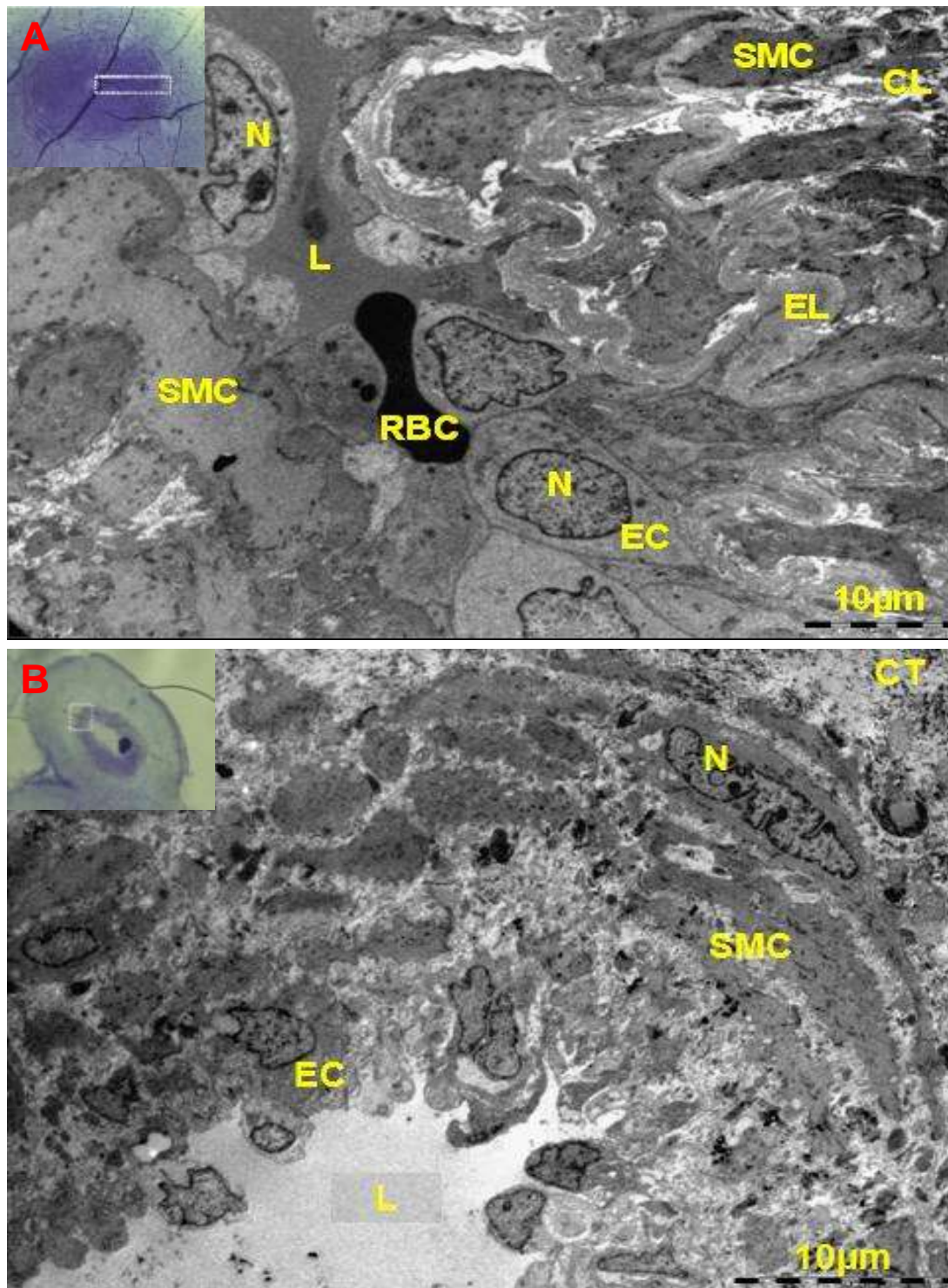


Figure VI showing TEM micrographs of human placental CPA (A) and SVA (B) (n=1 from N=1). The inserts show the original tissue slice and the region that was magnified (white box). The SMC layer can be seen with CPA with a single RBC inside the lumen. In contrast three distinct cell regions including the EC, SMC and CT can be seen with SVA imaged at the same magnification. Collagen (CL), Connective tissue (CT), Endothelial cell (EC), Elastic lamina (EL), Lumen (L), Nucleus (N), Red blood cell (RBC), Smooth muscle cell (SMC). *Scale bar 10µm.*